Rôle de la signalisation des enképhalines par les récepteurs opioïdergiques delta dans la résilience au stress chronique

Thèse

Mathilde Henry

Doctorat en neurobiologie
Philosophiæ doctor (Ph. D.)

Québec, Canada

RÔLE DE LA SIGNALISATION DES ENKÉPHALINES PAR LES RÉCEPTEURS OPIOÏDERGIQUES DELTA DANS LA RÉSILIENCE AU STRESS CHRONIQUE

Thèse

Mathilde Henry

Sous la direction de :

Guy Drolet, directeur de recherche
Marie-Ève Tremblay, codirectrice de recherche

RÉSUMÉ

La survie d'un individu repose essentiellement sur sa capacité d'adaptation à des conditions de vie en constante évolution. Il existe une grande variabilité entre les individus concernant leur réponse au stress chronique, définissant le concept de résilience. Il s'agit d'un mécanisme d'adaptation actif correspondant à la capacité d'un individu à éviter les conséquences négatives sociales, psychologiques et biologiques d'un stress extrême, qui compromettraient son bien-être psychologique ou physique. Le phénomène est complexe et fait intervenir de nombreuses structures cérébrales et de nombreux neurotransmetteurs. Parmi les systèmes neuropeptidergiques, les opioïdes endogènes, comme les enképhalines (ENKs), seraient des cibles potentiellement impliquées dans ces variations naturelles et pourraient ainsi, être un élément déterminant de la capacité d'adaptation individuelle, au cours de l'exposition au stress chronique. Dans une précédente étude de l'équipe du Dr Guy Drolet, il avait été démontré que les niveaux d'expression de l'ARNm des ENKs étaient diminués dans le noyau basolatéral de l'amygdale (BLA) chez les rats vulnérables après un stress chronique de défaite sociale (SCDS). De plus, l'inhibition des ENKs dans la BLA permettait de reproduire un phénotype de vulnérabilité chez le rat, démontrant ainsi le rôle prépondérant de la circuiterie des ENKs dans le développement de la résilience.

Cette thèse a pour objectif principal de comprendre la contribution dans la résilience au stress chronique du circuit des ENKs via les récepteurs opioïdergiques Delta (DOPr), tant au niveau neuroanatomique que fonctionnel. Nous avons, tout d'abord, examiné par hybridation *in situ*, les niveaux d'expression des ENKs dans la BLA chez la souris après un SCDS : comme chez le rat, les souris vulnérables présentaient une diminution de l'ARNm des ENKs dans la BLA par rapport aux animaux résilients et contrôles. Ce résultat confirme une conservation entre les rongeurs concernant l'implication des ENKs dans la résilience. Par la suite, nous avons évalué les niveaux d'expression de DOPr dans les structures cibles de la BLA. Nous avons spécifiquement ciblé l'hippocampe qui entretient un dialogue privilégié avec l'amygdale dans la réponse au stress et dans lequel, DOPr est fortement exprimé. L'expression de l'ARNm de DOPr était réduite dans la région CA1 de l'hippocampe ventral (CA1-vHPC) chez les souris vulnérables tandis que le niveau était

maintenu chez les animaux résilients comme chez les témoins. Afin de disséquer l'importance de la signalisation DOPr dans le développement de la résilience, une activation pharmacologique a été effectuée : l'administration d'un agoniste de DOPr, le SNC80, dans la circulation systémique, a augmenté la proportion de souris résilientes après le SCDS.

Dans un second temps, nous avons fait l'hypothèse que le maintien du niveau d'expression de DOPr au niveau du CA1-vHPC permettait de maintenir un statut oxydatif contrôlé dans les neurones, conduisant au phénotype de résilience. En effet, le rôle neuroprotecteur de l'activation de DOPr contre les dommages oxydatifs cellulaires (*i.e.* stress oxydatif, SO) a été démontré dans différents contextes, notamment chez le rat ischémique. Nous avons ainsi observé des marqueurs du SO - comme les neurones « sombres » ou la dilatation du réticulum endoplasmique - par microscopie électronique à transmission (MET) après un SCDS, avec ou sans traitement au SNC80. Nous avons spécifiquement ciblé les neurones excitateurs et inhibiteurs du CA1-vHPC. Nous avons pu mettre en évidence que le SNC80 diminuait la proportion de certains marqueurs du SO, autant chez les animaux résilients que vulnérables, tandis que pour d'autres marqueurs, il restaurait les dommages oxydatifs induits par le SCDS, uniquement chez les vulnérables. Enfin, une étude ultrastructurelle des mitochondries - comme leur nombre et leur taille - par MET, a confirmé ces résultats où le SNC80 restaure les effets délétères du stress uniquement chez les souris vulnérables. Ces résultats ont permis de démontrer que l'activation de la signalisation DOPr est responsable de la résilience en maintenant un statut oxydatif contrôlé dans les neurones excitateurs et inhibiteurs du CA1-vHPC. Pour finir, une étude moléculaire a été effectuée par western blot, dans l'hippocampe total, afin de déterminer la cible moléculaire de DOPr impliquée dans le SO permettant la résilience. Les complexes de la chaîne respiratoire mitochondriale et des enzymes antioxydantes ont été ciblés. L'activation de DOPr a résulté en une diminution de l'expression de certains complexes sans dévoiler la cible moléculaire exacte de DOPr permettant la résilience au stress chronique. Collectivement, ces études proposent un nouveau mécanisme par lequel la signalisation ENK-DOPr permettrait le développement de la résilience au stress chronique en favorisant un état oxydatif contrôlé dans les neurones de l'hippocampe.

ABSTRACT

The survival of an individual is essentially based on his ability to adapt to ever-changing living conditions. There is a great variability among individuals regarding their response to chronic stress, defining the concept of resilience. Resilience is an active coping mechanism corresponding to an individual's ability to avoid the negative social, psychological and biological consequences of extreme stress that would compromise their psychological or physical well-being. The phenomenon is complex and recruits many brain structures and several neurotransmitters. Among the neuropeptidergic systems, endogenous opioids, such as enkephalins (ENKs), could be potential targets involved in the occurrence of these natural variations and could thus be a crucial determinant of an individual's capacity to adapt to chronic stress. In a previous study by Dr Guy Drolet's team, ENK mRNA expression levels were shown to be decreased in the nucleus of basolateral amygdala (BLA) in vulnerable rats after chronic social defeat stress (CSDS). In addition, the inhibition of ENKs in the BLA reproduced this vulnerability phenotype in rats, thus demonstrating the preponderant role of the ENK circuitry in the development of resilience. The main objective of this thesis was to investigate the contribution of the ENKs circuit via the Delta opioid receptors (DOPr) in the chronic stress resilience, both at the neuroanatomical and functional levels. We first examined, by *in situ* hybridization, the expression levels of ENKs in BLA in mice after CSDS: as in rats, susceptible mice showed a decrease in ENK mRNA in BLA compared to resilient and controls animals. This result confirmed the implication of the ENKs in resilience in rodents. Subsequently, we evaluated the expression levels of DOPr in the target structures of the BLA. We specifically targeted the hippocampus, which maintains a privileged dialogue with the amygdala in the response to stress and in which DOPr is strongly expressed. DOPr mRNA expression was reduced in the ventral hippocampal CA1 region (CA1-vHPC) in vulnerable mice while the level was preserved in both resilient and control animals. In order to dissect the importance of DOPr signaling in the development of resilience, pharmacological activation was performed: the administration of a DOPr agonist, SNC80, into the systemic circulation, increased the proportion of resilient mice after the CSDS.

In a second step, we hypothesized that the maintenance of DOPr mRNA expression in CA1-vHPC allowed the preservation of a controlled oxidative status in neurons, leading to the phenotype of resilience. Indeed, the neuroprotective role of DOPr activation against cellular oxidative damages (*i.e.* oxidative stress, OS) was demonstrated in different contexts, particularly in ischemic rats. Thus, we observed markers of OS - such as dark neurons and endoplasmic reticulum dilation - by transmission electron microscopy (TEM) after CSDS, with or without SNC80 treatment. We specifically targeted excitatory and inhibitory neurons of CA1-vHPC. We were able to demonstrate that the SNC80 decreased the proportion of some OS markers in both resilient and vulnerable animals, while for other markers, it restored CSDS-induced oxidative damages only in vulnerable mice. Finally, an ultrastructural study of mitochondria by TEM, confirmed these results where the SNC80 restored the deleterious effects of stress only in vulnerable mice. These results demonstrated that activation of DOPr signaling is responsible for resilience by the preservation of a controlled oxidative status in excitatory and inhibitory neurons of CA1-vHPC. Finally, a molecular study was performed by western blot, in the total hippocampus, to determine the molecular target of DOPr involved in OS, allowing stress resilience. Complexes of the mitochondrial respiratory chain and antioxidant enzymes were measured. The activation of DOPr showed a decrease in the expression of certain complexes without revealing the exact molecular target of DOPr allowing resilience to chronic stress. Overall, these studies propose a novel mechanism by which ENK-DOPr signaling promotes resilience to chronic stress by enhancing a controlled oxidative status in hippocampal neurons.

TABLE DES MATIÈRES

RÉSUMÉ ..... **III**
ABSTRACT ..... **V**
TABLE DES MATIÈRES ..... **VII**
LISTE DES FIGURES ..... **XI**
LISTE DES TABLEAUX ..... **XII**
LISTE DES ABRÉVIATIONS ..... **XIII**
REMERCIEMENTS ..... **XV**
AVANT-PROPOS ..... **XVIII**
1 INTRODUCTION **1**
1.1 Le stress **1**
1.1.1 Incidence et facteurs de risque 2
1.1.2 L'histoire du stress 3
1.1.3 La perception de l'organisme face à l'évènement stressant 4
1.1.4 Les circuits neuronaux impliqués dans la réponse au stress 6
1.1.5 Les réponses physiologiques engendrées par le stress 9
1.1.5.1 Le système nerveux autonome 9
1.1.5.2 L'axe hypothalamo-hypophyso-surrénalien 11
1.1.6 Les réponses émotionnelles et comportementales liées au stress 13
1.1.7 Le système opioïdergique 14
1.1.7.1 Structure, voies de signalisation et régulation des récepteurs opioïdergiques 15
1.1.7.2 Distribution des récepteurs opioïdergiques MOPR et DOPr dans le système nerveux central 17
1.2 La signalisation enképhalinergique et le stress : « Enkephalins : endogenous analgesics with an emerging role in stress resilience » **20**
1.2.1 Résumé 20
1.2.2 Abstract 20
1.2.3 Introduction 22
1.2.4 Enkephalins and their opioid receptors 23
1.2.4.1 Biochemistry and anatomical distribution of enkephalins and their receptors, DOPr and MOPr, in the CNS 23
1.2.4.2 Roles in emotional behavior 25
1.2.4.2.1 Fear conditionning 26
1.2.4.2.2 Stress and anxiety 29
1.2.5 Role in resilience to chronic stress 33
1.2.6 Conclusion 36
1.3 « Le stress oxydatif est le nouveau stress » **38**
1.3.1 Définition du stress oxydatif 38
1.3.2 Les marqueurs cellulaires du stress oxydatif 42
1.3.2.1 Les cellules « sombres » 42
1.3.2.2 Le stress du réticulum endoplasmique et la dilatation de l'appareil de Golgi 44
1.3.2.3 Les mitochondries 46
1.3.2.4 Autres marqueurs 47
1.3.3 Le stress oxydatif et les pathologies liées au stress chronique 48
1.3.4 Le stress oxydatif et le système opioïdergique 50
1.4 Objectifs de recherche **52**

2 CHAPITRES 53
2.1 Chapitre 1 53
2.1.1 Résumé 54
2.1.2 Abstract 55
2.1.3 Introduction 56
2.1.4 Materials and Methods 58
2.1.4.1 Animals 58
2.1.4.2 Repeated social defeat 58
2.1.4.3 Pharmacological treatment 59
2.1.4.4 Perfusion and tissue preparation 60
2.1.4.5 Corticosterone ELISA in plasma 61
2.1.4.6 Radioactive in situ hybridization 61
2.1.4.7 Electron microscopy 62
2.1.4.8 Statistical analyses 62
2.1.5 Results 64
2.1.5.1 Vulnerable mice display a strong social avoidance behavior upon repeated social defeat. 64
2.1.5.2 Decreased expression levels of ENK and DOPr are associated with vulnerability to stress. 67
2.1.5.3 Administration of a DOPr agonist, SNC80, promotes a resilience phenotype. 70
2.1.5.4 SNC80 treatment prevents oxidative stress in hippocampal CA1 neurons. 73
2.1.6 Discussion 82
2.1.7 Funding and disclosure 85
2.1.8 Acknowledgments 86
2.1.9 Supplementary data 87
2.2 Chapitre 2 92
Les résultats évoqués dans ce chapitre font partie d'une étude en collaboration avec Dr Louis Gendron et Dr Jean-Luc Parent de l'Université de Sherbrooke et seront integrés au sein d'un article de plus grande envergure. 92
2.2.1 Résumé 93
2.2.2 Abstract 94
2.2.3 Introduction 95
2.2.4 Material and Methods 98
2.2.4.1 Animals 98
2.2.4.2 Social defeat stress 98
2.2.4.3 Pharmacological treatment 98
2.2.4.4 Perfusion 98
2.2.4.5 Electron microscopy 99
2.2.4.6 Western Blot 100
2.2.4.7 Statistical analyses 101
2.2.5 Results 102
2.2.5.1 SNC80 restores healthy mitochondrial morphology in vulnerable mice. 102
2.2.5.1.1 Number of mitochondria 102
2.2.5.1.2 Mean grey value 103
2.2.5.1.3 Area and perimeter 104
2.2.5.1.4 Shape descriptor 104
2.2.5.2 SNC80 increases expression of complex III and V of mitochondrial respiratory chain. .. 111
2.2.6 Conclusion 114
2.2.7 Supplemental information 115
3 DISCUSSION GÉNÉRALE 117
3.1 Le modèle de stress chronique de défaite sociale 118
3.2 Un dialogue privilégié ENK/DOPr entre la BLA et le *oriens*-CA1-vHPC dans la résilience au stress chronique 120

3.3 L'expression des ARNm DOPr est diminuée dans le *oriens*-CA1-vHPC des souris vulnérables : Que sont ces neurones exprimant DOPr? 121
3.4 Le SNC80 : avantages et inconvénients 122
3.5 Perspectives : première partie du chapitre 1 123
3.6 DOPr favorise naturellement la résilience en réduisant les effets délétères du stress oxydatif induit par le stress chronique 125
3.7 Hypothèses de mécanismes entre l'activation endogène de DOPr et le maintien d'un statut oxydatif contrôlé chez les résilients 129
3.8 Thérapies 130

4 CONCLUSION 134

5 RÉFERENCES BIBLIOGRAPHIQUES 135

6 CONTRIBUTION SCIENTIFIQUE / COLLABORATION – ANNEXE 159
6.1 Résumé 160
6.2 Abstract 161
6.3 Introduction 162
6.4 Methods 164
6.4.1 Animals and ethical approval 164
6.4.2 Mating and neonatal maternal separation (NMS) procedures 164
6.4.3 Series I – Gonadectomy and whole-body plethysmography 164
6.4.3.1 Surgical procedures 164
6.4.3.2 Ventilatory measurements 165
6.4.3.3 Protocol 165
6.4.3.4 Blood sampling and hormone analyses 165
6.4.4 Series II – Quantification of c-fos immunoreactive cells during baseline and hypercapnia 166
6.4.4.1 Brain tissue harvesting 166
6.4.4.2 Regions of interest 166
6.4.4.3 Immunohistochemistry 166
6.4.5 Data analysis 167
6.4.5.1 Ventilatory measurements 167
6.4.5.2 Immunohistochemistry 167
6.4.6 Statistics 167
6.5 Results 169
6.5.1 Effectiveness of the castration procedure, body weight, and impact on basal ventilatory activity. 169
6.5.2 Ventilatory response to hypercapnia (HCVR) 171
6.5.3 c-fos expression in the PVN at rest (room air) and following hypercapnic exposure (10% CO_2) 172
6.5.4 c-fos expression in the amygdala at rest (room air) and following hypercapnic exposure (10% CO_2) 174
6.5.5 c-fos expression in the dorsomedial hypothalamus (DMH) at rest (room air) and following hypercapnic exposure (10% CO_2) 176
6.5.6 c-fos expression in the medial amygdala is inversely proportional to the intensity of the hyperventilatory response to CO_2. 177
6.6 Discussion 179
6.6.1 Neonatal maternal separation, castration, and breathing at rest 179
6.6.2 Impact of neonatal maternal separation and castration on basal c-fos expression in the hypothalamus and amygdala 180
6.6.3 Impact of neonatal maternal separation and castration on the ventilatory, hypothalamic, and amygdalar responses to CO_2 inhalation 181

6.6.4 Limitations, Conclusions, and Perspectives 183
6.7 Acknowledgments 184

LISTE DES FIGURES

Figure 1 : Système modélisant la réponse au stress chez l'humain.
Figure 2 : Schéma général des voies régulées par un stress.
Figure 3 : Organisation des efférences limbiques.
Figure 4 : Les voies efférentes du SNA.
Figure 5 : Organisation de l'axe hypothalamo-hypophyso-adrénal (axe HPA).
Figure 6 : Structure générale d'un récepteur couplé à une protéine G (RCPG).
Figure 7 : Voies de signalisation intracellulaires associées aux récepteurs opioïdes.
Figure 8 : Distribution neuroanatomique du récepteur opioïdergique μ (MOPr) chez la souris grâce à une construction MOPr-mcherry.
Figure 9 : Distribution neuroanatomique du récepteur opioïdergique δ (DOPr) chez la souris grâce à une construction DOPr-eGFP.
Figure 10 : Cartography of main connectivities involved in fear, stress, and resilience, as well as demonstrated ENK pathways between areas and expression of ENK, MOPr, and DOPr.
Figure 11 : Production de radicaux libres lors de la respiration aérobie.
Figure 12 : Les sources et les réponses cellulaires induites par la production d'espèces réactives à l'oxygène (ROS).
Figure 13 : Exemple de cellules « sombres ».
Figure 14 : Déclenchement du stress du réticulum endoplasmique (« ER stress ») et la balance du yin-yang entre la survie cellulaire et l'apoptose.
Figure 15 : La réponse au stress de la mitochondrie en condition de stress aigu et chronique.
Figure 16 : Vulnerable mice display a strong social avoidance behavior upon repeated social defeat.
Figure 17 : Decreased expression levels of ENK and DOPr are associated with vulnerability to social stress.
Figure 18 : Administration of a DOPr agonist, SNC80, promotes a resilience phenotype.
Figure 19 : SNC80 treatment prevents oxidative stress in pyramidal cells of CA1 hippocampus.
Figure 20 : SNC80 treatment reduces oxidative stress in interneurons from *stratum oriens* of CA1 hippocampus.
Figure 21 : SNC80 treatment reduces oxidative stress in interneurons from *stratum radiatum* of CA1 hippocampus.
Figure 22 : Summary of experiments**.**
Figure 23 : Sense probe versus antisense probe DOPr.
Figure 24 : Representative pictures illustrating different shapes of mitochondria as observed using transmission electron microscopy (TEM).
Figure 25 : SNC80 treatment prevents oxidative stress in *stratum pyramidale* of CA1 hippocampus.
Figure 26 : SNC80 treatment prevents oxidative stress in interneurons of *stratum oriens* of CA1 hippocampus.
Figure 27 : SNC80 treatment prevents oxidative stress in interneurons of *stratum radiatum* of CA1 hippocampus.
Figure 28 : SNC80 treatment reduces expression level of complexes in mitochondrial respiratory chain in hippocampus.
Figure 29 : Structures chimiques d'agonistes de DOPr.

LISTE DES TABLEAUX

Tableau 1 : Les opioïdes endogènes (gènes, peptides et séquences d'acide aminé).
Tableau 2 : Evidence for ENK signaling involvement using different behavioral tests.
Tableau 3 : Evidence for ENK signaling involvement under different stress paradigms.
Tableau 4 : Quantification of DOPr mRNA levels across hippocampus after repeated social defeat stress.
Tableau 5 : Statistical analysis (Two-way ANOVA with Bonferroni *post-hoc* analysis) for prevalence of different oxidative stress markers in *stratum pyramidale* described by electron microscopy.
Tableau 6 : Statistical analysis (Two-way ANOVA with Bonferroni *post-hoc* analysis) for prevalence of different oxidative stress markers in *stratum oriens* described by electron microscopy.
Tableau 7 : Statistical analysis (Two-way ANOVA with Bonferroni *post-hoc* analysis) for prevalence of different oxidative stress markers in *stratum radiatum* described by electron microscopy.
Tableau 8 : Statistical analysis (Two-way ANOVA with Bonferroni *post-hoc* analysis) for diverse morphological features of mitochondria in *stratum pyramidale* described by electron microscopy.
Tableau 9 : Statistical analysis (Two-way ANOVA with Bonferroni *post-hoc* analysis) for diverse morphological features of mitochondria in *stratum oriens* described by electron microscopy.
Tableau 10 : Statistical analysis (Two-way ANOVA with Bonferroni *post-hoc* analysis) for diverse morphological features of mitochondria in *stratum radiatum* described by electron microscopy.

LISTE DES ABRÉVIATIONS

ACTH : Hormone adénocorticotrope
AMG : Amygdala / amygdale
AVP : Arginine-vasopressine
BDNF : Brain-derived neurotrophic factor / facteur neurotrophique derivé du cerveau
BLA : Basolateral nucleus of amygdala / amygdale basolatérale
BST : Bed nuclei of the stria terminalis / noyau de la strie terminale
CAT : Catalase
CEA : Central part of amygdala / amygdale centrale
CEAl : Lateral part of central amygdala / partie latérale de l'amygdale centrale
CNS : Central nervous system / système nerveux central (SNC)
CRF : Corticotropin-releasing factor
CRH : Hormone corticolibérine
DMH : Noyau dorsomédian de l'hypothalamus
DOPr : δ opioid peptide receptor
DPDPE : [D-Pen 2,5]-enkephalin
ENK : Enkephalin
EPM : Elevated plus maze / labyrinthe en croix surélevé
ERAD : Endoplasmic reticulum associated degradation
FST : Forced swim test / test de nage forcée
GC : Glucocorticoïde
GPx : Glutathion peroxydase
HPA : Axe hypothalamo-hypophyso-surrénalien
HPC : Hippocampus / hippocampe
HPT : Hypothalamus
IC : Intercalated nuclei of amygdala / noyaux intercalaires de l'amygdale
IL : Cortex infralimbique
KD : Knock down
KI : Knock in
KO : Knockout
KOPr : κ opioid peptide receptor
LC : Locus coeruleus
LDB : Light-dark box
LDCVs : Large dense-core vesicles
Leu-ENK : Leucine-enkephalin
MEA : Medial part of amygdala / noyau médian de l'amygdale
MEAP : Met-ENK-Arg6Phe7
Met-ENK : Methionine-enkephalin
MOPr : μ opioid peptide receptor
mPFC : Medial prefrontal cortex / cortex préfrontal médian
NAc : Nucleus accumbens
NTS : Noyau du tractus solitaire
OF : Open-field
OPr : Opioid peptide receptor
PAG : Periaqueducal grey

PET : Positron emission tomography
PGi : Paragigantocellularis nucleus
PKC-δ : Protein kinase C-δ
PL : Cortex prélimbique
Pro-ENK : Proenkephalin
PTSD : Posttraumatic stress disorder
PVN : Paraventricular nucleus of HPT / noyau paraventriculaire de l'hypothalamus
RE : Réticulum endoplasmique
RNS : Espèces réactives de l'azote
ROS : Espèces réactives à l'oxygène
RSD : Repeated social defeat
SI : Social interaction
SN : Substantia nigra
SNA : Système nerveux autonome
SNS : Système nerveux sympathique
SOD : Superoxide dismutase
SR : Startle response
TMT : 2,5-Dihydro-2,4,5-trimethylthiazoline
UPR : Unfolded protein response
vSUB : Subiculum ventral
VTA : Ventral tegmental area / aire tegmentaire ventrale

REMERCIEMENTS

J'ai entrepris mon doctorat en septembre 2013 au sein du laboratoire de Dr Guy Drolet. Tout d'abord, je tiens à remercier Guy pour m'avoir fait faire ces 6000 km et vivre cette incroyable expérience du Québec et du doctorat. Il a su avec brio me transmettre sa passion pour la recherche, mais surtout pour les enképhalines et le stress. En plus d'être un chercheur passionné et brillant, Guy est humain, intègre et m'a toujours montrée beaucoup d'attention.

À l'époque où je suis arrivée, le laboratoire était en mutation. Sylvie Laforest, la professionnelle de recherche était sur le départ et Mélaine Henry venait d'arriver. Je tiens à remercier chaleureusement Sylvie pour m'avoir initiée à l'hybridation *in situ* radioactive qui aura été ma manip phare durant deux ans. Je remercie très chaudement Mélaine qui m'a accompagnée pendant un an, elle m'a appris les nombreuses techniques que j'ai utilisées tout au long de mon doctorat. Mais je la remercie surtout pour sa bonne humeur et son humour. Elle m'a aussi soutenue dans les moments difficiles par la suite, même si elle n'était plus au laboratoire. Nathalie Vernoux a succédé à Mélaine et m'a accompagnée jusqu'à la fin de mon doctorat. Je la remercie car elle a su m'accompagner avec sa gentillesse, son franc parler et son humour qui resteront gravés à jamais dans ma mémoire. Je remercie chaleureusement les PRs des équipes avoisinantes Claudia, Françoise et Sandrine pour leur aide constante et leurs conseils avisés.

Je tiens également à remercier Marie-Ève d'avoir accepté d'être ma co-directrice. Je ne la remercierai jamais assez de m'avoir pris en charge comme elle l'a fait, avec beaucoup de douceur et de gentillesse. Elle a montré énormément de patience et de disponibilité à mon égard dans l'apprentissage difficile de l'écriture d'articles scientifiques sans jamais pointer du doigt mes failles. Son optimisme naturel, sa persévérance et ses encouragements continuels pendant ces deux dernières années ont été d'une extraordinaire aide. Marie-Ève est une brillante chercheuse, en plus d'exceller dans l'encadrement de ses étudiants.

Je souhaite aussi remercier tous les membres de l'équipe de Marie-Ève, qui m'ont rapidement acceptée et intégrée, et avec qui je m'entends très bien. J'adresse mes remerciements en particulier à Julie, pour sa vivacité d'esprit, Cynthia pour sa générosité, Kanchan pour les discussions social defeat dans les couloirs sans oublier Marie-Kim,

Thomas, Katherine, Kaushik et Fernando (et les nombreux stagiaires qui nous auront bien aidés!).

Je souhaite également remercier Dr Louis Gendron qui a été d'une précieuse aide pour l'écriture de la revue et de l'article mais aussi pour ses conseils avisés en matière de statistiques.

Je remercie les membres de l'animalerie pour leur compréhension et leur aide lors de mes expériences de stress, notamment France, Mélanie, Karine et Denis.

Je tiens à remercier ma famille qui malgré la distance, a toujours été présente pour moi et m'a toujours soutenue. Ils sont tous venus et parfois plusieurs fois au Québec pour m'accompagner dans l'aventure. Un énorme merci à ma maman et mon papa ainsi qu'à Marie, Jean-Pierre et Piton pour leur encouragement continuel, pour avoir cru en moi quand moi, je n'y croyais plus. Une dédicace spéciale pour mes deux grandes sœurs adorées, Anaïs et Juliette, qui ont été les plus difficiles à quitter. Par contre, je ne remercie pas Juju de ne pas avoir attendu pour donner naissance à mes deux adorables neveux, Abdoul Shlomo et Loulou, que malheureusement, je vois grandir de beaucoup trop loin. Je souhaite aussi remercier mes amis qui m'ont beaucoup soutenue, une pensée notamment pour Paulette, Saranounette, Titi, Cha, Alixm et Jeanette, mes supers copines de très longue date.

Comme tout le monde le sait (enfin surtout ceux qui le vivent), le doctorat est une expérience extrêmement difficile, parfois douloureuse, frustrante et qui demande des ressources que l'on n'imaginait même pas avoir! Au laboratoire, on se construit comme une deuxième famille constituée d'étudiants avec qui on souffre en simultané, mais aussi avec qui on rigole beaucoup (parfois nerveusement) : une famille parfois un peu « boule de nerfs » mais qui se soutient, quoi qu'il arrive. Alors, un remerciement très spécial à mes supers copains de labo qui resteront dans mon petit cœur pour toute la vie, même si on risque d'être très éloignés les uns des autres pour les années à venir : Julia, Maud, Mélo et Nico. L'aventure « doctorat » aurait été sans aucun intérêt si ils n'avaient pas été là. Je remercie aussi Audrey, Léa, Sara, Franck, André-Anne, Emmanuelle et Baya (en particulier) que j'ai adoré côtoyer au laboratoire et en privé.

Enfin, je pense que je dois des remerciements à vie à mon mari, Anto, qui a fait 6000 km pour mes beaux yeux, pour suivre mes rêves tout en mettant les siens en sourdine, et qui en plus a du se marier avec moi pour ça! Je n'aurai de cesse de le remercier parce que sans son

soutien, sans une ombre, sans une seule faille, rien n'aurait été possible, parce qu'il excelle dans son rôle unique d'anxiolytique et parce que même après huit ans, il me fait toujours autant rire.

Merci aux membres de mon jury, Dr Claude Rouillard, Dr Martin Parent et Dre Brigitte Kieffer, d'avoir accepté d'évaluer ce manuscrit et de participer à ma soutenance.

AVANT-PROPOS

Le sujet de cette thèse porte sur la compréhension du rôle de la signalisation des enképhalines via les récepteurs opioïdergiques Delta dans la résilience au stress chronique. Elle se compose d'une introduction, de deux chapitres ainsi que d'une discussion générale et d'une conclusion. L'introduction fait état de la littérature concernant le stress : cette partie détaille les étapes permettant de répondre efficacement à une situation de stress, allant de la perception du stimulus à la réponse comportementale en passant par les circuits empruntés et les réponses physiologiques qui y sont associées. La seconde partie de l'introduction présente une version intégrale de la revue publiée, le 11 juillet 2017, dans le journal *Neural Plasticity* écrite avec Dr Guy Drolet et Dre Marie-Ève Tremblay en collaboration avec Dr Louis Gendron (Université de Sherbrooke). Cette revue s'intitule « Enkephalins : endogenous analgesics with an emerging role in stress resilience ». Elle fait état de ce qui est connu des enképhalines, de leurs récepteurs associés, de leur rôle dans la régulation des émotions et enfin, dans la résilience au stress chronique. La troisième partie introduit la récente littérature concernant le possible lien entre les pathologies associées au stress chronique et le stress oxydatif et d'autre part, entre le stress oxydatif et le système opioïdergique. À la suite de cette introduction, deux chapitres présentent ma contribution scientifique dans le cadre de mon projet principal de thèse. Le premier chapitre renferme la version intégrale d'un article intitulé « Delta opioid receptor signaling promotes resilience to stress under the repeated social defeat paradigm in mice », publié dans le journal *Frontiers in Molecular Neuroscience en* 2018 (M.S. Henry, K. Bisht, N. Vernoux, L. Gendron, A. Torres-Berrio, G. Drolet, M.-E. Tremblay). Le second chapitre correspond à l'étude d'un autre marqueur bien connu du stress oxydatif, l'altération mitochondriale induite par le stress chronique et l'effet neuroprotecteur des opioïdes dans ce contexte. Les résultats évoqués ici font partie d'une étude à plus grande échelle en collaboration avec Dr Louis Gendron et Dr Jean-Luc Parent. Ils seront présentés sous forme d'un article (en anglais) intitulé «Delta Opioid Receptor blunts oxidative stress to promote resilience to chronic stress: A morphological and molecular study of mitochondria».

J'ai écrit la revue sur les enképhalines avec l'aide de Marie-Ève, Guy et Louis. J'ai effectué la mise au point du protocole de stress chronique de défaite sociale en collaboration avec

Kanchan Bisht et Angélica Torres-Berrio (Université McGill, Montréal) à l'initiative de Guy et de Marie-Ève. Guy a participé à l'élaboration du projet concernant la première partie de l'article (chapitre 1) tandis que la seconde partie de l'article et le second chapitre sont à l'initiative de Marie-Ève (chapitres 1 et 2). Ce projet a d'autre part été élaboré en collaboration avec Louis concernant la drogue utilisée (chapitres 1 et 2). J'ai effectué le paradigme de stress, les expériences d'hybridation *in situ*, les quantifications et les analyses (chapitre 1). J'ai, d'autre part, effectué les expériences de microscopie électronique, les quantifications et les analyses avec l'aide de Marie-Ève. Les quantifications morphologiques des mitochondries ont conjointement été effectuées par moi-même et Gabrielle Duvoisin, stagiaire au laboratoire de Marie-Ève Tremblay (chapitre 2). Les Western Blot ont été effectués par moi-même au sein du laboratoire de Dr Sébastien Hébert (prêt de matériels et d'anticorps). Dr Michel Lebel a aussi prêté des anticorps.

Les collaborations effectuées durant mon doctorat ont donné lieu, en outre, à deux articles et à une revue. J'ai participé à l'écriture d'une revue intitulée « Microglia gone rogue: impacts on psychiatric disorders across the lifespan », publiée le 4 janvier 2018, dans le journal *Frontiers in Molecular Neuroscience*, où j'ai écrit les sections sur la dépendance à l'alcool et aux drogues, ainsi que les troubles liés au sommeil (T. Leng Tay, C. Bechade, I. D'Andrea, M.K. St-Pierre, M.S. Henry, A. Roumier, M.-E. Tremblay). Une riche collaboration avec Dr Richard Kinkead et Dre Luana Tenorio-Lopes a donné naissance à un article intitulé « Neonatal maternal separation opposes the facilitatory effect of castration on the respiratory response to hypercapnia of the adult male rat: evidence for the involvement of the medial amygdala *»,* publié le 24 octobre 2017, dans le *Journal of Neuroendocrinology* (L. Tenorio-Lopes, M.S. Henry, D. Marques, M.-E. Tremblay, G. Drolet, F. Bretzner, R. Kinkead). Cet article est présenté en annexe de ce manuscrit. Dans cet article, j'ai fait la capture d'images et les quantifications du marqueur *c-fos* dans les différentes régions examinées, aussi, j'ai préparé les figures et rédigé le matériel et méthode associés à cette expérience. Un second article à propos du rôle des orexines dans les troubles respiratoires liés au stress néonatal est en cours d'écriture. Pour celui-ci, j'ai effectué la mise au point et les expériences de double immunofluorescence pour les orexines et *c-fos* ainsi que la capture d'images et les quantifications. De la même manière, j'ai préparé la figure et le matériel et méthode associés à cette expérience.

1 INTRODUCTION

1.1 Le stress

La survie d'un individu est liée à sa capacité d'adaptation à des conditions de vie en perpétuel changement. Le concept de stress a beaucoup évolué au cours des siècles, et aucune définition consensuelle n'a réussi à émerger. L'association américaine des psychologues (*American Psychological Association*) utilise, de ce fait, la définition proposée par Dr Andrew Baum : le stress correspond à « une expérience émotionnelle accompagnée de changements biochimiques, physiologiques et comportementaux prévisibles » (Baum, 1990). Plus récemment, le stress se définit comme une « réponse multifactorielle de l'organisme en réaction à une contrainte de l'environnement jugée susceptible de perturber l'homéostasie de l'individu » (Day, 2005). Le stress apparait quand l'équilibre des paramètres physiologiques (homéostasie) est menacé ou est perçu comme tel. Différents mécanismes sont ainsi apparus au cours de l'évolution afin de maintenir l'homéostasie en situation de stress, indispensables à la survie de l'individu. Certains types de stress peuvent être bénéfiques produisant l'énergie et la motivation requises pour surmonter la situation. À l'inverse, des situations de stress extrêmes et prolongées peuvent avoir un effet délétère et conduire à des altérations neurologiques, neuroendocriniennes, immunitaires et cardiovasculaires (Anderson, 1998). Il existe une grande variabilité entre les individus en ce qui concerne les réponses physiologiques et comportementales observées face à une situation de stress. Les différents degrés de capacité d'adaptation définissent le concept de résilience ou à l'inverse, le concept de vulnérabilité (Charney, 2004; Russo *et al*, 2012; Wolff, 1995; Yehuda *et al*, 2006). Ces notions seront présentées en détail dans la deuxième partie de l'introduction. Après une brève introduction sur la nécessité d'étudier le stress chronique et un historique à propos du concept de stress, je décrierai comment le stress est perçu par l'organisme, les réponses physiologiques et comportementales générées par une situation de stress ainsi que les principaux circuits neuronaux qui y sont associés et en particulier, le système opioïdergique. La seconde partie de l'introduction présente la version complète d'une revue décrivant le rôle émergent des enképhalines (ENKs) et de leurs récepteurs dans la résilience au stress chronique. Une

brève introduction sur les ENKs et leurs récepteurs est présentée, suivie de leur rôle dans les comportements émotionnels ainsi que dans la capacité d'adaptation face à une situation de stress à long terme. Enfin, j'exposerai la littérature récente sur le stress oxydatif comme potentiel mécanisme sous-jacent les troubles associés au stress chronique, ainsi que les effets connus de la modulation du système opioïdergique sur le stress oxydatif.

1.1.1 Incidence et facteurs de risque

L'organisation mondiale de la santé a décrit les pathologies liées au stress comme l'épidémie du XXIe siècle. Chaque année, 20% des travailleurs canadiens présentent des troubles associés au stress (Statistique Canada (2003) Enquête sur la santé dans les collectivités canadiennes : santé mentale et bien-être). L'une des issues les plus dévastatrices du stress chronique est la dépression majeure : d'ici à 2020, cette pathologie sera classée au deuxième rang des causes d'incapacité au niveau mondial (Cambridge *et al*, 1996). L'exposition répétée et prolongée au stress peut conduire à de nombreux troubles endocriniens, métaboliques, comportementaux, cardiovasculaires et immunitaires. Chez la femme enceinte, le stress chronique peut induire des perturbations dans le développement et la croissance de l'enfant. Le développement et la sévérité de ces troubles dépendent de nombreux facteurs génétiques et épigénétiques, comme l'exposition au stress à des périodes critiques du développement ou encore, la présence de facteurs néfastes ou protecteurs de l'environnement (Chrousos, 2009). Le stress chronique peut précipiter ou induire des pathologies psychiatriques comme l'anxiété et la dépression majeure (Davidson and McEwen, 2012), des troubles cardiaques comme l'hypertension (Spruill, 2010), des troubles métaboliques comme l'obésité (Dallman *et al*, 2003), des troubles du sommeil comme l'hypersomnie ou l'insomnie (Han *et al*, 2012), ainsi que des troubles obsessifs comme l'alcoolisme (Becker, 2017) ou l'abus de drogues (Sinha, 2008). Les pathologies comportementales dues au stress chronique résultent de l'activation continue ou intermittente du système du stress (voir la section 1.1.5.) provoquant la sécrétion prolongée des médiateurs responsables de l'anxiété et de la dépression (Gold *et al*, 2005; Wong *et al*, 2000), des troubles alimentaires et du sommeil (Vgontzas *et al*, 2001). Ainsi, la recherche s'intéresse au stress depuis des décennies et semble être le sujet d'actualité phare de notre

siècle. En effet, le stress est, de plus en plus, présent dans notre société actuelle que ce soit au travail - où « productivité » est le nouveau mot d'ordre - ou en privé : des relations néfastes, des problèmes de santé, une insécurité financière ou encore le trafic automobile sont des sources quotidiennes de stress. Cependant, la thématique du stress trouve ses origines bien plus tôt dans le temps, au XIXe siècle.

1.1.2 L'histoire du stress

Le concept de stress a été introduit en biologie au XIXe siècle par Claude Bernard dans son œuvre *Introduction à la Médecine Expérimentale* (Bernard, 1865). Il y démontre la capacité de l'organisme à maintenir la stabilité de l'environnement interne, le « milieu intérieur », face aux perturbations de l'environnement externe, définissant ainsi la notion d'homéostasie, sans la nommer. C'est Walter Cannon qui invente le terme d'homéostasie. Il introduit le célèbre concept de « fight or flight », définissant ainsi les deux issues possibles face à une situation de stress à savoir « combattre ou fuir ». Il met en évidence les différentes réactions physiologiques induites par certaines émotions comme la peur ou la colère, et démontre la stimulation de la glande surrénale engendrée par la réaction de peur. Il décrit alors la réponse au stress comme un système où les réponses physiologiques et émotionnelles sont intimement liées et se produisent en simultané. Il découvre aussi une molécule responsable de l'activité du système nerveux autonome (SNA) sympathique (SNS) qu'il nommera sympathine, laquelle s'avèrera être la noradénaline (Cannon, 1929, 1939). À partir de 1936, Hans Selye, considéré comme le pionnier en matière de recherche sur le stress, redéfinit le terme de stress comme étant une « réponse non spécifique de l'organisme en réaction à toute demande d'adaptation qui lui est faite », définition encore utilisée de nos jours (Selye, 1956). Il décrit alors les nombreuses réactions physiologiques induites par le stress mettant en évidence l'activation de l'axe corticotrope et la sécrétion du cortisol, ainsi que l'activation du SNS et la sécrétion d'adrénaline. Enfin, Selye reprend le concept de « fight or flight » de Cannon en utilisant le terme de « syndrome général d'adaptation » qui décrit la réaction générale d'alarme correspondant à un effort de l'organisme pour s'adapter à de nouvelles conditions. Il s'agit donc de la réponse de l'organisme aux agressions auxquelles il est exposé. Il décrit alors à son tour, trois phases

de la réponse au stress : la phase d'alarme, la phase d'adaptation et celle d'épuisement (Selye, 1937, 1950; Selye and Fortier, 1950). Ainsi, les travaux de Walter Cannon et Hans Selye ont permis de mettre en évidence les réponses physiologiques engendrées par le stress à savoir le rôle crucial du SNS et de l'axe hypothalamo-hypophyso-surrénalien (« hypothalamo-pituitary-adrenergic axis », ou axe HPA) dans la réponse adaptative au stress (Goldstein and Kopin, 2007).

Les réponses physiologiques seront détaillées dans la section 1.1.5. Avant de les déclencher, l'organisme doit avant tout percevoir le stress, l'interpréter et intégrer l'information pour pouvoir répondre de façon efficace à la situation.

1.1.3 La perception de l'organisme face à l'évènement stressant

La Figure 1 propose un système modélisant les étapes suivies suite à un évènement stressant :

(1) Évènement stressant réel ou fictif ;
(2) Interprétation cognitive ;
(3) Intégration affective de l'information ;
(4) Déclenchement des mécanismes neurologiques ;
(5) Réponse physiologique du SNA et de l'axe HPA ;
(6) Activation des organes cibles ;
(7) Réponse comportementale.

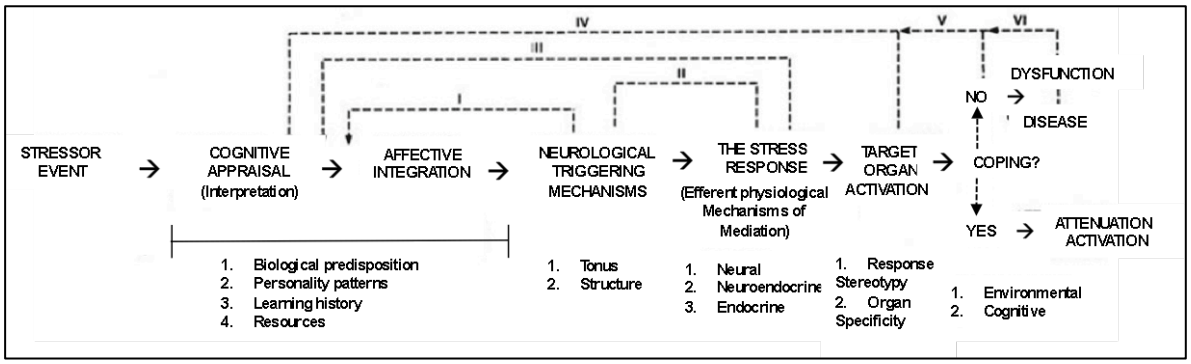

Figure 1 : Système modélisant la réponse au stress chez l'humain. Le cerveau interprète (2) et intègre l'information (3) du stress réel ou imaginé (1), des mécanismes neurologiques sont ensuite déclenchés (4). La réponse physiologique du SNA et de l'axe HPA a lieu (5) permettant d'activer les organes cibles (6) et enfin, la réponse comportementale permettant ou non de surmonter et maitriser la situation. Adaptée de (Everly and Lating, 2002).

D'un point de vue de la terminologie, il est important de distinguer le stimulus de la réponse au stress. Le terme « stress », utilisé par Hans Selye, fait référence à la réponse au stress. Le terme de « stresseur » fait ainsi référence au stimulus, que l'on peut diviser en deux catégories. On distingue le stresseur systémique - correspondant à une menace physique réelle – du stresseur psychogénique, qui dépend de la perception et de l'interprétation du stimulus stressant (Herman and Cullinan, 1997). La réponse liée à un stresseur systémique (*e.g.* perte de sang, infection, douleur) nécessite une réponse immédiate déclenchée par des mécanismes réflexes. Un stresseur systémique génère une réponse résultant d'une véritable perturbation de l'homéostasie physiologique et l'organisme n'a pas besoin de perception consciente pour que la réaction ait lieu. À l'inverse, le stresseur psychogénique menace l'homéostasie et perturbe l'état émotionnel de l'individu, nécessitant sa pleine conscience et faisant appel à la mémoire d'évènements antérieurs et donc, à l'intervention de structures cérébrales cognitives supérieures comme le cortex sensoriel et le système limbique (McDougall *et al*, 2005). La plupart des stresseurs sont psychogéniques. L'évaluation cognitive fait référence au processus d'interprétation cognitive : il s'agit de la signification que nous assignons à l'évènement tel qu'il se déroule devant nous. L'intégration affective correspond à l'émotion ressentie lors de l'interprétation cognitive. Ces deux étapes dépendent principalement des prédispositions biologiques, de la personnalité, de l'historique et de la capacité d'apprentissage de l'individu, ainsi que des

ressources d'adaptation disponibles (Figure 1). C'est la façon dont l'organisme perçoit le stimulus stressant qui va déterminer sa catégorie (systémique ou psychogénique) et ainsi les circuits neuronaux empruntés (Everly *et al*, 2002).

1.1.4 Les circuits neuronaux impliqués dans la réponse au stress

L'exposition à un stress active le tronc cérébral et les structures du système limbique qui à leur tour, contrôlent l'activation du SNS et de l'axe HPA. L'information de la réponse au stress est intégrée à différents niveaux, dont le nœud central est le noyau paraventriculaire de l'hypothalamus (PVN). Un stresseur systémique va induire une activation directe du PVN par l'intermédiaire d'afférences sensorielles provenant du tronc cérébral (neurones noradrénergiques du noyau du tractus solitaire ou NTS et organes circumventriculaires). Le PVN est aussi la cible de nombreux axones qui libèrent différents neuropeptides comme l'angiotensine II ou le neuropeptide Y qui vont moduler l'activité des neurones libérant l'hormone corticolibérine (« corticotropin-releasing-hormone » ou CRH). Les neurones CRH du PVN sont aussi la cible d'afférences glutamatergiques provenant de l'hypothalamus et du NTS ainsi que d'afférences sérotoninergiques du noyau du raphé (pour revue, (Ulrich-Lai and Herman, 2009)). À l'inverse, un stresseur psychogénique requiert l'intervention du système limbique. Aucun consensus universel n'a été trouvé quant à la définition des structures qui composent ce système, de par son hétérogénéité fonctionnelle. On y classe généralement le cortex limbique (gyrus cingulaire, cingulum, insula et gyrus parahippocampique), l'hippocampe, l'amygdale, le septum et l'hypothalamus (Rajmohan and Mohandas, 2007). Les régions limbiques n'ont pas de connections directes avec l'axe HPA ou le SNA mais sont capables de moduler les deux systèmes de façon indirecte. La réponse au stress via le système limbique nécessite l'intervention de noyaux intermédiaires comme le noyau de la strie terminale (BST) ou le noyau dorsomédian de l'hypothalamus (DMH) (Herman *et al*, 2016a). L'hippocampe et le cortex limbique sont connus pour apporter une régulation inhibitrice de l'axe HPA tandis que l'amygdale exerce une régulation activatrice de l'axe HPA (Figure 2).

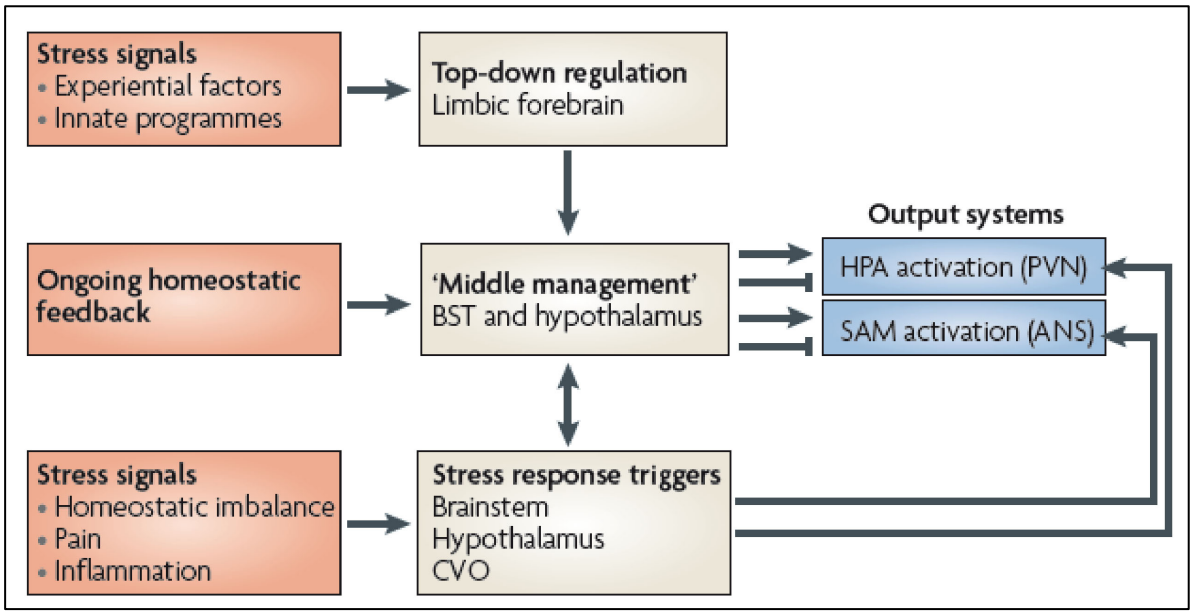

Figure 2 : Schéma général des voies régulées par un stress. Les stresseurs activent le tronc cérébral et/ou les structures limbiques. Le tronc cérébral est capable de générer des réponses rapides de l'axe HPA et du SNA via des projections directes aux neurones du PVN ou aux neurones pré-ganglionnaires (régulation ascendante, « stress response triggers»). En revanche, les régions limbiques n'ont aucune connexion directe avec l'axe HPA ou au SNA et nécessitent des synapses intermédiaires avant d'accéder aux neurones autonomes ou neuroendocriniens (régulation descendante, « top-down regulation »). Une forte proportion de ces neurones est située dans des noyaux hypothalamiques qui répondent également au statut homéostatique, fournissant un mécanisme par lequel les informations limbiques descendantes peuvent être modulées en fonction de l'état physiologique de l'animal (gestion intermédiaire, « middle management »). BST : noyau de la strie terminale; CVO : organe circumventriculaire; SAM : système sympatho-adreno-médullaire. Adaptée de (Ulrich-Lai *et al*, 2009).

La Figure 3 présente les afférences limbiques du PVN. La modulation limbique de la réponse au stress se produit principalement à partir des afférences au niveau du PVN et d'autres régions autonomes du cerveau. Les projections GABAergiques de l'amygdale centrale (CEA) régulent les réponses aux facteurs de stress systémique, tandis que celles de l'amygdale médiale (MEA) modulent préférentiellement les réponses aux facteurs de stress psychogénique. Grâce à des projections glutamatergiques à l'intérieur et à l'extérieur de l'amygdale, l'amygdale basolatérale (BLA) joue un rôle à la fois dans la réponse aigue au stress psychogénique et dans la régulation du stress chronique. Le subiculum ventral (vSUB) coordonne la sortie de l'hippocampe en fournissant une entrée glutamatergique au

niveau des relais inhibiteurs du PVN, limitant les réponses au stress psychogénique. Enfin, le cortex prélimbique (PL) inhibe les réponses au stress psychogénique, et cette inhibition est médiée principalement par des projections glutamatergiques au niveau des relais inhibiteurs du PVN. En revanche, le cortex infralimbique (IL) active les réactions autonomes et l'axe HPA, via des projections directes (NTS) ou indirectes (CEA).

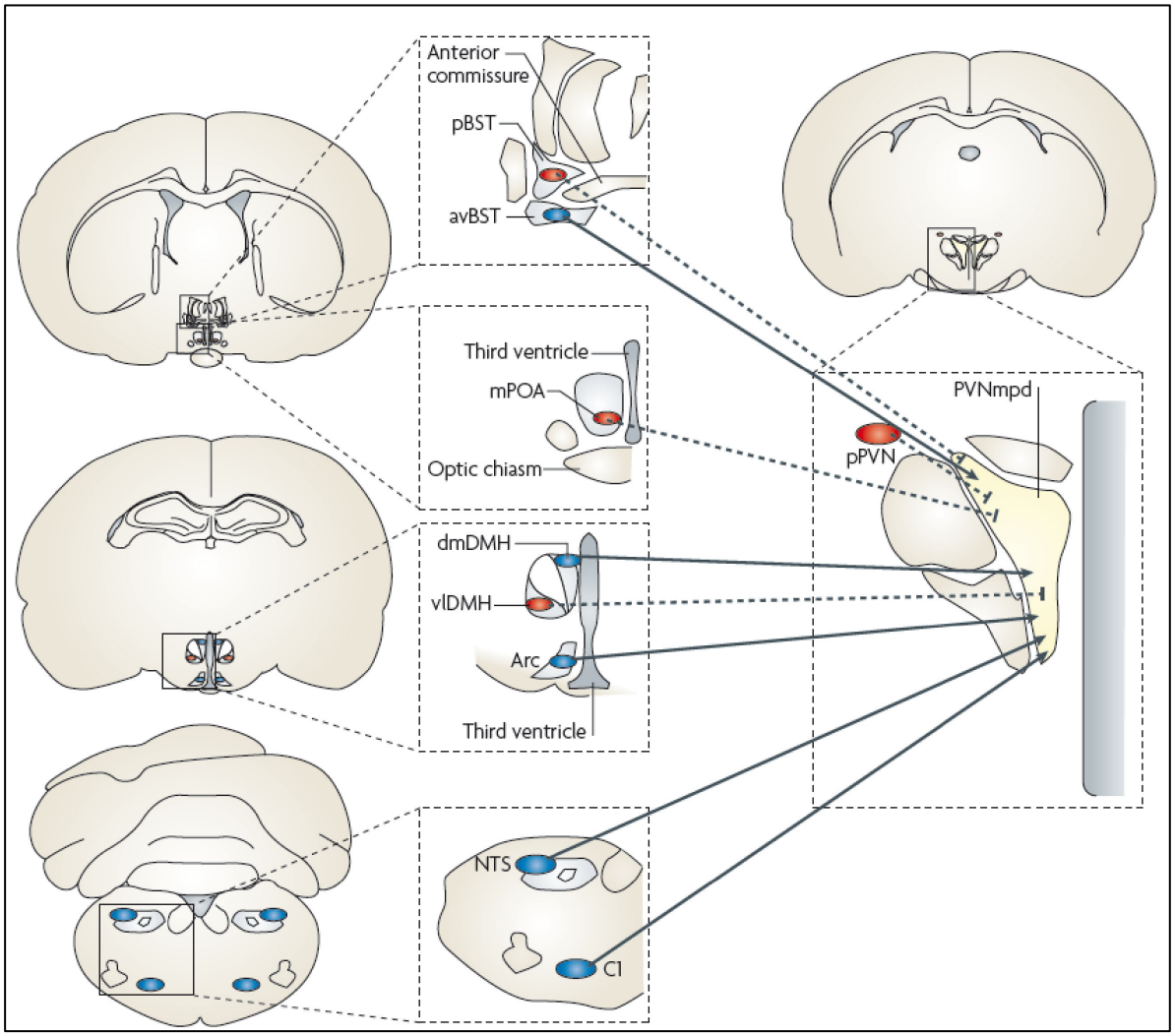

Figure 3 : Organisation des afférences limbiques. La modulation limbique de la réponse au stress se produit principalement à partir des afférences au niveau du PVN (PVNmpd; « the medial parvocellular paraventricular nucleus of the hypothalamus) et d'autres régions autonomes du cerveau. Les entrées excitatrices sont de couleur bleue avec des lignes solides et les régions avec entrées inhibitrices (GABA) sont représentées en rouge avec des lignes bleues pointillées. Panneau supérieur : le subiculum ventral (vSUB) coordonne la sortie de l'hippocampe en fournissant une entrée glutamatergique au niveau des relais inhibiteurs du PVN, limitant ainsi les réponses au stress psychogénique. Panneau central : les projections GABAergiques de l'amygdale centrale (CeA) régulent les réponses aux

facteurs de stress systémique, tandis que celles de l'amygdale médiale (MeA) modulent préférentiellement les réponses aux facteurs de stress psychogénique. Grâce à des projections glutamatergiques à l'intérieur et à l'extérieur de l'amygdale, l'amygdale basolatérale (BLA) joue un rôle à la fois dans la réponse aigue au stress psychogénique et dans la régulation du stress chronique. Panneau inférieur : le cortex prélimbique (PL) inhibe les réponses au stress psychogénique, et cette inhibition est médiée principalement par des projections glutamatergiques au niveau des relais inhibiteurs du PVN. En revanche, le cortex infralimbique (IL) active les réactions autonomes et l'axe HPA, via des projections directes (noyau de solitaire, NTS) ou indirectes (CeA). Adaptée de (Ulrich-Lai *et al*, 2009).

1.1.5 Les réponses physiologiques engendrées par le stress

1.1.5.1 Le système nerveux autonome

En condition de stress, les réponses physiologiques induites sont caractérisées par l'activation du SNS et de l'axe HPA agissant de manière coordonnée pour maintenir l'état d'alerte et favoriser le retour à l'homéostasie. Le SNA correspond à la partie du système nerveux responsable des fonctions non soumises au contrôle volontaire : il contrôle le muscle cardiaque, le muscle lisse (*e.g.* digestion), certaines glandes exocrines (*e.g.* sudation) et endocrines. Le SNA est constitué du SNS et du système nerveux parasympathique (SNP). Ces deux systèmes agissent, de façon antagoniste, directement sur les organes cibles via les ganglions vertébraux. La Figure 4 détaille les efférences respectives du SNP et du SNA.

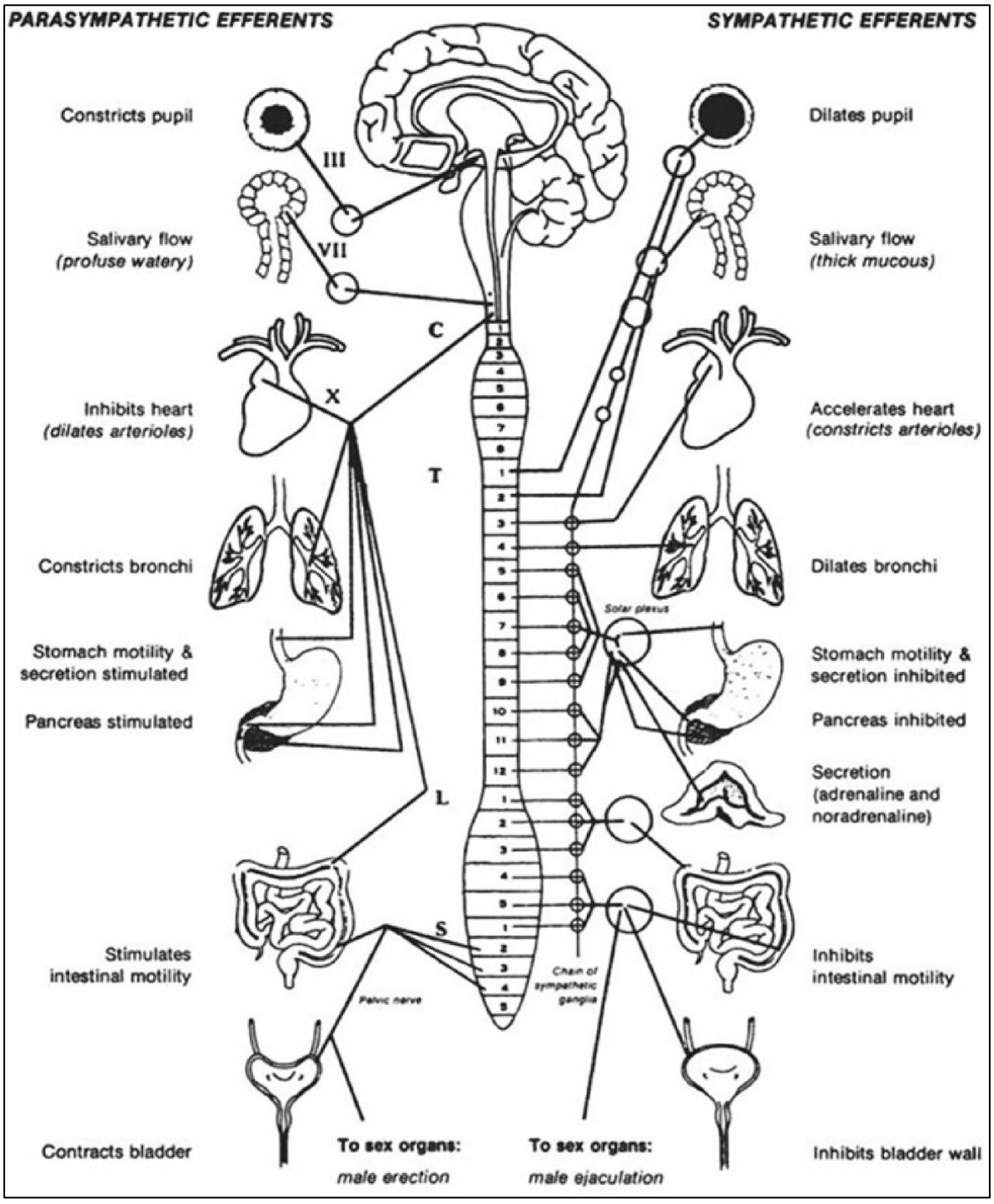

Figure 4 : Les voies efférentes du SNA présentant respectivement l'activité du SNP (à gauche) et du SNS (à droite) sur leurs organes cibles (yeux, cœur, estomac, intestin, vessie). Adaptée de (Everly *et al*, 2002).

Alors que le SNA prépare l'organisme à une action future, le SNP permet la restauration des fonctions « normales » de l'organisme en rétablissant l'homéostasie. La réponse au stress du SNS correspond à la phase d'alarme, décrite précédemment par Hans Selye.

Ainsi, l'activation du SNA est la réponse la plus immédiate à l'exposition au stress via l'action du SNS. L'exposition au stress provoque l'activation des neurones préganglionnaires sympathiques de la moelle épinière qui projettent aux ganglions vertébraux innervant les organes cibles et en particulier, la médullo-surrénale. L'activation du système induit une augmentation du niveau sanguin des catécholamines, adrénaline et noradrénaline (De Boer *et al*, 1990), une augmentation du rythme cardiaque et de la pression sanguine (Lucini *et al*, 2002; McDougall *et al*, 2000), une vasoconstriction périphérique (Cannon, 1929) et la redirection du flux sanguin de régions comme le système gastro-intestinal au profit du muscle squelettique et du SNC (Alper and Zink, 1994; Zhang *et al*, 1996) permettant ainsi la mobilisation de l'énergie nécessaire pour une réponse adaptée au stress (Cannon, 1929). L'intervention du SNP aide à contrôler la durée de la réponse autonomique sympathique (Porges, 1995; Thompson *et al*, 2003).

La réponse du SNA induite par le stress n'étant pas le sujet principal de cette thèse, elle ne sera pas évoquée plus en détail ici, néanmoins de nombreuses revues existent (McDougall *et al*, 2005; Ulrich-Lai *et al*, 2009).

1.1.5.2 L'axe hypothalamo-hypophyso-surrénalien

L'activation du système HPA est la seconde réponse centrale la plus immédiate. L'axe HPA est constitué du PVN, de l'adénohypophyse et de la glande corticosurrénale. La réponse au stress est caractérisée par l'activation successive de ces noyaux. Ainsi, l'exposition au stress active les neurones noradrénergiques du tronc cérébral (au niveau du NTS) qui innervent préférentiellement les neurones parvocellulaires du PVN producteurs de CRH (Antoni, 1986; Cunningham and Sawchenko, 1988). Ces neurones projettent via l'éminence médiane vers l'adénohypophyse qui libère ainsi l'hormone adénocorticotrope (« adenocorticotropic hormone » ou ACTH) (Whitnall, 1993). Enfin, l'ACTH stimule la production et la sécrétion des glucocorticoïdes par la glande corticosurrénale, qui sont alors libérés dans la circulation sanguine (Figure 5). Les glucocorticoïdes circulants favorisent la

mobilisation des réserves énergétiques issues du foie, des graisses et des muscles et potentialisent les effets induits par le SNS, afin de fournir à l'organisme les ressources nécessaires pour répondre adéquatement à la situation. Un rétrocontrôle négatif des glucocorticoïdes sur l'hypothalamus permet de diminuer la libération de CRH et de favoriser un retour rapide à l'homéostasie. Il permet aussi de limiter l'exposition prolongée aux glucocorticoïdes eux-mêmes, susceptible d'entraîner des pathologies importantes. De la même manière, ce sujet est détaillé dans une vaste littérature (Herman *et al*, 2016a; Myers *et al*, 2012).

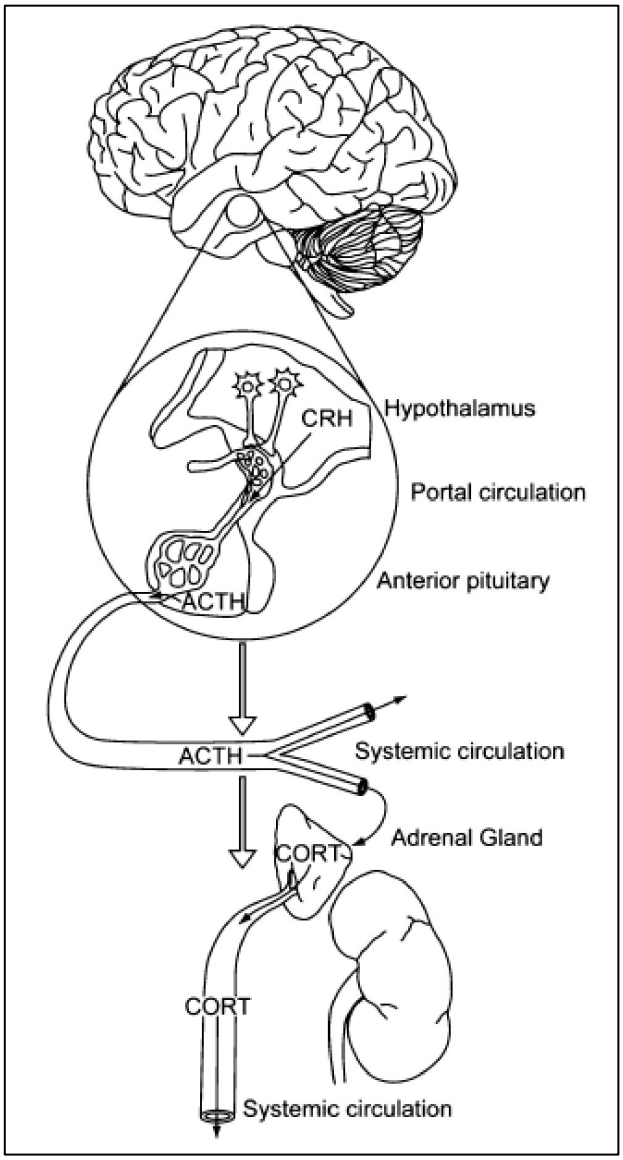

Figure 5 : Organisation de l'axe hypothalamo-hypophyso-adrénal (axe HPA). La réponse au stress de l'axe HPA est initiée par les neurones exprimant l'hormone corticotropine (CRH) dans le noyau paraventriculaire de l'hypothalamus (PVN). Un stress provoque la libération de CRH dans la veine porte hypophysaire transportant le peptide jusqu'à la glande antérieure pituitaire. Ceci induit la production puis la libération de l'hormone adrénocorticotrope dans la circulation systémique où elle va favoriser la synthèse et la sécrétion des glucocorticoïdes au niveau du cortex adrénal. Les glucocorticoïdes sont ensuite libérés dans la circulation systémique et pourront exercer leurs effets physiologiques via leurs récepteurs disponibles au niveau des nombreux organes cibles dont le cerveau. Adaptée de (Myers *et al*, 2012).

Le stress génère différentes réactions de l'organisme permettant au niveau physiologique de réagir efficacement face au stress et de rétablir l'homéostasie du système. La réponse comportementale est une composante essentielle permettant de maîtriser ou de tolérer la situation de stress.

1.1.6 Les réponses émotionnelles et comportementales liées au stress

En terme de comportement, l'exposition au stress se traduit par deux types d'émotions distinctes : la peur et l'anxiété. Elles sont associées à un phénomène émotionnel constituant un mécanisme de défense de l'organisme face à une menace quelconque. Autrement dit, il s'agit d'un processus d'ajustement cognitif destiné à maîtriser ou à tolérer la situation de stress. Ces réponses émotionnelles sont limitées dans le temps, elles dépendent du contexte et de la personnalité de l'individu. La peur est un comportement adaptatif caractérisé par la nécessité de se défendre et se traduisant dans un premier temps par une fuite ou un évitement. En effet, la peur est une émotion fondamentalement ancrée dans l'évolution, elle est indispensable à la survie de l'espèce. Même les organismes les plus primitifs ont développé ce mécanisme de défense contre les menaces extérieures. Le terme d'anxiété est utilisé pour décrire la sensation dysphorique associée à l'anticipation et l'appréhension d'un danger ou d'un problème futur plus ou moins réel (*American Psychological Association*). Ainsi, la peur se différencie de l'anxiété de par l'identification explicite du danger. Lorsque la stratégie d'adaptation créée par la peur ne permet pas de maitriser ou de tolérer le stress alors la peur se transforme en anxiété. L'anxiété peut se concrétiser par l'apparition d'attaque panique épisodique et lorsqu'elle est généralisée en pathologie du trouble panique (Öhman, 2000).

Ainsi, la réponse au stress implique de nombreux systèmes (axe HPA, SNA) et fait intervenir plusieurs structures cérébrales (tronc cérébral, système limbique). Les différents circuits empruntés pour une réponse au stress dépendent essentiellement de facteurs environnementaux comme le type de stresseur, sa durée, le besoin d'immédiateté de la réponse ou à l'inverse, le besoin de faire intervenir des structures cérébrales cognitives supérieures. La complexité de la réponse au stress nous suggère qu'il existe un grand éventail de systèmes de neurotransmetteurs et de neuromodulateurs impliqués.

L'implication d'un certain nombre d'entre eux a déjà été démontrée (*e.g.* systèmes GABAergique, glutamatergique, dopaminergique, sérotoninergique, cholinergique, neuropeptide Y, arginine-vasopressine, substance P, etc. (Kormos and Gaszner, 2013; Mora *et al*, 2012)). Le système opioïdergique fait partie des neuromodulateurs décrits de longue date dans la littérature du stress. Son rôle émergent dans la résilience au stress chronique sera évoqué dans la revue (section 1.2).

1.1.7 Le système opioïdergique

Le système opioïdergique se compose de différents neuropeptides dérivés de trois gènes : la prodynorphine (à l'origine des dynorphines et des néo-endorphines), la proenképhaline (à l'origine des enképhalines, ENKs) et la proopiomélanocortine (à l'origine des β-endorphines) (Akil *et al*, 1984). Le tableau 1 présente les peptides fonctionnels dérivés de ces trois gènes ainsi que leurs séquences d'acide aminé.

Gènes	Peptides	Séquences
Prodynorphine	Dynorphine A	Tyr-Gly-Gly-Phe-Leu-Arg-Arg-Ile-Arg-Pro-Lys-Leu-Lys-trp-Asp-Asn-Gln
	Dynorphine A (1-8)	Tyr-Gly-Gly-Phe-Leu-Arg-Arg-Ile
	Dynorphine B	Tyr-Gly-Gly-Phe-Leu-Arg-Arg-Gln-Phe-Lys-Val-Val-Trp
	α-Néoendorphine	Tyr-Gly-Gly-Phe-Leu-Arg-Lys-Tyr-Pro-Lys
	β-Néoendorphine	Tyr-Gly-Gly-Phe-Leu-Arg-Lys-Tyr-Pro
Proenképhaline	Leu-Enképhaline	Tyr-Gly-Gly-Phe-Leu
	Met-Enképhaline	Tyr-Gly-Gly-Phe-Met
	Octapeptide	Tyr-Gly-Gly-Phe-Met-Arg-Gly-Leu
	Heptapeptide	Tyr-Gly-Gly-Phe-Met-Arg-Phe
Proopioimélanocortine	β-Endorphine	Tyr-Gly-Gly-Phe-Met-Thr-Ser-Glu-Lys-Ser-Gln-Thr-Pro-Leu-Val-Thr-Leu-Phe-Lys-Asn-Ala-Ile-Ile-Lys-Asn-Ala-Tyr-Lys-Lys-Gly-Glu

Tableau 1 : Les opioïdes endogènes (gènes, peptides et séquences d'acide aminé).

Ces trois neuropeptides se fixent aux trois types de récepteurs avec différentes affinités : les récepteurs opioïdergiques μ (MOPr), δ (DOPr) et κ (KOPr).

1.1.7.1 Structure, voies de signalisation et régulation des récepteurs opioïdergiques

MOPr, DOPr et KOPr sont des récepteurs à sept domaines transmembranaires couplés à une protéine G inhibitrice (RCPG) (Chen *et al*, 1993; Evans *et al*, 1992; Kieffer *et al*, 1992; Yasuda *et al*, 1993). Ils sont aussi constitués de trois domaines extracellulaires et de trois domaines intracellulaires (Figure 6).

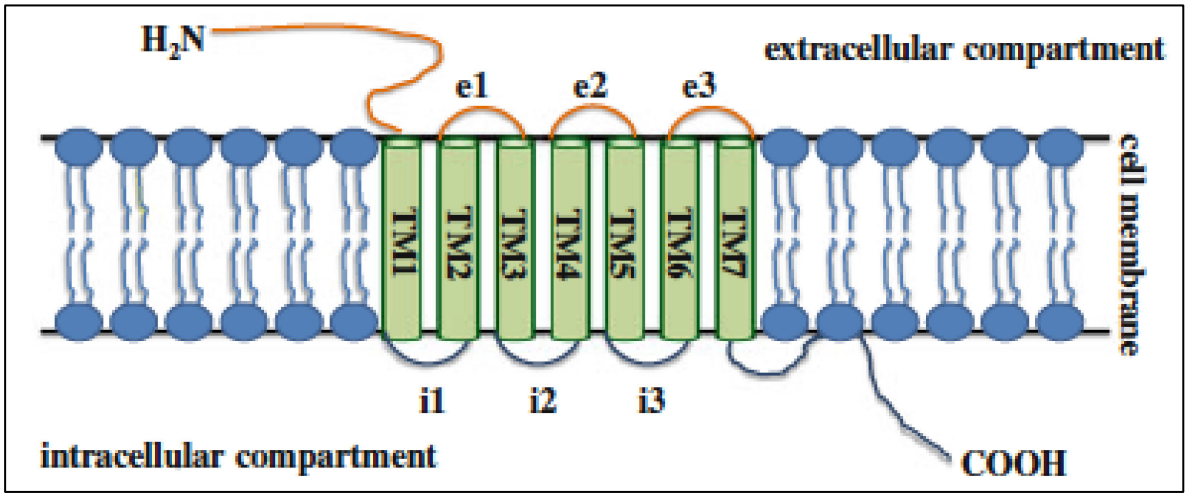

Figure 6 : Structure générale d'un récepteur couplé à une protéine G (RCPG). Les récepteurs opioïdergiques sont des protéines intégrées dans la membrane couplés à une protéine G hétérotrimérique. La structure consiste en sept domaines transmembranaires (TM 1 à 7), trois domaines intracellulaires hydrophobes (i1 à i3) et trois boucles extracellulaires (e1 à e3) ainsi qu'une queue N–terminale extracellulaire (NH_2) et une C-terminale intracellulaire (COOH). Adaptée de (Sobczak *et al*, 2014)

Les récepteurs opioïdergiques sont encodés par trois gènes OPRM1, OPRD1 et OPRK1, respectivement. Les séquences codant les sept domaines transmembranaires sont largement conservées entre les récepteurs mais celles codant les queues N-terminale et C-terminale sont très variables expliquant les différences d'affinité des ligands et les voies de signalisation induites. Suite à l'activation du récepteur par un agoniste, la conformation du récepteur change, activant ainsi la protéine G. Les sous-unités α et β/δ de la protéine G se

dissocient l'une de l'autre et vont activer différentes voies de signalisation intracellulaires. La sous-unité Gα va notamment inhiber la voie de l'adénosine monophosphate cyclique (Taussig *et al*, 1993) conduisant à l'inhibition de la protéine kinase A. Gα active également les canaux potassiques liés à la protéine G (GIRK) via une interaction directe, participant alors à l'hyperpolarisation du compartiment post-synaptique (Luscher and Slesinger, 2010). La sous-unité Gβ/δ est capable d'inhiber les canaux calciques voltage dépendants (de type, N et L) au niveau du compartiment pré-synaptique, conduisant à l'inhibition de la libération de neurotransmetteurs et de neuromédiateurs (Rhim and Miller, 1994; Rusin *et al*, 1997). Enfin, comme de nombreux RCPG, les récepteurs opioïdergiques peuvent également activer les voies des MAP kinases (« mitogen-activated-protein »). La signalisation intracellulaire induite par les RCPG dépend du nombre de récepteurs fonctionnels présents à la membrane cytoplasmique. Ils sont essentiellement régulés par la phosphorylation et l'internalisation. En effet, ils sont phosphorylés par les kinases associées aux RCPG, suite au relargage des sous-unités α et β/δ. Cette phosphorylation rend possible la liaison avec la β-arrestine, une protéine impliquée dans l'identification des récepteurs en vue de leur internalisation. L'internalisation des récepteurs induit la désensibilisation du récepteur : elle provoque la diminution du nombre de récepteurs à la membrane et donc diminue la réponse cellulaire en présence de ligands (Al-Hasani and Bruchas, 2011). Après l'internalisation des récepteurs dans les endosomes, ils peuvent être dirigés vers les lysosomes pour être dégradés ou être recyclés à la membrane (Whistler *et al*, 2002). Le nombre de récepteurs présents à la synapse est également régulé au niveau de l'expression. Les gènes sont autant régulés au niveau transcriptionnel qu'épigénétique (méthylation de l'ADN, méthylation, acétylation et phosphorylation, entre autres, des histones). De nombreux facteurs de transcription tels que CREB (« C-AMP Response Element-binding protein »), NFκB (« nuclear factor-kappa B »), AP2 (« activating protein 2 ») sont impliqués (Wei and Loh, 2011). Enfin, les gènes codant les récepteurs opioïdergiques subissent un épissage alternatif important (Pan, 2005; Wei et al, 2004). La Figure 7 résume brièvement les voies de signalisation induites par l'activation d'un récepteur opioïdergique ainsi que les mécanismes de régulation (phosphorylation, internalisation, dégradation ou recyclage).

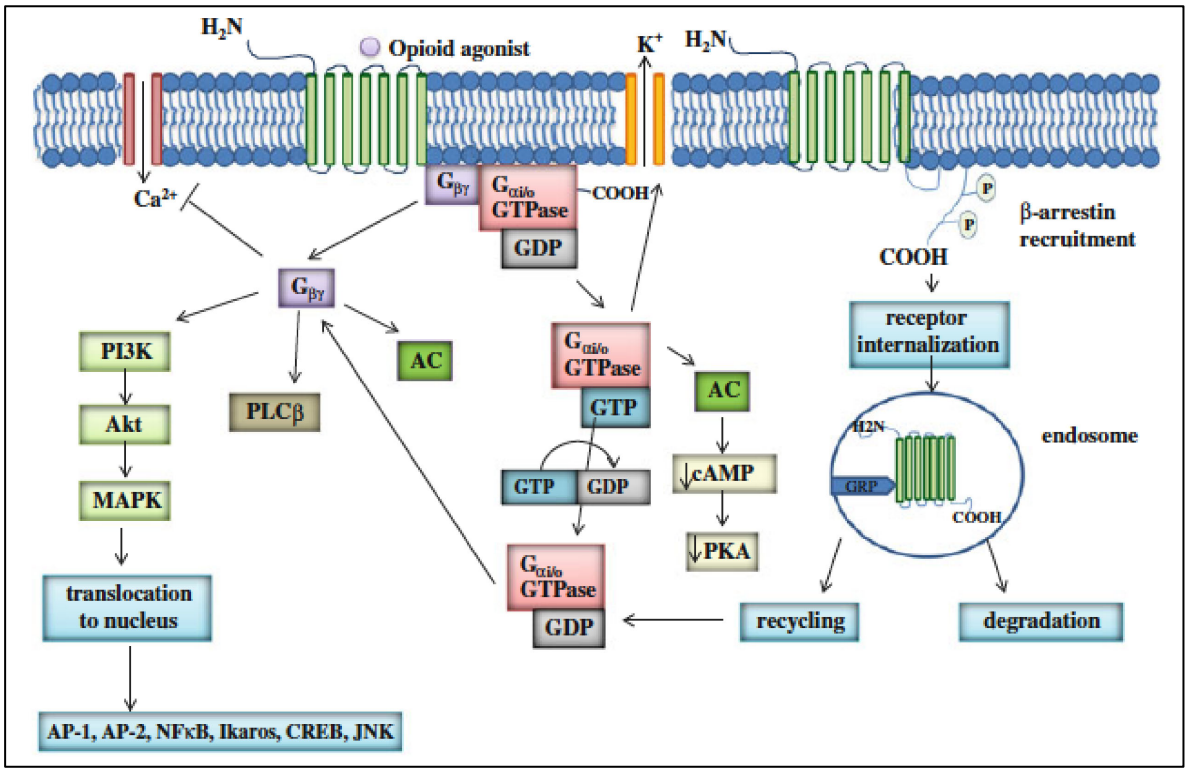

Figure 7: Voies de signalisation intracellulaires associées aux récepteurs opioïdergiques. Les récepteurs sont couplés à une protéine G. Les seconds messagers impliqués sont l'adénylate cyclase (AC), GPCR kinase 2/3 (GRK), la phospholipase C β (PLCβ), ainsi que la phospatidyl-inositol-3-kinase (PI3K). La libération de la sous-unité Gβγ inhibe aussi les canaux Ca^{2+} voltage-dépendant et active les canaux potassiques (K^{+}). Adaptée de (Sobczak *et al*, 2014).

1.1.7.2 Distribution des récepteurs opioïdergiques MOPR et DOPr dans le système nerveux central

Les ENKs ont une affinité plus élevée pour DOPr, même s'ils peuvent également se lier et activer MOPr et KOPr dans des cellules transfectées exprimant transitoirement MOPr ou KOPr (Mansour *et al*, 1995). Le rôle physiologique des ENKs est déterminé par leur capacité de liaison aux récepteurs et par la distribution anatomique de ces derniers. Des études décrivant la distribution des ENKs *in vivo*, dans le cerveau de rat, ont similairement montré une liaison préférentielle à DOPr et MOPr (Mansour *et al*, 1986). Ainsi, nous nous intéresserons ici uniquement à la distribution de MOPr et DOPr présentée dans les Figures

8 et 9, respectivement. Erbs et collègues ont développé un modèle de souris transgénique exprimant à la fois MOPr et DOPr associés à un fluorochrome, *mcherry* et *eGFP*, respectivement (Erbs *et al*, 2015). L'expression de MOPr est observée dans le bulbe olfactif, dans les couches corticales II et VI, dans le striatum, dans plusieurs noyaux thalamiques, dans le complexe amygdalien, et également, dans plusieurs structures du mésencéphale et du rhombencéphale (Figure 8).

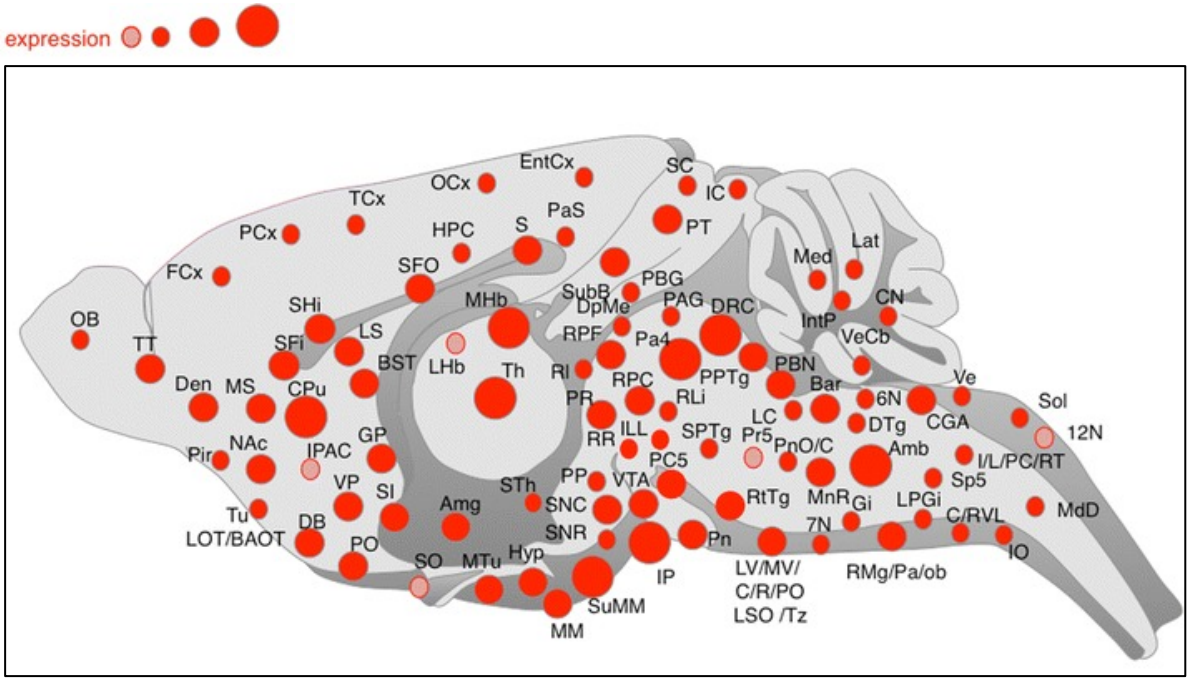

Figure 8 : Distribution neuroanatomique du récepteur opioïdergique μ (MOPr) chez la souris grâce à une construction MOPr-mCherry. La taille des cercles rouges est indicative de l'abondance de MOPr dans les différentes régions observées. Les cercles roses indiquent une faible expression. MOPr est exprimé à tous les niveaux du SNC. Adaptée de (Erbs *et al*, 2015).

La distribution des DOPr est présentée dans la Figure 9. DOPr est principalement observé au niveau du bulbe olfactif, du bulbe olfactif auxiliaire, des couches corticales II-III et V-VI, du striatum, du complexe amygdalien, de l'hypothalamus, dans l'hippocampe, ainsi que dans quelques noyaux du tronc cérébral. Il existe des différences importantes entre les distributions de DOPr et de MOPr dans plusieurs régions du SNC (*e.g.* thalamus et

complexe amygdalien) ce qui, entre autres, explique les différents effets pharmacologiques des agonistes de MOPr et de DOPr.

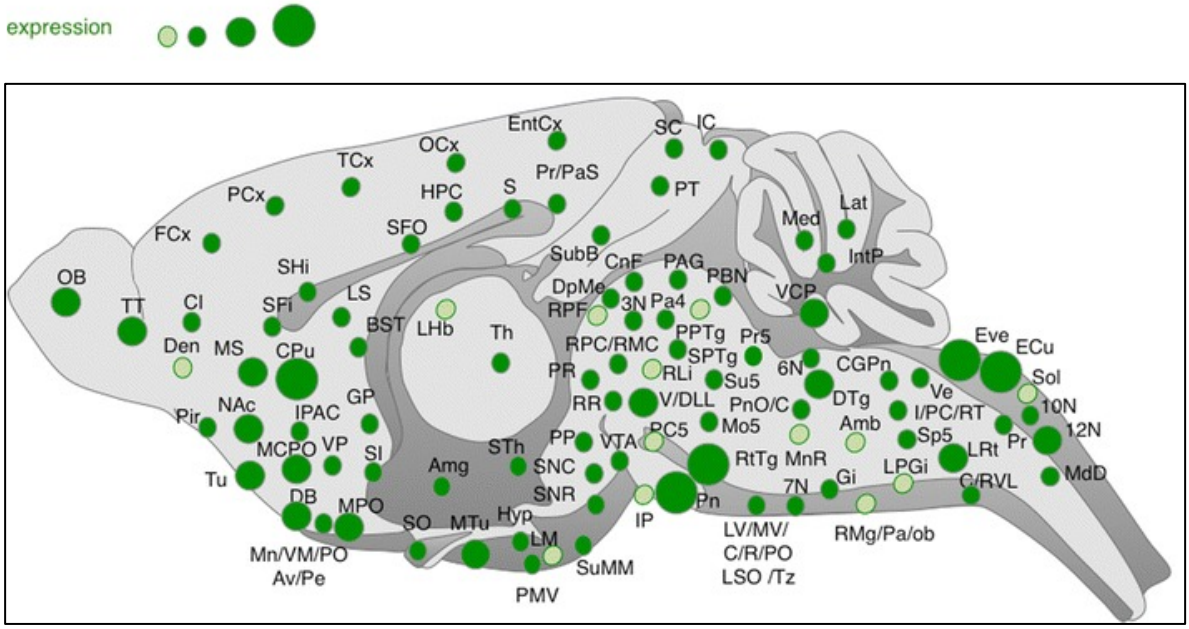

Figure 9 : Distribution neuroanatomique du récepteur opioïdergique δ (DOPr) chez la souris grâce à une construction DOPr-eGFP. La taille des cercles verts est indicative de l'abondance de DOPr dans les différentes régions observées. Les cercles vert pâle indiquent une faible expression. Adaptée de (Erbs *et al*, 2015).

Le système opioïdergique est universellement connu pour son rôle dans le contrôle de la douleur, des fonctions physiologiques, comme la fonction cardiaque ou la respiration, mais aussi dans la régulation des émotions. Le chapitre suivant contient une revue écrite en 2017 mettant en exergue le rôle émergent de la signalisation ENK via MOPr et DOPr dans la résilience au stress chronique.

1.2 La signalisation enképhalinergique et le stress : « Enkephalins : endogenous analgesics with an emerging role in stress resilience »

Neural Plast. 2017;2017:1546125. doi: 10.1155/2017/1546125. Epub 2017 Jul 11.

1.2.1 Résumé

Le stress psychologique est un état de tension mentale ou émotionnelle qui résulte de circonstances défavorables ou exigeantes de l'environnement. Le stress chronique est connu pour induire des troubles anxieux et la dépression majeure. Il est également considéré comme un facteur de risque pour la maladie d'Alzheimer. À l'inverse, la résilience au stress chronique est associée à la préservation des capacités cognitives et au vieillissement normal. La résilience présente des caractéristiques psychologiques et biologiques intrinsèques à un individu qui confèrent une protection contre le développement de psychopathologies. Comment pouvons-nous favoriser ou améliorer la capacité de résilience au stress chronique? De nombreuses études ont proposé des mécanismes permettant de favoriser l'apparition du phénomène. Les rôles de la transmission enképhalinergique dans le contrôle de la douleur, des fonctions physiologiques comme la respiration ou encore, des troubles affectifs, sont étudiés depuis plus de 30 ans. En revanche, leur rôle dans la résilience au stress chronique a reçu beaucoup moins d'attention. Cette revue compile la littérature mettant en évidence le rôle émergent de la signalisation des enképhalines via leurs deux récepteurs opioïdergiques associés, μ et δ, dans la capacité naturelle d'adaptation face à un style de vie stressant.

1.2.2 Abstract

Psychological stress is a state of mental or emotional strain or tension that results from adverse or demanding circumstances. Chronic stress is well known to induce anxiety disorders and major depression; it is also considered a risk factor for Alzheimer's disease. Stress resilience is a positive outcome that is associated with preserved cognition and healthy aging. Resilience presents psychological and biological characteristics intrinsic to an individual conferring protection against the development of psychopathologies in the

face of adversity. How can we promote or improve resilience to chronic stress? Numerous studies have proposed mechanisms that could trigger this desirable process. The roles of enkephalin transmission in the control of pain, physiological functions, like respiration, and affective disorders have been studied for more than 30 years. However, their role in the resilience to chronic stress has received much less attention. This review presents the evidence for an emerging involvement of enkephalin signaling through its two associated opioid receptors, μ opioid peptide receptor and δ opioid peptide receptor, in the natural adaptation to stressful lifestyles.

1.2.3 Introduction

Psychological stress is a state of mental or emotional strain or tension that results from adverse or demanding circumstances. It has multifaceted causes and occurs frequently over a lifetime with varying dimensions and intensity, affecting all walks of life, irrespective of a person's occupation or position within a society (Machado *et al*, 2014). While depression is often the devastating outcome of chronic stress (Davidson *et al*, 2012) and also a risk factor and common comorbidity in Alzheimer's disease (Green *et al*, 2003; Modrego, 2010), stress resilience, on the other hand, is a positive outcome that is associated with preserved cognition, reduced oxidative damage, and healthy aging (Charney, 2004; Pfau and Russo, 2015). The American Psychological Association defines resilience as "the process of adapting well in the face of adversity, trauma, tragedy, threats or even significant sources of threat." Heterogeneity in the response to chronic stress suggests that resilience is a complex neurobiological process that emerges from a multitude of gene-environment interactions. Several mechanisms are proposed to underlie the interindividual differences in resilience or vulnerability to chronic stress.

Within the neuropeptidergic system, the endogenous opioids enkephalins (ENK) which signal through the opioid peptide receptors (OPr), μ opioid peptide receptor (MOPr) and δ opioid peptide receptor (DOPr), could be interesting candidates to naturally promote the adaptation to chronic stress. ENK are members of the endorphin family and the first ones to be isolated in the brain (Hughes *et al*, 1975). Considering the binding of morphine and ENK to the same receptors, their role as a natural analgesic was rapidly proposed. Pioneered studies have provided the first experimental evidence supporting a role of ENK in analgesia and stress-induced analgesia (*i.e.* pain suppression after an exposure to stressful stimuli). More specifically, it was shown in the rat that 1) the cerebroventricular injection of ENK produces analgesia (Belluzzi *et al*, 1976; Pert *et al*, 1977); 2) stress increases blood concentrations of ENK (Madden *et al*, 1977); and 3) stress-induced analgesia, such as immobilization stress on a hot plate or cold water stress, could be reversed by an opioid antagonist (Amir and Amit, 1978; Bodnar *et al*, 1978). Subsequently, it was hypothesized that ENK were playing a major role in stress processes independently of their analgesic functions. Madden et al. reported that inescapable stress induced by footshocks (mimicking a posttraumatic stress disorder; PTSD) increases brain levels of

ENK (Madden *et al*, 1977). Another study showed a decrease of ENK immunoreactivity in the rat hypothalamus (HPT) after stress induced by footshocks (Rossier *et al*, 1978). More recently, ENK in the rat amygdala (AMG) were implicated in Pavlovian conditioned fear (Petrovich *et al*, 2000; Poulin *et al*, 2013) as well as in various behavioral and neuroendocrine aspects of the stress response (Berube *et al*, 2013; Berube *et al*, 2014; Hebb *et al*, 2004). The ENK are known to be involved in a large set of physiological and emotional processes, but their role in the individual capacity for stress adaptation has received less interest. In this review, the biochemistry of ENK and their anatomical distribution within the central nervous system (CNS) will be described first, followed by coverage of the well-known functions of ENK in emotional behaviors, including their key involvement in Pavlovian conditioned fear, anxiety, and stress response. Subsequently, the emerging role of ENK in the development of stress resilience will be discussed, with an emphasis on the recruitment of ENK projections coming from the AMG. The AMG is considered a key brain structure mediating the regulation of emotions and affective behavior, and the role of ENK in the stress response is notably suggested by their extended distribution in the AMG.

1.2.4 Enkephalins and their opioid receptors

1.2.4.1 Biochemistry and anatomical distribution of enkephalins and their receptors, DOPr and MOPr, in the CNS

ENK are produced from a propeptide precursor, proenkephalin (proENK), which is translated from preproenkephalin mRNA that is encoded by a gene distinct from the other endogenous opioid peptides (Kakidani *et al*, 1982; Noda *et al*, 1982). The maturation of propeptides into functional peptides is performed during the vesicular transport within large dense-core vesicles (LDCVs) and requires the joint action of several endopeptidases (cathepsin L, aminopeptidase B and E, and prohormone convertase 2) (Hokfelt *et al*, 2000; Seidah and Chretien, 1997; Steiner, 1998). In the rat, the proENK is cleaved proteolitycally to produce four copies of methionine-ENK (Met-ENK), one leucine-ENK (Leu-ENK), and two C-terminal extended Met-ENK. Subsequently, LDCVs are stored near release sites (*i.e.*

presynaptic, extrasynaptic, and dendritic) and released following an increase in intracellular calcium (Suudhof, 2008). Once released by neurons, ENK are degraded in order to control the diffusion and synchrony of the signal. Some studies demonstrated that radioactively labeled ENK are completely degraded in less than a minute upon injection (intracerebroventricular) in the rat brain (Noble and Roques, 2007). ENK degradation is performed by two neuropeptidases called metallopeptidases: aminopeptidase N and neutral endopeptidase (or neprilysin) (Noble *et al*, 2001; Waksman *et al*, 1986). In vitro, ENK have a slightly higher affinity for DOPr, even though they can also bind and activate MOPr and κ opioid peptide receptor (KOPr) in transfected cells transiently expressing MOPr, DOPr, or KOPr (Mansour *et al*, 1995). Studies describing the distribution of ENK in the rat brain have demonstrated their preferential binding to DOPr and MOPr by autoradiographic labelling (Mansour *et al*, 1986).

Given the vast extent of biological processes and physiological systems in which ENK are involved (cardiovascular system, thirst and feeding, pain and analgesia, gastrointestinal functions, respiration, etc. (Bodnar, 2017)), the expression of ENK, DOPr, and MOPr is ubiquitous. Indeed, ENK are distributed among the central, peripheral, and autonomous nervous systems, as well as in endocrine tissues (adrenal medulla, endocrine pancreas) and their target organs (liver, skin, bones, and lungs) (Denning *et al*, 2008; Eiden, 1987). For the purpose of this review, we will focus mainly on the neuroanatomical distribution of ENK and their receptors within the "emotional brain" known as the limbic system that includes the cingulate and entorhinal cortex, hippocampus (HPC), septum, HPT, and the extended AMG (Drolet *et al*, 2001). Most of neuroanatomic studies have been conducted in rats, although several studies have also been conducted in humans, showing a similar distribution across species, especially in the limbic system (Hurd, 1996). Fallon and Leslie extensively reported in 1986 the distribution of ENK neurons as well as ENK fibers in the rat brain using an indirect immunofluorescence technique (Fallon and Leslie, 1986). ENK neurons are found among the entorhinal, piriform, and medial prefrontal cortex (mPFC, infralimbic and prelimbic). Most nuclei of the HPT were shown to contain ENK neurons (paraventricular, posterior, ventromedial, dorsal, dorsomedial, and lateral nuclei). They are widely distributed in the central (CEA), medial (MEA), and basolateral (BLA) AMG and its intercalated (IC) nuclei. ENK neurons are also located in the lateral septum, preoptic

area, bed nuclei of the stria terminalis (BST), nucleus accumbens (NAc), and ventral tegmental area (VTA). In the HPC, ENK are present in mossy fibers and granular cells. ENK fibers mainly project from the dentate gyrus to the CA3 region of Ammon's horn, but also target some neurons of the CA1 and CA2, and dentate gyrus. Additionally, ENK fibers are found in the dorsal and ventral pallidum (Fallon *et al*, 1986; Gall *et al*, 1981).

Similar to ENK, OPr are extensively expressed throughout the CNS (Le Merrer *et al*, 2009). The anatomical distribution of MOPr and DOPr is relatively similar to that of ENK projections (Mansour *et al*, 1988). To study the relative distributions of MOPr and DOPr throughout the CNS, Scherrer and colleagues have generated a very useful mouse model. They first developed DOPr-eGFP *knock in* (KI) mice, presenting a complete functional receptor fused to an enhanced green fluorescent protein (eGFP) (Scherrer *et al*, 2006). These mutant mice were subsequently crossed to another model containing a similar construct, MOPr-mcherry KI mice (Erbs *et al*, 2015). This breeding generated a double KI mouse useful for in situ visualization of DOPr and MOPr simultaneously (Erbs *et al*, 2012; Erbs *et al*, 2015). The study of DOPr and MOPr distribution in the CNS showed that coexpression of DOPr and MOPr is observed in HPT, HPC, the lateral parabrachial nucleus and vestibular nuclei, circuitries which are involved in survival including water and food consumption, sexual behavior, and response to aversive stimuli (Erbs *et al*, 2015). The large distribution of ENK and their associated receptors in the limbic system of rodents and humans further suggests that ENK transmission plays a major role in emotional behaviors.

1.2.4.2 Roles in emotional behavior

ENK are indeed involved in several emotional behaviors, including fear conditioning (Asok *et al*, 2013; Haubensak *et al*, 2010; Petrovich *et al*, 2000; Poulin *et al*, 2013; Ragnauth *et al*, 2001; Szklarczyk *et al*, 2015), anxiety, and stress response (Bilkei-Gorzo *et al*, 2004; Broom *et al*, 2002a; Chu Sin Chung *et al*, 2015; Comings *et al*, 2000; Filliol *et al*, 2000; Granholm *et al*, 2015; Hernandez *et al*, 2015; Kennedy *et al*, 2006; Konig *et al*, 1996; Kung *et al*, 2010; Liberzon *et al*, 2007; Nozaki *et al*, 2014; Perrine *et al*, 2006; Rezayof *et al*, 2009; Saitoh *et al*, 2004; Saitoh *et al*, 2013; Sugiyama *et al*, 2014; Vergura *et al*, 2008; Zhu and Pan, 2004, 2005). This section will describe the experimental evidence for such a

role, mainly derived from studies conducted in rodents, using different approaches, neuroanatomical, silencing, pharmacological, and genetic, as well as stress paradigms varying in chronicity and intensity.

1.2.4.2.1 Fear conditionning

The fear conditioning paradigm allows assessment of learning and memory in association with fear (see Table 2). The first evidence that ENK participate in fear conditioning comes from an in situ hybridization study showing an increase in ENK mRNA levels in the CEA neurons of rats undergoing this paradigm (Petrovich *et al*, 2000). Thereafter, it was shown that ENK *knockout* (KO) mice exhibit an exaggerated immobility compared to wild-type controls during the auditory-conditioned fear acquisition (Ragnauth *et al*, 2001). A population of GABAergic neurons expressing protein kinase C-*δ* (PKC-*δ*) was identified in the lateral part of CEA (CEAl), using a molecular genetic approach in mice. Interestingly, this population appears to overlap with ENK neurons (Haubensak *et al*, 2010). In another study, it was shown that this neuronal population expressing PKC-*δ* in the CEAl is implicated in the inhibition of fear acquisition (Ciocchi *et al*, 2010). However, the exact role of ENK expressed by these PKC-*δ* GABAergic neurons is still undetermined.

Asok et al. also showed that exposure to a component of fox odor, 2,5-dihydro-2,4,5-trimethylthiazoline (TMT), which triggers innate fear in rats, increases ENK mRNA levels in the paraventricular nucleus (PVN) of the HPT (Asok *et al*, 2013). An increased expression of ENK mRNA levels is similarly observed after repeated footshocks, in the AMG of SWR/J mice, an inbred strain showing a reduced fear response, while this expression was unchanged in C57BL/6J mice, an inbred strain showing a high fear response (Szklarczyk *et al*, 2015). In the same study, administration of MOPr antagonist (naltrexone) or DOPr antagonist (naltrindole) increased fear response in SWR/J mice, which could be restored with a DOPr agonist. These results suggest that resistance in the face of traumatic experiences inducing fear involves ENK from the AMG and that vulnerability can be modulated by administration of OPr agonists (Szklarczyk *et al*, 2015). Finally, it has been shown by Poulin et al. that the downregulation of ENK in the rat CEA decreases unconditioned fear (Poulin *et al*, 2013). In this study, rats were submitted to a

contextual conditioning paradigm consisting of footshocks administered in a novel environment. ENK *knockdown* (KD) rats showed a reduced fear response during conditioning, while the context alone, presented 48 h later, did not produce change in freezing behavior. These results indicate that ENK release from CEA neurons is involved in the freezing behavior to an unconditioned stimulus, but not in the formation of an associative memory (Poulin *et al*, 2013). Results of ENK distribution studies in addition to pharmacological, silencing, and genetic studies demonstrate the prominent role of ENK, especially amygdalar ENK, in mediating fear behavior. This connection may further suggest a role for ENK in anxiety and stress responses, which are closely related to fear behavior.

Table 2: Evidence for ENK signaling involvement using different behavioral tests

Behavior	Paradigm	Principles and procedures	Evidence for involvement of ENK signaling
Fear	**Contextual fear conditioning**	In this paradigm, an animal learns to predict aversive events based on their environmental context. It is a form of learning and memory in which an aversive stimulus is associated to a neutral context and/or stimulus, resulting in fear responses upon presentation of the originally neutral context and/or stimulus. The animal is placed into a chamber to administer an aversive stimulus (*e.g.* electric footshocks). This procedure can be paired with another conditioning stimulus, a sound for example. After a delay, the animal is re-exposed to the environment and/or conditioning stimulus, without the aversive one. Freezing which is characterized by the total absence of movement except those required for respiration is then measured to assess fear responses.	- In rats, ENK mRNA levels are increased in CEA upon contextual fear conditioning (Petrovich *et al*, 2000); - ENK *knockout* (KO) mice show an exaggerated immobility during auditory fear conditioning (Ragnauth *et al*, 2001); - ENK neurons in CEAl overlap with PKC-δ GABAergic neurons, which are involved in fear behavior (Ciocchi *et al*, 2010; Haubensak *et al*, 2010); - In SWR/J mice (showing a reduced fear response induced by footshocks), ENK mRNA levels are increased in AMG (Szklarczyk *et al*, 2015); - In SWR/J mice (showing a reduced fear response induced by footshocks), administration of MOPr and DOPr antagonists increase fear response (Szklarczyk *et al*, 2015); - In rats, ENK *knockdown* (KD) of CEA decreased unconditioned fear (Poulin *et al*, 2013).

	Startle response	The startle reflex is considered as an innate and involuntary reaction that appears upon exposure to an unexpected or threatening stimuli. The response corresponds to a quick involuntary contraction of the animal's skeletal muscles. The test is conducted in an automated startle chamber that allows measurement of the reflex.	- ENK KO mice show an exaggerated startle response (Bilkei-Gorzo *et al*, 2004).
Anxiety	**Open-field**	This task is based on a rodent's preference for dark areas. The animal is placed in an open-field chamber, an arena with surrounding walls to prevent escape, and the exploratory behavior of the center (lit) versus periphery (dark) is assessed over time with a video-recording.	- ENK KO mice show a decreased exploratory behavior and avoid the central part of the open-field (OF) arena (Bilkei-Gorzo *et al*, 2004; Konig *et al*, 1996; Ragnauth *et al*, 2001); - ENK KO mice, exposed to stress induced by footshocks, present an anxiety-like behavior (Kung *et al*, 2010).
	Elevated-plus-maze	This task is based on a rodent's natural preference for dark and enclosed areas, compared to lit and uncovered areas, as well as on their natural exploratory behavior of a novel environment. The animal is placed in the maze and its exploratory behavior is assessed over time with a video-recording. The maze has a cross shape with two opposite arms surrounded by walls (dark and enclosed area) whereas the two other arms do not present walls (lit and uncovered).	- ENK KO mice present anxiety-like behavior in the elevated-plus-maze (EPM) (Bilkei-Gorzo *et al*, 2004); - ENK KO mice, exposed to stress induced by footshocks, present anxiety-like behavior in EPM (Kung *et al*, 2010); - In rats, ENK KD in CEA increases the exploratory behavior in EPM (Poulin *et al*, 2013); - Infusion of a DOPr agonist in CEA increases the number of entries and the time spent in open arms of the EPM (Randall-Thompson *et al*, 2010); - Administration of a DOPr antagonist diminishes the exploratory behavior in EPM (Perrine *et al*, 2006); - Administration of a DOPr agonist increases this behavior (Broom *et al*, 2002a; Nozaki *et al*, 2014; Saitoh *et al*, 2004; Saitoh *et al*, 2013; Vergura *et al*, 2008); - DOPr KO mice spent less time in the open arms of EPM (Filliol *et al*, 2000); - MOPr KO mice increases the exploratory behavior in EPM (Filliol *et al*, 2000); - Administration of MOPr agonist increases the exploratory behavior in EPM (Rezayof *et al*, 2009).

	Light-dark box	This task is based on a rodent's natural preference for dark areas, compared to lit ones. The box contains two chambers, one light and one dark. The animal is placed into the box and its exploratory behavior is assessed over time with a video-recording.	- ENK KO mice show a decreased exploratory behavior in the light-dark box (LDB) (Bilkei-Gorzo *et al*, 2004; Ragnauth *et al*, 2001); - ENK KO mice, exposed to stress induced by footshocks, present a anxiety-like behavior in LDB (Kung *et al*, 2010); - DOPr KO mice spent less time in the illuminated portions of the LDB (Filliol *et al*, 2000).
	Social interaction test	This test allows evaluating the propensity of an individual to socialize. The rodent is placed in an open-field arena alone in the first place and then with another individual. The time spent interacting with the intruder is measured.	- ENK KO mice present a reduced duration of social interaction (Bilkei-Gorzo *et al*, 2004).
	Forced swim test	This test is used to evaluate the antidepressant efficacy of new compounds. A rodent is placed in a pool containing approximately 15 cm^3 of water and its mobility is measured on a video-recording.	- Administration of a DOPr agonist increases mobility in the forced swim test (Nozaki *et al*, 2014).
Anhedonia	**Sucrose preference test**	This task is used as an indicator of anhedonia, characterized by a lack of interest for a reward. Two bottles, one containing a sucrose solution (between 1% and 5%) and another plain water, are presented to the animal. Its preference for the sweetened versus plain water reveals anhedonia state.	- After restraint stress, rats showing decreased anhedonia (assessed with the sucrose preference test) present a reduced expression of ENK mRNA in the NAc (Poulin *et al*, 2014).

1.2.4.2.2 Stress and anxiety

Several studies performed in humans showed the importance of ENK in anxiety, depression, and PTSD, a mental illness that appears after experiencing a traumatic event. Indeed, a polymorphism in the gene encoding neutral endopeptidase, involved in ENK metabolism, was identified in patients with anxiety disorder, tested with the SCL-90-R inventory of psychological symptoms (Comings *et al*, 2000). Positron emission tomography (PET) studies have shown that MOPr expression is decreased in the anterior cingulate cortex of patients with PTSD (Liberzon *et al*, 2007). In patients with depression, PET further revealed that the expression of MOPr is decreased in the HPT and AMG (Kennedy *et al*, 2006). These studies suggest that a reduced tone of ENK neurotransmission is a key component in the expression of anxiety.

In rodents, several behavioral paradigms are commonly used to assess the level of anxiety, including the elevated plus maze (EPM), open field (OF), and light-dark box (LDB) tests. These tests are based on the natural aversion of rodents for open, elevated, or illuminated

areas and their natural exploratory behavior in novel environments. In addition, the social interaction test (SI) allows evaluating the propensity to socialize. The startle response (SR) corresponds to an unconscious defensive response to unexpected or threatening stimuli. All behavioral tests discussed in our review are detailed in Table 2.

The ENK KO mice show an increased anxiety with the EPM, OF, and LDB tests, have an exaggerated SR, and a reduced duration of SI (Bilkei-Gorzo *et al*, 2004; Konig *et al*, 1996; Ragnauth *et al*, 2001). ENK KO mice exposed to a stress induced by footshocks, mimicking PTSD, similarly present anxiety- and depressive-like behaviors, contrary to wild-type controls, using the OF, EPM, and LDB tests (see Table 2) (Kung *et al*, 2010). However, the downregulation of ENK in CEA was shown to reduce anxiety as characterized by an increase of exploratory behavior (Poulin *et al*, 2013). ENK KO mice are resistant to anxiety- and depression-like behaviors after a chronic mild unpredictable stress consisting of daily exposure to different stressors, such as food deprivation and restraint stress for five weeks suggesting that ENK enhance the reactivity to chronic stress (Melo *et al*, 2014). ENK appear to have varying and even opposing effects on anxiety, depending on the considered CNS region and the type and intensity of stress.

The high levels of anxiety generally observed in ENK KO mice are also seen upon gene inactivation of DOPr (Filliol *et al*, 2000). Pharmacological studies conducted in rodents support these results obtained through gene inactivation of DOPr, since subcutaneous administration of naltrindole, a DOPr antagonist, induces anxiety (Perrine *et al*, 2006). Conversely, intraperitoneal injection of DOPr agonists (SNC80, UFP-512, (+)BW373U86) was shown to be anxiolytic (Broom *et al*, 2002a; Saitoh *et al*, 2004; Vergura *et al*, 2008). Moreover, infusion of [D-Pen 2,5]-ENK (DPDPE), a DOPr agonist, in CEA exerted similar effects, which could be reversed by the administration of naltrindole, a DOPr antagonist. Recently, a new DOPr agonist, KNT-127, has received an increasing interest as a potential therapeutic treatment for anxiety and depression, although the efficacy of this molecule has not yet been investigated in clinical trials. In rodents, KNT-127 produces anxiolytic and antidepressant-like effects in a dose-dependent manner (see Table 2) (Nozaki *et al*, 2014; Saitoh *et al*, 2013). These results are consistent between models and suggest that signaling onto DOPr mainly exerts anxiolytic effects.

In contrast to these findings, a conditional KO mouse for DOPr (Dlx-DOR) in forebrain

GABAergic neurons showed a reduced level of anxiety compared to wild-type littermates, demonstrating that stimulation of DOPr in GABAergic neurons of the forebrain is anxiogenic (see Table 2) (Chu Sin Chung *et al*, 2015). In the same way, the gene inactivation of MOPr has anxiolytic effects, with MOPr KO mice presenting an increased time spent in the open arms of an EPM (Kung *et al*, 2010). Nevertheless, several pharmacological studies instead demonstrated that MOPr activation is anxiolytic. For example, intraperitoneal administration of morphine, a MOPr agonist, decreases vocalizations in rats exposed to a predator and anxiety assessed with the EPM test (Rezayof *et al*, 2009). Overall, MOPr appear to have varying effects on anxiety, depending on the methodological approaches used.

A few recent studies explored the neuroanatomical specificity of ENK projections that are recruited in steady-state conditions or upon stress in rats. Single housing (see Table 3) in early life was shown to decrease immunoreactivity of Met-ENK-Arg6Phe7 (MEAP) in the brain areas that include the AMG, substantia nigra (SN), HPT, and periaqueductal grey (PAG) (Granholm *et al*, 2015). Hernández et al. also measured ENK neuropeptidase activities in the three main regions of the stress response circuitry (AMG, HPC, and mPFC) after acute restraint in rats (see Table 3; (Hernandez *et al*, 2015)). Neuropeptidases regulate the expression of neuropeptides at the release sites. Peptidase activity can thus be used to indicate the functional status of neuropeptides. This neuropeptidase activity was found to be more intense in AMG than in HPC or mPFC both in control and stressful conditions, suggesting that ENK metabolism is preponderant in the AMG. After acute restraint stress, ENK-degrading activity was reduced in AMG and increased in HPC, while it remained unchanged in the mPFC. In stressed rats, a positive correlation was described between the AMG and HPC, while in control rats, a negative correlation was observed between the mPFC and HPC. These results suggest a neuropeptidergic functional connection between the mPFC, HPC, and AMG, which could be triggered by stress and involved in some of the adaptive functions performed by this circuit.

Overall, these contradictory results found in the literature regarding the influence of ENK signaling on anxiety could be attributed first, to the technical approaches (pharmacological, genetic), then to the considered nucleus (CEA for example) or associated neurotransmitters (GABA), and finally to the type (acute, chronic stress) and intensity of stress. It still

remains unknown whether the many effects of ENK circuitry acting in such a diverse array of brain circuits might all be recruited together in response to a variety of different stressors and different modalities. Different brain circuits could synergistically contribute to the stress response, highlighting the huge challenge we face in understanding the functions of ENK signaling. Taken together, the combined findings from these silencing, pharmacological, genetic, and neuroanatomical studies suggest that the stimulation of ENK transmission onto DOPr and/or MOPr might enhance the natural strategies to cope with stress.

Table 3: Evidence for ENK signaling involvement under different stress paradigms

Paradigm	Principles and procedures	Evidence for involvement of ENK signaling
Single housing	Given the social behavior of rodents, chronic or acute single housing is used to mimic the stress due to social isolation. The animal is placed alone in its home cage.	- Prolonged single housing in early life decreases ENK immunoreactivity in AMG, substantia nigra, HPT and PAG (Granholm *et al*, 2015).
Restraint stress	The animal is placed in a tube in such a way that all movements are prevented. The psychological and physiological effects due to restraint stress result from the distress and aversive nature of the forced immobility.	- After acute restraint stress, ENK-degrading activity is reduced in AMG and increased in HPC (Hernandez *et al*, 2015); - After chronic restraint stress, ENK *knockout* (KO) mice do not exhibit anxiety nor depression-like behavior (Melo *et al*, 2014); - After chronic restraint stress, rats showing decreased anhedonia present a reduced expression of ENK mRNA in the NAc (Poulin *et al*, 2014).
Social defeat stress **(or resident-intruder paradigm)**	This task exploits the social conflict between two individuals to initiate psychological stress. This experiment can be related to the intimidation or victimization in humans. An intruder is placed in the home cage of a resident each day for a given period of time.	- After a chronic social defeat, *Oprm1* A112G mice show a strong resilience (Briand *et al*, 2015); - After a chronic social defeat, resilient rats demonstrate a high recruitment of ENK afferents from PGi to LC (Reyes *et al*, 2015); - After a chronic social defeat in rats and mice, ENK mRNA levels decrease in BLA of vulnerable individuals (Berube *et al*, 2013; Henry *et al*, 2016).
Chronic unpredictable stress	This test allows to mimic the unpredictable disruptions of daily life. An animal is subjected to different stressors each day for a given period of time. Stressors can include restraint stress, electric footschocks, wet bedding, group housing, mild shaking of the home cage, cold water swim, etc.	- ENK *knockdown* (KD) in BLA increases anxiety reproducing behavioral responses encountered in individuals vulnerable to chronic unpredictable stress (Berube *et al*, 2014).

1.2.5 Role in resilience to chronic stress

An extreme amount of stress can lead to maladaptive behavioral changes such as anhedonia and social avoidance, in rodents and humans, as well as serious health consequences by impacting on the nervous, endocrine, and immune systems. However, chronic exposure to stress can also engender compensatory physiological responses in order to reduce these deleterious effects of stress. This mechanism of defense allows maintaining homeostasis in the face of adversity. This phenomenon of "resilience" corresponds to the ability of an individual to maintain normal psychological and physical functioning in the front of stress or trauma, in order to avoid mental and physical illnesses (Russo *et al*, 2012).

Recent findings regarding the functions of ENK transmission in stress resilience revealed the involvement of different brain areas such as the NAc (Poulin *et al*, 2014; Sweis *et al*, 2013) or septum, PVN and PAG (Berube *et al*, 2013; Berube *et al*, 2014; Briand *et al*, 2015), or locus coeruleus (LC) and paragigantocellularis nucleus (PGi) (Reyes *et al*, 2015), in addition to the BLA as we will discuss below, thus suggesting a high level complexity of ENK circuitry in stress resilience.

Sweis et al. associated the resilience to chronic stress measured by a lack of memory impairment poststress to an increased expression of ENK mRNA in the rat NAc, proposing that an ENK-mediated increase of dopaminergic tone could improve motivation-based cognitive performance (Sweis *et al*, 2013). This predominant role of ENK projections from the NAc is supported by the results of another study. Indeed, it was shown that after 14 days of restraint stress, rats showing increased anhedonia (as measured by their preference for sucrose see Table 2) also presented in the NAc a reduced expression of ENK mRNA and ΔFosB, a transcription factor that is expressed by ENK neurons. These results suggest that the individual vulnerability to chronic stress, determined here by measuring anhedonia, is associated with a ΔFosB-mediated downregulation of ENK (Poulin *et al*, 2014). The relationship between ΔFosB and the resilience to chronic stress was already known (Vialou *et al*, 2010).

Downstream of ENK, Akil et al. also studied in rats the effects of dominance status and housing conditions on the response to a DOPr agonist, SNC80 (Akil *et al*, 1984). This study revealed that single housing for 50 days leads to a stronger DOPr activation in the mPFC, CEA, and NAc. Triad housing for the same period of time also increases DOPr

activation in the mPFC, CEA, and NAc, in addition to the median eminence and thalamus, of β rats that we can assimilate to stress resilient individuals considering their defensive behaviors and frequent aggressive interactions with α dominant rats, which instead display an offensive behavior (Akil *et al*, 1984). This mechanism could be involved in the regulation of ENK transmission upon stress.

Two types of behavioral paradigms are commonly conducted in rodents for studying stress resilience (see Table 3). The social defeat paradigm, also named resident-intruder paradigm, in which intruder animals are repeatedly submitted to daily interactions with a home-cage unfamiliar resident over a given period of time, induces stress resilience by mimicking the unpredictable social disruptions of daily life. This paradigm has been shown to present excellent etiological, predictive, discriminative, and face validity (Golden *et al*, 2011). Moreover, unlike other stress paradigm, social defeat stress leads to long-lasting changes in hypothalamic-pituitary-adrenal axis function, making it a stress paradigm of choice (Bhatnagar and Vining, 2003). The majority of rodents exposed to this paradigm exhibits reduced motivation, anhedonia, and avoids social interactions (Rygula *et al*, 2005). Conversely, despite the deleterious effects of social stress, around 30% of the population presents a phenotype of stress resilience, being resistant to the emergence of depressive-like behavior. In rats, the daily interaction between individuals results in subordination of the intruder, indicated by adoption of a supine position. The latency to assume a defeated posture is recorded, and the averaged latency over stress exposition is used as a predictive value to define resilience or vulnerability to stress. In mice, the resilience or vulnerability to stress is instead assessed at the end of this experiment by using a SI test (see Table 2). The second chronic stress paradigm that is commonly used to study stress resilience is chronic unpredictable stress. In this experiment, individuals are daily submitted to different stressors that include restraint stress, wet bedding, food deprivation, and footshocks. The phenotype of resilience or vulnerability to stress is assessed at the end of the experiment in mice and rats using behavioral tests previously described such as SI, EPM, and OF (also see Table 2).

For example, Briand et al. used the repeated social defeat paradigm in a mouse model of OPRM1 A118G polymorphism (single nucleotide polymorphism, SNP) corresponding to a genetic mutation of MOPr observed in humans that is associated with an overall reduction

of baseline MOPr availability in regions implicated in pain and affective regulation (Pecina *et al*, 2015), thus allowing to unravel a potential role of MOPr in the resilience to chronic stress (Briand *et al*, 2015). This model presents increased home-cage dominance and nonaggressive social interactions, similar to the human carriers of this mutation. In the presence of an aggressor during social defeat stress, it also showed a strong resilience to chronic stress, determined by a blunted anhedonia and social avoidance following the social defeat. Neuronal activation measured by c-fos staining was additionally increased in the NAc, septum, BLA, PVN, and PAG, thus suggesting an increased release of endogenous opioids upon stress (Briand *et al*, 2015). In humans, Troisi et al. demonstrated that the carriers of this mutation have a greater capacity to experience social reward and are more prone to fearful attachment, a personality trait that is related to rejection sensitivity, regardless of the quality of maternal care (Troisi *et al*, 2011; Troisi *et al*, 2012).

Reyes et al. also revealed involvement of the ENK circuitry between the LC and PGi in stress resilience in rats. In this study, fluorogold, a retrograde tracer, was injected into the LC to determine involvement of different afferents (corticotropin-releasing factor, CRF neurons from CEA and ENK neurons from PGi) in resilience under the resident-intruder paradigm (Reyes *et al*, 2015). Individuals presenting a reduced latency to present a defeated posture (defined as vulnerable rats) showed an increased activation of LC neurons and afferents of CRF neurons from CEA. Conversely, resilient rats (longer latency to present a defeated posture) demonstrated a higher recruitment of ENK afferents from PGi. Thus, two different afferent pathways to the LC, from CRF neurons in the CEA and ENK neurons from the PGi, would partly define the interindividual variation with regard to the capacity to resist chronic stress.

Two studies conducted in our laboratory demonstrated that resilience to social defeat and chronic unpredictable stress share common variations of expression among the ENK systems within specific brain regions in rats (Berube *et al*, 2013; Berube *et al*, 2014). ENK mRNA (transcripts) were quantified in 23 nuclei of the mPFC, NAc, dorsal striatum, and AMG. Only one significant difference between control, resilient, and vulnerable individuals was found in the BLA of vulnerable individuals; ENK mRNA levels were decreased in vulnerable rats compared to control and resilient rats. In contrast, no difference was found in ENK expression in the BLA between controls and resilient animals (Berube *et al*, 2013).

In addition to revealing these associations, the functional role of ENK in the AMG was evaluated. The downregulation of ENK in the BLA was shown to increase anxiety both in the SI test and EPM thus reproducing certain behavioral responses encountered in individuals that are vulnerable to chronic stress (Berube *et al*, 2014). Finally, the chronic social defeat stress was conducted in mice in order to assess ENK signature in the BLA. The expression of ENK mRNA was found to be decreased by 33% in vulnerable mice, only in the BLA. No difference was found between the control and resilient individuals (Henry *et al*, 2016). These combined results suggest that specific neuroadaptations mediated by ENK neurotransmission in the BLA could represent a key mediator of stress resilience. Based on these results, we can hypothesize that the decrease in ENK transmission from the BLA is a maladaptive mechanism, which mediates the behavioral dichotomy observed between vulnerable and resilient animals experiencing chronic stress.

1.2.6 Conclusion

Overall, most of animal studies covered in this review suggest that ENK signaling could be targeted for promoting resilience to chronic stress. Resilience to chronic stress is a very complex process involving several brain structures and neurotransmitters. When considering only one neuropeptidergic system, the ENK acting through DOPr and MOPr, numerous implicated brain structures and circuits emerge (see Figure 10 for a schematic representation that we overlapped with the cartography of main connectivities known to be involved in stress response, fear, and resilience). While the roles of ENK signaling within certain brain structures such as AMG, HPT, and NAc were largely described, its involvement in other brain regions remains unknown with regard to stress resilience. For example, the preoptic area, BST, and piriform cortex express ENK without evidence for a potential role in resilience to chronic stress, to our knowledge. All of these circuits must be individually dissected. Complete ENK KO models may thus be inadequate for characterizing the involvement of ENK signaling in stress resilience. Hence, modulating ENK or DOPr/MOPr expression within circumscribed regions or modulating selected neuronal circuits appear to be more appropriate. In this regard, optogenetic tools could provide a unique opportunity to modulate ENK transmission among selected neuronal

circuits, over the course of chronic stress and associated pathologies, as required to unravel the mechanisms through which distinct ENK pathways exert their functional role in stress resilience. Understanding the synergistic involvement of different circuits in stress resilience could additionally provide accurate, powerful, and effective therapeutic strategies to prevent or treat long-term anxiety and depression, in addition to a variety of stress- and anxiety-related disorders.

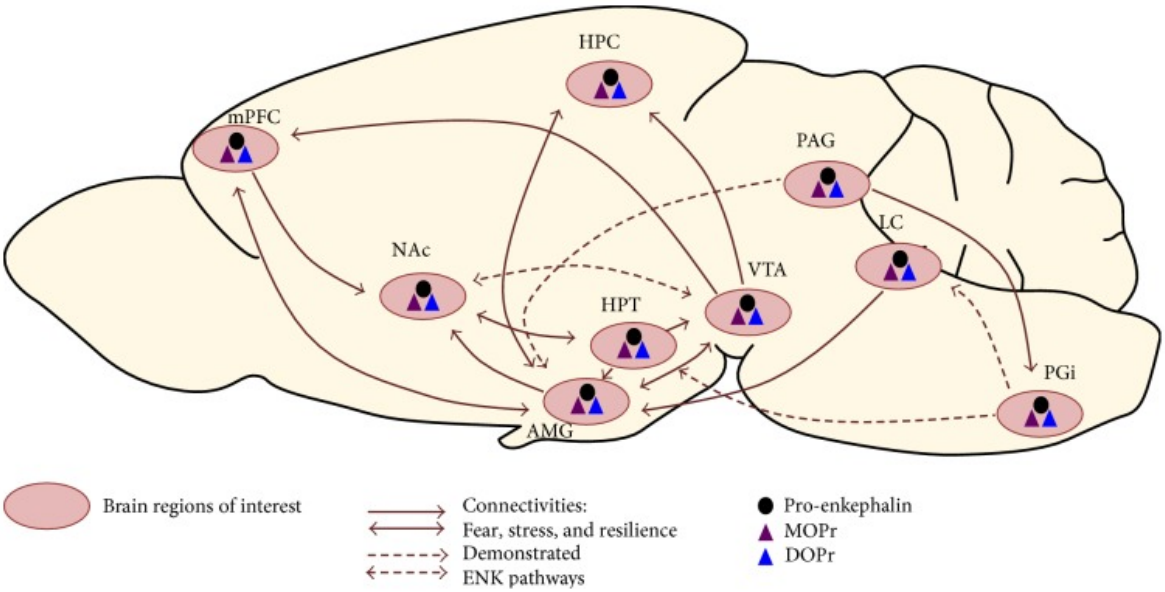

Figure 10: Cartography of main connectivities involved in fear, stress, and resilience, as well as demonstrated ENK pathways between areas and expression of ENK, MOPr, and DOPr. Pink circles represent brain regions of interest. Full arrows correspond to circuitries of stress, fear, and resilience. Dotted arrows represent demonstrated ENK circuitries. The black dot corresponds to expression of pro-enkephalin, and purple and blue triangles correspond to MOPr and DOPr expression, respectively. AMG: amygdala; HPC: hippocampus; HPT: hypothalamus; LC: locus coeruleus; mPFC: medial prefrontal cortex; NAc: nucleus accumbens; PAG: periaqueducal grey; PGi: paragigantocellularis nucleus; VTA: ventral tegmental area.

1.3 « Le stress oxydatif est le nouveau stress »

Lors de mon doctorat, nous avons émis l'hypothèse que la médiation par le système opioïdergique de la résilience au stress chronique pouvait faire intervenir le stress oxydatif (SO). En effet, certaines pathologies liées au stress psychologique ont été associées à une augmentation du SO (Miller *et al*, 2011; Miller and Sadeh, 2014). De plus, quelques études ont montré que l'activation ou l'inhibition des différents récepteurs opioïdergiques modifierait le statut oxydatif de la cellule, néfaste ou bénéfique pour celle-ci, en fonction de la voie empruntée (Nunez *et al*, 2011; Ozmen *et al*, 2007; Skrabalova *et al*, 2013; Yang *et al*, 2009). Dans la prochaine partie, je me suis appliquée à tenter de relier ces trois éléments : stress chronique, SO et système opioïdergique.

1.3.1 Définition du stress oxydatif

L'organisme dispose d'un système d'oxydation indispensable à tous les organismes à métabolisme aérobie afin de produire de l'énergie sous forme d'ATP, par phosphorylation oxydative. Cette énergie est captée dans des réactions d'oxydation pour permettre la construction et le maintien de structures cellulaires, ainsi que leur bon fonctionnement. L'énergie utilisée provient alors du mouvement des électrons issus des molécules oxydables. Il en résulte un environnement globalement réducteur dans les cellules et les tissus. Les couples de molécules d'oxydo-réduction (redox) dans les cellules sont sensibles aux mouvements d'électrons et aux changements redox de l'environnement. L'état redox décrit le rapport de la forme réduite à la forme oxydée d'un couple redox spécifique. Ce système d'oxydation est à l'origine de la production d'espèces réactives à l'oxygène (ROS) et de l'azote (RNS), pouvant être néfastes à la fonction cellulaire en cas d'excès. Néanmoins, la production contrôlée de ROS/RNS est aussi essentielle pour maintenir l'homéostasie cellulaire. Par exemple, la génération de ROS/RNS par les cellules phagocytiques constitue un mécanisme de défense important pour combattre les infections. De la même manière, les ROS/RNS, produites en réponse à la stimulation par des facteurs de croissance, sont impliquées dans la régulation de la réponse prolifératives (Finkel and Holbrook, 2000). La production de composés réactifs peut être de source endogène - mitochondriale par exemple – ou exogène (ultraviolet, radiations ionisantes, toxines, chimiothérapie…). Un système complexe d'antioxydants contre les ROS/RNS permet la

détoxification cellulaire, il est essentiel au maintien d'une bonne santé physique, à la longévité de l'organisme et à la survie cellulaire. Les mécanismes de défense contre les ROS/RNS sont assurés par de nombreuses enzymes (*e.g.* superoxyde dismutase, catalase, glutathion peroxydase) ou d'autres constituants cellulaires (*e.g.* albumine, glutathion, vitamine C) (Lobo *et al*, 2010; Mates *et al*, 1999). La respiration aérobie est l'exemple le plus couramment présenté : lors de celle-ci, certains électrons échappent à la chaîne de transport d'électrons et convertissent le dioxygène (O_2) en radical hydroperoxylique, pouvant conduire à la production de molécules hautement réactives, les radicaux superoxydes. L'anion du radical hydroperoxylique est neutralisé en présence d'une enzyme, la superoxyde dismutase, en peroxyde d'hydrogène. Celui-ci est converti en molécule d'eau par la réaction de Fenton ou en présence de catalase et de glutathion peroxydase (Maurya *et al*, 2016) (Figure 11).

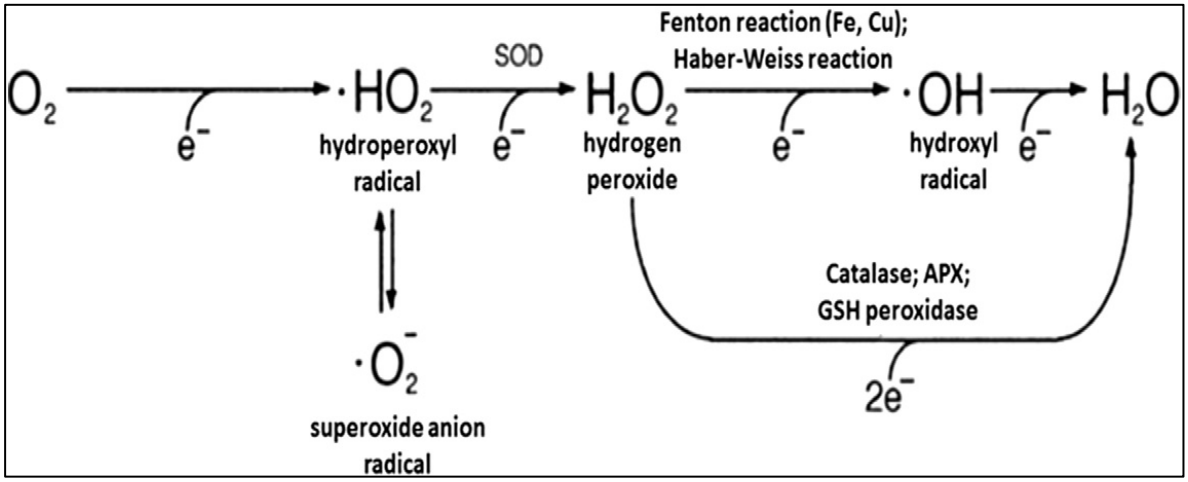

Figure 11 : Production de radicaux libres lors de la respiration aérobie. Pendant la respiration aérobie, certains électrons échappent à la chaîne de transport d'électrons et convertissent l'oxygène moléculaire (O_2) en radical hydroperoxylique ($\cdot HO_2$), convertible de manière réversible en radical superoxyde ($\cdot O_2$). Cet anion $\cdot O_2$, hautement réactif, est neutralisé en présence de l'enzyme superoxyde dismutase (SOD) en peroxyde d'hydrogène (H_2O_2). L'H_2O_2 est converti, par la réaction de Fenton, en molécule d'eau en utilisant deux électrons. L'H_2O_2 peut également être converti en eau en présence de catalase antioxydante enzymatique et de glutathion peroxydase. Adaptée de (Maurya *et al*, 2016).

Le SO correspond au déséquilibre entre une quantité excessive de ROS/RNS produite et une disponibilité ou une activité de défense insuffisante des antioxydants. Autrement dit, l'équilibre oxydatif de la cellule est compromis quand la production de ROS/RNS et de radicaux libres est trop importante ou que l'activité antioxydante est trop faible (Sies, 1997). Les radicaux libres correspondent à des composés intermédiaires des ROS/RNS, néfastes pour la cellule. Les principaux radicaux libres sont les radicaux superoxydes, hydroxyles ou l'oxyde nitrique. L'excès des composés réactifs peut endommager un certain nombre de constituants de la cellule comme l'ADN, les protéines ou encore les lipides. Les effets sur la cellule sont multiples : des dommages à la membrane et à l'ADN, la perte de fonction des organites et la fuite des électrolytes, en sont les principaux. Le SO accélère, de façon prématurée, le vieillissement cellulaire et conduit ultimement à la mort cellulaire par nécrose ou apoptose (Czerska *et al*, 2015). Toutefois, il s'agit d'un mécanisme réversible (Cole *et al*, 2010). La Figure 12 présente les différentes sources de composés réactifs et les réponses cellulaires associées à leur production.

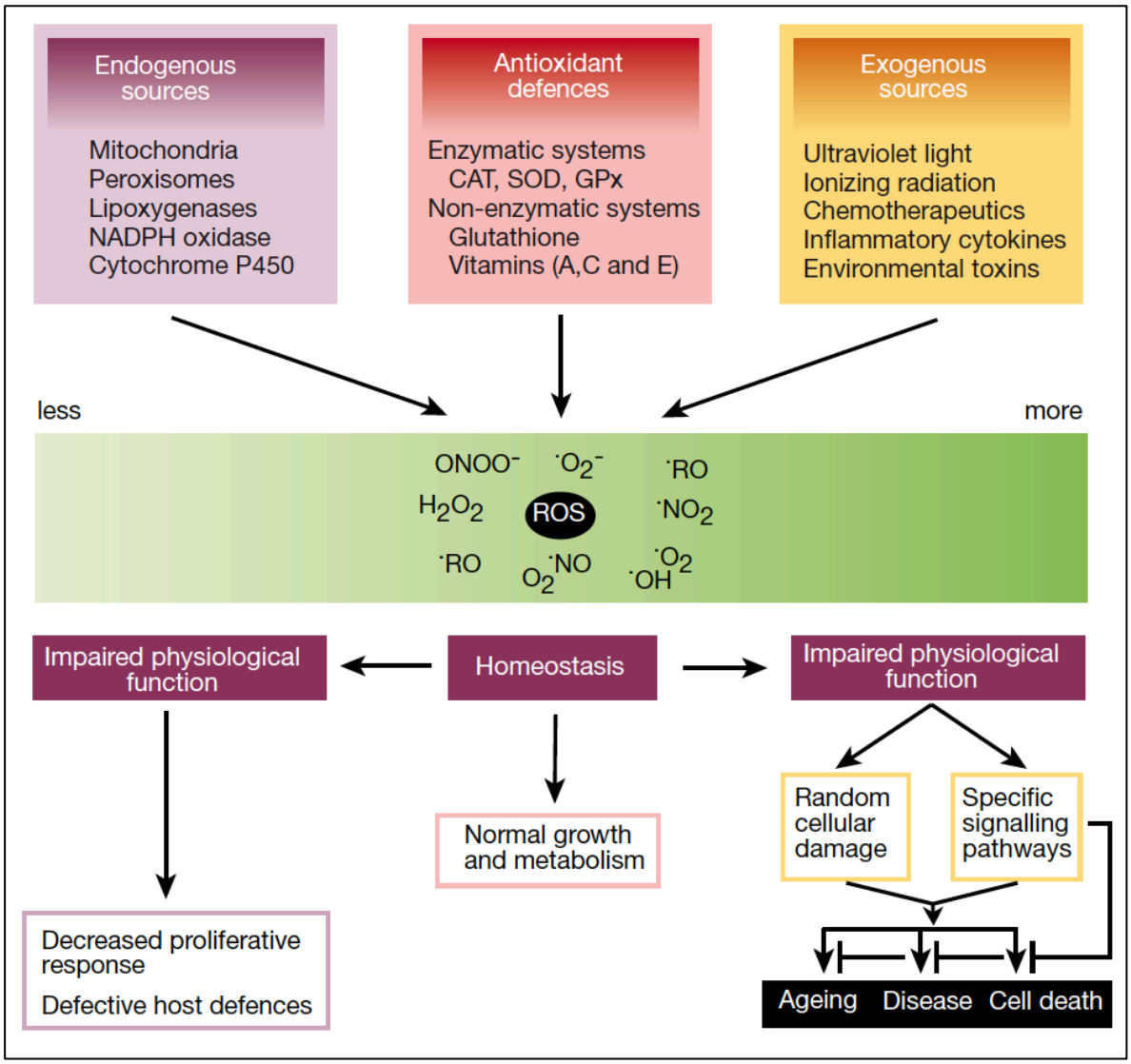

Figure 12: Les sources et les réponses cellulaires induites par la production d'espèces réactives à l'oxygène (ROS). Les oxydants sont générés par le métabolisme intracellulaire normal dans les mitochondries et les peroxysomes, ainsi que par une variété de systèmes enzymatiques du cytosol. En outre, un certain nombre d'agents externes peuvent déclencher la production de ROS. Un système de défense, antioxydant enzymatique et non enzymatique, sophistiqué, comprenant la catalase (CAT), la superoxyde dismutase (SOD) et la glutathion peroxydase (GPx), contrecarre et régule les niveaux de ROS pour maintenir l'homéostasie physiologique. L'abaissement des niveaux de ROS en dessous d'un seuil critique permettant l'homéostasie peut interrompre le rôle physiologique des oxydants dans la prolifération cellulaire et la défense de l'hôte. La surproduction de ROS peut être néfaste et conduire à la mort cellulaire ou à une accélération du vieillissement et mener à des maladies liées à l'âge. L'augmentation des ROS provoque des dommages aléatoires au niveau des protéines, des lipides et à l'ADN. En plus de ces effets, les ROS constituent un signal de stress qui active des voies de signalisation spécifiques au système d'oxydo-réduction. Une fois activées, ces diverses voies de signalisation peuvent soit endommager ou protéger la cellule. Adaptée de (Finkel *et al*, 2000)

Lors de mon doctorat, je me suis intéressée aux dommages des constituants cellulaires induits par le SO. En effet, il existe de nombreux marqueurs pour évaluer les effets du SO. Ils sont facilement observables et quantifiables en microscopie électronique : parmi eux, les cellules « sombres » dues à leur forte densité du cytoplasme et du nucléoplasme, la dilatation du réticulum endoplasmique (RE) et de l'appareil de Golgi ainsi que l'altération architecturale de la mitochondrie. La structure de ces organites est modifiée de façon plus ou moins drastique lors d'un SO. Dans la partie suivante, j'exposerai la littérature connue à propos des changements de l'ultrastructure cellulaire engendrés par le SO.

1.3.2 Les marqueurs cellulaires du stress oxydatif

1.3.2.1 Les cellules « sombres »

Les neurones sombres peuvent être observés en microscopie optique : ils présentent une apparence foncée homogène et semblent rétrécis. De plus, ils ont une affinité accrue pour les différents colorants utilisés en histologie : leurs noyaux et leurs cytoplasmes apparaissent de couleur bleu foncé avec l'hématoxyline et l'éosine (Figure 13A). Leurs dendrites peuvent aussi être irrégulières. En microscopie électronique, le nucléoplasme, le cytoplasme et les dendrites de ces neurones sont denses aux électrons et apparaissent plus ou moins foncés (Figure 13B). L'observation de neurones sombres dans le SNC fait débat, depuis leur découverte en 1885, où ils ont été décrits au niveau des ganglions spinaux chez diverses espèces. Différentes écoles de pensées sont nées de ce débat : (1) les neurones sombres sont un artéfact, (2) ils sont issus d'un phénomène non spécifique, (3) ils correspondent à une modification fonctionnelle spécifique résultant d'une activité cellulaire particulière, de l'administration d'une drogue, d'un processus pathologique ou lié à l'âge, (4) ils résultent d'une combinaison de (1) et (3). Les neurones sombres peuvent apparaître à la perfusion aux aldéhydes ou pendant le retrait du cerveau de la boite crânienne (Csordas *et al*, 2003; Johnson, 1975; Jortner, 2006).

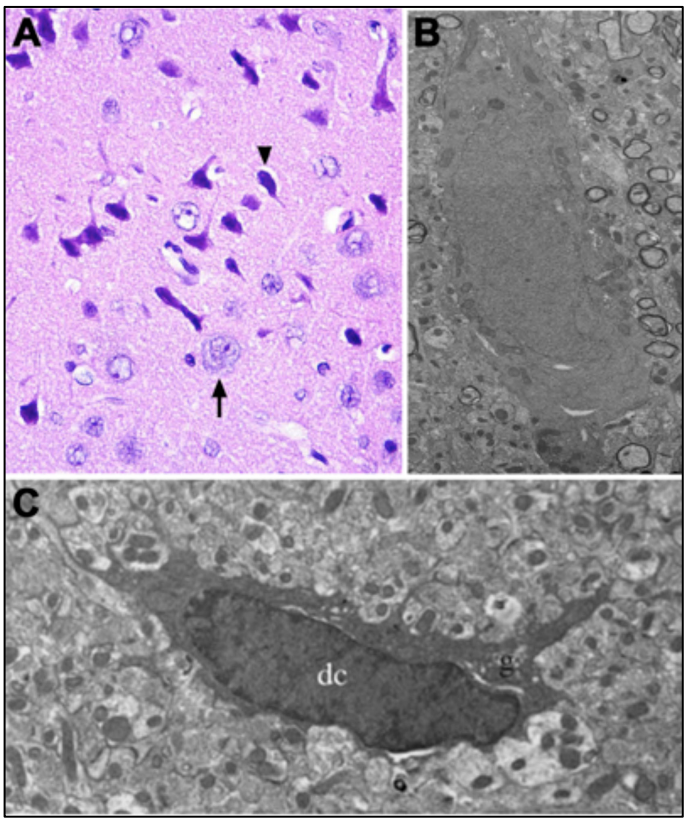

Figure 13 : Exemple de cellules « sombres ». (A) Neurones « sombres » (tête de flèche), à côté de neurones en santé (flèche), observés au niveau du cortex chez le rat, grâce à un marquage à l'hématoxyline et éosine par microscopie optique. Adaptée de (Jortner, 2006). (B) Exemple d'un neurone « sombre » dans la région CA1 de l'hippocampe ventral (couche pyramidale) chez la souris en condition de stress chronique, observé en microscopie électronique à transmission. (C) Exemple d'une microglie sombre dans la région CA1 de l'hippocampe ventral (*stratum lacunosum-moleculare*) chez la souris stressée déficiente en récepteur CX_3CR1. Adaptée de (Bisht *et al*, 2016b).

De nombreuses études ont cherché à démontrer que leur apparition résultait essentiellement de certaines conditions pathologiques. Une étude, réalisée en 1975, présente une analyse des neurones sombres par microscopie optique et électronique, au niveau du noyau vestibulaire latéral du rat, en condition normale ou suivant une lésion au niveau des afférences vestibulaires (Johnson, 1975). Les auteurs observèrent une présence de neurones « sombres » plus importante chez les animaux lésés par rapport aux contrôles. De la même manière, le retrait du cortex moteur, chez le chat, permet l'observation de motoneurones « sombres » dans la moelle épinière en controlatéral de la lésion (Young and Rowley, 1970). Les cellules sombres ont ainsi été observées dans différentes conditions autant au niveau des neurones (Oster-Granite *et al*, 1996; Peters *et al*, 1998; Tremblay *et al*, 2012) - en vieillissement normal dans le cortex préfrontal chez le singe (Peters *et al*, 1998) ou dans le système visuel et auditif chez la souris (Tremblay *et al*, 2012) - que des cellules gliales (Figure 13C) (Bisht *et al*, 2016b). Elles ont aussi été décrites en condition pathologique : notamment, dans des modèles murins de la maladie d'Alzheimer (Bisht *et al*, 2016b; Oster-

Granite *et al*, 1996), dans le cerveau de rat ischémique (Kirino *et al*, 1984), dans un modèle d'épilepsie chez le rat (Atillo *et al*, 1983) et en condition de stress chronique chez la souris (Bisht *et al*, 2016b). Les cellules sombres présentent un certain nombre de caractéristiques du SO comme la dilatation du RE et de l'appareil de Golgi ainsi qu'une altération architecturale des mitochondries.

1.3.2.2 Le stress du réticulum endoplasmique et la dilatation de l'appareil de Golgi

Le RE est un organite crucial au sein de la cellule eucaryote, qui est étroitement lié à la membrane nucléaire. Il est localisé en continuité de la surface membranaire nucléaire externe et est relié à l'appareil de Golgi. Il est constitué de saccules et de tubules interconnectés, ainsi que de vésicules. Ses fonctions sont multiples : il assure le stockage du calcium, la synthèse des lipides et le bon repliement des protéines, en plus de leur transport. Le RE lisse est indispensable à la synthèse des acides gras et des phospholipides ainsi qu'à l'assemblage des doubles couches lipidiques et à l'homéostasie calcique. Le RE rugueux, dont la surface est constituée de ribosomes, assure les fonctions de synthèse et de sécrétion des protéines (Cooper, 2000). Le bon repliement des protéines nécessite l'intervention de nombreuses protéines (chaperonnes, enzymes) mais aussi, d'un microenvironnement adéquat (niveau de calcium, statut redox). De nombreux paramètres intrinsèques à la cellule et à son microenvironnement peuvent influencer les fonctions du RE. L'hypoxie, l'hypoglycémie, l'hyperthermie, l'acidose, le statut redox, le niveau d'énergie ou encore de calcium représentent les principales causes du stress du RE, conduisant à l'accumulation de protéines mal repliées dans sa lumière. Cette accumulation provoque la dilatation du RE, particulièrement visible en microscopie électronique. En réponse à ces perturbations, le RE induit des voies de signalisation favorisant la survie cellulaire via l'intervention de GRP78 (ou BiP, protéine chaperonne), ou à l'inverse, provoquant l'apoptose cellulaire via CHOP (facteur de transcription « CCAAT-enhancer-binding protein homologous protein »). La Figure 14 présente un schéma des paramètres pouvant affecter le RE et induire son stress, conduisant ultimement soit à la survie, soit à l'apoptose de la cellule.

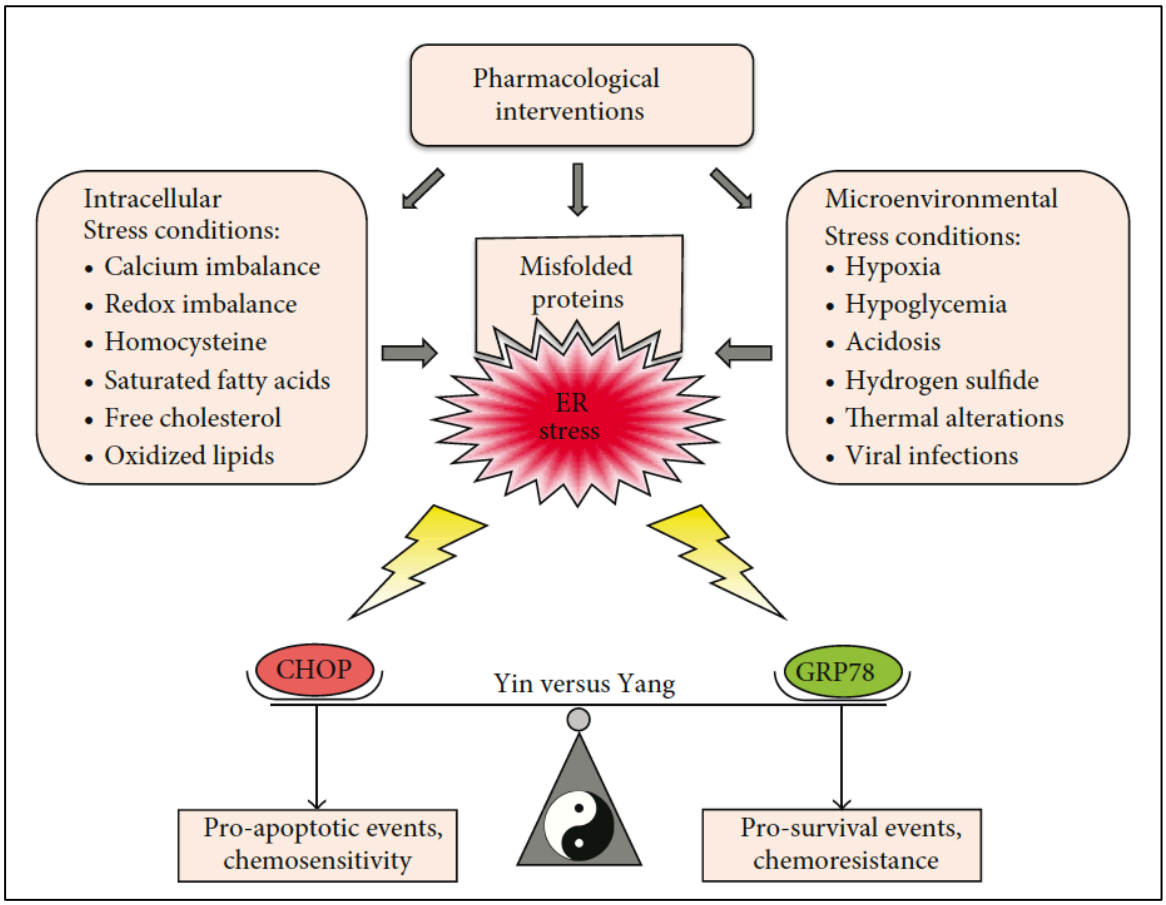

Figure 14 : Déclenchement du stress du réticulum endoplasmique (« ER stress ») et la balance du yin-yang entre la survie cellulaire et l'apoptose. Une grande variété de conditions et de composés pharmacologiques perturbe l'homéostasie du RE conduisant à son stress et à l'accumulation de protéines mal-conformées. En réponse à cette perturbation, le RE induit des voies de signalisation favorisant la survie cellulaire dont le médiateur principal est GRP78. À l'inverse, si le stress est trop important, les voies de signalisation, dont CHOP est le principal médiateur, vont être activées pour induire l'apoptose cellulaire. Adaptée de (Schonthal, 2012).

Le stress du RE provoque l'activation de la « réponse aux protéines ayant un problème de conformation» (« Unfolded protein response », UPR) permettant de replier correctement les protéines et faisant intervenir de nombreuses protéines chaperonnes. Si le but n'est pas atteint, deux systèmes sont mis en place : (1) la « dégradation associée au RE» (*Endoplasmic reticulum associated degradation*, ERAD) conduisant à la dégradation de la protéine par le protéasome et (2) la formation de vésicules où les protéines sont stockées avec d'autres débris cellulaires et qui seront recyclées par autophagie (Kim *et al*, 2008; Ron

and Walter, 2007; Schonthal, 2012).

L'étude présentée en chapitre 1 de ce manuscrit fait état d'un autre marqueur du SO qui est beaucoup moins documenté : il s'agît de la dilatation de l'appareil de Golgi. Celui-ci étant étroitement lié au RE et participant au traitement des protéines et des lipides (synthèse des glycolipides et de la sphingomyéline), il semble logique d'associer le stress du RE et de l'appareil de Golgi. L'appareil de Golgi reçoit les protéines provenant du RE (entrée *cis*) afin d'assurer leur traitement (modifications post-traductionnelles : *N* et *O*-glycosylation, phosphorylation) et les orienter vers leur destination suivante (lysosome, membrane plasmique, sécrétion ; sortie *trans*). Il est constitué de sacs membranaires aplatis (citernes) et de vésicules (Cooper, 2000). En 1985, Welch et Suhan présentaient une étude morphologique des changements des organites, lors d'un stress thermique, sur des fibroblastes de rat par microscopie électronique. Après le choc thermique, les cellules montraient une désorganisation complète des citernes de l'appareil de Golgi et une augmentation du nombre de vésicules dans la région perinucléaire (Welch and Suhan, 1985).

1.3.2.3 Les mitochondries

La mitochondrie est constituée d'un système de double membrane : une membrane externe et une membrane interne qui sont séparées par un espace inter-membranaire. La membrane interne forme des invaginations (crêtes) qui s'étendent jusqu'à la matrice de la mitochondrie. La matrice contient le matériel génétique de la mitochondrie, ainsi que toutes les enzymes nécessaires au métabolisme oxydatif. La mitochondrie joue un rôle majeur dans le métabolisme énergétique des cellules eucaryotes. La glycolyse transformant le glucose en pyruvate a lieu dans le cytoplasme de la cellule, le pyruvate est alors transporté au sein de la mitochondrie où il est converti en acetyl Co-enzyme A, lui-même oxydé en CO_2 via le cycle de l'acide citrique. Cette oxydation est couplée à la réduction du nicotinamide adénine dinucleotide (NAD+ en NADH) et flavine adénine dinucleotide (FAD en $FADH_2$). La réaction de transfert des électrons, du NADH et $FADH_2$ à l'O_2 membranaire, est à l'origine de l'énergie nécessaire à la production d'ATP. Les acides gras

sont aussi convertis en acetyl Co-enzyme A et suivent le même processus pour permettre la synthèse d'ATP. Par phosphorylation oxydative, les acides gras et les sucres sont convertis en ATP (Cooper, 2000). La mitochondrie est la première source de ROS dans la cellule et sa production de ROS varie en réponse aux modifications intracellulaires du niveau d'O_2. L'hypoxie induit l'expression d'un facteur de transcription (*hypoxia-inducible-factor 1*, HIF1) régulant la glycolyse, la consommation d'O_2 par la mitochondrie et la survie cellulaire. À l'inverse, l'hyperoxie conduit à une forte production de ROS, à une diminution de la production d'ATP et à la mort cellulaire (Chandel and Budinger, 2007). Les modifications structurelles de la mitochondrie reflètent ses altérations fonctionnelles (Brocard *et al*, 2003). En effet, il a été montré qu'un stress thermique, appliqué sur des fibroblastes de rat, conduisait au gonflement de la mitochondrie, à la désorganisation des crêtes et à l'élargissement des espaces entre les crêtes (Welch *et al*, 1985).

1.3.2.4 Autres marqueurs

Deux autres marqueurs ont été identifiés : les granules de lipofuscine et les indentations nucléaires. Ces marqueurs ne relèvent pas directement du SO mais y sont étroitement liés. En effet, les granules de lipofuscine sont des marqueurs de vieillissement qui ont largement été documentés dans ce domaine, il s'agit de granules cytoplasmiques résultant de l'oxydation d'acides gras insaturés, cette composition les rend particulièrement visibles en microscopie électronique (Sohal and Wolfe, 1986). Enfin, les indentations nucléaires, correspondant au repliement de la membrane nucléaire dans le noyau, ont principalement été identifiées dans les années 1980 dans le contexte de la maladie d'Huntington où elles apparaissaient comme un marqueur pathologique de stress (Roos and Bots, 1983). Cependant, une étude récente montre que ces indentations résultent de la tension exercée par les fibres de stress d'actine et qu'elles correspondent à des sites de condensation de la chromatine. Ceci suggère une forte activité transcriptionnelle au niveau de ces sites présentant alors les indentations nucléaires comme des marqueurs de plasticité cellulaire pouvant être bénéfiques aussi bien que néfastes (Versaevel *et al*, 2014).

Le SO joue un rôle majeur dans le développement de nombreuses pathologies comme l'hypertension (Harrison and Gongora, 2009), le diabète (Maritim *et al*, 2003), l'ischémie et

différentes maladies neurodégénératives telles que la maladie d'Alzheimer (Multhaup *et al*, 1997) ou la maladie de Parkinson (Zhou *et al*, 2008). Ces pathologies ne sont pas sans rappeler celles associés à l'exposition répétée et prolongée au stress. De plus, le SO a été relié au vieillissement, il y a plus de 50 ans (Harman, 1956) et les pathologies associées au stress chronique sont décrites comme un vieillissement accéléré (Wolkowitz *et al*, 2010). Ainsi, depuis quelques années, une modeste littérature fait état d'un lien entre le SO, l'anxiété et le stress chronique (Aschbacher *et al*, 2013; Ditzen *et al*, 2006; Gingrich, 2005; Hovatta *et al*, 2005; Kromer *et al*, 2005; Kuloglu *et al*, 2002a; Kuloglu *et al*, 2002b; Patki *et al*, 2013).

1.3.3 Le stress oxydatif et les pathologies liées au stress chronique

Le cerveau est un des organes les plus vulnérables au SO de par son importante consommation en oxygène, ses faibles défenses antioxydantes et la présence de constituants cellulaires riches en lipide. Historiquement, la recherche sur les troubles associés à l'anxiété s'est principalement concentrée sur les systèmes régulateurs comme le système GABAergique ou le système sérotoninergique. En effet, les traitements par excellence, utilisés contre l'anxiété, sont les benzodiazépines et les inhibiteurs sélectifs de la recapture de la sérotonine (ISRS). Les benzodiazépines provoquent une sédation, une tolérance et une dépendance. Les ISRS ont un temps d'action qui se compte en semaines, avec des effets secondaires non négligeables. Cependant, des études du début des années 2000, effectuées chez des patients atteints de différentes pathologies associées à l'anxiété (*i.e.* troubles obsessionnels compulsifs, trouble panique), ont permis de proposer un autre système régulateur, impliqué dans l'anxiété, à savoir le SO (Kuloglu *et al*, 2002a; Kuloglu *et al*, 2002b). En 2005, une étude démontra l'implication de deux enzymes fondamentales du métabolisme oxydatif (glyoxalase 1 et gluthathion reductase 1) chez des souris de fonds génétiques différents présentant des niveaux d'anxiété variables. L'expression de celles-ci - dont le rôle majeur est de diminuer les dommages cellulaires liés au SO - était augmentée chez les souris les plus « anxieuses », à l'inverse, les souris les moins « anxieuses » présentaient une faible expression. De plus, la surexpression de ces enzymes augmentait le niveau d'anxiété chez les différentes souches de souris testées, tandis que leur inhibition

exerçait l'effet inverse (Hovatta *et al*, 2005). L'hypothèse incongrue d'un rôle du métabolisme oxydatif dans la régulation de l'anxiété donna lieu à la publication d'une lettre au titre provocateur « le stress oxydatif est le nouveau stress » (Gingrich, 2005). D'autres études ont suivi au sujet du lien possible entre ces enzymes et le comportement anxieux chez d'autres souches de souris, observant des résultats opposés à ceux d'Hovatta *et al.* (Ditzen *et al*, 2006; Kromer *et al*, 2005). Ces divergences de résultats pourraient s'expliquer par les différentes souches de souris utilisées, ainsi que les éventuelles différences d'intensité de l'anxiété des animaux. Néanmoins, ces découvertes ont permis d'établir le lien entre les deux systèmes sans en déterminer le mécanisme sous-jacent et un lien de causalité évident. Des études plus récentes se sont concentrées sur le rôle du SO dans le stress chronique. En effet, la dépression, l'anxiété et les troubles de la mémoire mis en évidence après un stress chronique social chez le rat, ont été associés à l'augmentation du SO et de l'inflammation (Patki *et al*, 2013). Aschbacher *et al.* (2013) a émis l'hypothèse que le cortisol, sécrété lors d'un stress aigu, aurait la capacité de favoriser la résistance aux dommages oxydatifs dépendamment de l'exposition à un stress chronique. Enfin, les fonctions d'oxydation de la mitochondrie ont été associées à de nombreux médiateurs du stress comme les glucocorticoïdes (GC), les catécholamines ou encore les cytokines (Manoli *et al*, 2007). L'exposition courte à un stress induit une régulation de la biogenèse mitochondriale et une activité enzymatique de la chaîne respiratoire par les GC tandis qu'une exposition prolongée aux GC conduit à la perturbation de la chaîne respiratoire, une forte production de ROS et des anomalies structurelles de la mitochondries (Duclos *et al*, 2004; Manoli *et al*, 2005). La Figure 15 présente les différentes réponses de la mitochondrie, en condition de stress aigu, comparées à celles observées lors d'un stress chronique, exposées par Manoli *et al.* (2007) dans leur revue.

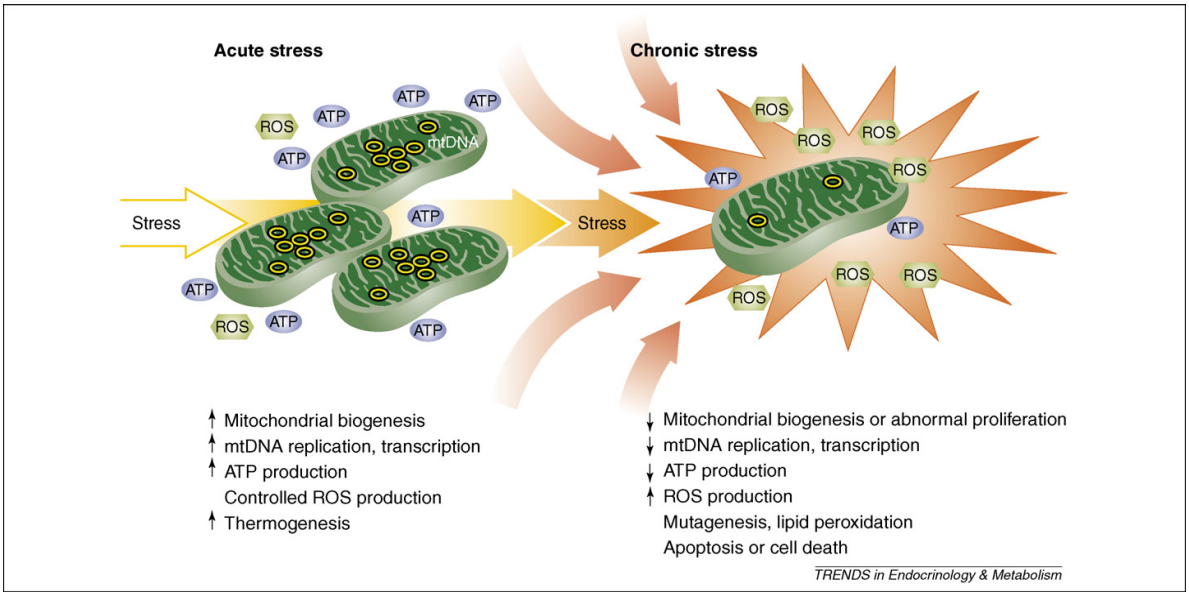

Figure 15 : La réponse de la mitochondrie en condition de stress aigu et chronique. L'exposition limitée et aigue aux glucocorticoïdes, ou à d'autres médiateurs du stress, est associée avec l'augmentation de la biogenèse mitochondriale et l'activité enzymatique de diverses sous unités du complexe de la chaîne respiratoire, pour satisfaire la demande croissante en énergie de la cellule. La production contrôlée de ROS, la thermogenèse et l'apoptose servent de mécanismes de protection contre les infections et d'autres dommages cellulaires. À l'inverse, l'exposition à un stress prolongé conduit à un déséquilibre de l'homéostasie mitochondriale provoquant une prolifération mitochondriale anormale et une altération de la chaîne respiratoire. Adaptée de (Manoli *et al*, 2007).

La plupart des études sont principalement corrélatives : le lien de causalité entre le SO et le stress psychologique est rarement établi et les mécanismes sont encore peu élucidés. De la même manière, le rôle du système opioïdergique dans le SO a fait l'objet de peu de littérature et les mécanismes sont encore mal compris.

1.3.4 Le stress oxydatif et le système opioïdergique

La relation entre ces deux systèmes a d'abord été établie dans le cadre des dépendances aux opiacés et des traitements opiacés contre la douleur. En effet, les traitements chroniques contre la douleur, utilisant la morphine, seraient à l'origine d'une importante production de ROS et de RNS. Une forte diminution de glutathion a aussi été observée dans le cerveau et le foie de rongeurs traités à court ou long terme avec de la morphine, mais aussi chez

l'humain. Il a été montré que la morphine réduisait significativement l'activité de nombreuses enzymes antioxydantes comme la superoxyde dismutase (SOD), la catalase, la peroxydase gluthation (Skrabalova *et al*, 2013; Zhang *et al*, 2004). L'administration spinale de morphine diminue le niveau d'acides gras en augmentant le SO (Ozmen *et al*, 2007). Enfin, le métabolisme de la morphine, lui-même, induit du SO (Smith, 2009). Puisque la morphine a une affinité préférentielle pour les MOPr (Reisine and Pasternak), les effets ainsi observés par l'administration de morphine sur l'augmentation du SO seraient essentiellement régulés par les MOPr. À l'inverse, des études ont démontré que l'activation de DOPr produisait l'effet opposé sur le SO. En effet, l'activation de DOPr a un effet protecteur contre l'ischémie et l'hypoxie dans divers modèles comme des neurones en culture en condition hypoxique, dans des tranches de cerveaux exposées à une hypoxie ou exposées à une privation de glucose et d'O_2 et *in vivo*, ainsi que dans le cerveaux de rat ischémique (Chao *et al*, 2007; Ma *et al*, 2005; Yang *et al*, 2009; Zhang *et al*, 2000). Cet effet neuroprotecteur de l'activation de DOPr fait notamment intervenir la réduction du SO en augmentant l'activité de nombreuses enzymes antioxydantes et en diminuant l'activité des caspases (Yang *et al*, 2009). Cependant, le mécanisme moléculaire par lequel DOPr diminue le SO n'est pas détaillé dans ces articles. Une étude a suggéré que le rôle neuroprotecteur de DOPr passerait par une action directe sur la chaîne respiratoire mitochondriale. L'administration d'un agoniste de DOPr, sur des neurones corticaux, réduit les altérations neuronales (évaluées par la sécrétion de lactate déshydrogenase) induites par un inhibiteur de la chaîne respiratoire mitochondriale, soit le sodium azide (Zhu *et al*, 2009).

1.4 Objectifs de recherche

L'objectif général de cette thèse est de mettre en lumière la contribution fonctionnelle de la transmission ENK via DOPr dans le développement de la résilience au stress chronique chez la souris. Pour répondre à cette question, le paradigme de stress chronique de défaite sociale a été effectué. Les réponses comportementales observées, dans le test d'interaction sociale, ont permis de distinguer un groupe d'individus vulnérables au stress chronique et un groupe d'individus résilients. Dans un deuxième temps, ce paradigme a été réalisé sous traitement avec un agoniste de DOPr permettant l'activation pharmacologique du récepteur. Enfin, différents marqueurs du SO ont été évalués, par microscopie électronique à transmission et par western blot. Cette thèse présente deux chapitres répondant à deux objectifs :

Objectif 1 : Dans quelle mesure le système opioïdergique participe t-il à la résilience au stress chronique? (Chapitre 1)

(1) Existe t-il une signature de l'expression des ENKs chez les rongeurs dans la résilience au stress chronique? Caractérisation du niveau d'expression de l'ARNm des ENKs dans la BLA chez la souris après un SCDS.

(2) Quelle structure cible la BLA dans le contexte de la résilience au stress chronique? Caractérisation du niveau d'expression de l'ARNm de DOPr au niveau de l'HPC.

(3) L'activation pharmacologique de DOPr, par l'agoniste SNC80, permet-elle d'induire un phénotype de résilience au stress chronique?

Objectif 2 : Le maintien d'un statut oxydatif contrôlé permet-il d'expliquer le lien entre la signalisation ENK/DOPr et la résilience au stress chronique? (Chapitre 1 et 2)

(1) L'activation pharmacologique de DOPr modifie t-elle les marqueurs du SO au niveau de l'ultrastructure cellulaire? Caractérisation des marqueurs du SO en condition de SCDS et en présence de SNC80 (Chapitre 1).

(2) L'activation pharmacologique de DOPr modifie t-elle la morphologie des mitochondries, et l'expression de protéines associées à son fonctionnement? Étude morphologique et moléculaire de la mitochondrie en condition de SCDS et en présence de SNC80 (Chapitre 2).

2 CHAPITRES

2.1 Chapitre 1

Delta opioid receptor signaling promotes resilience to stress under the repeated social defeat paradigm in mice

Mathilde S. Henry[1], Kanchan Bisht[1], Nathalie Vernoux, Ph.D.[1], Louis Gendron, Ph.D.[2,3,4], Angélica Torres-Berrio[5], Guy Drolet, Ph.D.[1,6*], and Marie-Ève Tremblay, Ph.D.[1,7#*]

[1] Axe neurosciences, Centre de Recherche du CHU de Québec – Université Laval, Québec, QC, Canada.

[2] Centre de recherche du CHU de Sherbrooke and Institut de pharmacologie de Sherbrooke, Université de Sherbrooke, Sherbrooke, QC, Canada.

[3] Département de pharmacologie-physiologie, Université de Sherbrooke, Sherbrooke, QC, Canada.

[4] Quebec Pain Research Network, Sherbrooke, QC, Canada.

[5] Douglas Mental Health University Institute, Montréal, QC, Canada.

[6] Département de psychiatrie et neurosciences, Université Laval, Québec, QC, Canada.

[7] Département de médecine moléculaire, Université Laval, Québec, QC, Canada.

* Equal contribution as senior authors

KEYWORDS: enkephalin, opioid receptor, chronic stress, resilience, oxidative stress, electron microscopy

Ce chapitre renferme la version intégrale d'un article publié dans le journal *Frontiers in Molecular Neuroscience*. *Front. Mol. Neurosci., 06 April 2018 | https://doi.org/10.3389/fnmol.2018.00100.*

2.1.1 Résumé

L'adaptation au stress chronique est très variable entre les individus. La résilience au stress est un processus complexe qui recrute de nombreuses structures cérébrales et de nombreux systèmes de neurotransmetteurs. Le but de cette étude était d'élucider l'implication de la signalisation de certains opioïdes endogènes, les enképhalines (ENK), dans le développement de la résilience au stress, chez la souris. Le modèle translationnel du stress répété de la défaite sociale a été choisi pour reproduire les perturbations imprévisibles de la vie quotidienne et induire la résilience ou la vulnérabilité au stress. Les niveaux d'expression de l'ARNm de ENK et de leurs récepteurs delta-opioïdes (DOPr) ont été quantifiés respectivement dans le noyau basolatéral de l'amygdale (BLA) et dans les régions cibles de la BLA par hybridation *in situ*. Les niveaux d'ARNm ENK se sont révélés être diminués dans la BLA et ceux de DOPr, dans la région CA1 de l'hippocampe chez la souris vulnérables uniquement. La stimulation de la voie DOPr, pendant la défaite sociale par un traitement pharmacologique avec l'agoniste DOPr, le SNC80, a induit un phénotype résilient chez la majorité des animaux stressés. Les analyses ultrastructurelles ont, en outre, révélé une réduction du stress oxydatif dans les cellules pyramidales et les interneurones de l'hippocampe CA1 lors du traitement avec le SNC80, proposant un mécanisme par lequel la signalisation ENK-DOPr pourrait permettre de prévenir les effets délétères du stress social chronique.

2.1.2 Abstract

The adaptation to chronic stress is highly variable across individuals. Resilience to stress is a complex process recruiting various brain regions and neurotransmitter systems. The aim of this study was to investigate the involvement of endogenous opioid enkephalin (ENK) signaling in the development of stress resilience in mice. The translational model of repeated social defeat (RSD) stress was selected to mimic the unpredictable disruptions of daily life and induce resilience or vulnerability to stress. As in humans, adult C57BL/6J mice demonstrated a great variability in their response to stress under this paradigm. A social interaction (SI) test was used to discriminate between the phenotypes of resilience or vulnerability to stress. After social defeat, the expression levels of ENK mRNA and their delta opioid receptors (DOPr) were quantified in the basolateral amygdala (BLA) and BLA-target areas by in situ hybridization. In this manner, ENK mRNA levels were found to decrease in the BLA and those of DOPr in the ventral hippocampus (HPC) CA1 of vulnerable mice only. Stimulating the DOPr pathway during social defeat by pharmacological treatment with the nonpeptide, selective DOPr agonist SNC80 further induced a resilient phenotype in a majority of stressed animals, with the proportion of resilient ones increasing from 33% to 58% of the total population. Ultrastructural analyses additionally revealed a reduction of oxidative stress markers in the pyramidal cells and interneurons of the ventral HPC CA1 upon SNC80 treatment, thus proposing a mechanism by which ENK-DOPr signaling may prevent the deleterious effects of chronic social stress.

2.1.3 Introduction

The survival of an individual relies on its adaptation to living conditions in constant evolution. The response to chronic stress is highly variable from one individual to another. Resilience is defined as ‘‘the process of adapting well in the face of adversity, trauma, tragedy, threats or even significant sources of threat’’ (The American Psychological Association). Heterogeneity in the response to stress suggests that resilience is a complex neurobiological process that emerges from a multitude of gene-environment interactions. Several mechanisms have been proposed to underlie the inter-individual difference in resilience or vulnerability to stress. Numerous studies support an important contribution of endogenous ENKs in the modulation and regulation of stress responses. The potential role of ENKs in stress resilience is suggested by their extensive distribution in the basal forebrain, especially the prefrontal cortex, nucleus accumbens, dorsal striatum, ventral tegmental area, hippocampus (HPC) and amygdala (Le Merrer *et al*, 2009). The opioid enkephalin (ENK) is critical to maintain hedonic and emotional balance, as it attenuates endocrine, autonomous and stress-induced behavioral responses (Bali *et al*, 2015; Henry *et al*, 2017). We have recently shown how ENK transmission is central to the neurobiology of stress resilience (Berube *et al*, 2013; Berube *et al*, 2014; Henry *et al*, 2017). Expression levels of ENKs mRNA were specifically decreased in the basolateral amygdala (BLA) of vulnerable rats, while ENK knockdown in the BLA reproduced a vulnerability phenotype in rats (Berube *et al*, 2013; Berube *et al*, 2014). In vivo, ENK have a preferential affinity for two types of opioid receptors: mu opioid receptor (MOPr) and delta opioid receptor (DOPr; (Mansour *et al*, 1986)). Genetic inactivation of ENK as well as DOPr in mice induces a high level of anxiety whereas mice deficient for MOPr display reduced anxiety (Bilkei-Gorzo *et al*, 2004; Filliol *et al*, 2000). Moreover, DOPr antagonists promote anxiety while treatments with agonists exert the opposite effect in rats (Perrine *et al*, 2006). Recently, chronic psychological stress during childhood, post-traumatic stress disorder (PTSD), and several other stress related conditions, were found to be associated with increased levels of oxidative stress (Miller *et al*, 2011; Miller *et al*, 2014). Conversely, reducing anxiety-like behavior in mice using benzodiazepine treatment prevents the exacerbated production of reactive oxygen species that is induced by chronic restraint stress

(Nunez *et al*, 2011). Oxidative stress corresponds to the disturbed balance between free radicals and antioxidant molecules. Higher levels of toxic reactive species impair cellular functions by affecting lipids, proteins, as well as nucleic acids (Czerska *et al*, 2015). Moreover, the neuroprotective effects of DOPr have been linked to reduced oxidative stress (Ma *et al*, 2005; Wallace *et al*, 2006; Yang *et al*, 2009). In particular, Wallace et al. (2006) demonstrated that DOPr activation, using [D-Pen2, D-Pen5)]-Enkephalin (DPDPE) or SNC80, counteracts the oxidative stress induced by human immunodeficiency virus toxins in vitro. In addition, DOPr pharmacological activation using intraperitoneal injection of [D-Ala2, D-Leu5]-Enkephalin (DADLE) is protective against brain hypoxic injury in rats, resulting in an attenuation of oxidative damage exerted through increased activity of antioxidant enzymes (Yang *et al*, 2009). On the opposite, morphine (MOPr agonist) administration in rat spinal cord exacerbates oxidative stress (Ozmen *et al*, 2007). The purpose of this study was to investigate the functional contribution of ENK/DOPr pathway to the emergence of stress resilience in mice, using a combination of stress paradigm, behavioral testing, molecular biology and ultrastructural analyses. Social stress was specifically targeted considering that social interactions (SIs) represent the main source of stress from the environment. We performed the repeated social defeat (RSD) paradigm, which results in either vulnerability or resilience to stress. This variance in behavioral outcome makes it an excellent model to study the underlying mechanisms of stress resilience (Duclot and Kabbaj, 2013; Golden *et al*, 2011; Krishnan *et al*, 2007). Our results first confirmed the proportion generally obtained for resilient and vulnerable phenotypes in mice, as mentioned in Golden et al. (2011). Indeed, 33% of mice displayed a resilient phenotype while the rest of them showed vulnerability to stress. The expression levels of ENK and DOPr mRNA in the BLA and the HPC, respectively, were measured in animals exposed to RSD and their non-stressed controls. The mRNA levels of ENK were found to be decreased in the BLA and those of DOPr in the ventral HPC CA1 of vulnerable mice compared to control and resilient ones. To assess the functional impact of this pathway on stress resilience under RSD, we next hypothesized that activation of DOPr signaling by SNC80 treatment throughout RSD could promote resilience. SNC80 is a nonpeptide, selective DOPr agonist able to cross the blood brain barrier (Bilsky *et al*, 1995). This compound was previously shown to induce DOPr-mediated anxiolytic (Saitoh *et al*, 2004;

Saitoh *et al*, 2005), antidepressive (Broom *et al*, 2002a), as well as analgesic effects in rodents (Bilsky *et al*, 1995). In our experiments, administration of SNC80 induced a resilient phenotype in a majority of stressed animals, with the proportion of resilient ones increasing from 33% to 58% of the total population. We lastly tested the hypothesis that DOPr signaling enhances resilience to chronic social stress by preventing oxidative damage to excitatory and inhibitory neurons of the ventral HPC CA1. Ultrastructural analyses were thus conducted using transmission electron microscopy (TEM), which revealed a major effect of SNC80 on dampening oxidative stress, both in interneurons and pyramidal cells, when quantifying changes in several of their features. Indeed, SNC80 reduced the proportion of cells with cytoplasmic/nucleoplasmic condensation, nuclear indentation, as well as endoplasmic reticulum (ER) and Golgi apparatus dilation, among other markers of oxidative stress.

2.1.4 Materials and Methods

2.1.4.1 Animals

All experiments were performed under approval of the institutional animal ethics committees, in conformity with the Canada Council on Animal Care guidelines (animal protocols n° 2014-037, 2016-073 and 242-14B). Male mice were used as detailed below. C57BL/6J mice were acquired from Jackson Laboratories (Bar Harbor, ME, USA) and all other mice from Charles River (St. Constant, QC, Canada). The animals were housed under a 12 h light-dark cycle at 22–25°C with free access to food and water.

2.1.4.2 Repeated social defeat

First, CD1 retired breeders (4–6 months old) were screened for their level of aggressiveness in presence of naïve C57BL/6 mice (8–20 weeks old) for 3 days. C57BL/6J mice (7–8 weeks old) were randomly assigned to social defeat (N = 30, for 3 cohorts; see Supplementary Figure 22 for schematic representation) or control groups (N = 26, 3 cohorts). Mice from the social defeat group (intruders) were subjected to 10 consecutive days of stress as described in Golden et al. (2011). In brief, intruders were daily housed with an aggressive CD1 mouse in its home cage for 5 min of interaction. For the next 24 h, i.e., until the next defeat, the intruders were housed on the other side of the cage, separated by a perforated divider allowing for visual, olfactory and auditory contact. Each intruder

was exposed to the same group of resident CD1 mice, in a different order, and to a different resident daily. The experimental mice were weighed every 2 days and their health status monitored carefully. Control C57BL/6J mice were paired-housed in defeat boxes and changed partners every day. One day after the final defeat, both defeated and control mice underwent a SI test. At first, each mouse was placed alone for 150 s in the middle of an open-field arena (42 cm x 42 cm x 42 cm). A CD1 mouse screened for aggressiveness not previously used for defeat was then introduced in the social interaction zone (IZ) for 150 s, within a wire-mesh enclosure. Videos were recorded and analyzed with ANY-maze (Stoelting Co, Wood Dale, IL, USA). The test was performed by an observer blind to the experimental conditions. Despite the stress experience, mice still interacting with the CD1, i.e., spending more time in the IZ, were considered resilient. Vulnerable mice had a tendency to freeze in front of the CD1 and head toward the corner zones (CZs), showing social avoidance. Thus, a SI ratio was calculated as the time spent in the SI zone in the presence of a CD1 mouse divided by the time spent in the SI zone in the absence of a CD1 mouse. To discriminate between resilient and vulnerable populations, as generally done in mice, a theoretical cut-off criterion was set to 1 for the SI ratio (Berton *et al*, 2006; Golden *et al*, 2011; Krishnan *et al*, 2007; Menard *et al*, 2017). Resilient individuals presented a SI ratio superior or equal to 1, and vulnerable ones a SI ratio inferior to 1. Non stressed controls included in the experiment had a ratio above 1 and those presenting a SI ratio below 1 were excluded, reducing the number of controls from 26 to 18 mice.

2.1.4.3 Pharmacological treatment

SNC80 is a selective and nonpeptidic DOPr agonist (Bilsky *et al*, 1995). Effectiveness of the treatment was confirmed using the forced-swim test (FST) and tail suspension test (TST) on a cohort of 32 C57BL/6 mice (7–8 weeks old) not exposed to RSD (see Supplementary Figure 22). The mice were treated with SNC80 s.c. (10 mg/kg) or administered a saline solution s.c. (0.9%) 1 h (FST) or 30 min (TST) before the test. For the FST, 6 mice per group were each placed in a transparent plastic cylinder (30 cm tall x 20 cm wide), filled with water (25°C ± 1°C, 15 cm deep), for two swimming sessions: an initial 10 min of training, followed, 24 h later, by a 6 min test session. Results were normalized to the last 4 min of test session. Videos were recorded with ANY-maze and the time spent immobile was measured by an observer blind to the experimental conditions.

For the TST, 10 mice per group were suspended by the tail with adhesive tape for 6 min in a suspension chamber. An automated tail-suspension apparatus (TS100 Tail Suspension, Hamilton Kinder, CA, USA) was used to measure total time of immobility. Four animals were tested simultaneously on separate units. The last 5 min of testing were recorded. The data were clustered in 2 s periods and analyzed (Vibration Monitor software, Hamilton Kinder). Settings used in the TST experiments were as follow: threshold 0.40 Newton, off delay 40 ms, full scale 4.00 Newton. For the RSD experiments with SNC80 treatment (N(control) = 16 and N(defeated) = 26 mice; see Supplementary Figure 22), the compound was administered for 2 days of habituation before RSD and then, 1 h prior to the defeat, on each day of social stress. SNC80 can induce epileptic seizures. Although we did not extensively study this effect, seizures were observed in approximately 80% of the mice treated with SNC80. At a dose of 10 mg/kg s.c., the mice experienced mild, epileptic-like seizures 6–8 min after the injection. The clonic seizures were observed over a period of 2–5 min after their first appearance, in accordance with what has been described by others (Chu Sin Chung *et al*, 2015). Most importantly, no signs of convulsions were observed when the animals were submitted to any of our behavioral tests (TST, FST, RSD).

2.1.4.4 Perfusion and tissue preparation

The experimental C57BL/6J mice were sacrificed 1 day after the SI test. For in situ hybridization, 11 non-stressed control, 7 resilient and 13 vulnerable mice (see Supplementary Figure 22) were anesthetized with ketamine/xylazine (80 and 10 mg/kg, i.p.) and perfused with 0.9% saline (142.5 mM, pH 7). Brains were fixed by immersion in 4% paraformaldehyde (PFA; in 0.1 M borax buffer, pH 9.5) for 5 days at 4°C, followed by 20% sucrose in PFA/borax solution for one additional day at 4°C. Twenty micrometer coronal slices were cut with a microtome (Leica SM 2000R) and stored at -20°C in cryoprotectant. For TEM, 3 mice per group (control, resilient, or vulnerable, treated or non-treated with SNC80; see Supplementary Figure 22) were anesthetized with sodium pentobarbital (80 mg/kg, i.p.) and perfused with 3.5% acrolein followed by 4% PFA (both in phosphate buffer PB 100 mM, pH 7.4). Fifty micrometer-coronal sections were cut in sodium phosphate buffer (PBS; 50 mM, pH 7.4) with a vibratome (Leica VT1000S) and stored at -20°C in cryoprotectant.

2.1.4.5 Corticosterone ELISA in plasma

Blood samples were collected from all the experimental C57BL/6J mice through the mandibular vein, without anesthesia, 1 h prior to sacrifice. Blood was collected in a microvette tube (CB300; Sarstedt, Montréal, QC, Canada). Corticosterone levels were determined by immunoassay using a commercial ELISA kit (Cayman Chemical, Ann Arbor, MI, USA). Plates were read at 405 nm with a Microplate Reader (iMarkTM, Biorad, Hercules, CA, USA). Samples were diluted at 1:100 and corticosterone standards prepared. Samples concentrations were determined using a standard curve (logarithmic scale) followed by a four-parameter logistic fit analysis.

2.1.4.6 Radioactive in situ hybridization

Slices from Bregma 1.94 mm to -3.64 mm (The Mouse Brain in Stereotaxic Coordinates, Paxinos and Franklin, 3rd edition) were used for in situ hybridization. Protocols for riboprobe synthesis and in situ hybridization are described in Bérubé et al. (2013). The cRNA probe directed against ENK (938bp) was generated from a plasmid targeting nucleotides -104 to +832, and the probe against DOPr (1366bp) targeted nucleotides +48 to +1412. Plasmids were generously provided by Drs. Steven L. Sabol (National Institutes of Health, Bethesda, MD, USA; (Yoshikawa *et al*, 1984)) and Mary E. Abood (Lewis Katz School of Medicine at Temple University, Philadelphia, PA, USA). Hybridization of brain slices was revealed after 18 h (ENK) or 45 h (DOPr) on KODAK BioMax MR Films (Kodak, Rochester, NY, USA) exposed with a Precision illuminator B95 (Imaging Research, St. Catharines, ON, Canada). Autoradiographic images were digitally acquired with a Retiga-2000R camera (QImaging, Surrey, BC, Canada). Optical density was quantified using ImageJ and normalized with C14 standard slides (American Radiolabeled Chemicals, St. Louis, MO, USA). Mean gray value was measured in each C14 standard corresponding to a value of radioactivity in μCi/g of tissue, and then a standard curve was calculated. The same measure of gray value was performed for each brain region and reported on the standard curve. To identify the different hippocampal regions in which DOPr mRNA levels were quantified, The Mouse Brain in Stereotaxic Coordinates (Paxinos and Franklin, 2nd edition) was used as a reference. Pyramidal cell layers, in which DOPr mRNAs are strongly expressed, served as boundaries to delineate the other layers.

2.1.4.7 Electron microscopy

1) Tissue processing and imaging: Brain sections from Bregma 2.92 mm to -3.52 mm were rinsed in PBS (50 mM, pH 7.4), postfixed flat in 1% osmium tetroxide, dehydrated in ascending concentrations of ethanol, treated with propylene oxide, and impregnated in Durcupan (Sigma-Aldrich, Oakville, ON, Canada) overnight at room temperature as described (Bisht *et al,* 2016b). After resin polymerization at 55°C for 72 h, the areas of interest containing ventral HPC CA1 were cut at 70 nm with an ultramicrotome (Leica Ultracut UC7). Ultrathin sections were collected on square-mesh grids and examined at 80kV using a FEI Tecnai Spirit G2 microscope. For analysis, 16 pyramidal cells and 10 interneurons on average, in each of *strata oriens* and *radiatum*, were randomly photographed at magnifications between 890X and 4800X using an ORCA-HR camera (10 MP; Hamamatsu). *Strata radiatum* and *oriens* were identified based on their cellular and subcellular contents, and position relative to the CA1 pyramidal layer.

2) Ultrastructural analysis: Only neurons showing a nuclear profile above 3 **m**m in diameter (measured with ImageJ) were included in the analysis. Well-characterized ultrastructural features were used to assess cellular stress. Cytoplasmic and nucleoplasmic condensation (Peters *et al*, 1998) induces a ‘‘dark’’ appearance of neuronal soma, nucleus as well as dendrites and axons. Soma whose mean gray value was below 125 arbitrary units were considered as ‘‘dark’’. Rough ER and Golgi apparatus dilation was identified by the expansion of lumen widths above 100 nm. Soma presenting at least one of these features were scored (Schonthal, 2012; Welch *et al*, 1985). Nuclear membrane indentation above 600 nm (Davies *et al*, 1997) and lipofuscin granules recognized by their darker, granular, heterogeneous matrix and considered a hallmark of aging (Sohal *et al*, 1986) were also quantified. The proportion of neurons displaying at least one of each of these features was determined for each subpopulation analyzed (pyramidal cells, interneurons from *stratum oriens*, and from *stratum radiatum*).

2.1.4.8 Statistical analyses

Statistical significance and normality were calculated using GraphPad version 6.0 (La Jolla, CA, USA). All variables were normally distributed based on Bartlett’s test. Statistical

outliers which were identified using Grubb's test were removed from the analyses. Student t-test was used to assess effectiveness of SNC80 treatment. Multiple comparisons were performed by one-way ANOVA followed by Bonferroni *post hoc* analyses for behavioral characterization and in situ hybridization. Two-way ANOVA with Bonferroni *post hoc* analyses were used to assess the behavioral characterization as well as the effects of SNC80 treatment in other experiments. For the behavioral characterization, the two examined factors are the stress phenotype (non-stressed control, resilient or vulnerable mice) and the presence or absence of a CD1 mouse in the wire mesh enclosure during the SI test. Regarding electron microscopy (EM) analyses, the two examined factors are the stress phenotype and the presence or absence of SNC80 treatment. All data are presented as means ± standard error of the mean (SEM).

2.1.5 Results

2.1.5.1 Vulnerable mice display a strong social avoidance behavior upon repeated social defeat.

A chronic social defeat stress in mice was performed for 10 days followed by a SI test on the next day. Behavioral results are presented in Figure 16. Figure 16A presents a schematic overview of the open-field arena used for the SI test, which is divided into three main zones (interaction, corners, center). Figure 16B provides examples of movement track plots inside the SI test arena in the absence (off target) vs. presence of an aggressive CD1 in the wire mesh container (with target). The tested mice freely explored the entire arena in the absence of a CD1 mouse (top panel), and this pattern was modified when a CD1 mouse was introduced: control and resilient mice tend to spend more time interacting with the CD1 (bottom left and middle panels) while a progression toward the CZs was generally observed with the vulnerable mice (bottom right panel). This exploration pattern was quantified, thus allowing to determine the SI and CZ ratios. Resilient mice with a SI ratio above or equal to 1 accounted for 33% of the population (10 resilient mice out of 30), whereas vulnerable mice with a SI ratio inferior to 1 accounted for 67% of the population (20 vulnerable mice out of 30; Figure 16C), as expected for the RSD paradigm in mice (Golden *et al*, 2011). Non-stressed control mice presenting a SI ratio below 1 (suggesting a stressed phenotype) were removed from the experiment, as shown by the encircled symbols in Figure 16C.

Two-way ANOVA was performed to assess differences in the time spent in the IZ and CZs between stress phenotypes, in the presence vs. in the absence of a CD1 mouse (Figures 16E, G). ANOVA analysis of the time spent in the IZ revealed main effects of stress phenotype (Figure 1E: $F_{(2,90)} = 9.318$, $p = 0.0002$), and interaction target by stress phenotype ($F_{(2,90)} = 25.81$, $p < 0.0001$). *Post hoc* analysis especially revealed that control and resilient mice spent more time interacting with the CD1 mouse than vulnerable ones (Figure 16E). Consequently, vulnerable individuals presented a reduced SI ratio compared to control and resilient mice (Figure 16F: $F_{(2,45)} = 51.21$, $p < 0.0001$). The time spent in the CZs showed main effects of stress phenotype (Figure 16H: $F_{(2,90)} = 6.397$, $p = 0.0025$) and interaction ($F_{(2,90)} = 8.697$, $p = 0.0004$). In presence of a CD1 mouse, vulnerable mice spent

more time in the CZs than control and resilient mice without significant difference between control and resilient mice (Figure 16G). Thus, vulnerable mice had an increased CZ ratio as compared with control and resilient mice (Figure 16H: $F_{(2,44)} = 7.738$, $p = 0.0013$), indicating a strong social avoidance behavior in the SI test. These results are in accordance with the Nature Protocol described by Golden et al. (2011). Confirming efficacy of our stress paradigm, we found that stressed mice, whether resilient or vulnerable, presented higher plasmatic corticosterone levels than non-stressed controls (Figure 16D: $F_{(2,45)} = 7.244$, $p = 0.0019$).

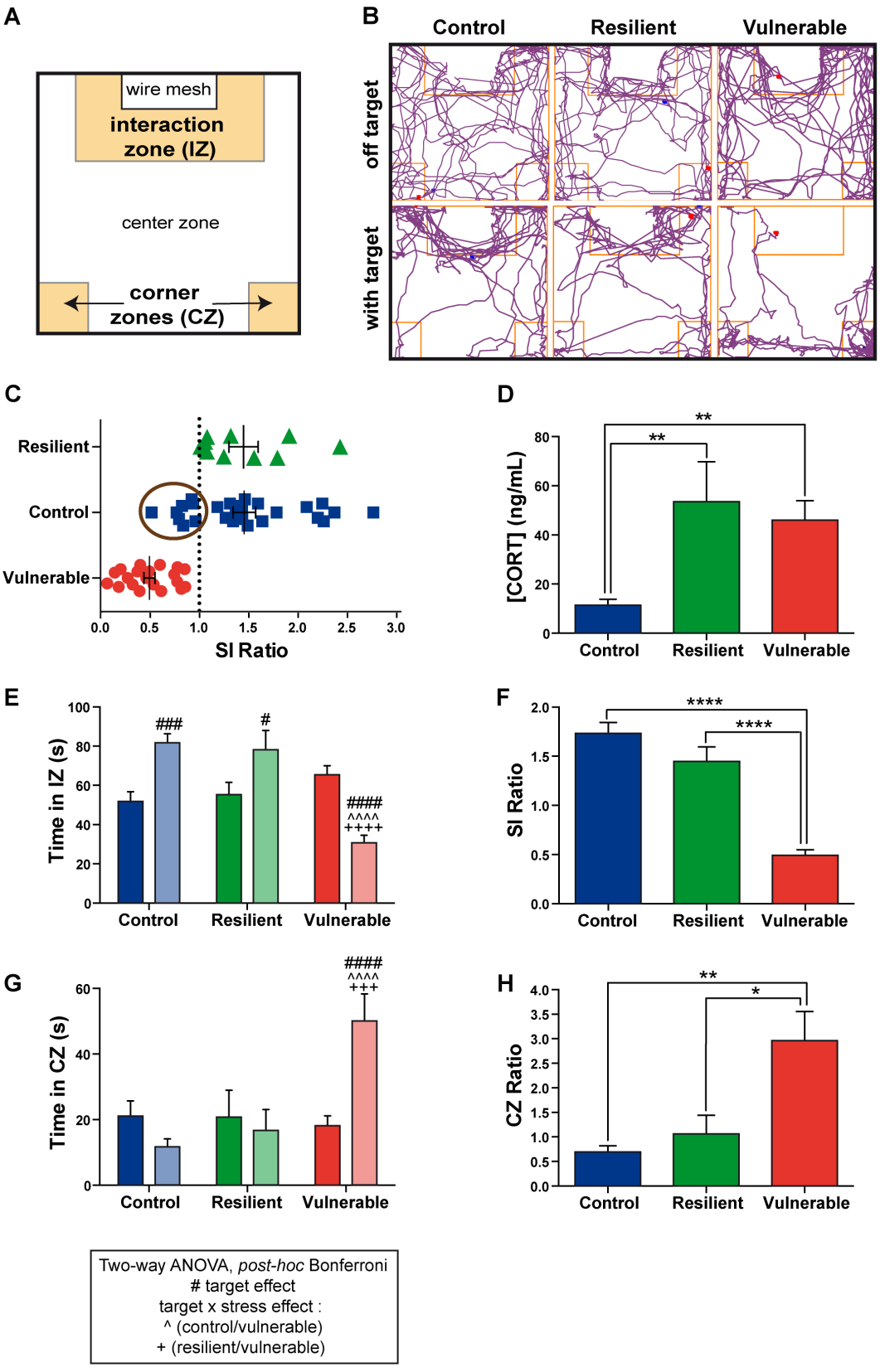
A
wire mesh
interaction zone (IZ)
center zone
corner zones (CZ)
B
Control
Resilient
Vulnerable
off target
with target
C
Resilient
Control
Vulnerable
0.0
0.5
1.0
1.5
2.0
2.5
3.0
SI Ratio
D
[CORT] (ng/mL)
**
**
Control
Resilient
Vulnerable
E
Time in IZ (s)
###
#
####
^^^^
++++
Control
Resilient
Vulnerable
F
SI Ratio
****
****
Control
Resilient
Vulnerable
G
Time in CZ (s)
####
^^^^
+++
Control
Resilient
Vulnerable
H
CZ Ratio
**
*
Control
Resilient
Vulnerable
Two-way ANOVA, post-hoc Bonferroni
target effect
target x stress effect :
^ (control/vulnerable)
+ (resilient/vulnerable)

Figure 16. Vulnerable mice display a strong social avoidance behavior upon repeated social defeat (RSD). (A) Schematic overview of the social interaction (SI) arena. (B) Examples of movement track plots for control, resilient and vulnerable mice inside the SI test arena in the absence (off target) vs. presence of an aggressive CD1 (with target). (C) Distribution of SI ratio among the mouse population. N(control, C) = 26, N(resilient, R) = 10, N(vulnerable, V) = 20. Error bars are mean standard error of the mean (SEM). (D) The plasmatic corticosterone levels are increased in resilient and vulnerable mice compared to controls as measured by ELISA, confirming effectiveness of the stress paradigm. Error bars are mean ± SEM. (E) Control and resilient mice spend more time, and vulnerable mice less time, in the interaction zone (IZ) in the presence vs. absence of an aggressive CD1 mouse. (F) Vulnerable mice present a reduced SI ratio compared to control and resilient mice. (G) Control and resilient mice spend the same time, while vulnerable mice spend more time, in the corner zones (CZs) in the presence or absence of an aggressive CD1 mouse. (H) Vulnerable mice present an increased CZ ratio compared to control and resilient mice. For (E, G): Two-way ANOVA, Bonferroni *post hoc* analysis, n(C) = 18, n(R) = 10, n(V) = 20, $^{\#}p < 0.05$, $^{\#\#\#}$, $^{+++}p < 0.001$, $^{\#\#\#\#}$, $^{\wedge\wedge\wedge\wedge}$, $^{++++}p < 0.0001$. The two analyzed factors are the stress phenotype (blue, green and red bars for control, resilient and vulnerable mice, respectively) and the presence (pale shades) or absence (dark shades) of a CD1 mouse. $^{\#}$for target effect, for stress x target effect, $^{\wedge}$(Control vs. Vulnerable), $^{+}$(Resilient vs. Vulnerable). For (D, F, H): One-way ANOVA, Bonferroni *post hoc* analysis, N(C) = 18, N(R) = 10, N(V) = 20, $^{*}p < 0.05$, $^{**}p < 0.01$, $^{****}p < 0.0001$. Error bars are mean ± SEM.

2.1.5.2 Decreased expression levels of ENK and DOPr are associated with vulnerability to stress.

To study the involvement of ENK signaling in stress resilience under the RSD, we performed radioactive in situ hybridization and quantified the expression levels of ENKs mRNA in BLA of control, resilient and vulnerable mice. Representative schematic of BLA is provided in Figure 17A (Bregma -1.94 mm). Representative autoradiography images from control, resilient and vulnerable mice are presented in Figure 17C. Resilience to chronic stress was previously associated with reduced ENKs mRNA levels in BLA of vulnerable rats upon social defeat, and inactivation of ENKs in the same area reproduced a vulnerability phenotype (Berube *et al*, 2013; Berube *et al*, 2014). Similarly, our current analysis revealed a significant reduction of ENKs mRNA in the BLA of vulnerable mice compared to control and resilient ones (Figure 17B: $F_{(2,28)} = 6.491$, $p = 0.0048$), without significant difference between resilient and control animals (Figure 17B). The combined results suggest conservation across rodent species of ENK involvement in the resilience to chronic social stress. To dissect the ENK circuitry mediating stress resilience, radioactive in situ hybridization against DOPr was next performed. Neurons from the BLA are known to

innervate the dorsolateral caudoputamen, prefontal cortex, HPC, and several hypothalamic nuclei in rodents (Hoover and Vertes, 2007; Petrovich *et al*, 2001). Our analyses focused on the HPC, considering its critical regulation of the hypothalamic-pituitary-adrenal axis during stress (McEwen *et al*, 2015), the known interplay between the amygdala and the HPC in chronic stress response (Vyas *et al*, 2002), and the abundant expression of DOPr in the HPC (Erbs *et al*, 2012). The analyses were performed across the dorsal, central, and ventral HPC (Bregma at -2.06 mm, -2.70 mm and -3.08 mm), comparing the CA1, CA3, and ventral *subiculum* regions (Figure 17D). Quantitative analysis revealed that DOPr mRNA expression levels are significantly reduced in vulnerable mice vs. control and resilient animals, in only one examined region: *stratum oriens* of the CA1 from ventral HPC (Figure 17E: $F_{(2,29)} = 7.588$, $p = 0.0022$). Representative autoradiography images are shown in Figure 17F. To support specificity of the probe against DOPr, pictures for negative control are shown in Supplementary Figure 23. A table is provided in the Supplemental information presenting data from all the hippocampal regions analyzed by in situ hybridization (Supplementary Table 4).

ENK mRNA in BASOLATERAL AMYGDALA under the repeated social defeat paradigm

A Basolateral amygdala (BLA)

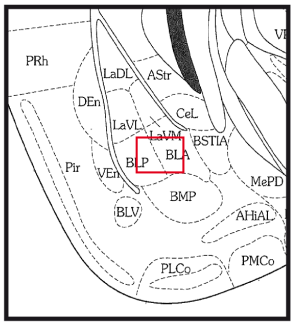

B ENK mRNA in BLA

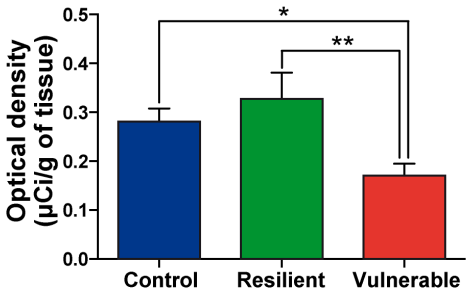

C

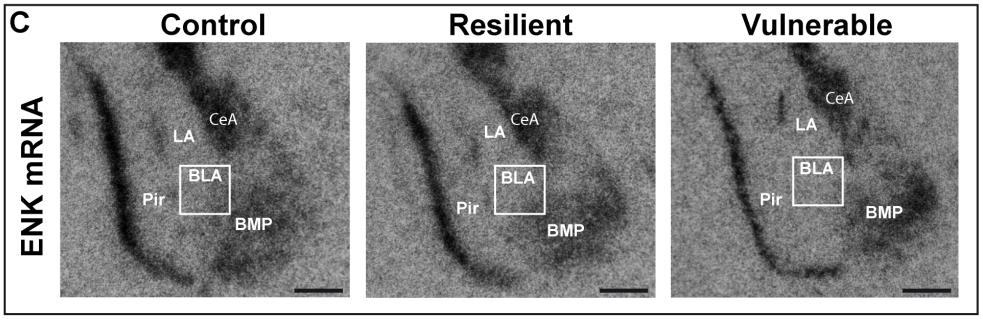

DOPr mRNA in HIPPOCAMPUS under the repeated social defeat paradigm

D Hippocampus (HPC)

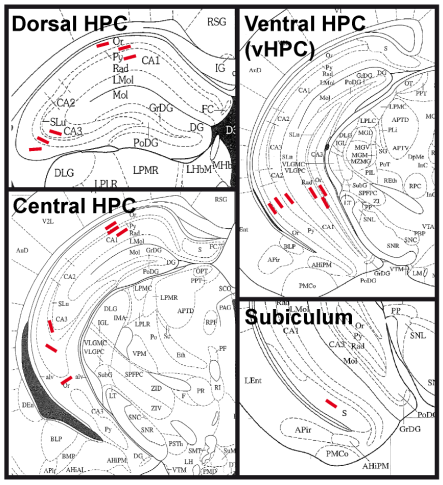

E DOPr mRNA in vHPC-CA1-*oriens*

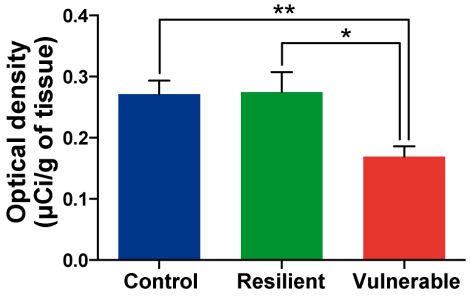

F

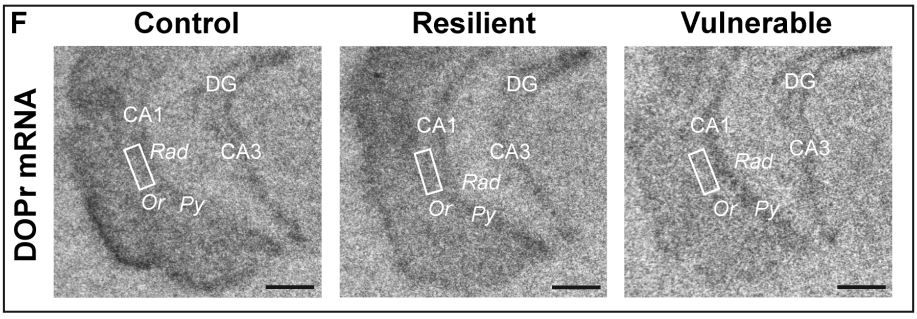

Figure 17. Decreased expression levels of enkephalin (ENK) and delta opioid receptors (DOPr) mRNA are associated with vulnerability to social stress. (A) Schematic overview of amygdala region (Bregma -1.94 mm), Image credit: *Franklin and Paxinos, 2nd edition*. (B) ENK mRNA are decreased in the basolateral nucleus of amygdala (BLA) of vulnerable mice after RSD. (C) Magnified view of representative autoradiographs showing the amygdalar region selected (Bregma -1.94 mm) for ENK mRNA quantification by radioactive in situ hybridization. Scale bar = 0.5 mm. (D) Schematic overview of Hippocampus (HPC) for quantification in dorsal (Bregma -1.82 mm), central (Bregma -2.54 mm) and ventral HPC (Bregma -3.08 mm), and subiculum region (Bregma -3.52 mm), Image credit: *Franklin and Paxinos, 2nd edition*. (E) DOPr mRNA are decreased in the *oriens* layer (Or) of CA1 HPC in vulnerable mice after RSD. (F) Magnified view of representative autoradiographs showing the ventral HPC region selected (Bregma -3.08 mm) for DOPr mRNA quantification by radioactive *in situ* hybridization. Scale bar = 0.5 mm. For (B, E) One-way ANOVA, Bonferroni *post hoc* analysis, N(C) = 11, N(R) = 7, N(V) = 13, $^{*}p < 0.05$, $^{**}p < 0.01$. Error bars are mean ± SEM. The nomenclature used is from *the Mouse brain atlas, Paxinos and Franklin, 2nd edition*. BMP, posterior basomedial nucleus of amygdala; CeA, central amygdala; LA, lateral amygdala; BLA, basolateral amygdala; Pir, piriform cortex; CA1/CA3, regions in HPC; DG, dentate gyrus; Py, *stratum pyramidale*; Rad, *stratum radiatum*; Or, *stratum oriens*.

2.1.5.3 Administration of a DOPr agonist, SNC80, promotes a resilience phenotype.

To study the functional role of DOPr signaling in stress resilience under the RSD in mice, the DOPr agonist SNC80 was injected 1 h prior to each social defeat session. First, we confirmed the effectiveness of 10 mg/kg SNC80 using the FST and TST: individuals treated with SNC80 showed reduced immobility time compared to saline-treated ones in both paradigms (Figure 18A: $t = 3.635$, $p = 0.0034$; Figure 18B: $t = 3.249$, $p = 0.0045$), indicating that the dose we used induced as expected antidepressant effects. The RSD paradigm was next performed on another cohort of naive mice to determine the effects of SNC80 treatment on social stress responses (Figures 18C–G). Figure 3C displays the distribution of SI ratio and Figures 18D–G the strong social avoidance behavior of vulnerable mice. Resilient and control mice displayed a SI ratio above 1 whereas vulnerable ones showed a SI ratio below 1 (Figure 18C). Two-way ANOVA was performed to address significant differences in the time spent in the IZ and CZs between stress phenotypes in the presence vs. in the absence of a CD1 mouse (Figures 18D, F). Control and resilient mice spent more time interacting with a CD1, while vulnerable ones decreased their interaction thus reducing the SI ratio (Figures 18D, E). Vulnerable mice spent more time in the CZs than control and resilient ones and thus presented a higher CZ ratio (Figures 18F, G). The

SI ratio of both resilient and vulnerable mice was significantly increased when SNC80 treatment was administered throughout the RSD, compared to the SI ratio calculated without SNC80 (Figure 18H: $t = 2.662$, $p = 0.0103$). The proportion of resilient mice increased from 33% to 58% of the total population (Figure 18I), demonstrating the capacity of SNC80 to prevent the emergence of depressive-like behavior upon RSD.

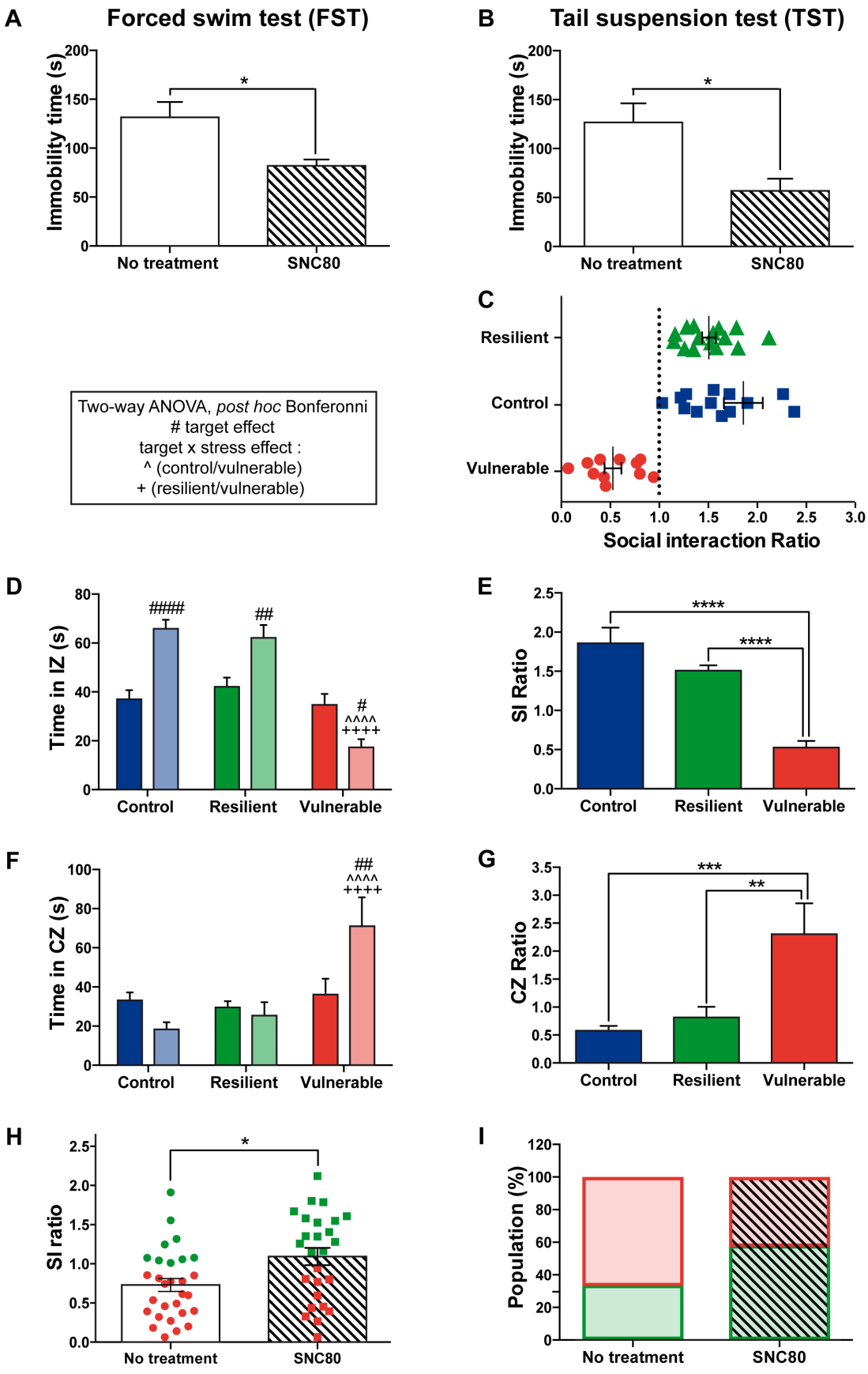
A
Forced swim test (FST)
Immobility time (s)
200
150
100
50
0
*
No treatment
SNC80
B
Tail suspension test (TST)
Immobility time (s)
200
150
100
50
0
*
No treatment
SNC80
C
Resilient
Control
Vulnerable
0.0
0.5
1.0
1.5
2.0
2.5
3.0
Social interaction Ratio
Two-way ANOVA, post hoc Bonferonni
target effect
target x stress effect :
^ (control/vulnerable)
+ (resilient/vulnerable)
D
Time in IZ (s)
80
60
40
20
0
####
##
#
^^^^
++++
Control
Resilient
Vulnerable
E
SI Ratio
2.5
2.0
1.5
1.0
0.5
0.0
****
****
Control
Resilient
Vulnerable
F
Time in CZ (s)
100
80
60
40
20
0
##
^^^^
++++
Control
Resilient
Vulnerable
G
CZ Ratio
3.5
3.0
2.5
2.0
1.5
1.0
0.5
0.0
***
**
Control
Resilient
Vulnerable
H
SI ratio
2.5
2.0
1.5
1.0
0.5
0.0
*
No treatment
SNC80
I
Population (%)
120
100
80
60
40
20
0
No treatment
SNC80

Figure 18. Administration of a DOPr agonist, SNC80, promotes a resilience phenotype. (A) Validation of SNC80 effectiveness in the forced swim test (FST). The time spent immobile is decreased with SNC80 treatment. White bar corresponds to no treatment and the streaky pattern to SNC80 treatment. Unpaired t-test, two tailed, *p < 0.05. N = 6 for each group. Error bars are mean ± SEM. **(B)** Validation of SNC80 effectiveness in the tail suspension test (TST). The time spent immobile is decreased with SNC80 treatment. White bar corresponds to no treatment and the streaky pattern to SNC80 treatment. Unpaired t-test, two tailed, *p < 0.05. N = 10 for each group. Error bars are mean ± SEM. **(C)** Distribution of SI ratio among the mouse population. N(C) = 16, N(R) = 15, N(V) = 11. Error bars are mean ± SEM. **(D)** Control and resilient mice spend more time, and vulnerable mice less time, in the IZ in the presence vs. absence of an aggressive CD1 mouse. **(E)** Vulnerable mice present a reduced SI ratio compared to control and resilient mice. **(F)** Control and resilient mice spend the same time, while vulnerable mice spend more time, in the CZs in the presence or absence of an aggressive CD1 mouse. **(G)** Vulnerable mice present an increased CZ ratio compared to control and resilient mice. For **(D, F)**: two-way ANOVA, Bonferroni *post hoc* analysis, N(C) = 16, N(R) = 15, N(V) = 11, $^{\#}$p < 0.05, $^{\#\#}$p < 0.01, $^{\#\#\#\#}$, $^{\wedge\wedge\wedge\wedge}$, $^{++++}$ p < 0.0001. The two analyzed factors are the stress phenotype (blue, green and red bars for control, resilient and vulnerable mice, respectively) and the presence (pale shades) or absence (dark shades) of a CD1 mouse. $^{\#}$for target effect, for stress x target effect, $^{\wedge}$(Control vs. Vulnerable), $^{+}$(Resilient vs. Vulnerable). For **(E, G)**: One-way ANOVA, Bonferroni post hoc analysis, N(C) = 16, N(R) = 15, N(V) = 11, **p < 0.01, ***p < 0.001, ****p < 0.0001. Error bars are mean ± SEM. **(H)** SNC80 (No treatment) during RSD increases the SI ratio compared to a classical RSD (No treatment). Green dots and squares correspond to resilient mice while the red ones represent vulnerable mice. Solid bar corresponds to no treatment and the streaky pattern to SNC80 treatment. Unpaired t-test, N(no treatment, NT) = 29; N(SNC80) = 26, *p < 0.05. Error bars are mean ± SEM. **(I)** Chronic treatment with SNC80, administered 1 h prior to the defeat during the 10 days of stress, increases the proportion of resilient mice after a classical protocol of RSD (No treatment). Resilient mice are represented by green squares while vulnerable ones are in red. Solid bar corresponds to no treatment and the streaky pattern to SNC80 treatment. N(NT) = 29, N(SNC80) = 26.

2.1.5.4 SNC80 treatment prevents oxidative stress in hippocampal CA1 neurons.

To identify mechanisms by which stimulating DOPr signaling promotes stress resilience in mice, we tested the hypothesis that SNC80 reduces oxidative stress in the ventral HPC CA1. The ventral HPC CA1 was specifically targeted considering that: (1) in the current study a significant difference of DOPr mRNA expression between resilient and vulnerable mice was only observed in this region among the entire HPC; (2) dense neuronal projections from BLA to the ventral HPC CA1 were described (Petrovich *et al*, 2001) as well as implicated in anxiety (Felix-Ortiz *et al*, 2013); and (3) this region plays a prominent role in social memory (Okuyama *et al*, 2016). To address this question, TEM was used to

measure well-established features of cellular stress among CA1 neurons of control, resilient, and vulnerable mice, with or without SNC80 treatment. Considering that DOPr is strongly expressed by CA1 *stratum oriens* GABAergic interneurons (Stumm *et al*, 2004) that make synapses onto pyramidal cells and *stratum radiatum* interneurons (Maccaferri, 2005), the three neuronal subpopulations were selected for analysis. Representative images are respectively provided in Figures 19A–J (*stratum pyramidale*), Figures 20A–J (*stratum oriens*) and Figures 21A–J (*stratum radiatum*). Two-way ANOVA was systematically performed to address significant differences in oxidative features between stress phenotypes in the presence vs. in the absence of SNC80 treatment (Figures 19, 20, 21). The condensation of cytoplasmic and nucleoplasmic contents, resulting in a ‘‘dark’’ appearance in EM, has been associated with the shrinkage of cells undergoing oxidative stress (Bisht *et al*, 2016a; Oster-Granite *et al*, 1996; Tremblay *et al*, 2012). ANOVA analysis of dark neurons revealed main effects of stress phenotype (Figure 19K: $F_{(2,282)} = 4.453$, $p = 0.0125$) and SNC80 treatment on their prevalence in the CA1 *stratum pyramidale* (Figure 19K: $F_{(1,282)} = 19.76$, $p < 0.0001$). *Post hoc* analysis especially revealed an increased prevalence of dark pyramidal cells in vulnerable mice compared to resilient and non-stressed ones (Figure 19K). After treatment with SNC80, this increased prevalence observed upon stress in vulnerable mice was prevented (Figure 19K). ANOVA further identified treatment effects in both *strata oriens* (Figure 20K: $F_{(1,157)} = 5.403$, $p = 0.0214$) and *radiatum* (Figure 21K: $F_{(1,142)} = 13.15$, $p = 0.0004$), and a stress phenotype by treatment interaction in *stratum radiatum* (Figure 21K: $F_{(2,142)} = 8.918$, $p = 0.0002$). In particular, control and vulnerable mice treated with SNC80 displayed a decreased prevalence of dark interneurons in *stratum radiatum* compared to non-treated control and vulnerable mice (Figure 21K). However, post hoc analysis did not reveal significant differences in *stratum oriens* (Figure 20K). Surprisingly, control mice, which were housed in the room where RSD occurred, displayed a significant proportion of ‘‘dark neurons’’ in *stratum radiatum* (Figure 21K) suggesting some degree of stress in these animals witnessing the social defeat. The analysis of neurons with a dilated ER, considered the best characterized feature of cellular stress at the ultrastructural level (Schonthal, 2012), revealed main effects for both treatment (Figure 19L: $F_{(1,282)} = 67.46$, $p < 0.0001$) and interaction (Figure 19L: $F_{(2,282)} = 6.240$, $p < 0.0022$) in *stratum pyramidale*, and treatment effects in *strata oriens* (Figure 20L: $F_{(1,157)} = 22.43$, p

< 0.0001) and *radiatum* (Figure 21L: $F_{(1,142)} = 24.12$, $p < 0.0001$). Precisely, the proportion of neurons with a dilated ER was reduced by SNC80 treatment in *stratum pyramidale* from control and vulnerable mice compared to non-treated control and vulnerable ones (Figure 19L). For the interneurons, this reduction induced by SNC80 was observed in resilient and vulnerable mice (*stratum oriens*, Figure 20L and *stratum radiatum*, Figure 21L). The proportion of neurons displaying a dilated Golgi apparatus, documented as another cellular stress marker (Welch *et al*, 1985), revealed main treatment (Figure 19M: $F_{(1,282)} = 7.664$, $p = 0.0060$) and interaction (Figure 19M: $F_{(2,282)} = 3.263$, $p = 0.0397$) effects in pyramidal cells. A main stress phenotype effect was also observed in *stratum oriens* (Figure 20M: $F_{(2,257)} = 4.109$, $p < 0.0001$), but failed to reach significance in *stratum radiatum* (Figure 21M). *Post hoc* analysis revealed a decreased proportion of neurons displaying a dilated Golgi apparatus upon SNC80 treatment in *stratum pyramidale* of vulnerable mice (Figure 19M). No significant differences were observed for interneurons of *oriens* and *radiatum* layers (Figures 20M, 21M). Finally, quantitative analyses of lipofuscin granules, i.e., cytoplasmic granules resulting from the oxidation of unsaturated fatty acids which are related to cellular aging (Sohal *et al*, 1986), were conducted. Although stress phenotype and treatment effects failed to reach statistical significance in ANOVA for all layers (Figures 19N, 20N, 21N), the number of neurons showing lipofuscin granules was found to be significantly reduced upon *post hoc* analyses in pyramidal cells of SNC80-treated vulnerable mice compared to non-treated ones (Figure 19N). Nuclear indentations, also related to cellular aging (Roos *et al*, 1983), displayed a main stress phenotype effect (Figure 19O: $F_{(2,282)} = 6.106$, $p = 0.0025$) and a main stress phenotype by treatment effect in *stratum pyramidale* (Figure 4O: $F_{(2,282)} = 8.742$, $p = 0.0002$) while only a stress phenotype effect was identified in *stratum radiatum* (Figure 21O: $F_{(2,142)} = 4.656$, $p = 0.0110$). Thus, treated vulnerable mice exhibited an increased prevalence of neurons presenting indentations compared to treated resilient and control mice in *stratum pyramidale* (Figure 19O). Moreover, the prevalence of neurons showing nuclear indentations was specifically increased in *stratum pyramidale* of treated vulnerable mice vs. non-treated ones (Figure 19O). Finally, *post hoc* analyses revealed a significant increase of *strata oriens* and *radiatum* interneurons with indentations in treated vulnerable mice compared to treated controls (Figures 20O, 21O). Tables are provided in Supplemental information presenting

values for the two-way ANOVAs followed by Bonferroni *post hoc* analyses for each analyzed layer (Supplementary Tables 5, 6, 7). Overall, these findings suggest that SNC80 treatment prevents the occurrence of cellular stress among CA1 pyramidal cells and interneurons, ultimately promoting resilience to chronic social stress.

NEURONS from *stratum PYRAMIDALE*

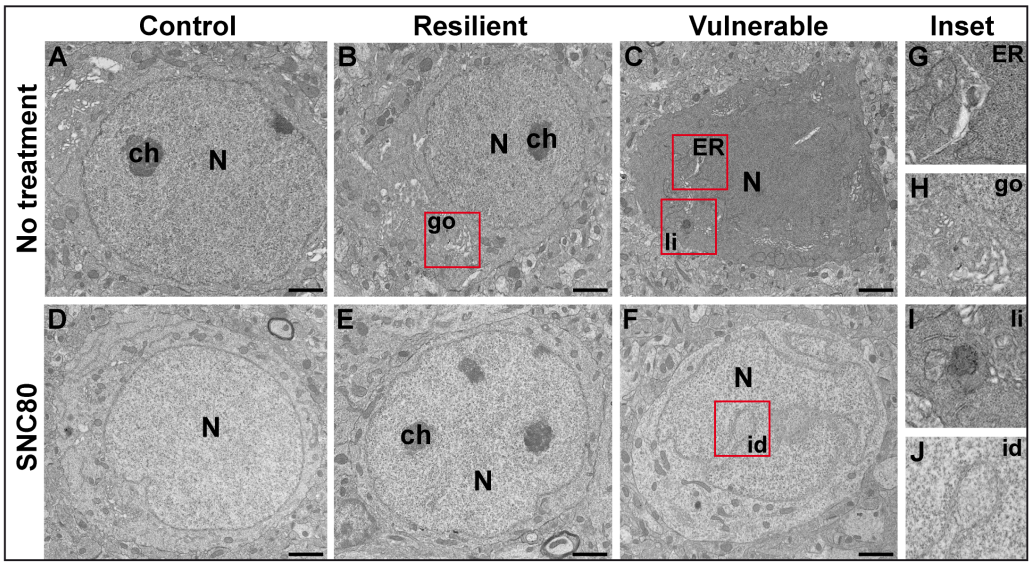

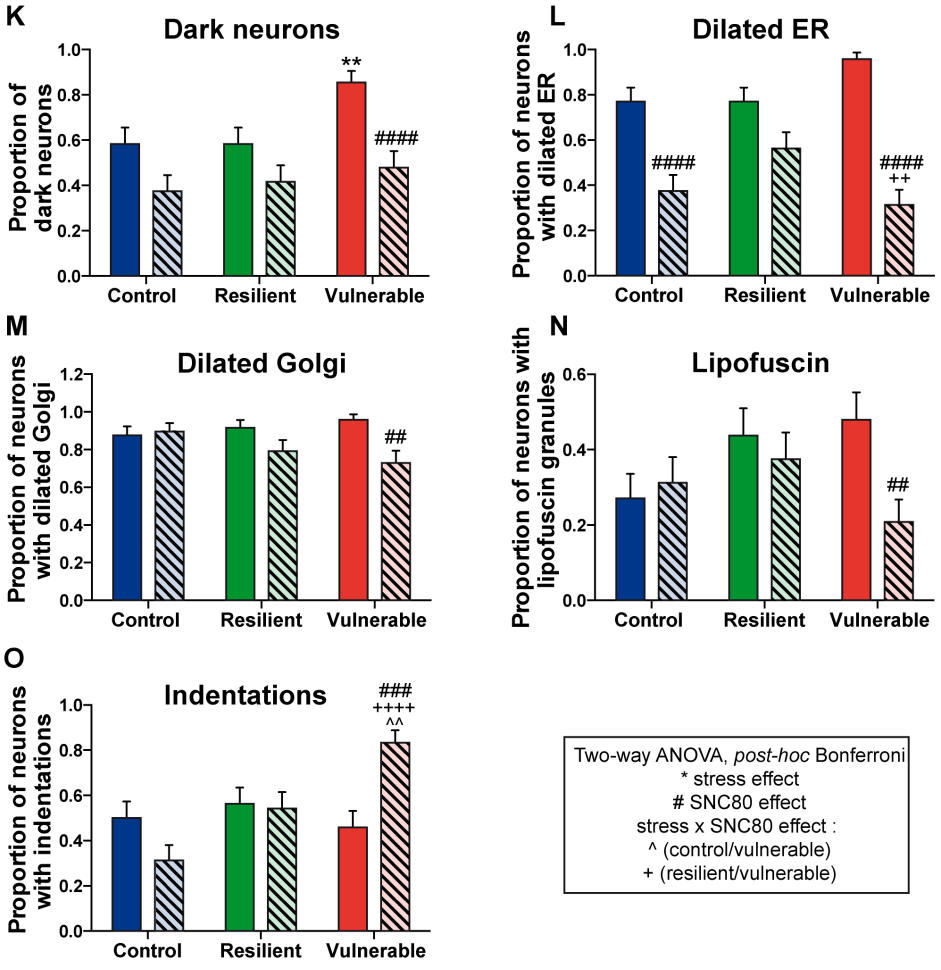

Two-way ANOVA, *post-hoc* Bonferroni
* stress effect
\# SNC80 effect
stress x SNC80 effect :
^ (control/vulnerable)
\+ (resilient/vulnerable)

Figure 19. SNC80 treatment prevents oxidative stress in pyramidal cells of CA1 HPC. In **(A–C)**, representative pictures of neurons (N) in the pyramidal layer (Py) of CA1 region in ventral HPC after RSD without treatment (NT), in control, resilient and vulnerable mice, are shown respectively. In **(D–F)**, pictures of neurons from the Py layer of CA1 in vHPC after RSD with SNC80 treatment (SNC80), in control, resilient and vulnerable mice, respectively. Scale bar = 500 nm. In **(G–J)**, magnified views of dilated endoplasmic reticulum (ER), dilated Golgi apparatus (go), lipofuscin granule (li) and nuclear indentation (id), respectively. In **(K–O)**, graphs for Py layer representing the proportion of dark neurons, the proportion of neurons presenting dilated ER, dilated Golgi apparatus, lipofuscin granules and indentations, respectively, without and with SNC80 treatment. Two-way ANOVA, Bonferroni *post hoc* analysis, N = 48 cells for each condition. The two analyzed factors are the stress phenotype (blue, green and red bars for control, resilient and vulnerable mice under RSD, respectively) and the presence or absence of SNC80 treatment (dark blue, green and red bars for control, resilient and vulnerable mice under RSD without SNC80 treatment, respectively, and pale blue, green and red bars with a streaky pattern for control, resilient and vulnerable mice under RSD with SNC80 treatment, respectively). Significance: *for stress phenotype effect or $^{\#}$for SNC80 treatment effect or for stress x treatment effect, $^{\wedge}$(Control vs. Vulnerable), $^{+}$(Resilient vs. Vulnerable) = **, $^{\#\#}$, $^{\wedge\wedge}p < 0.01$, $^{\#\#\#}p < 0.001$, $^{\#\#\#\#}$, $^{++++}p < 0.0001$. Error bars are mean ± SEM.

NEURONS from *stratum ORIENS*

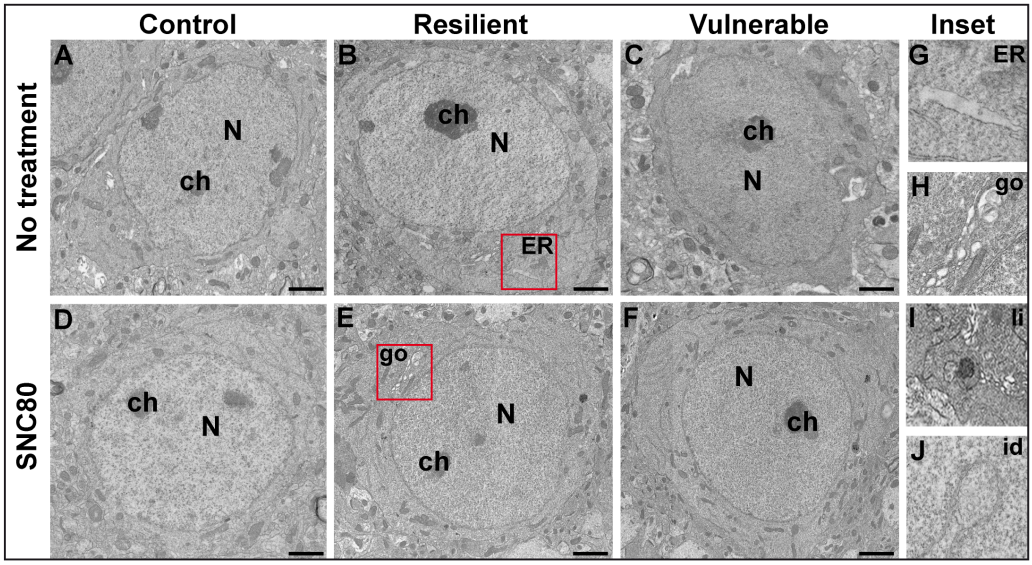

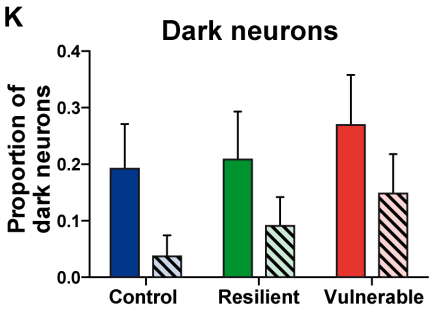

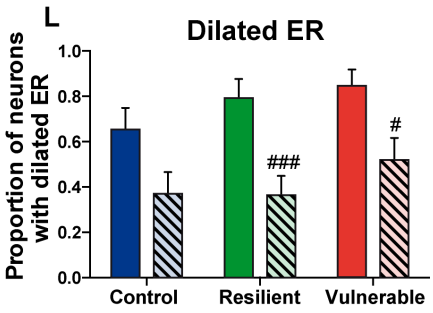

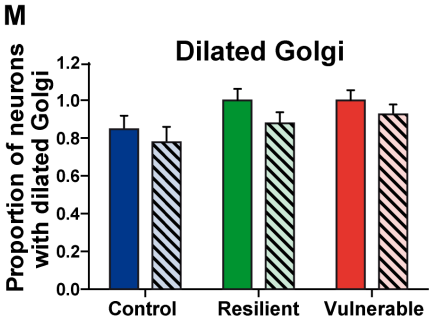

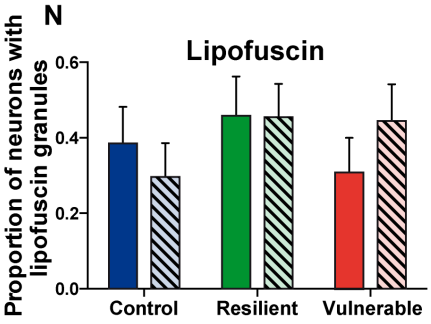

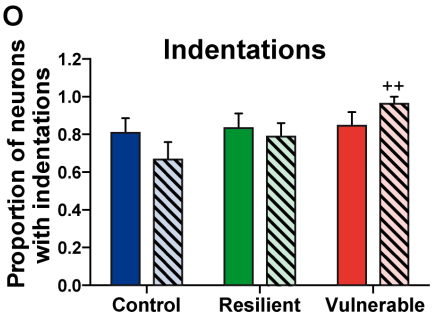

Two-way ANOVA, *post-hoc* Bonferroni
* stress effect
\# SNC80 effect
stress x SNC80 effect :
^ (control/vulnerable)
\+ (resilient/vulnerable)

Figure 20. SNC80 treatment reduces oxidative stress in interneurons from stratum oriens of CA1 HPC. In (A–C), representative pictures of neurons (N) in the *oriens* layer (Or) of CA1 region in ventral HPC after RSD without treatment (NT), in control, resilient and vulnerable mice, are shown respectively. In (D–F), pictures of neurons from the Or layer of CA1 in vHPC after RSD with SNC80 treatment (SNC80), in control, resilient and vulnerable mice, respectively. Scale bar = 500 nm. In (G–J), magnified views of dilated ER, dilated Golgi apparatus (go), lipofuscin granule (li), and nuclear indentation (id), respectively. In (K–O), graphs for Or layer representing the proportion of dark neurons, the proportion of neurons presenting dilated ER, dilated Golgi apparatus, lipofuscin granules and indentations, respectively, without and with SNC80 treatment. Two-way ANOVA, Bonferroni *post hoc* analysis, N(NT: C; R; V) = 26; 24; 26 cells and N(SNC80: C; R; V) = 27; 33; 27 cells. The two analyzed factors are the stress phenotype (blue, green and red bars for control, resilient and vulnerable mice under RSD, respectively) and the presence or absence of SNC80 treatment (dark blue, green and red bars for control, resilient and vulnerable mice under RSD without SNC80 treatment, respectively, and pale blue, green and red bars with a streaky pattern for control, resilient and vulnerable mice under RSD with SNC80 treatment, respectively). Significance: *for stress phenotype effect or $^{\#}$for SNC80 treatment effect or for stress x treatment effect, $^{\wedge}$(Control vs. Vulnerable), $^{+}$(Resilient vs. Vulnerable) = $^{\#}p < 0.05$, $^{\wedge\wedge}p < 0.01$, $^{\#\#\#}p < 0.001$. Error bars are mean ± SEM.

NEURONS from *stratum RADIATUM*

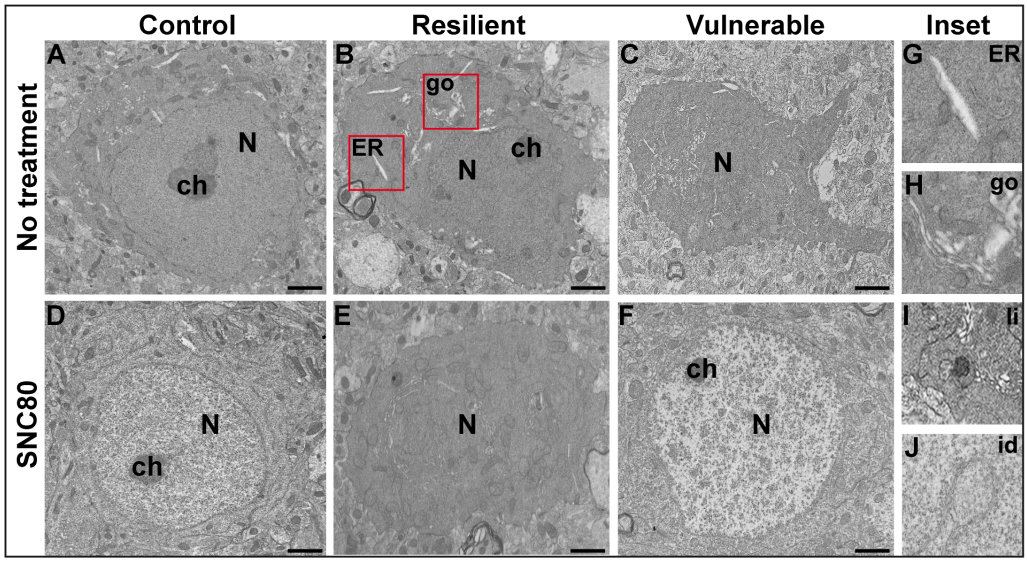

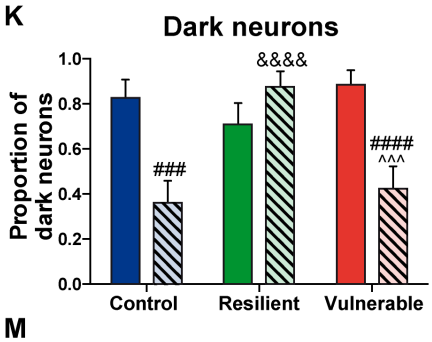

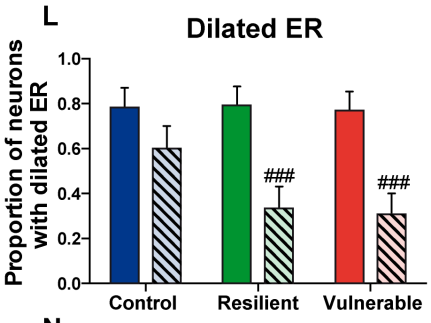

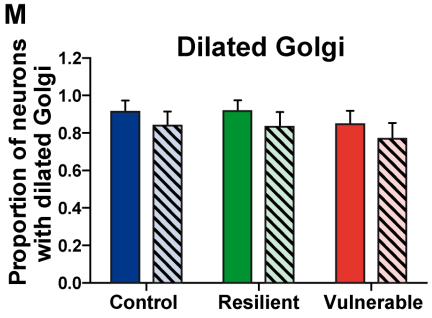

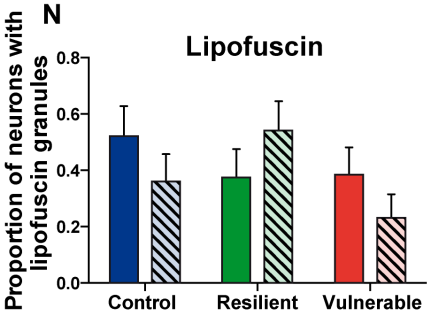

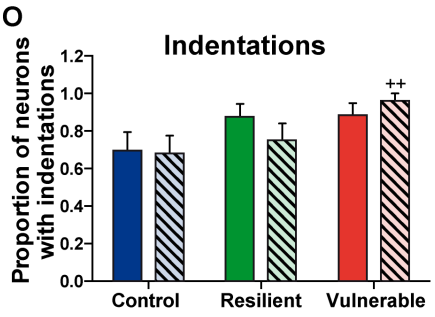

Two-way ANOVA, *post-hoc* Bonferroni
* stress effect
\# SNC80 effect
stress x SNC80 effect :
^ (control/vulnerable)
\+ (resilient/vulnerable)
& (control/resilient)

Figure 21. SNC80 treatment reduces oxidative stress in interneurons from *stratum radiatum* of CA1 HPC. In (A–C), representative pictures of neurons (N) in the *radiatum* layer (Rad) of CA1 region in ventral HPC after RSD without treatment (NT), in control, resilient and vulnerable mice, are shown respectively. In (D–F), pictures of neurons from the Rad layer of CA1 in vHPC after RSD with SNC80 treatment (SNC80), in control, resilient and vulnerable mice, respectively. Scale bar = 500 nm. In (G–J), magnified views of dilated ER, dilated Golgi apparatus (go), lipofuscin granule (li), and nuclear indentation (id), respectively. In (K–O), graphs for Rad layer representing the proportion of dark neurons, the proportion of neurons presenting dilated ER, dilated Golgi apparatus, lipofuscin granules and indentations, respectively, without and with SNC80 treatment. Two-way ANOVA, Bonferroni *post hoc* analysis, N(NT: C; R; V) = 23; 24; 26 cells, and N(SNC80: C; R; V) = 25; 24; 26 cells. The two analyzed factors are the stress phenotype (blue, green and red bars for control, resilient and vulnerable mice under RSD, respectively) and the presence or absence of SNC80 treatment (dark blue, green and red bars for control, resilient and vulnerable mice under RSD without SNC80 treatment, respectively, and pale blue, green and red bars with a streaky pattern for control, resilient and vulnerable mice under RSD with SNC80 treatment, respectively). Significance: *for stress phenotype effect or $^{\#}$for SNC80 treatment effect or for stress x treatment effect, $^{\wedge}$(Control vs. Vulnerable), $^{\&}$(Control vs. Resilient), $^{+}$(Resilient vs. Vulnerable) = $^{++}p < 0.01$, $^{\#\#}$, $^{\wedge\wedge\wedge}p < 0.001$, $^{\#\#\#\#}$, $^{\&\&\&\&}p < 0.0001$. Error bars are mean ± SEM.

2.1.6 Discussion

Elucidating the underlying mechanisms of resilience is a pressing medical challenge in the 21st century, especially considering the devastating outcomes of chronic stress on major depression (Davidson *et al*, 2012), cognitive aging, and neurodegenerative diseases (Green *et al*, 2003; Modrego, 2010). The aim of this study was to investigate the involvement of opioid ENK signaling in the development of stress resilience in mice. The RSD paradigm was selected to reproduce the unpredictable disruptions of daily life and study the underlying mechanisms of stress resilience. As expected from previous RSD studies in mice (Golden *et al*, 2011), we obtained 33% of animals displaying a resilient phenotype among the total population. To validate our paradigm, we showed that vulnerable and resilient mice demonstrated an increase of their plasmatic corticosterone levels. RSD is considered the most demanding paradigm in terms of hypothalamic pituitary-adrenal axis activation (Koolhaas *et al*, 1997). When comparing control and defeated rodents, an important variation of plasmatic corticosterone levels was previously reported throughout RSD, with a peak measured during the first and the last defeat days in mice and with a return to basal levels appearing 1 week after (Keeney *et al*, 2006). Krishnan et al. (2007) obtained a result comparable to ours where vulnerable mice as well as resilient ones had an

increase in plasma corticosterone levels on the day following the last defeat. Our results indicate that mRNA levels of ENK decrease in the BLA of vulnerable mice compared to resilient ones without significant differences between resilient and control animals. Previous studies demonstrated a similar reduction of ENKs mRNA levels in the BLA of vulnerable rats, while inactivation of ENKs in the same area reproduced a vulnerability phenotype (Berube *et al*, 2013; Berube *et al*, 2014). These findings provide support to the hypothesis that BLA-ENK neurotransmission contributes to the development of stress resilience in both rats and mice, raising the intriguing possibility that a similar role might be exerted in humans. Reduced mRNA levels of ENK (in the BLA) under the RSD paradigm were also associated to a decreased mRNA expression of its DOPr (in BLA targeted CA1 *stratum oriens* of ventral HPC) in vulnerable mice only. These findings suggest that signaling between BLA-ENK projections and their targets, DOPr-expressing neurons in the CA1 *stratum oriens* of ventral HPC, is preserved during resilience to social stress. Considering that changes in mRNA signals do not necessarily reflect the protein levels (Hatzimanikatis *et al*, 1999), additional experiments determining the changes in ENK and DOPr protein expression are however warranted to provide a comprehensive picture of their association with stress resilience. In addition, several other, possibly indirect, neuroanatomical connections of non-enkephalinergic neurochemical nature such as glutamatergic projections (Felix-Ortiz *et al*, 2013; Rei *et al*, 2015) may have contributed to this phenomenon. Also considering that social stress recruits several brain regions including classical ones mediating the stress response, comprising the hypothalamus, septum, bed nucleus of stria terminalis, preoptic area and some nuclei in brainstem, as shown by mapping experiments with the immediate-early gene c-fos (Martinez *et al*, 2002), and that DOPr is widely expressed across the brain (Scherrer *et al*, 2006), it would be important in future experiments to investigate the role of additional brain areas. Pharmacological activation of DOPr with the agonist SNC80 throughout RSD further increased the proportion of resilient animals, indicating that the endogenous ENK-DOPr system could be targeted to promote coping behavior and adaptation in the face of chronic social adversity. ENKs are known to reduce stress-induced neuroendocrine and autonomic responses, and also to stimulate these effector systems under normal, non-stressful conditions. A distinctive feature of ENKs analgesic action is their blunting of pain's

distressing, affective component, without dulling the sensation itself. Therefore, our findings propose that ENK-DOPr signaling may diminish the impact of social stress on depressive-like behavior by attenuating physiological responses during resilience, including emotional and affective states, leading to reduced anxiety. Indeed, the results from several rodent studies consistently indicate that ENK-DOPr signaling mainly exerts anxiolytic effects (Drolet *et al*, 2001; Gendron *et al*, 2015; Henry *et al*, 2017). To provide insights into the underlying mechanisms, considering that anxiety levels in mice are tightly related to antioxidant enzymes expression (Hovatta *et al*, 2005), ultrastructural analyses of oxidative damage to neurons were conducted in the CA1 region (*strata oriens*, *pyramidale*, *radiatum*) of ventral HPC. Electron density was first examined considering that the condensation of cytoplasmic and nucleoplasmic contents is strongly associated with oxidative challenges to neurons (Peters *et al*, 1998) and glial cells (Bisht *et al*, 2016a; Bisht *et al*, 2016b). Dark neurons were previously described in elderly monkeys (Peters *et al*, 1998) as well as rodent models of Huntington's and Alzheimer's diseases (Oster-Granite *et al*, 1996; Turmaine *et al*, 2000; Yang *et al*, 2008), ischemia (Kirino *et al*, 1984), epilepsy (Atillo *et al*, 1983) and aging (Tremblay *et al*, 2012). In our analyses, social stress and SNC80 were found to exert different effects on the electron density between neuronal subpopulations. Among these, dark pyramidal cells became more prevalent in vulnerable mice compared to control and resilient ones, while SNC80 treatment prevented this increase. Stimulating ENK-DOPr signaling may thus reduce the deleterious impact of chronic social stress by preventing oxidative damage. This finding is supported by the reduced prevalence of dilated ER that we measured upon SNC80 treatment in CA1 interneurons and pyramidal cells from the experimental groups analyzed. The best-characterized sign of cellular disturbance at the ultrastructural level is ER stress, since the pathological accumulation of unfolded or misfolded proteins makes its lumen appear dilated in EM (Malhotra and Kaufman, 2007; Ron *et al*, 2007; Schonthal, 2012). The unfolded protein response (UPR) is triggered upon ER stress to stop protein translation, degrade unfolded proteins or activate signaling pathways leading to refolding (Ron *et al*, 2007). During the refolding process, reactive oxygen species are produced, leading to impaired redox balance resulting in oxidative stress. Since the refolding process depends on redox homeostasis, oxidative stress can disrupt proper folding mechanisms thus exacerbating further the ER stress. Similarly,

dilation of Golgi cisternae, also associated with oxidative stress (Welch *et al*, 1985), was found to be prevented in pyramidal cells of SNC80-treated vulnerable mice. Whether SNC80 treatment decreases ER and Golgi stress directly, or preserves homeostasis by activating the UPR pathway, among others, remains to be investigated. Additional signs of cellular stress were also reduced upon stimulation of DOPr signaling, such as the prevalence of lipofuscin granules, which are long-considered the major hallmark of cellular aging (Sohal *et al*, 1986), in pyramidal cells of SNC80-treated vulnerable mice. This finding indicates that pharmacological treatment with DOPr agonists might prevent the accelerated-aging effect induced by stress (Green *et al*, 2003). Additionally, nuclear indentations became more frequent in pyramidal cells and interneurons of vulnerable mice treated with SNC80. Considering that nuclear indentations have been associated with the remodeling of cellular morphology (Versaevel *et al*, 2014), their appearance might reflect an increased neuronal plasticity induced by SNC80 treatment. Indeed, DOPr are known to induce long-term plasticity of hippocampal GABAergic synapses (Rozov *et al*, 2017). Overall, this study suggests that ENK/DOPr signaling between the BLA and CA1 (*stratum oriens*) of ventral HPC is preserved in resilient mice and impaired in vulnerable ones under the RSD paradigm. Moreover, this study highlighted a key role of DOPr signaling in promoting social stress resilience through its protective effect against cellular stress among excitatory and inhibitory neurons of the ventral HPC CA1. Additional research focusing on the functional role of DOPr in preventing cellular stress in the face of adversity may provide novel insights into how the intimate relationship between oxidative stress and psychosocial stress influences resilience. The current work underlines the importance of studying endogenous opioids as novel therapeutic targets for stress-related disorders, and suggests that pharmacological activation of DOPr could be an interesting candidate to prevent the exacerbation of cellular stress induced by psychosocial stress.

2.1.7 Funding and disclosure

This study was supported by grants from the Canadian Institutes of Health Research (CIHR) to Louis Gendron, Guy Drolet and Marie-Eve Tremblay. Louis Gendron holds a Chercheur boursier, senior scholar, and Marie-Eve Tremblay a Canada Research Chair Tier 2 in *Neuroimmune Plasticity in Health and Therapy*. The authors declare no conflict of interest.

2.1.8 Acknowledgments

We are grateful to Julie-Christine Lévesque at the Bioimaging Platform of CRCHU de Québec- Université Laval for technical assistance with electron microscopy, and to Cecilia Flores at the Douglas Mental Health University Institute for helping to set-up the repeated social defeat experiments. We also thank Julie C. Savage for her insightful suggestions.

2.1.9 Supplementary data

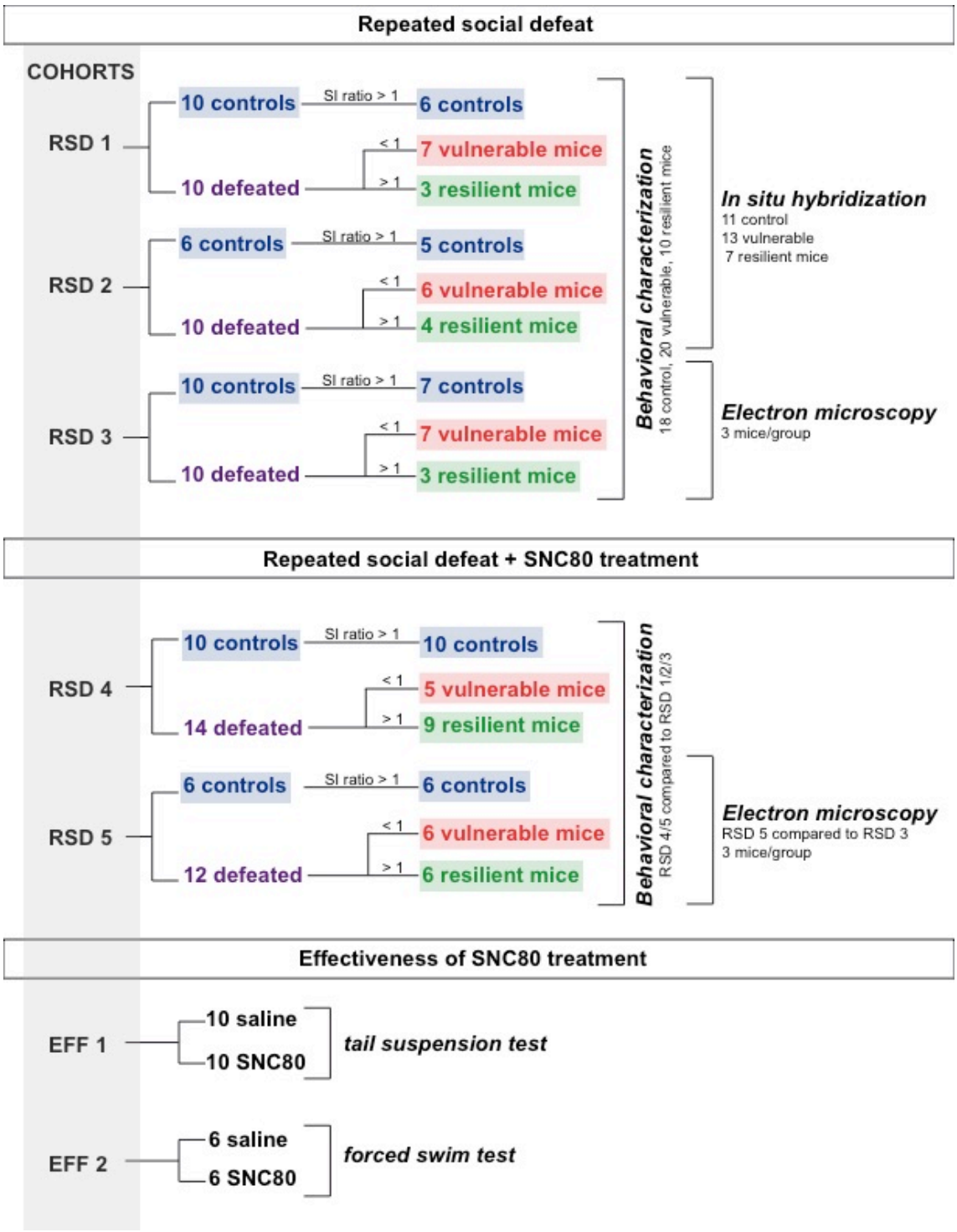

Figure 22. Summary of experiments. Schematic representation of animal cohorts including the number of animals used for each experiment.

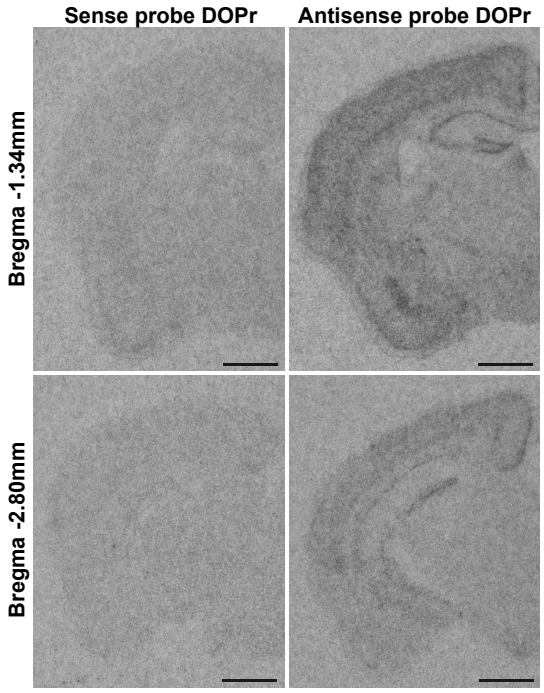

Figure 23. Sense probe versus antisense probe DOPr.
Magnified views of brain sections (Bregma -1.34mm and -2.80mm) tested with sense probe *versus* antisense probe for DOPr. Scale bar = 1mm.

Bregma Levels in Hippocampus	Regions	Layers	Control	Resilient	Vulnerable	p values
	CA1	*Pyramidal*	0.608	0.590	0.576	0.8179
		Radiatum	0.232	0.249	0.265	0.6941
		Oriens	0.323	0.283	0.326	0.642
	CA3	*Pyramidal*	0.513	0.467	0.498	0.7778
		Radiatum	0.215	0.230	0.230	0.42
Dorsal Hippocampus (Bregma = -2.06mm)		*Oriens*	0.270	0.259	0.248	0.9277
	CA1	*Pyramidal*	0.491	0.492	0.495	0.8551
		Radiatum	0.196	0.217	0.207	0.752
		Oriens	0.260	0.256	0.274	0.8788
	CA3	*Pyramidal*	0.561	0.542	0.568	0.8637
		Radiatum	0.224	0.233	0.249	0.6991
Ventral Hippocampus (Bregma = -2.70mm)		*Oriens*	0.235	0.247	0.276	0.157
	CA1	*Pyramidal*	0.464	0.484	0.458	0.7607
		Radiatum	0.194	0.219	0.223	0.5551
		Oriens	**0.271**	**0.275**	**0.169**	**0.0022**
	CA3	*Pyramidal*	0.502	0.534	0.515	0.7921
		Radiatum	0.224	0.248	0.240	0.6897
		Oriens	0.219	0.248	0.249	0.3355
Ventral Hippocampus (Bregma = -3.08mm)	SUBv		0.368	0.467	0.406	0.1962

Table 4. Quantification of DOPr mRNA levels across hippocampus after repeated social defeat stress.
Mean values for all regions in hippocampus quantified for DOPr mRNA levels. Dorsal (Bregma 2.06mm), central (Bregma -2.70mm) and ventral hippocampus (Bregma -3.08mm) were quantified in CA1 and CA3 regions in three different *strata* (*pyramidale*, *oriens* and *radiatum*) as well as in ventral subiculum (SUBv).

MARKERS		F(DFn, DFd)	p values
Dark cells	INTERACTION	F (2, 282) = 1,281	P = 0,2794
	STRESS	F (2, 282) = 4,453	**P = 0,0125**
	TREATMENT	F (1, 282) = 19,76	**P < 0,0001**
Dilated ER	INTERACTION	F (2, 282) = 6,240	**P = 0,0022**
	STRESS	F (2, 282) = 1,181	P = 0,3086
	TREATMENT	F (1, 282) = 67,46	**P < 0,0001**
Dilated Golgi	INTERACTION	F (2, 282) = 3,263	**P = 0,0397**
	STRESS	F (2, 282) = 0,3892	P = 0,6780
	TREATMENT	F (1, 282) = 7,664	**P = 0,0060**
Lipofuscin	INTERACTION	F (2, 282) = 2,731	P = 0,0669
	STRESS	F (2, 282) = 1,420	P = 0,2434
	TREATMENT	F (1, 282) = 3,058	P = 0,0814
Indentations	INTERACTION	F (2, 282) = 8,742	**P = 0,0002**
	STRESS	F (2, 282) = 6,106	**P = 0,0025**
	TREATMENT	F (1, 282) = 0,9697	P = 0,3256

	No treatment			SNC80		
	Control vs Resilient	Control vs Vulnerable	Resilient vs Vulnerable	Control	Resilient	Vulnerable
Significance?	No	**Yes**	**Yes**	No	No	**Yes**
t values	0.000	**2.781**	**2.781**	2.139	1.710	**3.850**
p values	1	**0.0058**	**0.0058**	0.0333	0.0884	**0.0001**
Significance?	No	No	No	**Yes**	No	**Yes**
t values	0.000	2.134	2.134	**4.506**	2.371	**7.352**
p values	1	0.0337	0.0337	**0.0001**	0.0184	**0.0001**
Significance?	No	No	No	No	No	**Yes**
t values	0.600	1.198	0.598	0.299	1.798	**3.295**
p values	0.549	0.2319	0.5503	0.7652	0.0732	**0.0011**
Significance?	No	No	No	No	No	**Yes**
t values	1.731	2.164	0.433	0.433	0.649	**2.814**
p values	0.0845	0.0313	0.6653	0.6653	0.5169	**0.0052**
Significance?	No	No	No	No	No	**Yes**
t values	0.640	0.427	1.066	1.919	0.213	**3.837**
p values	0.5227	0.6697	0.2873	0.056	0.8315	**0.0002**

	Interaction stress x SNC80		
Significance?	Control vs Resilient	Control vs Vulnerable	Resilient vs Vulnerable
t values	No	No	No
p values	0.428	1.070	0.642
Significance?	0.6690	0.2855	0.5214
t values	No	No	**Yes**
p values	2.134	0.711	**2.845**
Significance?	0.0337	0.4777	**0.0048**
t values	No	No	No
p values	1.497	2.396	0.899
Significance?	0.1355	0.0172	0.3694
t values	No	No	No
p values	0.649	1.082	1.731
Significance?	0.5169	0.2802	0.0845
t values	No	**Yes**	**Yes**
p values	2.345	**5.329**	**2.984**
	0.0197	**0.0001**	**0.0031**

Table 5. Statistical analysis (Two-way ANOVA with Bonferroni *post-hoc* analysis) for prevalence of different oxidative stress markers in *stratum pyramidale* described by electron microscopy. Left part of the table provides statistical data of main effects and the right part (purple) provides statistical data for Bonferroni *post-hoc*. Bold numbers are considered as significant.

MARKERS		F(DFn, DFd)	p values
Dark cells	INTERACTION	F (2, 157) = 0,04531	P = 0,9557
	STRESS	F (2, 157) = 0,9301	P = 0,3967
	TREATMENT	F (1, 157) = 5,403	**P = 0,0214**
Dilated ER	INTERACTION	F (2, 157) = 0,3465	P = 0,7077
	STRESS	F (2, 157) = 1,810	P = 0,1671
	TREATMENT	F (1, 157) = 22,43	**P < 0,0001**
Dilated Golgi	INTERACTION	F (2, 157) = 0,1345	P = 0,8743
	STRESS	F (2, 157) = 4,109	**P = 0,0182**
	TREATMENT	F (1, 157) = 3,648	P = 0,0580
Lipofuscin	INTERACTION	F (2, 157) = 0,7054	P = 0,4955
	STRESS	F (2, 157) = 0,7926	P = 0,4545
	TREATMENT	F (1, 157) = 0,03681	P = 0,8481
Indentations	INTERACTION	F (2, 157) = 1,522	P = 0,2215
	STRESS	F (2, 157) = 2,520	P = 0,0837
	TREATMENT	F (1, 157) = 0,1471	P = 0,7018

	No treatment			SNC80		
	Control vs Resilient	Control vs Vulnerable	Resilient vs Vulnerable	Control	Resilient	Vulnerable
Significance?	No	No	No	No	No	No
t values	0.158	0.773	0.600	1.575	1.220	1.229
p values	0.8747	0.4407	0.5494	0.1173	0.2243	0.2209
Significance?	No	No	No	No	**Yes**	No
t values	1.048	1.493	0.414	2.220	**3.434**	2.567
p values	0.2962	0.1374	0.6794	0.0279	**0.0008**	0.0112
Significance?	No	No	No	No	No	No
t values	1.858	1.897	0.000	0.851	1.545	0.922
p values	0.065	0.0597	1	0.3961	0.1244	0.3579
Significance?	No	No	No	No	No	No
t values	0.528	0.563	1.079	0.652	0.029	1.009
p values	0.5982	0.5742	0.2822	0.5154	0.9769	0.3145
Significance?	No	No	No	No	No	No
t values	0.235	0.361	0.118	1.334	0.440	1.105
p values	0.8145	0.7186	0.9062	0.1841	0.6605	0.2709

	Interaction stress x SNC80		
Significance?	Control vs Resilient	Control vs Vulnerable	Resilient vs Vulnerable
t values	No	No	No
p values	0.579	1.137	0.614
Significance?	0.5634	0.2573	0.5401
t values	No	No	No
p values	0.056	1.171	1.285
Significance?	0.9554	0.2434	0.2007
t values	No	No	No
p values	1.331	1.861	0.621
Significance?	0.1851	0.0646	0.5355
t values	No	No	No
p values	1.237	1.104	0.079
Significance?	0.2179	0.2713	0.9371
t values	No	**Yes**	No
p values	1.214	**2.830**	1.754
	0.2266	**0.0053**	0.0814

Table 6. Statistical analysis (Two-way ANOVA with Bonferroni *post-hoc* analysis) for prevalence of different oxidative stress markers in *stratum oriens* described by electron microscopy. Left part of the table provides statistical data of main effects and the right part (purple) provides statistical data for Bonferroni *post-hoc*. Bold numbers are considered as significant.

MARKERS		F(DFn, DFd)	p values
Dark cells	INTERACTION	F (2, 142) = 8,918	**P = 0,0002**
	STRESS	F (2, 142) = 2,758	P = 0,0668
	TREATMENT	F (1, 142) = 13,15	**P = 0,0004**
Dilated ER	INTERACTION	F (2, 142) = 1,507	P = 0,2251
	STRESS	F (2, 142) = 1,599	P = 0,2057
	TREATMENT	F (1, 142) = 24,12	**P < 0,0001**
Dilated Golgi	INTERACTION	F (2, 142) = 0,002508	P = 0,9975
	STRESS	F (2, 142) = 0,6046	P = 0,5477
	TREATMENT	F (1, 142) = 1,728	P = 0,1908
Lipofuscin	INTERACTION	F (2, 142) = 1,789	P = 0,1709
	STRESS	F (2, 142) = 1,440	P = 0,2404
	TREATMENT	F (1, 142) = 0,3817	P = 0,5377
Indentations	INTERACTION	F (2, 142) = 0,8587	P = 0,4259
	STRESS	F (2, 142) = 4,656	**P = 0,0110**
	TREATMENT	F (1, 142) = 0,1124	P = 0,7379

	No treatment			SNC80		
	Control vs Resilient	Control vs Vulnerable	Resilient vs Vulnerable	Control	Resilient	Vulnerable
Significance?	No	No	No	**Yes**	No	**Yes**
t values	0.950	0.481	1.466	**3.796**	1.359	**3.915**
p values	0.3437	0.6313	0.1449	**0.0002**	0.1763	**0.0001**
Significance?	No	No	No	No	**Yes**	**Yes**
t values	0.069	0.103	0.175	1.390	**3.492**	**3.659**
p values	0.9451	0.9181	0.8613	0.1667	**0.0006**	**0.0004**
Significance?	No	No	No	No	No	No
t values	0.035	0.649	0.693	0.703	0.804	0.772
p values	0.9721	0.5174	0.4894	0.4832	0.4227	0.4414
Significance?	No	No	No	No	No	No
t values	1.030	0.981	0.069	1.146	1.183	1.136
p values	0.3048	0.3283	0.9451	0.2537	0.2388	0.2579
Significance?	No	No	No	No	No	No
t values	1.596	1.714	0.088	0.141	1.125	0.720
p values	0.1127	0.0887	0.9300	0.8881	0.2625	0.4727

	Interaction stress x SNC80		
	Control vs Resilient	Control vs Vulnerable	Resilient vs Vulnerable
Significance?	Yes	No	**Yes**
t values	4.241	0.530	**3.757**
p values	0.0001	0.5969	**0.0003**
Significance?	No	No	No
t values	2.052	2.295	0.199
p values	0.0420	0.0232	0.8425
Significance?	No	No	No
t values	0.065	0.703	0.630
p values	0.9483	0.4832	0.5297
Significance?	No	No	No
t values	1.302	0.945	2.249
p values	0.1950	0.3463	0.0261
Significance?	No	**Yes**	No
t values	0.636	**2.611**	1.941
p values	0.5258	**0.0100**	0.0542

Table 7. Statistical analysis (Two-way ANOVA with Bonferroni *post-hoc* analysis) for prevalence of different oxidative stress markers in *stratum radiatum* described by electron microscopy. Left part of the table provides statistical data of main effects and the right part (purple) provides statistical data for Bonferroni *post-hoc*. Bold numbers are considered as significant.

2.2 Chapitre 2

Delta Opioid Receptor blunts oxidative stress to promote resilience to chronic stress: A morphological and molecular study of mitochondria

Mathilde S. Henry[1], Kanchan Bisht[1], Nathalie Vernoux, Ph.D.[1], Louis Gendron, Ph.D.[3,4,5], Angélica Torres-Berrio[2], Guy Drolet, Ph.D.[1,6], and Marie-Ève Tremblay, Ph.D.[1,7#]

[1] Axe neurosciences, Centre de Recherche du CHU de Québec – Université Laval, Québec, QC, Canada.

[2] Centre de recherche du CHU de Sherbrooke and Institut de pharmacologie de Sherbrooke, Université de Sherbrooke, Sherbrooke, QC, Canada.

[3] Département de pharmacologie-physiologie, Université de Sherbrooke, Sherbrooke, QC, Canada.

[4] Quebec Pain Research Network, Sherbrooke, QC, Canada.

[5] Douglas Mental Health University Institute, Montréal, QC, Canada.

[6] Département de psychiatrie et neurosciences, Université Laval, Québec, QC, Canada.

[7] Département de médecine moléculaire, Université Laval, Québec, QC, Canada.

Les résultats évoqués dans ce chapitre font partie d'une étude en collaboration avec Dr Louis Gendron et Dr Jean-Luc Parent de l'Université de Sherbrooke et seront integrés au sein d'un article de plus grande envergure.

2.2.1 Résumé

Il existe une grande variabilité entre les individus en ce qui concerne les réponses physiologiques et comportementales observées dans une situation stressante. La résilience au stress est un processus complexe qui recrute de nombreuses structures cérébrales et de nombreux neurotransmetteurs. La signalisation des récepteurs opioïdergiques Delta (DOPr) a récemment été impliquée dans ce processus. En effet, le niveau d'expression des ARNm de DOPr a montré une diminution dans la région CA1 de l'hippocampe ventral (CA1-vHPC) chez les souris vulnérables après un stress chronique de défaite sociale (SCDS), tout en demeurant inchangé chez les animaux résilients comme chez les contrôles. De plus, l'activation pharmacologique du DOPr avec un agoniste, le SNC80, induisait un phénotype résilient chez la majorité des animaux stressés. Dans cette étude, nous avons émis l'hypothèse que la signalisation DOPr favorise naturellement la résilience au stress en agissant sur l'équilibre oxydatif des neurones de la région CA1. En effet, l'activation de DOPr a un effet neuroprotecteur contre le stress oxydatif en condition hypoxique et ischémique chez le rat. Le but de cette étude était d'étudier l'effet de la stimulation de la voie DOPr, en utilisant le SNC80, sur la morphologie mitochondriale après SCDS par microscopie électronique. Nous avons spécialement ciblé le CA1-vHPC pour répondre à cette hypothèse. Les analyses ultrastructurelles de la morphologie mitochondriale ont révélé que le traitement SNC80 réduit le stress oxydatif dans les cellules pyramidales et les interneurones en modifiant leur forme et en améliorant leur intégrité architecturale sans affecter leur taille, en particulier chez les souris vulnérables. Ces résultats suggèrent que le traitement par SNC80 pourrait restaurer les effets délétères du stress chronique en ciblant directement les mitochondries. Nous avons également effectué des western blot sur l'hippocampe total pour identifier les cibles moléculaires associées aux effets bénéfiques de la signalisation DOPr sur la résilience. Le SNC80 a augmenté l'expression des complexes de la chaîne respiratoire indiquant une amélioration de leur activité dans la production d'ATP. Toutefois, le SNC80 n'a pas altéré l'expression d'enzymes antioxydantes telles que la superoxyde dismutase ou la catalase. Des études futures seront requises afin d'identifier le mécanisme par lequel DOPr favorise la résilience au stress.

2.2.2 Abstract

There is a great variability among individuals with respect to the physiological and behavioral responses observed in a stressful situation. Resilience to stress is a complex process recruiting various brain regions and neurotransmitter systems. Delta opioid receptors (DOPr) signaling was recently involved in this process. In particular, DOPr mRNA levels were shown to be reduced in the ventral hippocampus CA1 region (CA1-vHPC) of vulnerable mice upon chronic social defeat stress (RSD) while remaining unchanged in resilient ones as in controls. Moreover, pharmacological activation of DOPr using an agonist, SNC80, significantly induced a resilient phenotype in a majority of stressed animals. In this current study, we hypothesized that DOPr signaling naturally promotes stress resilience by acting on the oxidative balance of CA1 region neurons. Indeed, DOPr activation is neuroprotective against oxidative stress during hypoxia and ischemia in rats. The aim of this study was to investigate the effect of stimulating DOPr pathway using SNC80 on mitochondrial morphology under RSD by electron microscopy. We specially targeted the CA1-vHPC to address this hypothesis. Ultrastructural analyses of mitochondrial morphology revealed that SNC80 treatment reduces oxidative stress in pyramidal cells and interneurons by modifying their shape and improving their architectural integrity without affecting their size, particularly in vulnerable mice. These results suggest that SNC80 treatment might restore the deleterious effects of chronic stress by directly targeting mitochondria. We also performed western blot in total hippocampus to identify molecular targets associated with the beneficial effects of DOPr signaling on stress resilience. SNC80 increased the expression of specific complexes in the respiratory chain indicating an enhanced ATP production activity. However, SNC80 did not alter the expression of antioxidant enzymes such as superoxide dismutase and catalase. Future studies will be required to identify the mechanism by which DOPr activation promotes stress resilience.

2.2.3 Introduction

Chronic stress is known to induce major depression, which is the leading cause of disability affecting 350 million people all around the world. Stress is described as an uncomfortable « emotional experience accompanied by predictable biochemical, physiological and behavioral changes » (Baum, 1990). Some stress can be beneficial producing a boost that provides energy to help people get through situations. However, exposure to extreme and prolonged stress can lead to health consequences by adversely affecting the immune, cardiovascular, neuroendocrine and central nervous systems (Anderson, 1998). There is a great variability among individuals with respect to the physiological and behavioral responses observed in a stressful situation. The different degrees of adaptability define resilience or vulnerability to chronic stress. Resilience is a common concept used in psychology to define an active coping mechanism referring to « the capacity of an individual to avoid negative social, psychological, and biological consequences of extreme stress that would otherwise compromise their psychological or physical well-being » (Russo *et al*, 2012).

Several stress-related conditions such as chronic psychological stress during childhood and post-traumatic stress disorder (PTSD) were shown to elevate oxidative stress (Miller *et al*, 2011; Miller *et al*, 2014). All aerobic organisms possess an oxidation system essential to the production of cellular energy. This oxidation system is at the origin of the production of reactive oxygen (ROS) and nitrogen (RNS) species, which could be harmful to cellular function in case of excess. Oxidative stress is defined as a state in which the level of oxidation exceeds the ability of cells to eliminate ROS/RNS leading to impairment in cellular functions by damaging lipids, proteins, as well as nucleic acids (Czerska *et al*, 2015).

Delta opioid receptors (DOPr), G protein-coupled receptors for endogenous and exogenous opioids, are known to play a critical role in mood disorders (Lutz and Kieffer, 2013). Especially, we previously demonstrated that the expression levels of DOPr mRNA were positively correlated in hippocampus with resilience under the repeated social defeat stress (RSD) paradigm in mice (Henry *et al*, 2018). DOPr activation was also found to be neuroprotective against oxidative stress in rat cortex and hippocampus during hypoxia and ischemia (Yang *et al*, 2009; Zhang *et al*, 2000) as well as against mitochondrial respiratory

chain injury induced by sodium azide leading to oxidative stress in cultured cortical rat neurons (Zhu *et al*, 2009).

In our previous study, we hypothesized that resilience to chronic stress may recruit DOPr signaling, leading to a reduction of oxidative stress in hippocampal neurons. To address this question, the RSD paradigm was performed in mice, with or without DOPr pharmacological activation treatment. Expression levels of DOPr mRNA were found to be reduced in the CA1 region of ventral hippocampus of vulnerable mice while remaining unchanged in resilient mice and controls. Then, using electron microscopy, we quantified different ultrastructural markers of oxidative stress including cytoplasmic/nucleoplasmic condensation ("dark" neurons) and endoplasmic reticulum dilation, among others, in CA1 hippocampus. Thus we showed that pharmacological activation of DOPr using SNC80 improves resilience to chronic social stress. It also restores cellular health in hippocampal pyramidal cells and interneurons of vulnerable mice, by preventing the deleterious effects of oxidative stress induced during chronic stress. Taken together, these results suggest that DOPr naturally promotes resilience to chronic stress by blunting oxidative stress (Henry *et al*, 2018).

Manoli and colleagues exposed in a review the critical role of mitochondria under acute and chronic stress conditions. Mitochondria play a vital role in cellular homeostasis by constantly sensing the internal milieu and environmental changes. They provide the enormous energy demands essential for proper stress response (Manoli *et al*, 2007). The mitochondrial response to cellular needs involves signaling pathways in order to increase mitochondrial performance by recruiting more mitochondria or increasing their volume, enhancing activity of oxidative phosphorylation complexes, generating ROS for signaling or defense and inducing apoptosis according to stressors (Goldenthal and Marin-Garcia, 2004). Mitochondria are thus a potential target by which DOPr signaling could blunt oxidative stress. Mitochondria consist of a double membrane system: an outer membrane and an inner membrane separated by an inter-membrane space. The inner membrane forms invaginations (cristae) that extend to the matrix of the mitochondria. The matrix contains the genetic material of the mitochondria as well as all the enzymes necessary for oxidative metabolism. Morphological changes in mitochondria were proposed to reflect their functional alteration (Brocard *et al*, 2003). For example, a study using multiphoton

microscopy demonstrated in yeast that a change of substrate (from glucose to glycerol) induced a 3-fold increase in mitochondrial volume without affecting their number (Egner *et al*, 2002). Thermal stress on rat fibroblasts has been shown to lead to mitochondrial swelling, disruption of cristae, and widening of spaces between cristae *in vitro* (Welch *et al*, 1985). Thus, morphological analyses of mitochondria under the RSD paradigm in mice, with or without SNC80 treatment, were conducted by electron microscopy in the CA1 region of ventral hippocampus. These analyses included the quantification of mitochondria per cells, their gray-value, a size descriptor (area, perimeter) as well as a shape descriptor (aspect ratio, roundness, circularity, solidity). To identify potential molecular targets of DOPr signaling, western blot analyses targeting oxidative stress markers associated with mitochondrial function - including antioxidant enzymes and proteins from respiratory chain complexes - were also performed in total hippocampus.

2.2.4 Material and Methods

2.2.4.1 Animals

CD1 retired breeders (4-6 months old), naïve C57BL/6 screeners (8-20 weeks old), and C57BL/6 mice for forced-swim test and tail suspension test (7-8 weeks old) were provided by Charles River (St-Constant, QC, Canada), while experimental C57BL6/J mice (7-8 weeks old) were from Jackson Laboratories (Bar Harbor, ME, USA). Mice were housed under a 12h light-dark cycle with food and water available *ad libitum*. All experiments were strictly conducted according to the protocol approved by the institutional animal ethics committee, in conformity with the Canada Council on Animal Care guidelines.

2.2.4.2 Social defeat stress

The protocol for chronic social defeat stress was followed as described (Henry *et al*, 2018). Briefly, after a screening of CD1 mice to evaluate their aggressiveness, C57BL/6J were placed in the home-cage of CD1 aggressors for 5min per day during 10 days while non stressed mice (controls) were paired-housed and switched partners each day. After every session, defeated C57BL6/J went back to their home cage. On the eleventh day, controls and defeated mice were subjected to a social interaction test to assess their resilience or vulnerability phenotype with a calculated social interaction ratio (SI ratio) corresponding to the time spent interacting with a novel CD1 *versus* in absence. Despite the 10 days experiment, resilient mice still interacted with CD1 whereas vulnerable tended to avoid contact with aggressor. Thus, as shown in our previous study (Henry *et al*, 2018) resilient mice and control mice displayed a SI ratio above 1 while vulnerable ones had a ratio below.

2.2.4.3 Pharmacological treatment

The compound SNC80 used for this study as well as the protocol for administration were described in our previous work (Henry *et al*, 2018). Efficacy of the treatment was evaluated using a forced-swim test (FST) and a tail suspension test (TST) as previously described (Henry *et al*, 2018).

2.2.4.4 Perfusion

The experimental C57BL/6J mice were sacrificed one day after the social interaction test. Three animals per group (stress and treatment) were examined by electron microscopy. Mice were anesthetized with sodium pentobarbital (80mg/ml, i.p.) and perfused with 3.5%

acrolein followed by 4% PFA (both in phosphate buffer – PB 100mM, pH 7.4). Fifty micrometer-transverse sections were cut in sodium phosphate buffer (PBS ; 50 mM, pH 7.4) with a vibratome (Leica VT1000S) and stored at -20 °C in cryoprotectant. For western blot, mice were anesthetized with an intraperitoneal injection of ketamine/xylazine (80 and 10 mg/kg, respectively) and perfused with a 0.9% saline solution (285 mOsm/L, pH 7.4).

2.2.4.5 Electron microscopy

1) Tissues processing

As previously described (Henry *et al*, 2018), brain sections from Bregma 2.92mm to -3.52mm were used and processed for electron microscopy (postfixed in 1% osmium tetroxide, dehydrated in ethanol, treated with propylene oxide, and impregnated in resin). The areas of interest containing ventral hippocampus CA1 were cut at 70nm with an ultramicrotome (Leica Ultracut UC7). Ultrathin sections were collected on square-mesh grids and examined at 80kV using a FEI Tecnai Spirit G2 microscope. For analysis, pyramidal cells and interneurons (*strata oriens* and *radiatum*) were randomly photographed at magnifications ranging between 890x and 4800x using an ORCA-HR camera (10 MP; Hamamatsu).

2) Quantitative analyses of mitochondria

Neuronal mitochondria were quantified and their contours were drawn using free-hand tools of ImageJ 1.6 software. The quantification was performed blind to the experimental conditions. The parameters “area”, “perimeter”, “circularity”, “aspect ratio”, “roundness”, “solidity” and “mean grey value” were measured for each mitochondrion. The circularity, aspect ratio, roundness and solidity shape descriptors inform about the shape of mitochondria. Since a circularity of 1 corresponds to a perfect circle, the closest to 0, the more elongated is the mitochondrion. The aspect ratio corresponds to the major axis divided by the minor axis, while roundness is the opposite of the aspect ratio. Finally, solidity is the ratio of area divided by its convex hull area. The mean grey value testifies of mitochondrial cristae integrity since disruption in cristae leads to light grey holes whereas healthy mitochondria display a grey compacted structure. In this study, values correspond to the inverse of the mean grey values.

2.2.4.6 Western Blot

1) Protein extraction

After perfusion with saline solution, the brains were immediately removed and dissected on ice to extract the hippocampus. Hippocampal tissues were frozen on dry ice, and kept at − 80°C until processing. Hippocampi were homogenized in 5 times volume/weight of RIPA buffer (50 mM Tris, pH 8, 150 mM NaCl, 0.25% Na-deoxycholate, 2 mM EDTA, Triton 10X, 1 mM PMSF, 10 µl/ml of Phosphatases and Proteases Inhibitors Cocktail), using a mechanical homogenizer at 4°C. After 15min incubation on ice, samples were centrifuged for 15min at 12000g at 4°C. Supernatants were extracted and kept at − 80°C.

2) Immunoblot against oxidative stress markers

Detection of enzymes: 10 µg of protein from each sample were separated by SDS 10% of polyacrylamide gels and then, transferred onto Immobilon®-P Polyvinylidene difluoride membrane (Sigma-Aldrich, MO, USA). Detection of mitochondrial complexes: 10 µg of protein from each sample were separated by SDS-PAGE with 10% Tris-Glycine eXtended (TGX) Stain-Free™ polyacrylamide gels (Bio-Rad, Hercules, CA, USA). Stain-Free™ gels were activated by UV transillumination for 5 min using the Fusion FX5 imaging system (Vilbert Lourmat, France). Proteins were transferred to nitrocellulose membranes (Bio-Rad) and total proteins were visualized under UV using the Fusion FX5 imaging system. For both gels, non-specific binding sites were blocked with 5% nonfat dry milk in phosphate-buffered saline containing 0.1% Tween 20 (PBS-T) for 1 hour at room temperature and were afterwards incubated overnight at 4 °C with primary antibodies. Antibodies used in this study were: anti-Catalase (diluted at 1/1000, C0979, Sigma-Aldrich, MO, USA), anti-Mn-SOD (superoxide dismutase, 1/1000, 06984, Millipore, MA, USA) or Mito Profile (1/1000, AB110413, Abcam, MA, USA). The following day, membranes were washed 3 times in PBS-T and then incubated for 1 hour at room temperature with the corresponding secondary antibody in 5% nonfat dry milk in PBS-T, and the immunoreactive signal intensity was visualized by enhanced chemiluminescence (ECL, Biorad). The Fusion FX5 imaging system was used for immunoblot visualization. Band intensities were quantified using ImageJ 1.6 software and normalized to β-actine (1/50000, A5316, Sigma-Aldrich, MO, USA) or total proteins per lane.

2.2.4.7 Statistical analyses

Statistical significance and normality were calculated using the online software GraphPad version 7.0 and GraphPad version 6.0 (La Jolla, CA, USA). All variables were normally distributed based on Bartlett's test. Multiple comparisons were performed by two-way-ANOVA to assess the effects of stress and SNC80 treatment followed by Bonferroni *post hoc* analysis. All data are presented as means ± standard error of the mean (SEM).

2.2.5 Results

2.2.5.1 SNC80 restores healthy mitochondrial morphology in vulnerable mice.

Structural changes in mitochondria are tightly associated with their functional status, which determines their outcome between promoting cell death and protecting cells (Brocard *et al*, 2003). Diverse representative shapes of mitochondria as visualized using TEM are provided in Figure 24. Figure 24A corresponds to healthy round shape mitochondria while Figure 24B and 24C present a more elongated shape. Mitochondria from Figure 24D display an alteration of architecture with disruption of cristae, while severely damaged mitochondria from Figure 24E are devoid of contents. Finally, dumbbell-shaped mitochondria which might undergo fusion or fission events are presented in Figure 24F and 24G.

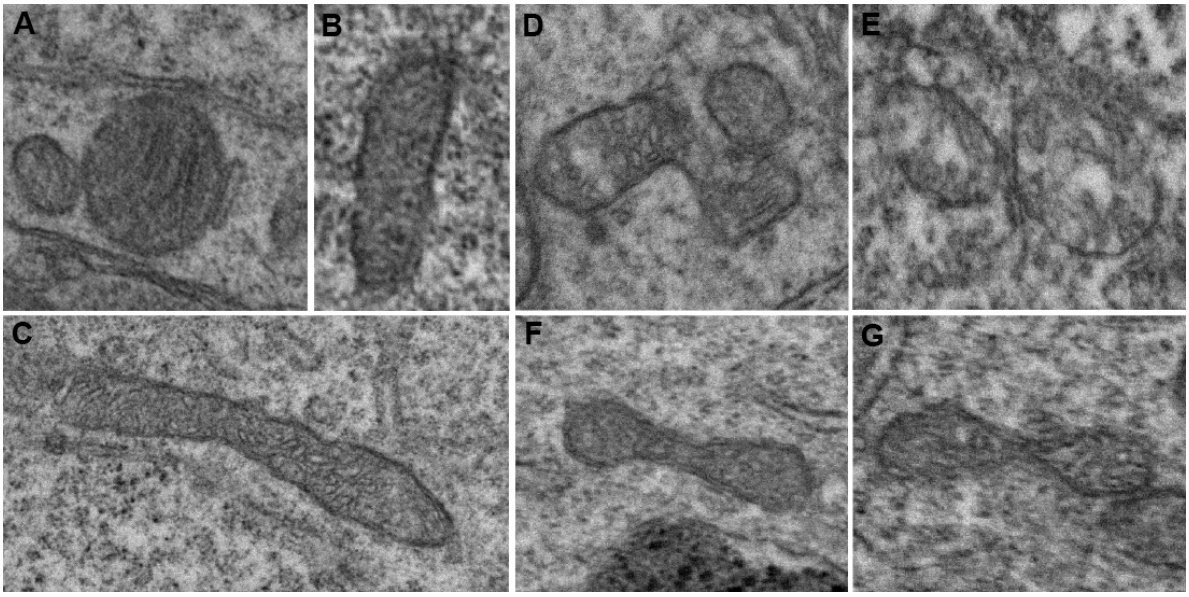

Figure 24. Representative pictures illustrating different shapes of mitochondria as observed using TEM. (A) Healthy round shape mitochondria. **(B)** and **(C)** Elongated shape. **(D)** and **(E)** Mitochondria with an altered architecture showing disruption of cristae. **(F)** and **(G)** Dumbbell-shaped mitochondria. Mitochondria are from pyramidal cells in CA1-vHPC. These TEM images come from our own library.

2.2.5.1.1 Number of mitochondria

Number of mitochondria displayed a main effect of stress and interaction (stress x treatment) in pyramidal cells (Figure 25A: $F_{(2,174)}$=4.262, p=0.0156 and $F_{(2,174)}$=7.492,

p=0.0008, respectively). *Post hoc* analyses revealed an increase of number in resilient mice compared to non-stressed ones. Moreover, controls treated with SNC80 exhibited an increase of number compared to non-treated. Finally, number of mitochondria was decreased in treated vulnerable mice compared to treated control and resilient ones. In *stratum oriens*, only stress by treatment effect was observed (Figure 26A: $F_{(2,145)}$=4.115, p=0.0183). Particularly, vulnerable treated with SNC80 showed a reduced number of mitochondria as compared to treated resilient. Mitochondria from *stratum radiatum* interneurons failed to show a significant difference (Figure 27A). As mentioned in Manoli *et al.* (2007), chronic stress can induce an uncontrolled proliferation of mitochondria as well as a decrease in their number. Indeed, in response to many stressors, the peroxisome proliferators-activated receptor gamma coactivator-1α (PGC-1α) signaling pathway (Puigserver and Spiegelman, 2003) is essential for mitochondrial biogenesis, but can eventually become maladaptive as observed in cardiomyopathy induced by cardiac PGC-1 α overexpression in mice (Russell *et al*, 2004). Moreover, a reduced mitochondrial biogenesis is observed in diabetic mouse models (Duncan *et al*, 2007) while abnormally proliferated mitochondria is a characteristic feature of mitochondrial myopathies (Bourgeois and Tarnopolsky, 2004).

2.2.5.1.2 Mean grey value

Stratum pyramidale revealed a main effect of stress, treatment and interaction (Figure 25B: $F_{(2,174)}$=3.973, p=0.0205, $F_{(2,174)}$=4.916, p=0.0279, $F_{(2,174)}$=7.591, p=0.0007, respectively) while mitochondria in interneurons displayed only a main effect of stress and treatment (Figure 26B: $F_{(2,145)}$=10.63, p<0.0001 and $F_{(2,145)}$=7.668, p=0.0064, Figure 27B: $F_{(2,132)}$=6.559, p=0.0019 and $F_{(2,132)}$=8.769, p=0.0036). Precisely, resilient and vulnerable mice presented an increase of mean grey value compared to control ones in pyramidal cells (Figure 25B) suggesting a better-preserved mitochondrial integrity in resilient and vulnerable animals which seem to be inconsistent. As previously mentioned, disruption in cristae leads to light grey holes (low mean grey value) whereas healthy mitochondria displays a grey compacted structure (high). However, mitochondria undergoing oxidative stress can show a darker grey value due to lipid oxidation. Indeed, osmium tretroxide used

for the treatment of the tissues for electron microscopy has a high affinity for lipid rich structures and oxidated components (Wigglesworth, 1981). This interpretation seems to be more plausible in this case.

On the contrary, in *strata oriens* and *radiatum,* vulnerable mice displayed a decreased mean grey value compared to control and resilient mice indicating a reduced integrity in vulnerable mice (Figure 26B and Figure 27B). SNC80 restored the mean grey value in *stratum radiatum* when treated vulnerable mice were compared to non-treated ones (Figure 27B) or when they were compared to treated control animal in *stratum oriens* (Figure 26B). Finally, in *stratum pyramidale*, the mean grey value was increased in controls treated with SNC80 compared to non-treated controls (Figure 25B) indicating that SNC80 improves mitochondrial integrity in general.

2.2.5.1.3 Area and perimeter

The analysis of mitochondrial area and perimeter did not reveal any effect of stress or treatment or interaction in *stratum pyramidale* (Figure 25D). However, mitochondrial perimeter in interneurons of *stratum radiatum* indicated a main effect of treatment (Figure 27D: $F_{(1,132)}$=4.944, p=0.0279) while *post hoc* analysis did not reach a significant difference. Similarly, although a stress by treatment effect was observed for mitochondrial area in *stratum oriens* (Figure 26D: $F_{(2,145)}$=4.127, p=0.0181), no significant difference was revealed after *post hoc* analysis. These results together suggest that stress and SNC80 treatment might not modify the size of mitochondria.

2.2.5.1.4 Shape descriptor

In *strata pramidale* and *oriens*, analysis of aspect ratio and roundness revealed a main effect of stress by treatment interaction (Figure 25E: $F_{(2,173)}$=12.38, p<0.0001; Figure 25F: $F_{(2,174)}$=7.149, p=0.0010; Figure 26E: $F_{(2,143)}$=3.339, p=0.0382, Figure 26F: $F_{(2,143)}$=4.834, p=0.0093) while treatment and interaction effects were described in *stratum radiatum* for the aspect ratio (Figure 27E: $F_{(1,132)}$=6.763, p=0.0104 and $F_{(2,132)}$=5.474, p=0.0052) and only an interaction effect for the roundness (Figure 27F: $F_{(2,132)}$=4.630, p=0.0114). Especially, treated vulnerable mice presented a reduced aspect ratio (and increased

roundness) compared to non-treated ones as well as to treated control and resilient animals in pyramidal layer. This result revealed that SNC80 induced a less elongated mitochondrial shape in vulnerable mice. This difference was not observed in *stratum radiatum* and *oriens*. ANOVA further identified interaction effect for mitochondrial circularity in interneurons of *strata oriens* (Figure 26G: $F_{(2,145)}$=4.444, p=0.0134) and *radiatum* (Figure 27G: $F_{(2,132)}$=6.256, p=0.0025) whereas it failed to reach significance in pyramidal cells. In particular, treated control mice showed reduced mitochondrial circularity compared to non-treated ones in *radiatum* layer. Moreover, circularity was increased in treated vulnerable animal compared to treated control and resilient ones. Solidity of mitochondria in *stratum radiatum* also revealed the same result as presented for circularity (Figure 27H). *Post hoc* analysis failed to present a significant difference in *stratum oriens* regarding circularity and solidity. Solidity analysis of mitochondria from pyramidal cells revealed a treatment and interaction effect (Figure 25H: $F_{(1,173)}$=4.440, p=0.0366 and $F_{(2,173)}$=4.193, p=0.0167). Precisely, treated vulnerable animal exhibited an increased solidity when compared to non-treated ones suggesting that SNC80 promotes a more uniform mitochondrial morphology in vulnerable mice. Altogether, the measurements with these shape descriptors indicate that SNC80 promotes a healthy circle-shape in vulnerable mice and suggest that SNC80 significantly modifies the shape of mitochondria both in pyramidal cells and interneurons, particularly in vulnerable mice, in order to restore the deleterious effects induced by chronic stress.

Tables presenting values for the two-way ANOVAs followed by Bonferroni *post hoc* analyses for each analyzed layer are provided in Tables 8 (*stratum pyramidale*), 9 (*stratum oriens*) and 10 (*stratum radiatum*) in the Supplemental information.

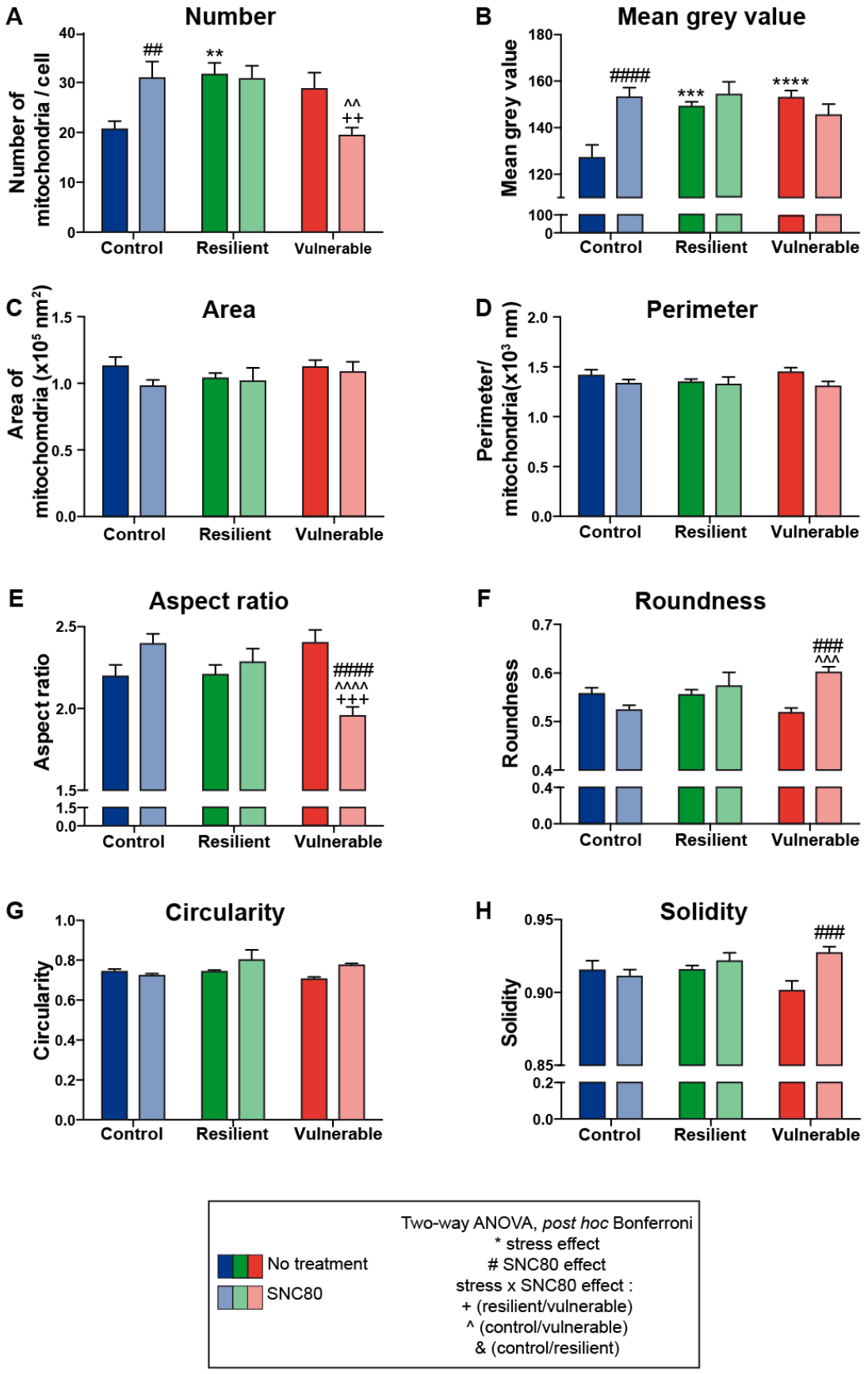
A
Number
Number of mitochondria / cell
##
**
^^
++
Control
Resilient
Vulnerable
B
Mean grey value
Mean grey value
####
***
****
Control
Resilient
Vulnerable
C
Area
Area of mitochomdria (x10⁵ nm²)
Control
Resilient
Vulnerable
D
Perimeter
Perimeter/ mitochondria(x10³ nm)
Control
Resilient
Vulnerable
E
Aspect ratio
Aspect ratio
####
^^^^
++++
Control
Resilient
Vulnerable
F
Roundness
Roundness
###
^^^
Control
Resilient
Vulnerable
G
Circularity
Circularity
Control
Resilient
Vulnerable
H
Solidity
Solidity
###
Control
Resilient
Vulnerable
No treatment
SNC80
Two-way ANOVA, post hoc Bonferroni
* stress effect
# SNC80 effect
stress x SNC80 effect :
+ (resilient/vulnerable)
^ (control/vulnerable)
& (control/resilient)

Figure 25. SNC80 treatment prevents oxidative stress in *stratum pyramidale* of CA1 hippocampus. (A) Graph representing the number of mitochondria per cell. **(B)** Graph representing the mean grey value in mitochondria. **(C)** and **(D)** Graphs representing area and perimeter of mitochondria respectively. **(E)** and **(F)** Graphs representing aspect ratio and roundness of mitochondria. **(G)** and **(H)** Graphs representing the circularity and solidity of mitochondria. Two-way ANOVA, Bonferroni *post hoc* analysis, n=30 cells/groups (3 animals/group). * for stress effect or # for SNC80 treatment effect or for stress x treatment effect, ^ (Control *versus* Vulnerable), & (Control *versus* Resilient), +(Resilient *versus* Vulnerable) = $p<0.05$, ** = $p<0.01$, *** = $p<0.001$, **** = $p<0.0001$. Error bars are mean ± SEM.

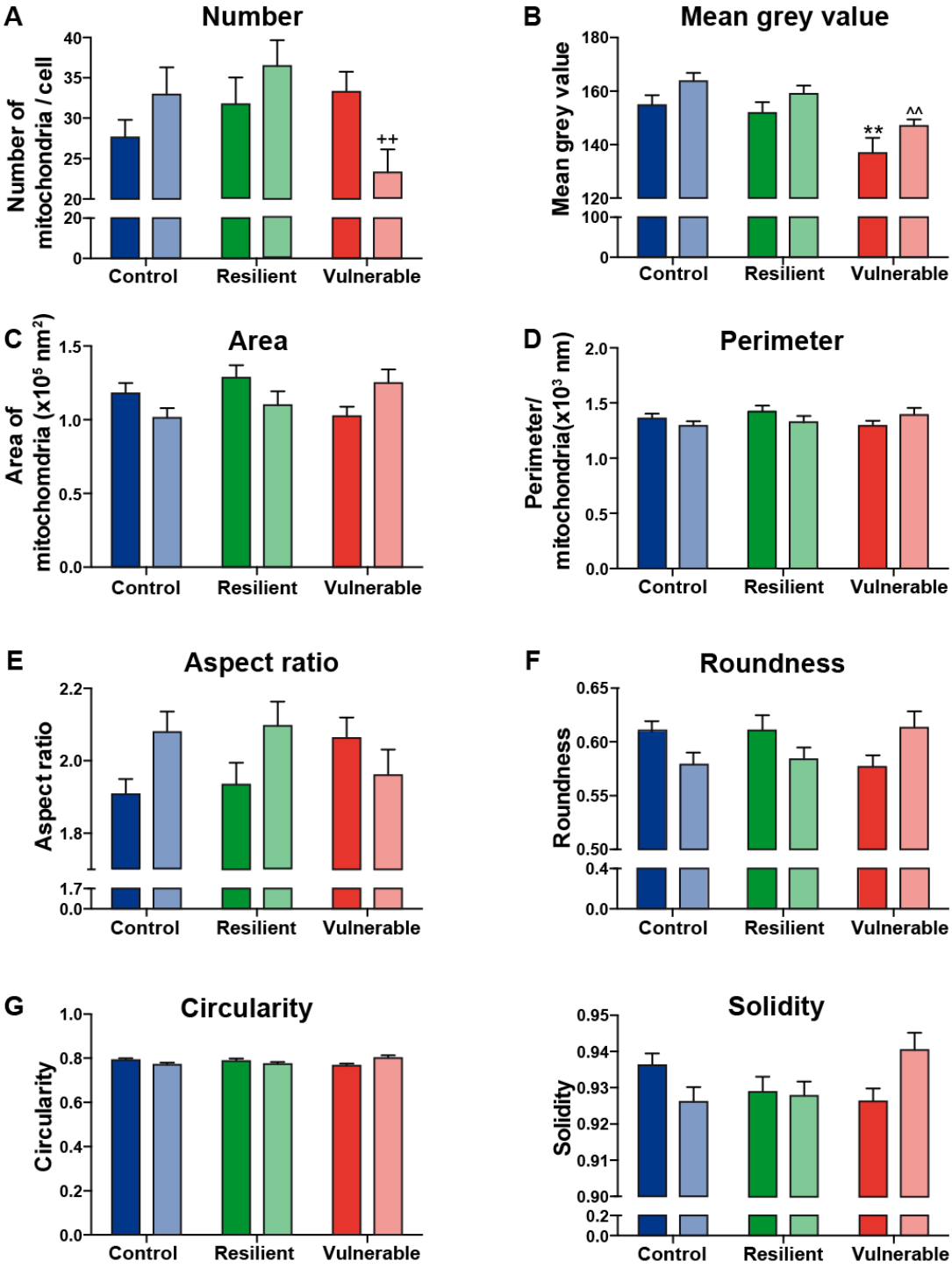
A
Number
Number of mitochondria / cell
++
Control
Resilient
Vulnerable
B
Mean grey value
Mean grey value
**
^^
C
Area
Area of mitochomdria (x10⁵ nm²)
D
Perimeter
Perimeter/ mitochondria(x10³ nm)
E
Aspect ratio
Aspect ratio
F
Roundness
Roundness
G
Circularity
Circularity
Solidity
Solidity
No treatment
SNC80
Two-way ANOVA, post hoc Bonferroni
* stress effect
# SNC80 effect
stress x SNC80 effect :
+ (resilient/vulnerable)
^ (control/vulnerable)
& (control/resilient)

Figure 26. SNC80 treatment prevents oxidative stress in interneurons of *stratum oriens* of CA1 hippocampus. (A) Graph for representing the number of mitochondria per cell. **(B)** Graph representing the mean grey value in mitochondria. **(C)** and **(D)** Graphs representing area and perimeter of mitochondria respectively. **(E)** and **(F)** Graphs representing aspect ratio and roundness of mitochondria. **(G)** and **(H)** Graphs representing the circularity and solidity of mitochondria. Two-way ANOVA, Bonferroni *post hoc* analysis, group without treatment: n(C)=27 cells, n(R)=24, n(V)=25 and group with treatment: n(C)=27 cells, n(R)=27, n(V)=21 (3 animals/group). * for stress effect or # for SNC80 treatment effect or for stress x treatment effect, ^ (Control *versus* Vulnerable), & (Control *versus* Resilient), +(Resilient *versus* Vulnerable) = $p<0.05$, ** = $p<0.01$, *** = $p<0.001$, **** = $p<0.0001$. Error bars are mean ± SEM.

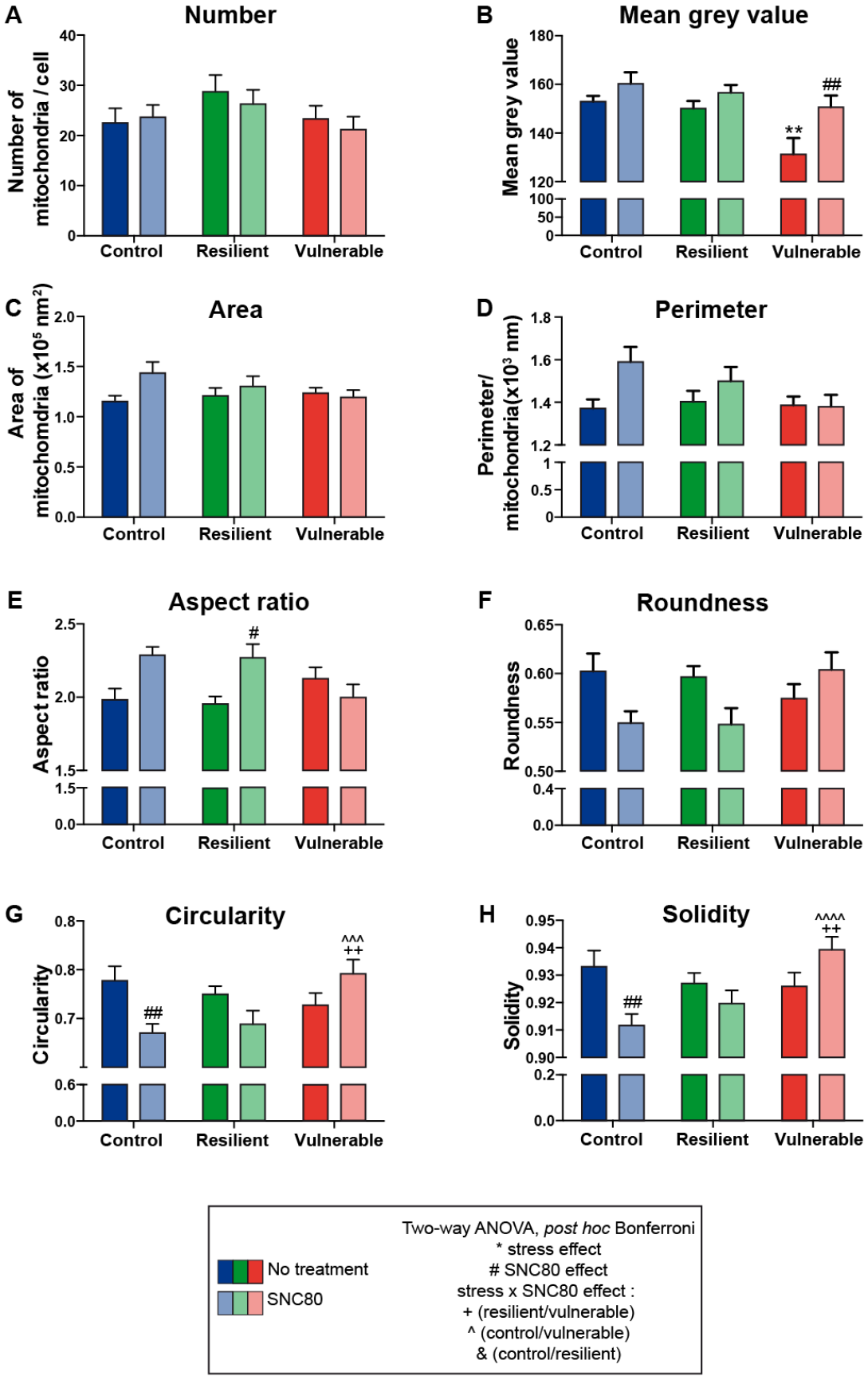
A
Number
Number of mitochondria / cell
40
30
20
10
0
Control
Resilient
Vulnerable
B
Mean grey value
Mean grey value
180
160
140
120
100
50
0
**
##
Control
Resilient
Vulnerable
C
Area
Area of mitochomdria (x10⁵ nm²)
2.0
1.5
1.0
0.5
0.0
Control
Resilient
Vulnerable
D
Perimeter
Perimeter/ mitochondria(x10³ nm)
1.8
1.6
1.4
1.2
1
0.5
0
Control
Resilient
Vulnerable
E
Aspect ratio
Aspect ratio
2.5
2.0
1.5
1.5
0.0
#
Control
Resilient
Vulnerable
F
Roundness
Roundness
0.65
0.60
0.55
0.50
0.4
0.0
Control
Resilient
Vulnerable
G
Circularity
Circularity
0.8
0.8
0.7
0.6
0.0
##
^^^
++
Control
Resilient
Vulnerable
H
Solidity
Solidity
0.95
0.94
0.93
0.92
0.91
0.90
0.2
0.0
##
^^^^
++
Control
Resilient
Vulnerable
No treatment
SNC80
Two-way ANOVA, post hoc Bonferroni
* stress effect
# SNC80 effect
stress x SNC80 effect :
+ (resilient/vulnerable)
^ (control/vulnerable)
& (control/resilient)

Figure 27. SNC80 treatment prevents oxidative stress in interneurons of *stratum radiatum* of CA1 hippocampus. (A) Graph for *radiatum* layer representing the number of mitochondria per cell. **(B)** Graph representing the mean grey value in mitochondria. **(C)** and **(D)** Graphs representing area and perimeter of mitochondria respectively. **(E)** and **(F)** Graphs representing aspect ratio and roundness of mitochondria. **(G)** and **(H)** Graphs representing the circularity and solidity of mitochondria. Two-way ANOVA, Bonferroni *post hoc* analysis, group without treatment: n(C)=20 cells, n(R)=22 n(V)=26 and group with treatment: n(C)=24 cells, n(R)=25, n(V)=21 (3 animals/group). * for stress effect or # for SNC80 treatment effect or for stress x treatment effect, ^ (Control *versus* Vulnerable), & (Control *versus* Resilient), +(Resilient *versus* Vulnerable) = $p<0.05$, ** = $p<0.01$, *** = $p<0.001$, **** = $p<0.0001$. Error bars are mean ± SEM.

2.2.5.2 SNC80 increases expression of complex III and V of mitochondrial respiratory chain.

Expression levels of different proteins involved in mitochondrial activity were assessed by western blot in the hippocampus. Figure 28A and 28G present representatives bands of expression level in proteins for each group. Respiratory chain is located in the inner membrane of mitochondria and closely related with the production of adenosine triphosphate (ATP). It consists of four linked membrane protein complexes named complex I, II, III and IV. Complex V corresponds here to a subunit of ATP synthase. Complex I possesses a NADH coenzyme Q reductase activity that retrieves electrons from NADH allowing transport of four protons from matrix to intermembrane space. Complex II is a succinate coenzyme Q reductase that retrieves electrons from $FADH_2$. Complexe III displays a coenzyme Q cytochrome C reductase activity allowing transport of four protons from matrix to inter membrane space. Complex IV is a cytochrome C oxidase transporting two protons. Finally, complex V is a subunit of the ATP synthase transporting protons into mitochondrial matrix to produce ATP (Green and Reed, 1998). Complexes I, II and IV failed to show a significant difference between non stressed animals and stressed ones as well as with treated mice (Figure 28D, 28E and 28F) while complexes III and V revealed a huge effect of SNC80 (Figure 28C: $F_{(1,30)}=46.86$, $p<0.0001$ and Figure 28B: $F_{(1,30)}=34.70$, $p<0.0001$). Indeed, expression of complex III was increased with SNC80 in all groups compared to non-treated mice (Figure 28C) while this increase was only observed in control and vulnerable mice for complex V (Figure 28B). However, resilient mice only displayed an increased trend toward for complex V expression with SNC80 (Figure 28B). Although a main effect of interaction was not observed for complex V, *post hoc* analyses

revealed an increased expression in treated vulnerable mice compared to treated resilient ones (Figure 28B). Overall, SNC80 showed a beneficial effect on complexes III and V without counteracting a stress effect. These results suggest that SNC80 improves their activity in order to generate a higher amount of cellular energy.

Superoxide dismutase (SOD) is an oxidoreductase, which is the major defense against superoxide ion and peroxynitrite. Three isoforms are known, catalyzing the same reaction but corresponding to distinct genes with different subcellular locations. Among them, Mn-SOD (Mn for manganese) is located in mitochondrial matrix and involves alternate reduction and reoxidation of catalytic metal (*i.e.* Mn) at the active site (Fukai and Ushio-Fukai, 2011). Catalase is also an oxidoreductase that catalyzes H_2O_2 to H_2O and oxygen, and is mainly located at peroxisome in the cytoplasm (Bai and Cederbaum, 2001). ANOVA analyses revealed that stress and SNC80 treatment do not modify the expression levels of superoxide dismutase (SOD; Figure 28H). On the contrary, expression levels of catalase showed a main effect of stress and stress by treatment (Figure 28I: $F_{(2,23)}$=6.397, p=0.0062 and $F_{(2,23)}$=3.517, p=0.0465). Especially, resilient and vulnerable mice displayed a reduced expression of catalase compared to controls without revealing any effect of SNC80 suggesting that SNC80 might not target catalase to promote stress resilience.

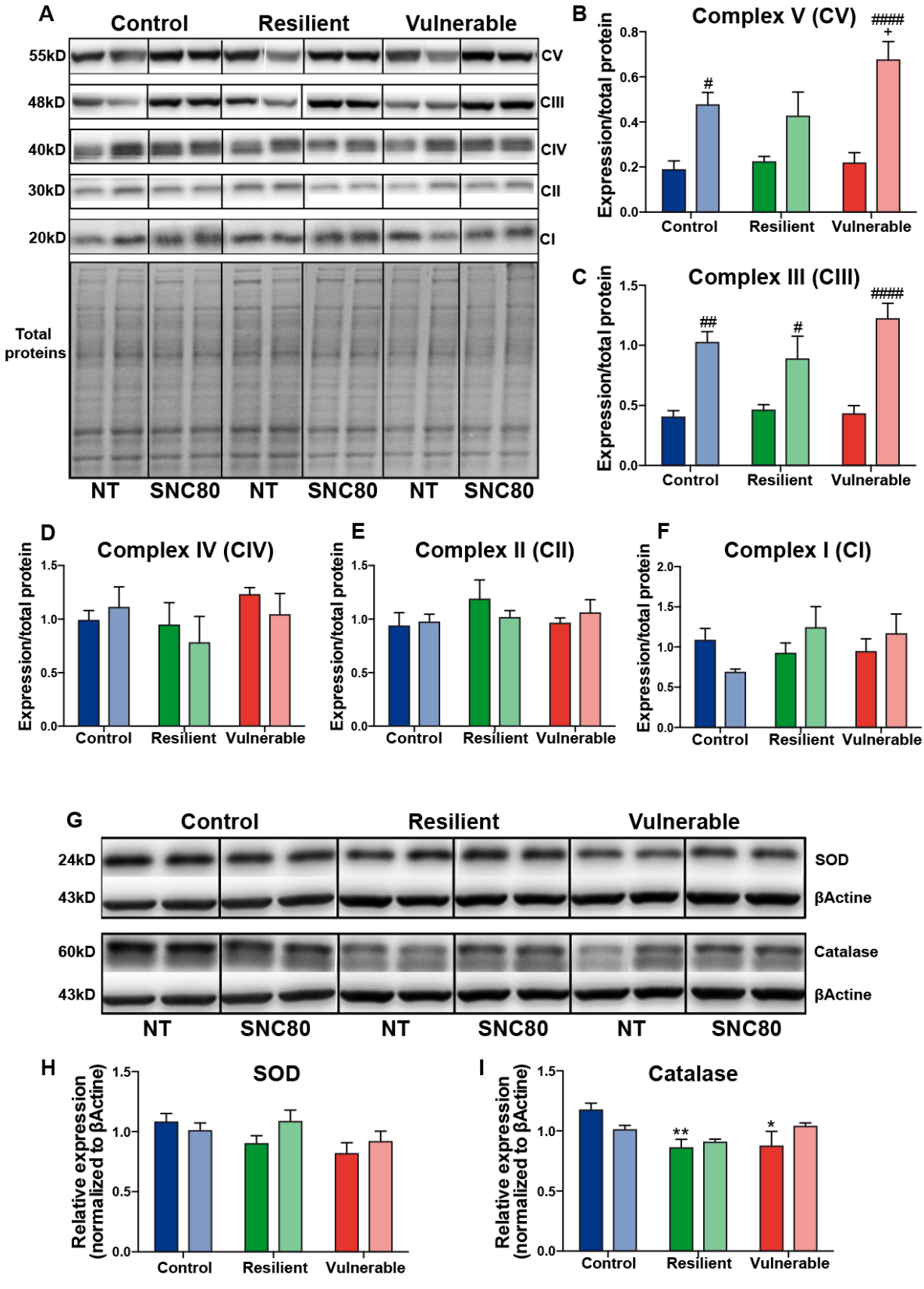
A
Control
Resilient
Vulnerable
55kD
48kD
40kD
30kD
20kD
CV
CIII
CIV
CII
CI
Total proteins
NT
SNC80
NT
SNC80
NT
SNC80
B
Complex V (CV)
Expression/total protein
Control
Resilient
Vulnerable
C
Complex III (CIII)
Expression/total protein
Control
Resilient
Vulnerable
D
Complex IV (CIV)
Expression/total protein
Control
Resilient
Vulnerable
E
Complex II (CII)
Expression/total protein
Control
Resilient
Vulnerable
F
Complex I (CI)
Expression/total protein
Control
Resilient
Vulnerable
G
Control
Resilient
Vulnerable
24kD
43kD
SOD
βActine
60kD
43kD
Catalase
βActine
NT
SNC80
NT
SNC80
NT
SNC80
H
SOD
Relative expression (normalized to βActine)
Control
Resilient
Vulnerable
I
Catalase
Relative expression (normalized to βActine)
Control
Resilient
Vulnerable

Figure 28. SNC80 treatment reduces expression level of mitochondrial respiratory chain complexes in hippocampus. (A) Representative bands for expression level in fives complexes of the respiratory chain (CI, CII, CIII, CIV, CV) and **(G)** Representative bands for expression level in superoxide dismutase (SOD) and catalase. From **(B)** to **(F)** Graphs for expression levels in CV, CIII, CIV, CII and CI in hippocampus for all groups. **(H)** and **(I).** Graphs for expression levels in SOD and Catalase in hippocampus for all groups. Two-way ANOVA, Bonferroni *post hoc* analysis, n=6/group, * for stress effect or # for SNC80 treatment effect or for stress x treatment effect, ^ (Control *versus* Vulnerable), & (Control *versus* Resilient), +(Resilient *versus* Vulnerable) = $p<0.05$, ** = $p<0.01$, *** = $p<0.001$, **** = $p<0.0001$. Error bars are mean ± SEM.

2.2.6 Conclusion

Our previous study demonstrated that pharmacological activation of DOPr improves resilience to chronic social stress by restoring the deleterious effects of oxidative stress induced by chronic stress (Henry *et al*, 2018). Different markers comprising cytoplasmic/nucleoplasmic condensation ("dark" neurons), dilation of the endoplasmic reticulum and Golgi apparatus, increased accumulation of lipofuscin granules, and prevalence of indentations were assessed by electron microscopy to determine changes in neuronal function. In this current study, we further observed structural changes in mitochondria accompanied by an increased expression of molecular markers associated with mitochondrial activity. Morphological analyses of mitochondria in stress condition with or without treatment revealed that SNC80 significantly modifies the shape of mitochondria, particularly in vulnerable mice, and improves mitochondrial integrity without changing significantly their size. These results suggest that SNC80 treatment might restore the deleterious effects of chronic stress by directly targeting mitochondria. Western Blot analyses further showed that SNC80 increases expression of specific complexes in the respiratory chain indicating an improvement in their activity to produce ATP. This study failed to decipher how SNC80 restores deleterious effect induced by chronic stress and thus, the exact contribution of endogenous DOPr in naturally promoting resilience to chronic stress remains unclear and warrants further investigation. Indeed, to promote stress resilience, DOPr signaling might target other antioxidant enzymes or negatively regulate the levels of free radicals such as nitric oxide.

2.2.7 Supplemental information

STRATUM PYRAMIDALE

					No treatment			SNC80			Interaction stress x SNC80		
MARKERS		**F(DFn, DFd)**	**p values**		Control vs Resilient	Control vs Vulnerable	Resilient vs Vulnerable	Control	Resilient	Vulnerable	Control vs Resilient	Control vs Vulnerable	Resilient vs Vulnerable
	INTERACTION	F (2, 174) = 7,492	**P = 0,0008**	**Significance?**	**Yes**	No	No	**Yes**	No	No	No	**Yes**	**Yes**
	STRESS	F (2, 174) = 4,262	**P = 0,0156**	**t values**	**3.054**	2.255	0.799	**2.859**	0.242	2.598	0.047	**3.202**	**3.155**
Number	**TREATMENT**	F (1, 174) = 0,0001149	P = 0,9915	**p values**	**0.0026**	0.0254	0.4254	**0.0048**	0.8091	0.0102	0.9626	**0.0016**	**0.0019**
	INTERACTION	F (2, 174) = 7,591	**P = 0,0007**	**Significance?**	**Yes**	**Yes**	No	**Yes**	No	No	No	No	No
	STRESS	F (2, 174) = 3,973	**P = 0,0205**	**t values**	**3.584**	**4.203**	0.619	**4.235**	0.847	1.222	0.195	1.254	1.450
Mean grey value	**TREATMENT**	F (1, 174) = 4,916	**P = 0,0279**	**p values**	**0.0004**	**0.0001**	0.5367	**0.0001**	0.3982	0.2234	0.8456	0.2115	0.1489
	INTERACTION	F (2, 174) = 0,5387	P = 0,5845	**Significance?**	No	No	No	No	No	No	No	No	No
	STRESS	F (2, 174) = 0,6521	P = 0,5222	**t values**	0.949	0.076	0.874	1.591	0.249	0.405	0.393	1.110	0.718
Area	**TREATMENT**	F (1, 174) = 1,681	P = 0,1965	**p values**	0.3439	0.9395	0.3833	0.1134	0.8037	0.6860	0.6948	0.2685	0.4737
	INTERACTION	F (2, 174) = 0,6393	P = 0,5289	**Significance?**	No	No	No	No	No	No	No	No	No
	STRESS	F (2, 174) = 0,3912	P = 0,6769	**t values**	0.910	0.448	1.358	1.113	0.326	1.915	0.122	0.353	0.231
Perimeter	**TREATMENT**	F (1, 174) = 3,716	P = 0,0555	**p values**	0.3641	0.6547	0.1762	0.2672	0.7448	0.0571	0.9030	0.7245	0.8176
	INTERACTION	F (2, 173) = 12,38	**P < 0,0001**	**Significance?**	No	No	No	No	No	**Yes**	No	**Yes**	**Yes**
	STRESS	F (2, 173) = 1,444	P = 0,2388	**t values**	0.103	2.103	2.001	2.049	0.786	**4.565**	1.159	**4.532**	**3.373**
Aspect ratio	**TREATMENT**	F (1, 173) = 1,036	P = 0,3103	**p values**	0.9181	0.0369	0.0470	0.0420	0.4329	**0.0001**	0.4329	**0.0001**	**0.0009**
	INTERACTION	F (2, 174) = 7,149	**P = 0,0010**	**Significance?**	No	No	No	No	No	**Yes**	No	**Yes**	No
	STRESS	F (2, 174) = 1,318	P = 0,2704	**t values**	0.101	1.789	1.689	1.529	0.833	**3.808**	2.261	**3.547**	1.286
Roundness	**TREATMENT**	F (1, 174) = 3,226	P = 0,0742	**p values**	0.9197	0.0754	0.0930	0.1281	0.4060	**0.0002**	0.0250	**0.0005**	0.2002
	INTERACTION	F (2, 174) = 2,181	P = 0,1160	**Significance?**	No	No	No	No	No	No	No	No	No
	STRESS	F (2, 174) = 1,574	P = 0,2101	**t values**	0.009	1.146	1.137	0.603	1.764	2.107	2.359	1.564	0.794
Circularity	**TREATMENT**	F (1, 174) = 3,553	P = 0,0611	**p values**	0.9928	0.2534	0.2571	0.5473	0.0795	0.0366	0.0194	0.1196	0.4283
	INTERACTION	F (2, 173) = 4,193	**P = 0,0167**	**Significance?**	No	No	No	No	No	**Yes**	No	No	No
	STRESS	F (2, 173) = 0,5860	P = 0,5576	**t values**	0.027	1.879	1.905	0.586	0.793	**3.451**	1.400	2.159	0.740
Solidity	**TREATMENT**	F (1, 173) = 4,440	**P = 0,0366**	**p values**	0.9785	0.0619	0.0584	0.5586	0.4289	**0.0007**	0.1633	0.0322	0.4603

Table 8. Statistical analysis (Two-way ANOVA with Bonferroni *post hoc* analysis) for diverse morphological features of mitochondria in *stratum pyramidale* described by electron microscopy. Left part of the table provides statistical data of main effects and the right part (orange) provides statistical data for Bonferroni *post hoc*. Bold numbers are considered as significant.

STRATUM ORIENS

					No treatment			SNC80			Interaction stress x SNC80		
MARKERS		**F(DFn, DFd)**	**p values**		Control vs Resilient	Control vs Vulnerable	Resilient vs Vulnerable	Control	Resilient	Vulnerable	Control vs Resilient	Control vs Vulnerable	Resilient vs Vulnerable
	INTERACTION	F (2, 145) = 4,115	**P = 0,0183**	**Significance?**	No	No	No	No	No	No	No	No	**Yes**
	STRESS	F (2, 145) = 1,968	P = 0,1434	**t values**	0.994	1.378	0.363	1.319	1.142	2.285	0.883	2.243	**3.070**
Number	**TREATMENT**	F (1, 145) = 2,139e-005	P = 0,9963	**p values**	0.3219	0.1703	0.7171	0.1892	0.2553	0.0238	0.3787	0.0264	**0.0026**
	INTERACTION	F (2, 145) = 0,07621	P = 0,9267	**Significance?**	No	**Yes**	No	No	No	No	No	**Yes**	No
	STRESS	F (2, 145) = 10,63	**P < 0,0001**	**t values**	0.535	**3.335**	2.715	1.710	1.327	1.782	0.893	**2.968**	2.133
Mean grey value	**TREATMENT**	F (1, 145) = 7,668	**P = 0,0064**	**p values**	0.5935	**0.0011**	0.0074	0.0894	0.1866	0.0768	0.3733	**0.0035**	0.0346
	INTERACTION	F (2, 145) = 4,127	**P = 0,0181**	**Significance?**	No	No	No	No	No	No	No	No	No
	STRESS	F (2, 145) = 0,7760	P = 0,4622	**t values**	0.958	1.418	2.317	1.552	1.689	1.927	0.798	2.060	1.314
Area	**TREATMENT**	F (1, 145) = 0,4416	P = 0,5074	**p values**	0.3397	0.1583	0.0219	0.1228	0.0934	0.0559	0.4262	0.0412	0.1909
	INTERACTION	F (2, 145) = 2,513	P = 0,0845	**Significance?**	No	No	No	No	No	No	No	No	No
	STRESS	F (2, 145) = 0,5650	P = 0,5696	**t values**	1.026	0.948	1.929	1.028	1.569	1.431	0.468	1.513	1.074
Perimeter	**TREATMENT**	F (1, 145) = 0,3706	P = 0,5436	**p values**	0.3066	0.3447	0.0557	0.3057	0.1188	0.1537	0.6405	0.1325	0.2846
	INTERACTION	F (2, 143) = 3,339	**P = 0,0382**	**Significance?**	No	No	No	No	No	No	No	No	No
	STRESS	F (2, 143) = 0,08006	P = 0,9231	**t values**	0.316	1.895	1.529	2.145	1.936	1.177	0.209	1.397	1.569
Aspect ratio	**TREATMENT**	F (1, 143) = 2,563	P = 0,1116	**p values**	0.7525	0.0601	0.1285	0.0336	0.0548	0.2412	0.8347	0.1646	0.1189
	INTERACTION	F (2, 143) = 4,834	**P = 0,0093**	**Significance?**	No	No	No	No	No	No	No	No	No
	STRESS	F (2, 143) = 0,03735	P = 0,9633	**t values**	0.090	1.996	2.027	1.880	1.607	2.082	0.280	1.973	1.677
Roundness	**TREATMENT**	F (1, 143) = 0,5222	P = 0,4711	**p values**	0.9284	0.0478	0.0445	0.0621	0.1103	0.0391	0.7799	0.0504	0.0957
	INTERACTION	F (2, 145) = 4,444	**P = 0,0134**	**Significance?**	No	No	No	No	No	No	No	No	No
	STRESS	F (2, 145) = 0,06017	P = 0,9416	**t values**	0.280	1.806	1.479	1.553	0.997	2.353	0.237	2.124	1.903
Circularity	**TREATMENT**	F (1, 145) = 0,0001125	P = 0,9916	**p values**	0.7799	0.0730	0.1413	0.1226	0.3204	0.0200	0.8130	0.0354	0.0590
	INTERACTION	F (2, 148) = 4,582	**P = 0,0117**	**Significance?**	No	No	No	No	No	No	No	No	No
	STRESS	F (2, 148) = 0,7765	P = 0,4619	**t values**	1.313	1.793	0.453	1.847	0.182	2.388	0.319	2.446	2.204
Solidity	**TREATMENT**	F (1, 148) = 0,09391	P = 0,7597	**p values**	0.1912	0.0750	0.6512	0.0667	0.8558	0.0182	0.7502	0.0156	0.0291

Table 9. Statistical analysis (Two-way ANOVA with Bonferroni *post hoc* analysis) for diverse morphological features of mitochondria in *stratum oriens* described by electron microscopy. Left part of the table provides statistical data of main effects and the right part (orange) provides statistical data for Bonferroni *post hoc*. Bold numbers are considered as significant.

STRATUM RADIATUM

					No treatment			SNC80			Interaction stress x SNC80		
MARKERS		**F(DFn, DFd)**	**p values**		Control vs Resilient	Control vs Vulnerable	Resilient vs Vulnerable	Control	Resilient	Vulnerable	Control vs Resilient	Control vs Vulnerable	Resilient vs Vulnerable
	INTERACTION	F (2, 132) = 0,2439	P = 0,7839	**Significance?**	No	No	No	No	No	No	No	No	No
	STRESS	F (2, 132) = 2,039	P = 0,1343	**t values**	1.500	0.203	1.392	0.278	0.634	0.538	0.679	0.607	1.269
Number	**TREATMENT**	F (1, 132) = 0,2546	P = 0,6147	**p values**	0.1360	0.8394	0.1663	0.7814	0.5272	0.5915	0.4983	0.5449	0.2067
	INTERACTION	F (2, 132) = 1,270	P = 0,2842	**Significance?**	No	**Yes**	**Yes**	No	No	**Yes**	No	No	No
Mean grey value	**STRESS**	F (2, 132) = 6,559	**P = 0,0019**	**t values**	0.431	**3.347**	**2.977**	1.091	1.020	**3.018**	0.578	1.474	0.930
	TREATMENT	F (1, 132) = 8,769	**P = 0,0036**	**p values**	0.6672	**0.0011**	**0.0035**	0.2773	0.3096	**0.0031**	0.5642	0.1429	0.3541
	INTERACTION	F (2, 132) = 0,2439	P = 0,7839	**Significance?**	No	No	No	No	No	No	No	No	No
	STRESS	F (2, 132) = 2,039	P = 0,1343	**t values**	0.452	0.685	0.221	2.295	0.777	0.351	1.147	1.988	0.899
Area	**TREATMENT**	F (1, 132) = 0,2546	P = 0,6147	**p values**	0.6520	0.4945	0.8254	0.0233	0.4385	0.7261	0.2535	0.0489	0.3703
	INTERACTION	F (2, 132) = 1,958	P = 0,1452	**Significance?**	No	No	No	No	No	No	No	No	No
	STRESS	F (2, 132) = 1,568	P = 0,2124	**t values**	0.383	0.186	0.217	2.674	1.214	0.088	1.177	2.611	1.499
Perimeter	**TREATMENT**	F (1, 132) = 4,944	**P = 0,0279**	**p values**	0.7023	0.8527	0.8285	0.0084	0.2269	0.9300	0.2413	0.0101	0.1363
	INTERACTION	F (2, 132) = 5,474	**P = 0,0052**	**Significance?**	No	No	No	No	**Yes**	No	No	No	No
	STRESS	F (2, 132) = 0,4473	P = 0,6403	**t values**	0.238	1.335	1.624	2.739	**2.930**	1.205	0.162	2.629	2.498
Aspect ratio	**TREATMENT**	F (1, 132) = 6,763	**P = 0,0104**	**p values**	0.8123	0.1842	0.1068	0.0070	**0.0040**	0.2304	0.8716	0.0096	0.0137
	INTERACTION	F (2, 132) = 4,630	**P = 0,0114**	**Significance?**	No	No	No	No	No	No	No	No	No
	STRESS	F (2, 132) = 0,6912	P = 0,5028	**t values**	0.252	1.283	1.048	2.390	2.283	1.375	0.077	2.495	2.592
Roundness	**TREATMENT**	F (1, 132) = 3,718	P = 0,0560	**p values**	0.8014	0.8014	0.2966	0.0183	0.0240	0.1715	0.9387	0.0138	0.0106
	INTERACTION	F (2, 132) = 6,256	**P = 0,0025**	**Significance?**	No	No	No	**Yes**	No	No	No	**Yes**	**Yes**
	STRESS	F (2, 132) = 1,579	P = 0,2101	**t values**	0.749	1.406	0.644	**2.960**	1.761	1.828	0.525	**3.395**	**2.921**
Circularity	**TREATMENT**	F (1, 132) = 2,905	P = 0,0907	**p values**	0.4552	0.1621	0.5207	**0.0036**	0.0806	0.0698	0.6005	**0.0009**	**0.0041**
	INTERACTION	F (2, 132) = 6,557	**P = 0,0019**	**Significance?**	No	No	No	**Yes**	No	No	No	**Yes**	**Yes**
	STRESS	F (2, 132) = 2,773	P = 0,0661	**t values**	0.859	1.053	0.165	**3.089**	1.101	1.987	1.218	**4.032**	**2.895**
Solidity	**TREATMENT**	F (1, 132) = 1,710	P = 0,1933	**p values**	0.3919	0.2943	0.8692	**0.0024**	0.2729	0.0490	0.2254	**0.0001**	**0.0044**

Table 10. Statistical analysis (Two-way ANOVA with Bonferroni *post hoc* analysis) for diverse morphological features of mitochondria in *stratum radiatum* described by electron microscopy. Left part of the table provides statistical data of main effects and the right part (orange) provides statistical data for Bonferroni *post hoc*. Bold numbers are considered as significant.

3 DISCUSSION GÉNÉRALE

Les études présentées dans cette thèse ont permis de mettre en lumière l'importance de la signalisation ENK/DOPr dans la neurobiologie de la résilience au stress chronique. L'expérience de stress chronique de défaite sociale mime les perturbations sociales quotidiennes et démontre l'existence d'une grande variabilité entre les individus quant à leur réponse comportementale. Ce paradigme permet, ainsi, de discriminer deux populations : les individus résilients et ceux qui sont vulnérables au stress chronique. Les résultats des études présentées dans cette thèse ont révélé que la signalisation ENK/DOPr est naturellement nécessaire pour favoriser la résilience, notamment grâce à son rôle neuroprotecteur face au stress oxydatif dans un contexte de stress social chronique.

Dans cette discussion générale, je présenterai les avantages et les limites du modèle de stress social chronique que nous avons utilisé, ainsi que ceux de l'agoniste DOPr employé, le SNC80. Je discuterai en détail des résultats obtenus dans les deux études qui constituent le corps de ma thèse, en proposant des perspectives de travail pour la suite. Enfin, je terminerai cette discussion sur le développement de thérapies potentielles pour le traitement des troubles anxieux chez l'humain, afin de prévenir le développement de pathologies plus sévères associées au stress chronique, comme la dépression majeure ou les maladies neurodégénératives.

3.1 Le modèle de stress chronique de défaite sociale

La recherche de thérapies pour traiter les pathologies psychiatriques stagne depuis des décennies, malgré quelques pistes prometteuses en cours d'investigation. En effet, les médicaments pour soigner la dépression majeure ou les troubles bipolaires ont peu évolué depuis leur première découverte et utilisation. Par exemple, le lithium est un régulateur de l'humeur prescrit dans le cadre des troubles bipolaires pour stabiliser les patients qu'ils soient en phase maniaque ou dépressive. Sa première prescription contre les troubles maniaques remonte à 1871 (Shorter, 2009), et il est encore largement utilisé aujourd'hui. Ses mécanismes d'action ont, en partie, été récemment élucidés (Beaulieu *et al*, 2009). De la même manière, l'hypothèse de l'implication des monoamines (sérotonine, norepinéphrine et dopamine) dans la dépression a émergé il y a 50 ans, et les traitements comme les inhibiteurs de monoamines oxydases ainsi que les inhibiteurs de la recapture de la sérotonine ont été développés par la suite (Hillhouse and Porter, 2015). Ces thérapies ont des effets secondaires importants, leur délai d'action peut être long, et l'efficacité reste modeste selon les patients (Medecine, 2017). La productivité modérée dans ce domaine résulte, entre autres, de la rareté des modèles animaux existants permettant de mimer un comportement dit « dépressif ». Le stress chronique de défaite sociale (SCDS) semble être à l'heure actuelle un des meilleurs paradigmes pour reproduire les perturbations sociales de la vie quotidienne et induire ainsi un comportement dit « dépressif » (Golden *et al*, 2011; Huhman, 2006; Krishnan *et al*, 2007). Il permet de mimer la symptomatologie du PTSD (Whitaker *et al*, 2014) et de la dépression (Bondar *et al*, 2017), comprenant l'exacerbation de la réponse de peur (PTSD), le comportement d'évitement et d'anxiété (PTSD, dépression ; DSM-V), ainsi qu'une altération au niveau de l'axe HPA (PTSD, dépression). Le phénotype vulnérable obtenu après un SCDS peut être reversé par l'administration chronique mais non aigue d'antidépresseurs (fluoxetine et imipramine) (Berton *et al*, 2006; Tsankova *et al*, 2006). De plus, le SCDS diffère d'autres paradigmes de stress, comme la contention ou la nage forcée, de par sa capacité à activer de façon continue et à long terme la réponse neuroendocrine via l'axe HPA et la libération des catécholamines (Koolhaas *et al*, 1997). Son intérêt réside principalement dans la possibilité d'étudier les différences individuelles quant à la capacité de résister ou non face à un stress chronique.

Un des problèmes majeurs associé à ce protocole est l'observation de nombreuses blessures physiques chez les souris subissant la défaite (Golden *et al*, 2011). Les blessures physiques infligées lors des expériences nous invitent à réfléchir quant à la pertinence d'utiliser ce paradigme dans le contexte de l'étude du système opioïdergique, dont le rôle premier est le contrôle de la douleur. En effet, la douleur engendrée par les blessures physiques pourrait déclencher la libération des ENK au niveau central dans les régions du contrôle sensitif et émotionnel de la douleur dont fait partie le système limbique (Ossipov *et al*, 2010; Waksman *et al*, 1985; Waksman *et al*, 1986). De plus, il a été démontré que le stress induit par des chocs électriques dans les pattes chez le rat provoque une analgésie via l'activation du système opioïdergique (Amit and Galina, 1986). L'hypothèse que les effets du stress sur l'ARNm des ENKs (Chapitre 1 – Figure 17B) résultent en partie de l'activation du système de la douleur ne peut donc être complètement éliminée. Toutefois, l'analgésie induite par les ENKs ferait intervenir l'activation des MOPr plutôt que des DOPr, comme démontré par l'injection intra-cérébro-ventriculaire d'agonistes spécifiques de MOPr et DOPr chez la souris (Chaillet *et al*, 1984). Ceci suggèrerait que les modifications de l'expression des ARNm de DOPr, que nous avons observées (Chapitre1 – Figure 17E), ne résultent peu ou pas de l'activation du système de la douleur.

Nous avons choisi le SCDS comme paradigme de stress chronique pour nos études car les interactions sociales sont la source principale de stress dans la vie quotidienne, rendant le modèle particulièrement pertinent d'un point de vue translationnel chez l'humain. Le stress chronique imprévisible consiste à exposer les animaux à un stress différent chaque jour (Berube *et al*, 2014) et permet aussi de distinguer les deux populations. Les deux paradigmes de stress chronique diffèrent par la nature des stress appliqués, la durée des protocoles et la méthode employée pour discriminer les résilients des vulnérables. Reproduire l'étude en utilisant le paradigme du stress chronique imprévisible permettrait donc d'investiguer la possibilité d'une signature commune, c'est-à-dire d'un mécanisme universel sous-jacent le rôle des ENKs et DOPr dans la résilience, quel que soit le paradigme de stress utilisé.

3.2 Un dialogue privilégié ENK/DOPr entre la BLA et le *oriens*-CA1-vHPC dans la résilience au stress chronique

Les articles de Patrick Bérubé ont mis en évidence la contribution fonctionnelle des ENKs de la BLA dans le développement de la résilience au stress chronique chez le rat (Berube *et al*, 2013; Berube *et al*, 2014). En effet, il a démontré une diminution de l'expression de l'ARNm des ENKs dans la BLA postérieure (BLAp) chez les animaux vulnérables avec un paradigme de SCDS (Berube *et al*, 2013). De plus, l'inhibition des ENKs, par ARN interférent dans ce noyau, a permis de reproduire un phénotype vulnérable, comme observé dans un modèle de stress chronique imprévisible (Berube *et al*, 2014). Dans le chapitre 1 de cette thèse, la même diminution du niveau des ARNm des ENKs dans la BLA a été observée chez la souris vulnérable avec un paradigme de SCDS (Chapitre 1 – Figure 17B). Ces résultats suggèrent qu'un rôle similaire serait exercé, par les ENKs de la BLA, dans la résilience entre les rongeurs et soulèvent l'hypothèse d'une conservation chez l'humain. Les études neuroanatomiques sont essentiellement effectuées chez le rat, où une distinction est faite entre la partie antérieure (BLAa) et la partie postérieure (BLAp) de l'amygdale basolatérale, à la différence de la souris. Pourtant, cette distinction existe bien dans l'atlas de Franklin et Paxinos (The Mouse Brain in Stereotaxic coordinates, 3^{éme} Édition). Chez le rat, les neurones exprimant ENK sont principalement localisés dans la BLAp tandis qu'ils sont peu observés dans la BLAa (Berube *et al*, 2013). Comme décrit précédemment, la diminution de l'expression de l'ARNm des ENKs chez les rats vulnérables a été observée dans la BLAp (Berube *et al*, 2013) tandis que chez la souris, la quantification a été effectuée dans le noyau au complet (Chapitre 1 – Figure 17B). Chez la souris, une réponse au niveau de l'expression de l'ARNm des DOPr a été observée dans la couche *oriens* de la région CA1 de l'hippocampe ventral (*oriens*-CA1-vHPF, Chapitre 1 – Figure 17E). Or, il a été rapporté, chez le rat, que les neurones de la BLAa projettent faiblement vers l'*oriens*-CA1-vHPF tandis que ceux de la BLAp y projettent massivement (Petrovich *et al*, 2001) suggérant ainsi des rôles bien distincts pour chacune de ces sous-parties. Ainsi, si la variation d'expression de l'ARNm des ENKs entre les souris résilientes et celles vulnérables ne s'applique que dans un des deux noyaux et que ceux-ci ont bien une contribution fonctionnelle distincte chez la souris comme les projections neuronales chez le

rat le suggèrent, le résultat obtenu est probablement « dilué » par l'absence de cette distinction anatomique.

L'établissement des différentes stratégies d'adaptation face à un stress chronique est associé à des changements dans l'activité des circuits neuronaux (Reyes *et al*, 2015). Par exemple, lors d'un stress aigu, l'activité du locus coeruleus (LC) est régulée à la fois par le CRH et les ENKs provenant d'afférences excitatrices de la CEA et celles inhibitrices du PGi, respectivement (Tjoumakaris *et al*, 2003). Dans l'étude de Reyes, l'injection d'un traceur rétrograde dans le LC - combiné à des marquages pour ENK, CRH et *cfos* (activation neuronale) - chez des rats ayant subi un SCDS, a révélé que les afférences excitatrices de la voie CRH (LC-CEA) sont engagées chez les rats vulnérables tandis que ce sont les afférences inhibitrices de la voie ENK (LC-PGi) qui sont engagées chez les rats résilients (2015). Ces observations nous invitent à investiguer l'activité du circuit neuronal entre la BLA et l'*oriens*-CA1-vHPF en condition de SCDS chez la souris. À cette fin, une étude neuroanatomique de traçage neuronal pourrait être effectuée en condition normale et de SCDS. Pour cela, injecter dans la BLA un virus anterograde Cre-dépendant dans des souris pENK-Cre (la recombinase Cre s'exprime uniquement dans les neurones ENK) préalablement croisées avec les souris *knockin* pour DOPr-eGFP (Scherrer et al, 2006) permettrait d'évaluer si les projections ENK de la BLA vers les neurones positifs pour DOPr dans l'*oriens*-CA1-vHPF sont engagées chez les animaux résilients à la différence des vulnérables.

3.3 L'expression des ARNm DOPr est diminuée dans le *oriens*-CA1-vHPC des souris vulnérables : Que sont ces neurones exprimant DOPr?

Notre première étude a montré que les souris vulnérables présentaient une diminution des ARNm de DOPr au niveau de *oriens*-CA1-vHPC (Chapitre 1 –Figure 17E). Une étude a montré que l'activation optogénétique des afférences glutamatergiques de la BLA vers le vHPC favoriserait un comportement anxieux chez la souris dans le labyrinthe en croix surélevé et dans le test de l'« open-field ». À l'inverse, son inhibition exercerait l'effet opposé (Felix-Ortiz *et al*, 2013). Ces travaux nous suggèrent que la signalisation

ENK/DOPr ferait partie de ces afférences inhibitrices projetant de la BLA vers le vHPC dans le but de moduler le comportement anxieux.

Nous pouvons alors nous questionner sur l'identité de ces neurones exprimant DOPr dans l'*oriens*-CA1-vHPC. Les neurones contenant DOPr dans l'*oriens*-CA1-vHPC comprennent des interneurones GABAergiques chez le rat (Commons and Milner, 1997). Les ARNm de DOPr sont connus pour être principalement exprimés dans les neurones positifs pour la parvalbumine (PV+) et moindrement, dans les neurones positifs pour la somatostatine (SOM+) tandis qu'ils sont complètement absents des neurones positifs pour la calrétinine chez le rat (Stumm *et al*, 2004). Une étude *in vitro,* sur coupe d'hippocampe de rat, a suggéré que les interneurones de l'*oriens* dans la région CA1 ciblant directement les neurones pyramidaux (cellules à panier et axo-axoniques) expriment principalement MOPr, tandis que DOPr serait contenu dans les neurones ciblant les autres couches (cellules *oriens-lacunosum moleculare,* OLM et cellules bistratifiées) (Svoboda *et al*, 1999).

3.4 Le SNC80 : avantages et inconvénients

Le SNC80 est un agoniste non-peptidique de DOPr (Bilsky *et al*, 1995) facilement disponible et peu dispendieux (structure chimique présentée en Figure 29 – section 3.8). Il est abondamment utilisé dans la recherche depuis sa synthèse en 1994 (Calderon *et al*, 1994). De plus, il peut être administré en périphérie tout en ayant un effet central, il traverse la barrière hémato-encéphalique à la différence des neuropeptides (Bilsky *et al*, 1995). Chez le rat, le SNC80 induit un effet supérieur aux antidépresseurs traditionnels dans le test de nage forcée (Broom *et al*, 2002a) et facilite l'exploration dans les bras ouverts du labyrinthe en croix surélevé (Perrine *et al*, 2006; Saitoh *et al*, 2005).

Un des inconvénients majeurs du SNC80 est sa propension à induire des crises épileptiques de courte durée mais non létales chez le rongeur, ainsi qu'une hyperlocomotion (Broom *et al*, 2002b; Jutkiewicz *et al*, 2005). Les crises peuvent induire une brève catalepsie susceptible d'affecter la capacité d'échappement de la souris pendant la défaite sociale. À l'inverse, l'hyperlocomotion augmenterait la capacité d'échappement de la souris (Jutkiewicz *et al*, 2005). Lors de mes expériences, le SNC80 a été injecté à 10 mg/kg entre 30 minutes et 1 heure avant le SCDS, le test de nage forcée ou le test de suspension par la

queue, afin d'éviter ces inconvénients (Chapitre 1- Figure 18). De plus, il a été montré, chez le rat, que les crises d'épilepsie n'interféraient pas avec l'effet anxiolytique du SNC80 dans un test de nage forcée (Jutkiewicz *et al*, 2005).

Dans le contexte du contrôle de la douleur chez la souris, il a été montré que l'administration aigüe du SNC80 permet une réponse analgésique. À la seconde injection, une forte internalisation du récepteur, due à sa phosphorylation et au découplage de la protéine G, est observée abolissant les effets analgésiques du SNC80. Cette désensibilisation du récepteur est transitoire car 24 heures plus tard, DOPr est à nouveau localisé à la membrane plasmique (Pradhan *et al*, 2009). Après 5 jours de traitement quotidien au SNC80, une tolérance aux effets analgésiques, locomoteurs et anxiolytiques est observée (Pradhan *et al*, 2010). Considérant que l'effet anxiolytique du SNC80 est aussi sujet à la tolérance, nous pouvons nous demander si la drogue n'aurait pas exercé un effet uniquement les premiers jours de traitement pendant le SCDS. Ainsi, continuer le traitement au SNC80 pour tenter d'augmenter davantage le nombre de résilients ou de diminuer le SO serait inutile. D'autres molécules peuvent être utilisées pour diminuer l'effet de tolérance. Cette option sera discutée dans la dernière partie de la discussion intitulée Thérapies.

3.5 Perspectives : première partie du chapitre 1

De nombreuses perspectives émergent directement des résultats obtenus dans le chapitre 1. En effet, les observations concernant les niveaux de DOPr se sont concentrées sur l'hippocampe. Cependant, le PFC (infralimbique, en particulier), l'AMG, la VTA et le NAc sont, entre autres, des régions à investiguer. Comme présenté dans la revue (Henry *et al*, 2017), l'activation de MOPr et DOPr semble produire des effets opposés en ce qui concerne l'anxiété : DOPr est généralement présenté comme anxiolytique tandis que MOPr exercerait un effet inverse (Filliol *et al*, 2000). Cependant, certaines études ne vont pas dans ce sens (Chu Sin Chung *et al*, 2015; Wilson and Junor, 2008). À l'aide d'un modèle murin de délétion de DOPr uniquement dans les neurones GABAergiques du cerveau antérieur (« forebrain »), l'étude de Chu Sin Chung *et al.* (2015) a mis en lumière un rôle anxiogénique d'une sous-population de neurones GABAergiques exprimant DOPr au sein

de ces structures. L'infusion d'un agoniste spécifique de MOPr dans la CEA chez le rat a révélé des effets opposés selon le modèle utilisé : la micro-injection de DAMGO a diminué le niveau d'anxiété dans le labyrinthe en croix surélevé tandis qu'elle l'augmentait dans le test d'enfouissement défensif (Wilson *et al*, 2008). Ces résultats suggèrent que l'effet de l'activation de MOPr et DOPr est spécifique aux contextes et aux structures étudiés. Ainsi, il semble indispensable de quantifier MOPr en condition de stress social dans l'*oriens*-CA1-vHPC mais aussi, dans les régions précédemment citées. Il serait aussi intéressant d'activer MOPr avec un agoniste comme le DAMGO dont la spécificité pour MOPr est avérée (Onogi *et al*, 1995). Enfin, inhiber de façon systémique et ponctuellement DOPr ou MOPr dans les structures clés du cerveau déjà mentionnées permettrait d'élucider davantage la contribution fonctionnelle de DOPr et MOPr dans la résilience au stress chronique. Pour cela, des approches génétiques (Chu Sin Chung *et al*, 2015), par ARN interférents (Berube *et al*, 2014), ou par micro-infusion d'agonistes et d'antagonistes (Wilson *et al*, 2008) peuvent être employées.

Les récepteurs opioïdergiques, comme de nombreux récepteurs couplés aux protéines G, sont capables de s'hétérodimériser (Bouvier, 2001; George *et al*, 2000; Jordan and Devi, 1999). L'hétérodimérisation permet d'exercer des effets distincts de ceux observés avec l'homodimérisation, suggérant des retombées majeures en matière de thérapie (Jordan *et al*, 1999). En effet, depuis la découverte de la formation d'un hétéromère MOPr-DOPr (George *et al*, 2000), une vaste littérature fait état notamment de l'importance de cet hétéromère dans le traitement des douleurs aigues et chroniques (Ong and Cahill, 2014). Gomes et al. ont démontré l'effet synergique résultant de l'activation simultanée des deux récepteurs (Gomes *et al*, 2004). Cependant, la formation des hétéromères entre récepteurs opioïdergiques est encore sujette à controverse : la plupart des études ont été menées *in vitro*, ne révélant pas forcément une réalité au niveau physiologique (Gendron *et al*, 2016; Kabli *et al*, 2014). Une étude a montré que le SNC80, connu pour cibler de façon sélective DOPr, est aussi capable d'activer l'hétéromère MOPr/DOPr *in vitro* (Metcalf *et al*, 2012). La co-localisation de MOPr et DOPr a été observée dans le CA1-vHPC des souris double *knockin* pour MOPr-*mcherry* et DOPr-*eGFP,* en condition basale par immunofluorescence. De plus, l'interaction de MOPr et DOPr a été démontré par co-immunoprécipitation sur

l'hippocampe total (Erbs *et al*, 2015). Ces études suggèrent que l'activation de l'hétéromère MOPr-DOPr pourrait aussi être responsable des effets observés du SNC80 (Chapitre 1 – Figure 18). Combiner agoniste/antagoniste de MOPr et DOPr, respectivement et inversement, permettraient d'évaluer quel récepteur est principalement responsable des effets observés (Jordan *et al*, 1999). Enfin, l'utilisation du modèle de souris double *knockin* pour MOPr-*mcherry* et DOPr-*eGFP* (Erbs *et al*, 2015) pourrait servir à révéler la potentielle formation d'hétéromères MOPr-DOPr par co-immunoprécipitation dans le contexte du SCDS.

Pour une perspective à plus long terme, l'optogénètique serait un outil intéressant pour décrire précisément la contribution fonctionnelle de la signalisation ENK/DOPr entre la BLA et l'*oriens*-CA1-vHPC dans le développement de la résilience au stress chronique. Un adénovirus, dépendant d'une recombinase Cre, exprimant une channelrhodopsin (sonde excitatrice) ou une halorhodopsin (sonde inhibitrice) serait injecté dans la BLA de souris pENK-Cre et la canule placée dans l'*oriens*-CA1-vHPC (Challis *et al*, 2014). Après rétablissement, les souris seraient soumises à un SCDS modifié (Challis *et al*, 2014; Challis *et al*, 2013): après les 5 minutes de contact physique avec l'agresseur, les souris seraient déplacées de l'autre côté de la paroi en plexiglas pour un contact sensoriel de 20 minutes durant lequel la souris recevrait une stimulation au laser pour stimuler ou inhiber la voie d'intérêt par la lumière. Les souris retourneraient ensuite dans leur cage jusqu'à la prochaine défaite pendant les 10 jours de protocole. En effet, il a été montré que la période critique, conduisant à l'évitement social caractéristique du phénotype vulnérable, correspond aux 20 minutes de contact sensoriel après le contact physique (Challis *et al*, 2013). Leur niveau d'anxiété serait évalué avec un test d'interaction sociale. Un phénotype vulnérable serait attendu suite à la photo-inhibition, tandis que la photo-stimulation devrait favoriser l'apparition d'un phénotype résilient.

3.6 DOPr favorise naturellement la résilience en réduisant les effets délétères du stress oxydatif induit par le stress chronique.

Nos analyses ultrastructurelles ont mis en évidence un nouveau mécanisme par lequel DOPr pourrait favoriser la résilience au stress social chronique (Chapitre 1 et 2 – Figures

19 à 21 et 25 à 27). Les neurones sombres étaient moins nombreux avec le traitement au SNC80 dans les différentes couches du CA1-vHPC analysées. L'aspect sombre de ces neurones en microscopie électronique serait dû au cytoplasme et au noyau devenus denses aux électrons. Les tissus cérébraux ont été post-fixés avec du tétroxyde d'osmium, qui oxyde les acides gras insaturés. La réduction du tétroxyde d'osmium conduit à un osmium métallique noir, dense aux électrons (Di Scipio *et al*, 2008). De plus, le tétroxyde d'osmium a une affinité pour les protéines oxydables (Wigglesworth, 1964). Cette haute affinité expliquerait la variabilité des niveaux de gris observés dans les organites, et l'apparence sombre des neurones, dans ce contexte, serait due à la modification des composants protéiques et lipidiques du cytoplasme et du nucléoplasme. Les neurones sombres ont déjà été documentés en condition pathologique chez l'humain, comme l'ischémie (Jenkins *et al*, 1981) ou l'épilepsie (Ingvar *et al*, 1988) et dans le développement post-natal du cortex chez le rat (Caley and Maxwell, 1968). Ils ont aussi été observés dans des modèles murins de vieillissement normal (Tremblay *et al*, 2012) ou pathologique comme la maladie d'Huntington (Turmaine *et al*, 2000) ou d'Alzheimer (Yang *et al*, 2008). Il a été montré que même si une majorité de neurones sombres sont dans une voie de dégénérescence, un sous-ensemble pourrait spontanément recouvrir leur état de santé normal (Csordas *et al*, 2003). Dans ce contexte, nous pouvons nous demander si le traitement au SNC80 empêcherait à l'origine les dommages oxydatifs s'accumulant au cours du paradigme de SCDS, ou s'il restaurerait après dommages l'état de santé des neurones sombres.

La dilatation du RE est la marque de SO la plus décrite dans la littérature (Schonthal, 2012). Notre étude a montré une diminution du nombre de neurones, pyramidaux et interneurones du CA1-vHPC, présentant un RE dilaté (Chapitre 1 – Figures 19 à 21). Le déséquilibre du milieu redox est un des nombreux facteurs susceptibles d'engendrer le stress du RE conduisant à une accumulation pathologique de protéines mal conformées dans sa lumière. Les cellules peuvent déclencher une réponse, appelée réponse cellulaire aux protéines mal conformées ou « Unfolded protein response » (UPR), afin de replier correctement leurs protéines. Chez les animaux stressés, le système est possiblement saturé et l'UPR provoque l'apoptose au lieu de restaurer l'homéostasie et de favoriser la survie neuronale (Ron *et al*, 2007). Comme suggéré dans la discussion de l'article, l'administration

de SNC80 pourrait directement favoriser l'UPR. Pour répondre à cette question, des analyses du stress du RE et de l'activité UPR pourraient être conduites aux niveaux cellulaires et moléculaires, notamment par l'évaluation de l'activation de plusieurs régulateurs de l'UPR ainsi que l'expression de protéines chaperonnes responsables du bon repliement des protéines. La quantification par western blot de la phosphorylation de IRE1α (« inositol-requiring enzyme 1 alpha ») et PERK (« protein kinase RNA (PKR)-like ER kinase »), des kinases localisées sur la membrane du RE qui s'auto-phosphorylent lors du stress du RE, permettrait d'évaluer efficacement l'activité UPR (Oslowski and Urano, 2011).

L'analyse morphologique par microscopie électronique des mitochondries, en condition de stress avec le traitement, a révélé que le SNC80 semblait améliorer l'intégrité mitochondriale sans aucun effet sur leur taille. De plus, le SNC80 a significativement modifié la forme des mitochondries, en particulier chez les souris vulnérables, ce qui suggère que le SNC80 serait capable de restaurer les effets délétères induits par le stress chronique (Chapitre 2 – Figures 25 à 27). Ces résultats confirment ceux obtenus dans le premier chapitre. Les changements morphologiques des mitochondries sont étroitement liés à leurs fonctions (Brocard *et al*, 2003). Elles subissent constamment un remodelage structurel tant en conditions normales que pathologiques. Deux phénomènes peuvent être observés : la fusion et la fission. Ces processus peuvent se produire en simultané et sont étroitement influencés par les changements métaboliques et pathologiques survenant au sein de la mitochondrie elle-même ou dans son environnement. Ils contribuent au contrôle de qualité de la mitochondrie. En effet, la fusion d'une mitochondrie avec celle(s) avoisinante(s) permet de maitriser un stress environnemental en diluant le contenu en ADN de la mitochondrie altérée, en plus de favoriser un échange de protéines et de lipides. La fission permet de créer de nouvelles mitochondries mais aussi, de générer des mitochondries de moindre taille plus faciles à éliminer par autophagie (Twig *et al*, 2008; van der Bliek *et al*, 2013; Youle and van der Bliek, 2012). Une étude a montré que la distinction entre les évènements de fusion et de fission pourrait renseigner sur la destinée de la mitochondrie. Le périmètre des mitochondries serait positivement corrélé avec un phénomène de fission tandis que leur solidité serait associée à la fusion. Les mitochondries

avec un plus grand périmètre témoignant d'un gonflement ont plus tendance à se fragmenter (Westrate *et al*, 2014). Comme mentionné dans les résultats du chapitre 2, la solidité représente le ratio de l'aire totale sur l'aire convexe (plus petit polygone formé autour de l'objet contenant tous les pixels de l'objet). Ainsi, une solidité tendant vers 0 correspond à une morphologie plus tortueuse avec davantage de branchements tandis qu'une solidité approchant 1 témoigne d'une structure plus uniforme et compacte. Dans notre étude, peu importe la couche du CA1-vHPC observée (*strata pyramidale, oriens, radiatum*), aucune différence significative n'a été observée quant au périmètre des mitochondries. En revanche, le SNC80 semble rétablir la solidité à un niveau proche de 1 pour les individus vulnérables. Ces résultats nous suggèrent que le SNC80 pourrait favoriser la fusion des mitochondries afin de les maintenir en santé. Ainsi, la fusion mitochondriale serait un des mécanismes par lequel l'activation endogène de DOPr favoriserait la résilience au stress chronique. La reconstruction 3D des mitochondries avec un microscope électronique à balayage aiderait à préciser les changements structurels survenus lors du stress et avec le traitement au SNC80 (Lea *et al*, 1994).

L'analyse moléculaire par western blot a montré que le SNC80 augmente l'expression des complexes III et V impliqués dans la chaîne respiratoire suggérant qu'il favorise aussi leur activité (Chapitre 2 – Figure 28). Néanmoins, la condition de stress n'a pas modifié l'expression de ces complexes suggérant que le SNC80 ne restaurerait pas leur niveau d'expression. Un stress chronique imprévisible, chez le rat, inhibe l'activité des complexes I, III et IV de la chaîne respiratoire dans le cortex et le cervelet (Rezin *et al*, 2008). Le stress chronique répété, chez le rat, augmente aussi le niveau des protéines des complexes I, II, III dans le PFC tandis qu'il diminue le niveau des protéines du complexe IV dans l'hippocampe (Xing *et al*, 2013). L'activation pharmacologique de DOPr diminue les dommages neuronaux induits par l'inhibition du complexe IV de la chaîne respiratoire mitochondriale (Zhu *et al*, 2009). Il a été montré que l'épicatechin, un puissant antioxydant, connu pour ses propriétés protectrices cardiaques chez l'humain, est capable de moduler la morphologie et la fonction des mitochondries via son activité de liaison à DOPr au niveau du cœur chez la souris (Panneerselvam *et al*, 2013). Dans notre étude, le stress n'a eu aucun effet significatif sur l'expression de la Mn-SOD (Chapitre 2 – Figure 28H) contredisant

Patki et collègues (2013) qui ont montré une diminution de l'expression de la Mn-SOD dans l'hippocampe de rat après un SCDS. La contradiction apparente entre nos résultats et la littérature peut s'expliquer par les différents modèles animaux et les stresseurs utilisés. De plus, nos études ultrastructurelles ont été conduites dans la région CA1-vHPC alors que le western blot a été effectué sur l'hippocampe complet pouvant expliquer, en partie, l'absence de résultats concluants avec le SNC80. En effet, la compartimentation dorsale/intermédiaire/ventrale de l'hippocampe n'est pas seulement une distinction anatomique mais révèle aussi des fonctions différentes, et il en va de même pour les régions CA1, CA2, CA3 et le gyrus denté (Fanselow and Dong, 2010).

Ainsi, l'étude moléculaire n'a pas permis de déterminer quelle(s) protéine(s) le SNC80 ciblerait pour rétablir l'effet délétère induit par le stress chronique. La/les cible(s) moléculaire(s) exacte(s) du DOPr endogène favorisant la capacité naturelle d'adaptation face au stress chronique demeure(nt) donc inconnue(s). Des recherches plus approfondies devront être conduites. Les enzymes gluthation peroxydase et réductase ainsi que le niveau d'oxydation des protéines pourraient être testées par western blot pour finaliser l'étude (Patki *et al*, 2013).

3.7 Hypothèses de mécanismes entre l'activation endogène de DOPr et le maintien d'un statut oxydatif contrôlé chez les résilients

L'effet neuroprotecteur de l'activation de DOPr contre le SO a été démontré dans le cerveau ischémique de rat (Yang *et al*, 2009). Dans cet article, l'activation de DOPr atténuait le SO induit par la blessure ischémique, effectué par suture de l'artère cérébrale pendant 2 heures, en favorisant la capacité antioxydante des neurones hippocampaux et corticaux. En effet, la stimulation de DOPr a réduit la production de radicaux libres en inhibant l'activité caspase, sans interférer avec l'augmentation de l'expression des cytokines pro-inflammatoires (interleukine IL1β et facteur de nécrose tumorale TNFα) induite par l'ischémie. Il avait été précédemment montré *in vitro* que l'effet neuroprotecteur de l'activation de DOPr recrutait la voie des kinases ERK (Ma *et al*, 2005; Narita *et al*, 2006). Cependant, *in vivo*, l'inhibition pharmacologique de la kinase ERK a conduit, dans cette étude de Yang *et al.,* à la mort prématurée des animaux ischémiques traités ou non

avec l'agoniste de DOPr, démontrant ainsi que l'activation de DOPr n'est pas suffisante pour rétablir les effets exacerbés de l'ischémie dus à l'inhibition de ERK (Yang *et al*, 2009). L'activation de DOPr semble aussi inhiber la production d'oxyde nitrique (NO) et par conséquent, l'activité de la caspase 3. En effet, une importante production de NO conduit à la libération du cytochrome c de la mitochondrie conduisant ultimement à l'apoptose (Ryter *et al*, 2007). Une autre étude a montré que l'activation de DOPr permet de restaurer les effets délétères provoqués par le dysfonctionnement mitochondrial, incluant la dépolarisation de la membrane mitochondriale, la surcharge calcique et la production de ROS. De la même manière, l'activation de DOPr inhiberait la libération de cytochrome c et l'activation de la caspase 3. Cet effet neuroprotecteur ferait aussi intervenir la voie PKC-ERK et en particulier, la kinase ERK mitochondriale (Zhu *et al*, 2011).

Une autre hypothèse, faisant intervenir le facteur neurotrophique dérivé du cerveau (BDNF), peut aussi être proposée pour expliquer le mécanisme d'action de la stimulation de DOPr sur le maintien du statut oxydatif contrôlé dans les neurones hippocampaux chez les résilients. Le BDNF est un médiateur clé de la résilience au stress chronique (Berton *et al*, 2006). Alors que l'expression du BDNF est augmentée dans le NAc chez la souris vulnérable (Krishnan *et al*, 2007), son expression est augmentée dans le gyrus denté des rats résilients au stress chronique (Duclot *et al*, 2013; Taliaz *et al*, 2011). D'autre part, des études ont montré que l'administration d'un agoniste de DOPr conduit à l'augmentation du BDNF dans l'hippocampe chez le rat, produisant un effet antidépresseur (Torregrossa *et al*, 2006; Zhang *et al*, 2006). Le SO a été associé à une diminution du BDNF dans certaines pathologies psychiatriques, comme les troubles bipolaires et la schizophrénie (Kapczinski *et al*, 2008; Zhang *et al*, 2015). La diminution du BDNF est davantage présentée comme une conséquence du SO et non l'inverse. Cependant, la littérature reste modeste à ce sujet et l'hypothèse est à approfondir.

3.8 Thérapies

Cette thèse avait pour objectif la caractérisation de la transmission ENK via DOPr dans le contexte de la résilience au stress. Elle visait à élucider les mécanismes fondamentaux

impliqués. J'ai donc très peu abordé le potentiel thérapeutique émanant de ces travaux. J'aborderai ce sujet dans la partie qui suit. Les récepteurs opioïdergiques sont pressentis comme cible thérapeutique pour les troubles de l'anxiété depuis des décennies (Emrich *et al*, 1982a; Emrich *et al*, 1982b). L'opium et la morphine sont utilisés depuis des siècles pour leurs effets euphorisants et anxiolytiques. Les nombreux effets secondaires, comme la constipation ou les risques d'arrêt respiratoire, et la dépendance qui y sont associés, ont limité leurs perspectives d'utilisation dans le cadre des troubles anxieux. Cependant, de nombreux composés ont été développés ces dernières années afin de réduire au maximum ces effets secondaires, tout en maintenant les effets anxiolytiques. Bien que le potentiel thérapeutique du SNC80 semble important, ce composé peut induire des convulsions, une hyperlocomotion et il induit une forte tolérance, limitant son utilisation en traitement chronique. Une revue de 2006 a mis l'accent sur les molécules ciblant DOPr développées à ce moment et dépourvues d'activité convulsivante (Jutkiewicz, 2006). Plus récemment, une revue a compilé la littérature à ce sujet (Dripps and Jutkiewicz, 2017). Les agonistes de DOPr (ARM390, ADL5747, ADL5859, KNT127, AZD2327), présentés dans le paragraphe suivant, ont été testés pour leur effet analgésique, antidépresseur ou anxiolytique (structures chimiques en Figure 29).

L'ARM390 et le SNC80 ont des propriétés communes considérant leur liaison à DOPr et leur effet analgésique. L'administration ponctuelle d'ARM390 chez la souris ne conduit pas à une désensibilisation du récepteur à la différence du SNC80 (Pradhan *et al*, 2009). Le traitement chronique induit toutefois une tolérance au niveau des effets analgésiques pour les deux drogues. Cependant, la tolérance n'est pas observée pour les effets locomoteurs et anxiolytiques avec l'administration de l'ARM390 faisant de cette molécule une amélioration concrète par rapport au SNC80 (Pradhan *et al*, 2010). L'ADL5747 et l'ADL5859 réduisent l'inflammation et la douleur neuropathique chez la souris, sans affecter la locomotion, ni conduire à l'internalisation du récepteur (Nozaki *et al*, 2012). L'ADL5859 montre une spécificité dix fois plus élevée pour DOPr que pour l'hétéromère MOPr-DOPr (van Rijn *et al*, 2013). Un traitement aigu avec le KNT127, chez la souris, exerce un effet analgésique dans la douleur inflammatoire induite et un effet antidépresseur, dans le test de nage forcée, sans affecter la locomotion ni induire une forte internalisation. Le traitement chronique conduit à une tolérance de l'effet analgésique mais pas pour l'effet

antidépresseur (Nozaki *et al*, 2014). Bien que les études chez les rongeurs et les singes aient révélé des effets antidépresseurs et anxiolytiques prometteurs pour l'AZD2327 sans effet de tolérance (Hudzik *et al*, 2011; Hudzik *et al*, 2014), l'étude préclinique chez des patients atteints de dépression anxieuse n'a pas permis d'obtenir des résultats concluants (Richards *et al*, 2016).

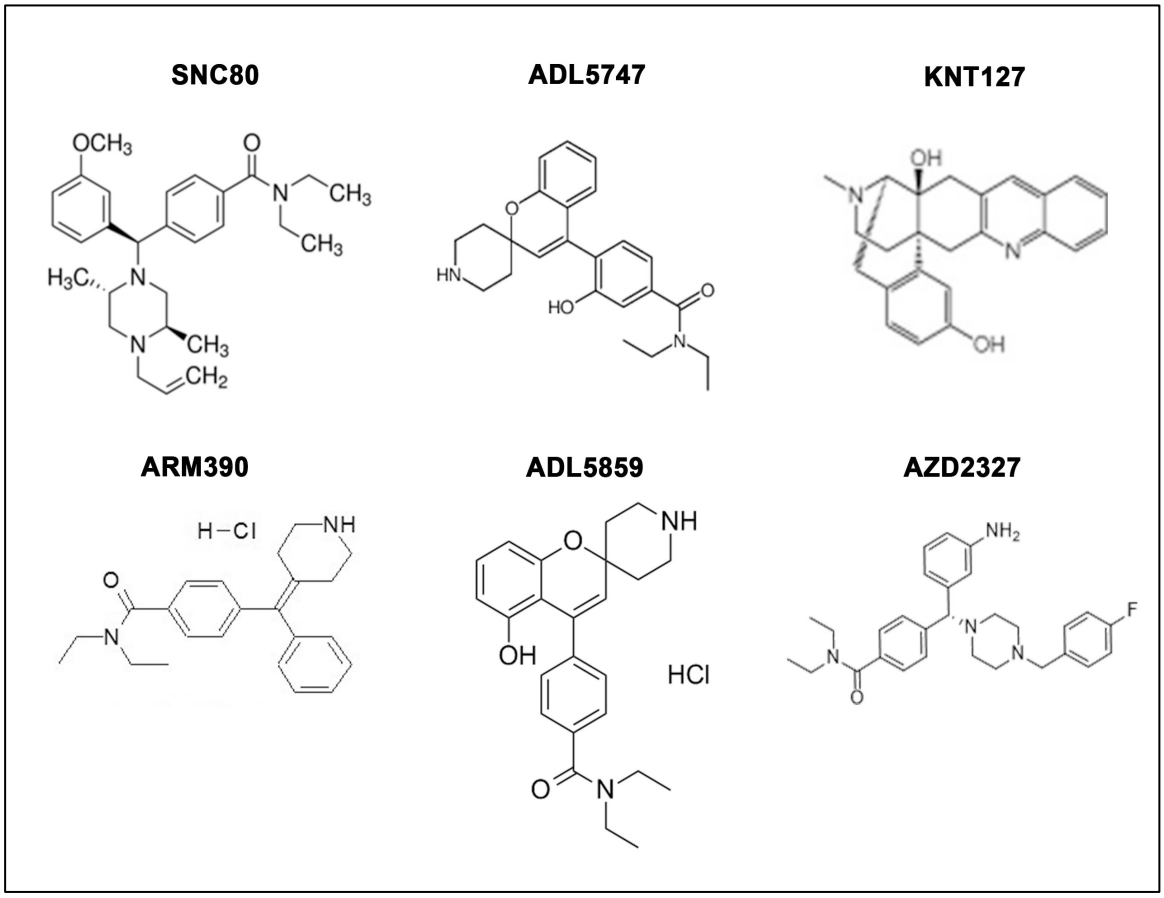

Figure 29 : Structures chimiques d'agonistes de DOPr (SNC80, ARM390, ADL5747, ADL5859, KNT127, AZD2327).

D'après les résultats et conclusions présentés dans cette thèse, une approche thérapeutique intéressante pour traiter les troubles liés au stress chronique et anxieux serait de conjuguer un agoniste de DOPr dépourvu d'effet secondaire avec des antioxydants. Les antioxydants se définissent comme toute molécule retardant, prévenant ou diminuant les dommages oxydatifs dans le but de prévenir le SO en contrant les effets délétères provoqués par l'excès de ROS (Halliwell and Gutteridge, 2007). Parmi ces molécules antioxydantes, on

compte les enzymes (superoxyde dismutase, catalase…) et les composés non enzymatiques, comme les vitamines ou encore les polyphénols contenus dans les fruits et les légumes. Les antioxydants sont déjà utilisés pour le traitement de certaines pathologies. L'edaravone est un composé mimant les phénols, utilisé au Japon pour diminuer les dommages dus à une ischémie. Ce composé présente une activité antioxydante *in vitro* (Nishinaka et al, 2010), réduit les dommages dans le cerveau ischémique de souris (Zhang *et al*, 2005) et montre de très bons résultats chez les patients (Miyaji *et al*, 2015). Son efficacité a aussi été rapportée dans l'encéphalopathie liée à une hypoxie-ischémie chez le nouveau-né (Noor *et al*, 2005). Il a aussi été testé dans un modèle murin de sclérose latérale amyotrophique (SLA (Takahashi, 2009)) et vient d'être validé pour le traitement de la SLA (Rothstein, 2017). Une abondante littérature fait état d'une potentielle utilisation d'antioxydants pour traiter d'autres maladies neurodégénératives comme la maladie d'Alzheimer et le Parkinson (McBean *et al*, 2017), mais aussi pour les désordres neuropsychiatriques comme la schizophrénie, les troubles bipolaires, les troubles anxieux et la dépression (Salim, 2014).

En 2013 et 2016, deux revues compilaient la littérature au sujet de nouvelles potentielles thérapies pour la dépression ciblant certaines molécules du SO et du stress nitrosatif (Lee *et al*, 2013; Maurya *et al*, 2016). Parmi celles-ci, l'acide ascorbique et le tocophérol sont capables de prévenir les altérations de l'activité des complexes II et IV de la chaîne respiratoire mitochondriale induit par un stress chronique chez le rat, tout en restaurant les perturbations cognitives associées au stress chronique (Tagliari *et al*, 2010; Tagliari *et al*, 2011). La minocycline, un antibiotique à fort pouvoir antioxydant normalisant l'activité microgliale, a montré des résultats prometteurs en complément d'un traitement pour la dépression majeure dans une étude préclinique (Dean *et al*, 2014). Enfin, le resvératrol, un polyphénol composant du raisin, connu pour ses propriétés antivieillissement (Pandey and Rizvi, 2013) a montré des effets antidépresseurs chez la souris par une régulation du BDNF au niveau de l'hippocampe (Ali *et al*, 2015). De nombreuses molécules antioxydantes sont en cours ou en voie d'être testées. Les résultats obtenus jusqu'alors sont souvent contradictoires démontrant la nécessité de la recherche dans ce domaine.

4 CONCLUSION

Le stress chronique est la pathologie du XXIe siècle dont l'issue la plus dévastatrice est la dépression chronique. Plus de 300 millions de personnes en sont atteintes dans le monde entier démontrant l'urgence de trouver des traitements pour guérir au mieux cette maladie très hétérogène. Les thérapies contre la dépression ont stagné depuis des décennies. Aujourd'hui, de nombreuses pistes prometteuses sont en cours d'investigation.

Le SO était au centre de l'attention il y a 15 ans, présenté comme un accélérateur du vieillissement. Il revient aujourd'hui à la mode, notamment avec l'utilisation d'un antioxydant, l'edaravone, comme traitement contre la sclérose latérale amyotrophique. Le lien avec le stress psychologique chronique est apparu en 2000, et a été ponctuellement étudié depuis, pointant du doigt une piste prometteuse pour le développement de thérapies.

Dans cette thèse, nous nous sommes principalement concentrés sur les mécanismes fondamentaux de la résilience au stress chronique via l'étude de la signalisation ENK/DOPr. Nos résultats indiquent qu'il existe un dialogue privilégié entre la BLA et le CA1-vHPC de cette signalisation ENK/DOPr, qui est préservé chez les individus résilients à la différence des individus vulnérables. Cette préservation rend possible le maintien d'un statut oxydatif viable pour les neurones pyramidaux et les interneurones du CA1-vHPC. Cette étude suggère qu'une attention toute particulière devrait être portée à l'altération du statut redox des neurones en condition de stress chronique. En plus d'approfondir les connaissances sur la circuiterie et les mécanismes fondamentaux qui régissent la résilience au stress chronique, ces investigations pourraient conduire à des thérapies prometteuses pour traiter la dépression mais aussi les pathologies neurodégénératives dont le stress chronique est un accélérateur bien connu.

5 RÉFERENCES BIBLIOGRAPHIQUES

Akil H, Watson SJ, Young E, Lewis ME, Khachaturian H, Walker JM (1984). Endogenous opioids: biology and function. *Annual review of neuroscience* **7**: 223-255.

Al-Hasani R, Bruchas MR (2011). Molecular mechanisms of opioid receptor-dependent signaling and behavior. *Anesthesiology* **115**(6): 1363-1381.

Ali SH, Madhana RM, K VA, Kasala ER, Bodduluru LN, Pitta S*, et al* (2015). Resveratrol ameliorates depressive-like behavior in repeated corticosterone-induced depression in mice. *Steroids* **101**: 37-42.

Alper RH, Zink MH, 3rd (1994). Adrenergic and nonadrenergic regulation of hindlimb blood flow during stress in rats. *J Pharmacol Exp Ther* **269**(1): 305-312.

Amir S, Amit Z (1978). Endogenous opioid ligands may mediate stress-induced changes in the affective properties of pain related behavior in rats. *Life Sci* **23**(11): 1143-1151.

Amit Z, Galina ZH (1986). Stress-induced analgesia: adaptive pain suppression. *Physiol Rev* **66**(4): 1091-1120.

Anderson NB (1998). Levels of analysis in health science. A framework for integrating sociobehavioral and biomedical research. *Annals of the New York Academy of Sciences* **840**: 563-576.

Antoni FA (1986). Hypothalamic control of adrenocorticotropin secretion: advances since the discovery of 41-residue corticotropin-releasing factor. *Endocr Rev* **7**(4): 351-378.

Aschbacher K, O'Donovan A, Wolkowitz OM, Dhabhar FS, Su Y, Epel E (2013). Good stress, bad stress and oxidative stress: insights from anticipatory cortisol reactivity. *Psychoneuroendocrinology* **38**(9): 1698-1708.

Asok A, Ayers LW, Awoyemi B, Schulkin J, Rosen JB (2013). Immediate early gene and neuropeptide expression following exposure to the predator odor 2,5-dihydro-2,4,5-trimethylthiazoline (TMT). *Behav Brain Res* **248**: 85-93.

Atillo A, Soderfeldt B, Kalimo H, Olsson Y, Siesjo BK (1983). Pathogenesis of brain lesions caused by experimental epilepsy. Light- and electron-microscopic changes in the rat hippocampus following bicuculline-induced status epilepticus. *Acta Neuropathol* **59**(1): 11-24.

Bai J, Cederbaum AI (2001). Mitochondrial catalase and oxidative injury. *Biol Signals Recept* **10**(3-4): 189-199.

Bali A, Randhawa PK, Jaggi AS (2015). Stress and opioids: Role of opioids in modulating stress-related behavior and effect of stress on morphine conditioned place preference. *Neuroscience and biobehavioral reviews* **51**: 138-150.

Battaglia M, Ogliari A, D'Amato F, Kinkead R (2014). Early-life risk factors for panic and separation anxiety disorder: insights and outstanding questions arising from human and animal studies of CO_2 sensitivity *Neuroscience & Biobehavioral Reviews* **46**(3): 455–464.

Baum A (1990). Stress, intrusive imagery, and chronic distress. *Health Psychol* **9**(6): 653-675.

Beaulieu JM, Gainetdinov RR, Caron MG (2009). Akt/GSK3 signaling in the action of psychotropic drugs. *Annu Rev Pharmacol Toxicol* **49**: 327-347.

Beck JG, Ohtake PJ, Shipherd JC (1999). Exaggerated anxiety is not unique to CO_2 in panic disorder: A comparison of hypercapnic and hypoxic challenges. *Journal of Abnormal Psychology* **108**(3): 473-482.

Becker HC (2017). Influence of stress associated with chronic alcohol exposure on drinking. *Neuropharmacology* **122**: 115-126.

Behan M, Kinkead R (2011). Neuronal Control of Breathing: Sex and Stress Hormones. *Comprehensive Physiology* **1**: 2101 - 2139.

Belluzzi JD, Grant N, Garsky V, Sarantakis D, Wise CD, Stein L (1976). Analgesia induced in vivo by central administration of enkephalin in rat. *Nature* **260**(5552): 625-626.

Bernard C (1865). *Introduction à l'étude de la médecine expérimentale*.

Berton O, McClung CA, Dileone RJ, Krishnan V, Renthal W, Russo SJ*, et al* (2006). Essential role of BDNF in the mesolimbic dopamine pathway in social defeat stress. *Science* **311**(5762): 864-868.

Berube P, Laforest S, Bhatnagar S, Drolet G (2013). Enkephalin and dynorphin mRNA expression are associated with resilience or vulnerability to chronic social defeat stress. *Physiology & behavior* **122**: 237-245.

Berube P, Poulin JF, Laforest S, Drolet G (2014). Enkephalin knockdown in the basolateral amygdala reproduces vulnerable anxiety-like responses to chronic unpredictable stress. *Neuropsychopharmacology : official publication of the American College of Neuropsychopharmacology* **39**(5): 1159-1168.

Bhatnagar S, Vining C (2003). Facilitation of hypothalamic-pituitary-adrenal responses to novel stress following repeated social stress using the resident/intruder paradigm. *Horm Behav* **43**(1): 158-165.

Bilkei-Gorzo A, Racz I, Michel K, Zimmer A, Klingmuller D, Zimmer A (2004). Behavioral phenotype of pre-proenkephalin-deficient mice on diverse congenic backgrounds. *Psychopharmacology (Berl)* **176**(3-4): 343-352.

Bilsky EJ, Calderon SN, Wang T, Bernstein RN, Davis P, Hruby VJ*, et al* (1995). SNC 80, a selective, nonpeptidic and systemically active opioid delta agonist. *J Pharmacol Exp Ther* **273**(1): 359-366.

Bisht K, Sharma K, Lacoste B, Tremblay ME (2016a). Dark microglia: Why are they dark? *Commun Integr Biol* **9**(6): e1230575.

Bisht K, Sharma KP, Lecours C, Gabriela Sánchez M, El Hajj H, Milior G*, et al* (2016b). Dark microglia: A new phenotype predominantly associated with pathological states. *Glia* **64**(5): 826-839.

Bodnar RJ (2017). Endogenous Opiates and Behavior: 2015. *Peptides* **88**: 126-188.

Bodnar RJ, Kelly DD, Spiaggia A, Ehrenberg C, Glusman M (1978). Dose-dependent reductions by naloxone of analgesia induced by cold-water stress. *Pharmacol Biochem Behav* **8**(6): 667-672.

Bondar N, Bryzgalov L, Ershov N, Gusev F, Reshetnikov V, Avgustinovich D*, et al* (2017). Molecular Adaptations to Social Defeat Stress and Induced Depression in Mice. *Molecular neurobiology*.

Bourgeois JM, Tarnopolsky MA (2004). Pathology of skeletal muscle in mitochondrial disorders. *Mitochondrion* **4**(5-6): 441-452.

Bouvier M (2001). Oligomerization of G-protein-coupled transmitter receptors. *Nature reviews Neuroscience* **2**(4): 274-286.

Briand LA, Hilario M, Dow HC, Brodkin ES, Blendy JA, Berton O (2015). Mouse model of OPRM1 (A118G) polymorphism increases sociability and dominance and confers resilience to social defeat. *The Journal of neuroscience : the official journal of the Society for Neuroscience* **35**(8): 3582-3590.

Brocard JB, Rintoul GL, Reynolds IJ (2003). New perspectives on mitochondrial morphology in cell function. *Biol Cell* **95**(5): 239-242.

Broom DC, Jutkiewicz EM, Rice KC, Traynor JR, Woods JH (2002a). Behavioral effects of delta-opioid receptor agonists: potential antidepressants? *Jpn J Pharmacol* **90**(1): 1-6.

Broom DC, Nitsche JF, Pintar JE, Rice KC, Woods JH, Traynor JR (2002b). Comparison of receptor mechanisms and efficacy requirements for delta-agonist-induced convulsive activity and antinociception in mice. *J Pharmacol Exp Ther* **303**(2): 723-729.

Calderon SN, Rothman RB, Porreca F, Flippen-Anderson JL, McNutt RW, Xu H*, et al* (1994). Probes for narcotic receptor mediated phenomena. 19. Synthesis of (+)-4-[(alpha R)-alpha-((2S,5R)-4-allyl-2,5-dimethyl-1-piperazinyl)-3- methoxybenzyl]-N,N-diethylbenzamide (SNC 80): a highly selective, nonpeptide delta opioid receptor agonist. *J Med Chem* **37**(14): 2125-2128.

Caley DW, Maxwell DS (1968). An electron microscopic study of neurons during postnatal development of the rat cerebral cortex. *The Journal of comparative neurology* **133**(1): 17-44.

Cambridge MA, Murray CJL, Lopez AD (1996). A comprehensive assessment of mortality and disability from diseases, injuries, and risk factors in 1990 and projected to 2020. In: Publié par la Harvard School of Public Health pour le compte de l'Organisation mondiale de la santé et de la Banque mondiale HUP (ed).

Cannon WB (1929). Bodily Changes in Pain Hunger Fear And Rage. New York: D. Appleton And Company.

Cannon WB (1939). The wisdom of the body New York: W.W. Norton.

Carter RN, Pinnock SB, Herbert J (2004). Does the amygdala modulate adaptation to repeated stress? *Neuroscience* **126**(1): 9-19.

Casanova JP, Contreras M, Moya EA, Torrealba F, Iturriaga R (2013). Effect of insular cortex inactivation on autonomic and behavioral responses to acute hypoxia in conscious rats. *Behav Brain Res* **253**: 60-67.

Chaillet P, Coulaud A, Zajac JM, Fournie-Zaluski MC, Costentin J, Roques BP (1984). The mu rather than the delta subtype of opioid receptors appears to be involved in enkephalin-induced analgesia. *Eur J Pharmacol* **101**(1-2): 83-90.

Challis C, Beck SG, Berton O (2014). Optogenetic modulation of descending prefrontocortical inputs to the dorsal raphe bidirectionally bias socioaffective choices after social defeat. *Frontiers in behavioral neuroscience* **8**: 43.

Challis C, Boulden J, Veerakumar A, Espallergues J, Vassoler FM, Pierce RC*, et al* (2013). Raphe GABAergic neurons mediate the acquisition of avoidance after social defeat. *The Journal of neuroscience : the official journal of the Society for Neuroscience* **33**(35): 13978-13988, 13988a.

Chandel NS, Budinger GR (2007). The cellular basis for diverse responses to oxygen. *Free Radic Biol Med* **42**(2): 165-174.

Chao D, Donnelly DF, Feng Y, Bazzy-Asaad A, Xia Y (2007). Cortical delta-opioid receptors potentiate K+ homeostasis during anoxia and oxygen-glucose deprivation. *J Cereb Blood Flow Metab* **27**(2): 356-368.

Charney DS (2004). Psychobiological mechanisms of resilience and vulnerability: implications for successful adaptation to extreme stress. *The American journal of psychiatry* **161**(2): 195-216.

Chen Y, Mestek A, Liu J, Hurley JA, Yu L (1993). Molecular cloning and functional expression of a mu-opioid receptor from rat brain. *Mol Pharmacol* **44**(1): 8-12.

Chichinadze K, Chichinadze N (2008). Stress-induced increase of testosterone: Contributions of social status and sympathetic reactivity. *Physiology & Behavior* **94**(4): 595-603.

Chrousos GP (2009). Stress and disorders of the stress system. *Nat Rev Endocrinol* **5**(7): 374-381.

Chu Sin Chung P, Keyworth HL, Martin-Garcia E, Charbogne P, Darcq E, Bailey A*, et al* (2015). A novel anxiogenic role for the delta opioid receptor expressed in GABAergic forebrain neurons. *Biological psychiatry* **77**(4): 404-415.

Ciocchi S, Herry C, Grenier F, Wolff SB, Letzkus JJ, Vlachos I*, et al* (2010). Encoding of conditioned fear in central amygdala inhibitory circuits. *Nature* **468**(7321): 277-282.

Cole NB, Daniels MP, Levine RL, Kim G (2010). Oxidative stress causes reversible changes in mitochondrial permeability and structure. *Exp Gerontol* **45**(7-8): 596-602.

Comings DE, Dietz G, Gade-Andavolu R, Blake H, Muhleman D, Huss M*, et al* (2000). Association of the neutral endopeptidase (MME) gene with anxiety. *Psychiatr Genet* **10**(2): 91-94.

Commons KG, Milner TA (1997). Localization of delta opioid receptor immunoreactivity in interneurons and pyramidal cells in the rat hippocampus. *The Journal of comparative neurology* **381**(3): 373-387.

Cooke BM (2006). Steroid-dependent plasticity in the medial amygdala. *Neuroscience* **138**(3): 997-1005.

Cooke BM, Woolley CS (2005). Sexually Dimorphic Synaptic Organization of the Medial Amygdala. *The Journal of Neuroscience* **25**(46): 10759-10767.

Cooper GM (2000). The Cell, a Molecular Approach. In: Associates SMS (ed), 2nd edition edn.

Csordas A, Mazlo M, Gallyas F (2003). Recovery versus death of "dark" (compacted) neurons in non-impaired parenchymal environment: light and electron microscopic observations. *Acta Neuropathol* **106**(1): 37-49.

Cunningham ET, Jr., Sawchenko PE (1988). Anatomical specificity of noradrenergic inputs to the paraventricular and supraoptic nuclei of the rat hypothalamus. *The Journal of comparative neurology* **274**(1): 60-76.

Czerska M, Mikolajewska K, Zielinski M, Gromadzinska J, Wasowicz W (2015). Today's oxidative stress markers. *Med Pr* **66**(3): 393-405.

Dallman MF, Pecoraro N, Akana SF, La Fleur SE, Gomez F, Houshyar H*, et al* (2003). Chronic stress and obesity: a new view of "comfort food". *Proceedings of the National Academy of Sciences of the United States of America* **100**(20): 11696-11701.

Davidson RJ, McEwen BS (2012). Social influences on neuroplasticity: stress and interventions to promote well-being. *Nature neuroscience* **15**(5): 689-695.

Davies SW, Turmaine M, Cozens BA, DiFiglia M, Sharp AH, Ross CA*, et al* (1997). Formation of neuronal intranuclear inclusions underlies the neurological dysfunction in mice transgenic for the HD mutation. *Cell* **90**(3): 537-548.

Day TA (2005). Defining stress as a prelude to mapping its neurocircuitry: no help from allostasis. *Prog Neuropsychopharmacol Biol Psychiatry* **29**(8): 1195-1200.

De Boer SF, Koopmans SJ, Slangen JL, Van der Gugten J (1990). Plasma catecholamine, corticosterone and glucose responses to repeated stress in rats: effect of interstressor interval length. *Physiology & behavior* **47**(6): 1117-1124.

de Souza Armini R, Bernabé CS, Rosa CA, Siller CA, Schimitel FG, Tufik S*, et al* (2015). In a rat model of panic, corticotropin responses to dorsal periaqueductal gray stimulation depend on physical exertion. *Psychoneuroendocrinology* **53**: 136-147.

Dean OM, Maes M, Ashton M, Berk L, Kanchanatawan B, Sughondhabirom A*, et al* (2014). Protocol and rationale-the efficacy of minocycline as an adjunctive treatment for major depressive disorder: a double blind, randomised, placebo controlled trial. *Clin Psychopharmacol Neurosci* **12**(3): 180-188.

Dempsey JA, Veasey SC, Morgan BJ, O'Donnell CP (2010). Pathophysiology of Sleep Apnea. *Physiol Rev* **90**(1): 47-112.

Denning GM, Ackermann LW, Barna TJ, Armstrong JG, Stoll LL, Weintraub NL*, et al* (2008). Proenkephalin expression and enkephalin release are widely observed in non-neuronal tissues. *Peptides* **29**(1): 83-92.

Di Scipio F, Raimondo S, Tos P, Geuna S (2008). A simple protocol for paraffin-embedded myelin sheath staining with osmium tetroxide for light microscope observation. *Microsc Res Tech* **71**(7): 497-502.

Ditzen C, Jastorff AM, Kessler MS, Bunck M, Teplytska L, Erhardt A*, et al* (2006). Protein biomarkers in a mouse model of extremes in trait anxiety. *Mol Cell Proteomics* **5**(10): 1914-1920.

Donner N, Lowry C (2013). Sex differences in anxiety and emotional behavior. *Pflügers Archiv - European Journal of Physiology* **465**(5): 601-626.

Dripps IJ, Jutkiewicz EM (2017). Delta Opioid Receptors and Modulation of Mood and Emotion. *Handb Exp Pharmacol*.

Drolet G, Dumont EC, Gosselin I, Kinkead R, Laforest S, Trottier JF (2001). Role of endogenous opioid system in the regulation of the stress response. *Prog Neuropsychopharmacol Biol Psychiatry* **25**(4): 729-741.

Drorbough JE, Fenn WO (1955). A Barometric method for measuring ventilation in newborn infants. *Pediatrics* **16**: 81-86.

Duclos M, Gouarne C, Martin C, Rocher C, Mormede P, Letellier T (2004). Effects of corticosterone on muscle mitochondria identifying different sensitivity to glucocorticoids in Lewis and Fischer rats. *Am J Physiol Endocrinol Metab* **286**(2): E159-167.

Duclot F, Kabbaj M (2013). Individual differences in novelty seeking predict subsequent vulnerability to social defeat through a differential epigenetic regulation of brain-derived neurotrophic factor expression. *The Journal of neuroscience : the official journal of the Society for Neuroscience* **33**(27): 11048-11060.

Duncan JG, Fong JL, Medeiros DM, Finck BN, Kelly DP (2007). Insulin-resistant heart exhibits a mitochondrial biogenic response driven by the peroxisome proliferator-activated receptor-alpha/PGC-1alpha gene regulatory pathway. *Circulation* **115**(7): 909-917.

Egner A, Jakobs S, Hell SW (2002). Fast 100-nm resolution three-dimensional microscope reveals structural plasticity of mitochondria in live yeast. *Proceedings of the National Academy of Sciences of the United States of America* **99**(6): 3370-3375.

Eiden LE (1987). The enkephalin-containing cell: strategies for polypeptide synthesis and secretion throughout the neuroendocrine system. *Cell Mol Neurobiol* **7**(4): 339-352.

Emrich HM, Vogt P, Herz A (1982a). Possible antidepressive effects of opioids: action of buprenorphine. *Annals of the New York Academy of Sciences* **398**: 108-112.

Emrich HM, Vogt P, Herz A, Kissling W (1982b). Antidepressant effects of buprenorphine. *Lancet* **2**(8300): 709.

Erbs E, Faget L, Scherrer G, Kessler P, Hentsch D, Vonesch JL*, et al* (2012). Distribution of delta opioid receptor-expressing neurons in the mouse hippocampus. *Neuroscience* **221**: 203-213.

Erbs E, Faget L, Scherrer G, Matifas A, Filliol D, Vonesch JL*, et al* (2015). A mu-delta opioid receptor brain atlas reveals neuronal co-occurrence in subcortical networks. *Brain structure & function* **220**(2): 677-702.

Evans CJ, Keith DE, Jr., Morrison H, Magendzo K, Edwards RH (1992). Cloning of a delta opioid receptor by functional expression. *Science* **258**(5090): 1952-1955.

Everly GS, Lating JM (2002). The Anatomy and Physiology of the Human Stress Response. In: York SSBMN (ed). *A Clinical Guide to the Treatment of the Human Stress Response*.

Fallon JH, Leslie FM (1986). Distribution of dynorphin and enkephalin peptides in the rat brain. *The Journal of comparative neurology* **249**(3): 293-336.

Fanselow MS, Dong HW (2010). Are the dorsal and ventral hippocampus functionally distinct structures? *Neuron* **65**(1): 7-19.

Feinstein JS, Buzza C, Hurlemann R, Follmer RL, Dahdaleh NS, Coryell WH*, et al* (2013). Fear and panic in humans with bilateral amygdala damage. *Nat Neurosci* **16**(3): 270-272.

Felix-Ortiz AC, Beyeler A, Seo C, Leppla CA, Wildes CP, Tye KM (2013). BLA to vHPC inputs modulate anxiety-related behaviors. *Neuron* **79**(4): 658-664.

Filliol D, Ghozland S, Chluba J, Martin M, Matthes HW, Simonin F*, et al* (2000). Mice deficient for delta- and mu-opioid receptors exhibit opposing alterations of emotional responses. *Nature genetics* **25**(2): 195-200.

Finkel T, Holbrook NJ (2000). Oxidants, oxidative stress and the biology of ageing. *Nature* **408**(6809): 239-247.

Forbes-Lorman R, Auger AP, Auger CJ (2014). Neonatal RU-486 (mifepristone) exposure increases androgen receptor immunoreactivity and sexual behavior in male rats. *Brain Research* **1543**: 143-150.

Fournier S, Gulemetova R, Baldy C, Joseph V, Kinkead R (2015). Neonatal stress affects the aging trajectory of female rats on the endocrine, temperature, and ventilatory responses to hypoxia. *Am J Physiol Regul Integr Comp Physiol* **308**(7): R659-R667.

Fournier S, Gulemetova R, Joseph V, Kinkead R (2014). Testosterone potentiates the hypoxic ventilatory response of adult male rats subjected to neonatal stress. *Exp Physiol* **99**(5): 824-834.

Francis DD, Meaney MJ (1999). Maternal care and the development of stress responses. *Curr Opin Neurobiol* **9**(1): 128-134.

Fukai T, Ushio-Fukai M (2011). Superoxide dismutases: role in redox signaling, vascular function, and diseases. *Antioxid Redox Signal* **15**(6): 1583-1606.

Gall C, Brecha N, Karten HJ, Chang KJ (1981). Localization of enkephalin-like immunoreactivity to identified axonal and neuronal populations of the rat hippocampus. *The Journal of comparative neurology* **198**(2): 335-350.

Gendron L, Cahill CM, von Zastrow M, Schiller PW, Pineyro G (2016). Molecular Pharmacology of delta-Opioid Receptors. *Pharmacol Rev* **68**(3): 631-700.

Gendron L, Mittal N, Beaudry H, Walwyn W (2015). Recent advances on the delta opioid receptor: from trafficking to function. *Br J Pharmacol* **172**(2): 403-419.

Genest SE, Balon N, Gulemetova R, Laforest S, Drolet G, Kinkead R (2007a). Neonatal maternal separation and enhancement of the hypoxic ventilatory response: the role of GABAergic neurotransmission within the paraventricular nucleus of the hypothalamus. *J Physiol* **583.1**: 299-314.

Genest SE, Gulemetova R, Laforest S, Drolet G, Kinkead R (2004). Neonatal maternal separation and sex-specific plasticity of the hypoxic ventilatory response in awake rat. *J Physiol* **554**(Pt 2): 543-557.

Genest SE, Gulemetova R, Laforest S, Drolet G, Kinkead R (2007b). Neonatal maternal separation induces sex-specific augmentation of the hypercapnic ventilatory response in awake rat. *J Appl Physiol* **102**: 1416-1421.

George SR, Fan T, Xie Z, Tse R, Tam V, Varghese G*, et al* (2000). Oligomerization of mu- and delta-opioid receptors. Generation of novel functional properties. *J Biol Chem* **275**(34): 26128-26135.

Gingrich JA (2005). Oxidative stress is the new stress. *Nat Med* **11**(12): 1281-1282.

Gold PW, Wong ML, Goldstein DS, Gold HK, Ronsaville DS, Esler M*, et al* (2005). Cardiac implications of increased arterial entry and reversible 24-h central and peripheral norepinephrine levels in melancholia. *Proceedings of the National Academy of Sciences of the United States of America* **102**(23): 8303-8308.

Golden SA, Covington HE, 3rd, Berton O, Russo SJ (2011). A standardized protocol for repeated social defeat stress in mice. *Nature protocols* **6**(8): 1183-1191.

Goldenthal MJ, Marin-Garcia J (2004). Mitochondrial signaling pathways: a receiver/integrator organelle. *Mol Cell Biochem* **262**(1-2): 1-16.

Goldstein DS, Kopin IJ (2007). Evolution of concepts of stress. *Stress* **10**(2): 109-120.

Gomes I, Gupta A, Filipovska J, Szeto HH, Pintar JE, Devi LA (2004). A role for heterodimerization of mu and delta opiate receptors in enhancing morphine analgesia. *Proceedings of the National Academy of Sciences of the United States of America* **101**(14): 5135-5139.

Gorman JM, Papp LA, Coplan JD, Martinez JM, Lennon S, Goetz RR*, et al* (1994). Anxiogenic effects of CO2 and hyperventilation in patients with panic disorder. *American Journal of Psychiatry* **151**(4): 547-553.

Graeff FG (2007). Anxiety, panic and the hypothalamic-pituitary-adrenal axis. *Revista Brasileira de Psiquiatria* **29**: s3-s6.

Granholm L, Roman E, Nylander I (2015). Single housing during early adolescence causes time-, area- and peptide-specific alterations in endogenous opioids of rat brain. *Br J Pharmacol* **172**(2): 606-614.

Green DR, Reed JC (1998). Mitochondria and apoptosis. *Science* **281**(5381): 1309-1312.

Green RC, Cupples LA, Kurz A, Auerbach S, Go R, Sadovnick D*, et al* (2003). Depression as a risk factor for Alzheimer disease: the MIRAGE Study. *Arch Neurol* **60**(5): 753-759.

Halliwell B, Gutteridge J (2007). Free radicals in Biology and Medicine **$th Edition, Oxford University Press, USA**.

Han KS, Kim L, Shim I (2012). Stress and sleep disorder. *Exp Neurobiol* **21**(4): 141-150.

Harman D (1956). Aging: a theory based on free radical and radiation chemistry. *J Gerontol* **11**(3): 298-300.

Harper RM, Frysinger RC, Trelease RB, Marks JD (1984). State-dependent alteration of respiratory cycle timing by stimulation of the central nucleus of the amygdala. *Brain Research* **306**(1–2): 1-8.

Harrison DG, Gongora MC (2009). Oxidative stress and hypertension. *Med Clin North Am* **93**(3): 621-635.

Hatzimanikatis V, Choe LH, Lee KH (1999). Proteomics: theoretical and experimental considerations. *Biotechnol Prog* **15**(3): 312-318.

Haubensak W, Kunwar PS, Cai H, Ciocchi S, Wall NR, Ponnusamy R*, et al* (2010). Genetic dissection of an amygdala microcircuit that gates conditioned fear. *Nature* **468**(7321): 270-276.

Hebb AL, Zacharko RM, Gauthier M, Trudel F, Laforest S, Drolet G (2004). Brief exposure to predator odor and resultant anxiety enhances mesocorticolimbic activity and enkephalin expression in CD-1 mice. *The European journal of neuroscience* **20**(9): 2415-2429.

Henry MS, Bisht K, Vernoux N, Gendron L, Torres-Berrio A, Drolet G*, et al* (2018). Delta opioid receptor signaling promotes resilience to stress under the repeated social defeat paradigm in mice. *Frontiers in Molecular Neuroscience*.

Henry MS, Bisht K, Vernoux N, Gendron L, Tremblay M, Drolet G (2016). Enkephalin and Delta opioid receptor promote the resilience to chronic stress. *Program No. 814.23. 2016 Neuroscience Meeting Planner*: San Diego, CA, Society for Neuroscience, 2016. Online.

Henry MS, Gendron L, Tremblay ME, Drolet G (2017). Enkephalins: Endogenous Analgesics with an Emerging Role in Stress Resilience. *Neural Plast* **2017**: 1546125.

Herman JP, Cullinan WE (1997). Neurocircuitry of stress: central control of the hypothalamo-pituitary-adrenocortical axis. *Trends Neurosci* **20**(2): 78-84.

Herman JP, McKlveen JM, Ghosal S, Kopp B, Wulsin A, Makinson R*, et al* (2016a). Regulation of the Hypothalamic-Pituitary-Adrenocortical Stress Response. *Compr Physiol* **6**(2): 603-621.

Herman JP, Tasker JG (2016b). Paraventricular Hypothalamic Mechanisms of Chronic Stress Adaptation. *Frontiers in Endocrinology* **7**(137).

Hernandez J, Prieto I, Segarra AB, de Gasparo M, Wangensteen R, Villarejo AB*, et al* (2015). Interaction of neuropeptidase activities in cortico-limbic regions after acute restraint stress. *Behav Brain Res* **287**: 42-48.

Hewitt SA, Wamsteeker JI, Kurz EU, Bains JS (2009). Altered chloride homeostasis removes synaptic inhibitory constraint of the stress axis. *Nat Neurosci* **12**(4): 438-443.

Hillhouse TM, Porter JH (2015). A brief history of the development of antidepressant drugs: from monoamines to glutamate. *Exp Clin Psychopharmacol* **23**(1): 1-21.

Hokfelt T, Broberger C, Xu ZQ, Sergeyev V, Ubink R, Diez M (2000). Neuropeptides--an overview. *Neuropharmacology* **39**(8): 1337-1356.

Hoover WB, Vertes RP (2007). Anatomical analysis of afferent projections to the medial prefrontal cortex in the rat. *Brain structure & function* **212**(2): 149-179.

Hoppe LJ, Ipser J, Gorman JM, Stein DJ (2012). Panic disorder. In: Michael J. Aminoff FB, Dick FS (eds). *Handbook of Clinical Neurology*. Elsevier. Vol Volume 106, pp 363-374.

Hovatta I, Tennant RS, Helton R, Marr RA, Singer O, Redwine JM*, et al* (2005). Glyoxalase 1 and glutathione reductase 1 regulate anxiety in mice. *Nature* **438**(7068): 662-666.

Hudzik TJ, Maciag C, Smith MA, Caccese R, Pietras MR, Bui KH*, et al* (2011). Preclinical pharmacology of AZD2327: a highly selective agonist of the delta-opioid receptor. *J Pharmacol Exp Ther* **338**(1): 195-204.

Hudzik TJ, Pietras MR, Caccese R, Bui KH, Yocca F, Paronis CA*, et al* (2014). Effects of the delta opioid agonist AZD2327 upon operant behaviors and assessment of its potential for abuse. *Pharmacol Biochem Behav* **124**: 48-57.

Hughes J, Smith TW, Kosterlitz HW, Fothergill LA, Morgan BA, Morris HR (1975). Identification of two related pentapeptides from the brain with potent opiate agonist activity. *Nature* **258**(5536): 577-580.

Huhman KL (2006). Social conflict models: can they inform us about human psychopathology? *Horm Behav* **50**(4): 640-646.

Hurd YL (1996). Differential messenger RNA expression of prodynorphin and proenkephalin in the human brain. *Neuroscience* **72**(3): 767-783.

Ingvar M, Morgan PF, Auer RN (1988). The nature and timing of excitotoxic neuronal necrosis in the cerebral cortex, hippocampus and thalamus due to flurothyl-induced status epilepticus. *Acta Neuropathol* **75**(4): 362-369.

Jenkins LW, Povlishock JT, Lewelt W, Miller JD, Becker DP (1981). The role of postischemic recirculation in the development of ischemic neuronal injury following complete cerebral ischemia. *Acta Neuropathol* **55**(3): 205-220.

Johnson JE, Jr. (1975). The occurrence of dark neurons in the normal and deafferentated lateral vestibular nucleus in the rat: observations by light and electron microscopy. *Acta Neuropathol* **31**(2): 117-127.

Johnson PL, Samuels BC, Fitz SD, Lightman SL, Lowry CA, Shekhar A (2012). Activation of the orexin 1 receptor is a critical component of CO_2-mediated anxiety and hypertension but not bradycardia. *Neuropsychopharmacology* **37**(8): 1911-1922.

Johnson PL, Truitt W, Fitz SD, Minick PE, Dietrich A, Sanghani S*, et al* (2010). A key role for orexin in panic anxiety. *Nat Med* **16**(1): 111-115.

Jordan BA, Devi LA (1999). G-protein-coupled receptor heterodimerization modulates receptor function. *Nature* **399**(6737): 697-700.

Jortner BS (2006). The return of the dark neuron. A histological artifact complicating contemporary neurotoxicologic evaluation. *Neurotoxicology* **27**(4): 628-634.

Jutkiewicz EM (2006). The antidepressant -like effects of delta-opioid receptor agonists. *Mol Interv* **6**(3): 162-169.

Jutkiewicz EM, Rice KC, Traynor JR, Woods JH (2005). Separation of the convulsions and antidepressant-like effects produced by the delta-opioid agonist SNC80 in rats. *Psychopharmacology (Berl)* **182**(4): 588-596.

Kabli N, Fan T, O'Dowd BF, George SR (2014). mu-delta opioid receptor heteromer-specific signaling in the striatum and hippocampus. *Biochemical and biophysical research communications* **450**(1): 906-911.

Kakidani H, Furutani Y, Takahashi H, Noda M, Morimoto Y, Hirose T*, et al* (1982). Cloning and sequence analysis of cDNA for porcine beta-neo-endorphin/dynorphin precursor. *Nature* **298**(5871): 245-249.

Kapczinski F, Frey BN, Andreazza AC, Kauer-Sant'Anna M, Cunha AB, Post RM (2008). Increased oxidative stress as a mechanism for decreased BDNF levels in acute manic episodes. *Rev Bras Psiquiatr* **30**(3): 243-245.

Keeney A, Jessop DS, Harbuz MS, Marsden CA, Hogg S, Blackburn-Munro RE (2006). Differential effects of acute and chronic social defeat stress on hypothalamic-pituitary-adrenal axis function and hippocampal serotonin release in mice. *J Neuroendocrinol* **18**(5): 330-338.

Kennedy SE, Koeppe RA, Young EA, Zubieta JK (2006). Dysregulation of endogenous opioid emotion regulation circuitry in major depression in women. *Arch Gen Psychiatry* **63**(11): 1199-1208.

Kessler RC, Chiu W, Jin R, Ruscio A, Shear K, Walters EE (2006). The epidemiology of panic attacks, panic disorder, and agoraphobia in the national comorbidity survey replication. *Archives of General Psychiatry* **63**(4): 415-424.

Kieffer BL, Befort K, Gaveriaux-Ruff C, Hirth CG (1992). The delta-opioid receptor: isolation of a cDNA by expression cloning and pharmacological characterization. *Proceedings of the National Academy of Sciences of the United States of America* **89**(24): 12048-12052.

Kim I, Xu W, Reed JC (2008). Cell death and endoplasmic reticulum stress: disease relevance and therapeutic opportunities. *Nat Rev Drug Discov* **7**(12): 1013-1030.

Kinkead R, Balon N, Genest SE, Gulemetova R, Laforest S, Drolet G (2008). Neonatal maternal separation and enhancement of the inspiratory (phrenic) response to hypoxia in adult rats: disruption of GABAergic neurotransmission in the nucleus tractus solitarius. *Eur J Neurosci* **27**(5): 1174-1188.

Kinkead R, Montandon G, Bairam A, Lajeunesse Y, Horner RL (2009). Neonatal maternal separation disrupts regulation of sleep and breathing in adult male rats. *Sleep* **32**(12): 1611-1620

Kinkead R, Tenorio L, Drolet G, Bretzner F, Gargaglioni L (2014). Respiratory manifestations of panic disorder in animals and humans: A unique opportunity to understand how supramedullary structures regulate breathing. *Respir Physiol Neurobiol* **204**(0): 3-13.

Kirino T, Tamura A, Sano K (1984). Delayed neuronal death in the rat hippocampus following transient forebrain ischemia. *Acta Neuropathol* **64**(2): 139-147.

Klein DF (1993). False suffocation alarms, spontaneous panics, and related conditions. An integrative hypothesis. *Arch Gen Psychiatry* **50**(4): 306-317.

Konig M, Zimmer AM, Steiner H, Holmes PV, Crawley JN, Brownstein MJ*, et al* (1996). Pain responses, anxiety and aggression in mice deficient in pre-proenkephalin. *Nature* **383**(6600): 535-538.

Koolhaas JM, De Boer SF, De Rutter AJ, Meerlo P, Sgoifo A (1997). Social stress in rats and mice. *Acta Physiol Scand Suppl* **640**: 69-72.

Kormos V, Gaszner B (2013). Role of neuropeptides in anxiety, stress, and depression: from animals to humans. *Neuropeptides* **47**(6): 401-419.

Krishnan V, Han MH, Graham DL, Berton O, Renthal W, Russo SJ*, et al* (2007). Molecular adaptations underlying susceptibility and resistance to social defeat in brain reward regions. *Cell* **131**(2): 391-404.

Kromer SA, Kessler MS, Milfay D, Birg IN, Bunck M, Czibere L*, et al* (2005). Identification of glyoxalase-I as a protein marker in a mouse model of extremes in trait anxiety. *The Journal of neuroscience : the official journal of the Society for Neuroscience* **25**(17): 4375-4384.

Kuloglu M, Atmaca M, Tezcan E, Gecici O, Tunckol H, Ustundag B (2002a). Antioxidant enzyme activities and malondialdehyde levels in patients with obsessive-compulsive disorder. *Neuropsychobiology* **46**(1): 27-32.

Kuloglu M, Atmaca M, Tezcan E, Ustundag B, Bulut S (2002b). Antioxidant enzyme and malondialdehyde levels in patients with panic disorder. *Neuropsychobiology* **46**(4): 186-189.

Kung JC, Chen TC, Shyu BC, Hsiao S, Huang AC (2010). Anxiety- and depressive-like responses and c-fos activity in preproenkephalin knockout mice: oversensitivity hypothesis of enkephalin deficit-induced posttraumatic stress disorder. *J Biomed Sci* **17**: 29.

Le Merrer J, Becker JA, Befort K, Kieffer BL (2009). Reward processing by the opioid system in the brain. *Physiol Rev* **89**(4): 1379-1412.

Lea PJ, Temkin RJ, Freeman KB, Mitchell GA, Robinson BH (1994). Variations in mitochondrial ultrastructure and dynamics observed by high resolution scanning electron microscopy (HRSEM). *Microsc Res Tech* **27**(4): 269-277.

Lee SY, Lee SJ, Han C, Patkar AA, Masand PS, Pae CU (2013). Oxidative/nitrosative stress and antidepressants: targets for novel antidepressants. *Prog Neuropsychopharmacol Biol Psychiatry* **46**: 224-235.

Lehmann J, Feldon J (2000). Long-term biobehavioral effects of maternal separation in the rat: consistent or confusing? *Rev Neurosci* **11**(4): 383-408.

Lehmann J, Russig H, Feldon J, Pryce CR (2002). Effect of a single maternal separation at different pup ages on the corticosterone stress response in adult and aged rats. *Pharmacol Biochem Behav* **73**(1): 141-145.

Levitan MN, Nardi AE (2009). Nocturnal panic attacks: clinical features and respiratory connections. *Expert review of neurotherapeutics* **9**(2): 245-254.

Liberzon I, Taylor SF, Phan KL, Britton JC, Fig LM, Bueller JA*, et al* (2007). Altered central micro-opioid receptor binding after psychological trauma. *Biological psychiatry* **61**(9): 1030-1038.

Liu D, Diorio J, Tannenbaum B, Caldji C, Francis D, Freedman A*, et al* (1997). Maternal care, hippocampal glucocorticoid receptors, and hypothalamic- pituitary-adrenal responses to stress. *Science* **277**(5332): 1659-1662.

Lobo V, Patil A, Phatak A, Chandra N (2010). Free radicals, antioxidants and functional foods: Impact on human health. *Pharmacogn Rev* **4**(8): 118-126.

Lovick TA (2014). Sex determinants of experimental panic attacks. *Neurosci Biobehav Rev* **46P3**: 465-471.

Luboshitzky R, Lavie L, Shen-Orr Z, Herer P (2005). Altered Luteinizing Hormone and Testosterone Secretion in Middle-Aged Obese Men with Obstructive Sleep Apnea. *Obesity Research* **13**(4): 780-786.

Lucini D, Norbiato G, Clerici M, Pagani M (2002). Hemodynamic and autonomic adjustments to real life stress conditions in humans. *Hypertension* **39**(1): 184-188.

Luscher C, Slesinger PA (2010). Emerging roles for G protein-gated inwardly rectifying potassium (GIRK) channels in health and disease. *Nature reviews Neuroscience* **11**(5): 301-315.

Lutz PE, Kieffer BL (2013). Opioid receptors: distinct roles in mood disorders. *Trends Neurosci* **36**(3): 195-206.

Ma MC, Qian H, Ghassemi F, Zhao P, Xia Y (2005). Oxygen-sensitive {delta}-opioid receptor-regulated survival and death signals: novel insights into neuronal preconditioning and protection. *J Biol Chem* **280**(16): 16208-16218.

Maccaferri G (2005). Stratum oriens horizontal interneurone diversity and hippocampal network dynamics. *J Physiol* **562**(Pt 1): 73-80.

Machado A, Herrera AJ, de Pablos RM, Espinosa-Oliva AM, Sarmiento M, Ayala A*, et al* (2014). Chronic stress as a risk factor for Alzheimer's disease. *Rev Neurosci* **25**(6): 785-804.

Madden Jt, Akil H, Patrick RL, Barchas JD (1977). Stress-induced parallel changes in central opioid levels and pain responsiveness in the rat. *Nature* **265**(5592): 358-360.

Malhotra JD, Kaufman RJ (2007). Endoplasmic reticulum stress and oxidative stress: a vicious cycle or a double-edged sword? *Antioxid Redox Signal* **9**(12): 2277-2293.

Manoli I, Alesci S, Blackman MR, Su YA, Rennert OM, Chrousos GP (2007). Mitochondria as key components of the stress response. *Trends Endocrinol Metab* **18**(5): 190-198.

Manoli I, Le H, Alesci S, McFann KK, Su YA, Kino T*, et al* (2005). Monoamine oxidase-A is a major target gene for glucocorticoids in human skeletal muscle cells. *FASEB J* **19**(10): 1359-1361.

Mansour A, Hoversten MT, Taylor LP, Watson SJ, Akil H (1995). The cloned mu, delta and kappa receptors and their endogenous ligands: evidence for two opioid peptide recognition cores. *Brain research* **700**(1-2): 89-98.

Mansour A, Khachaturian H, Lewis ME, Akil H, Watson SJ (1988). Anatomy of CNS opioid receptors. *Trends Neurosci* **11**(7): 308-314.

Mansour A, Lewis ME, Khachaturian H, Akil H, Watson SJ (1986). Pharmacological and anatomical evidence of selective mu, delta, and kappa opioid receptor binding in rat brain. *Brain research* **399**(1): 69-79.

Maritim AC, Sanders RA, Watkins JB, 3rd (2003). Diabetes, oxidative stress, and antioxidants: a review. *J Biochem Mol Toxicol* **17**(1): 24-38.

Martinez M, Calvo-Torrent A, Herbert J (2002). Mapping brain response to social stress in rodents with c-fos expression: a review. *Stress* **5**(1): 3-13.

Martinez RC, Carvalho-Netto EF, Ribeiro-Barbosa ÉR, Baldo MVC, Canteras NS (2011). Amygdalar roles during exposure to a live predator and to a predator-associated context. *Neuroscience*.

Mates JM, Perez-Gomez C, Nunez de Castro I (1999). Antioxidant enzymes and human diseases. *Clin Biochem* **32**(8): 595-603.

Matsumoto AM, Sandblom RE, Schoene RB, Lee KA, Giblin EC, Pierson DJ*, et al* (1985). Testosterone replacement in hypogonadal men: effects on obstructive sleep apnoea, respiratory drives, and sleep. *Clin Endocrinol (Oxf)* **22**(6): 713-721.

Maurya PK, Noto C, Rizzo LB, Rios AC, Nunes SO, Barbosa DS*, et al* (2016). The role of oxidative and nitrosative stress in accelerated aging and major depressive disorder. *Prog Neuropsychopharmacol Biol Psychiatry* **65**: 134-144.

McBean GJ, Lopez MG, Wallner FK (2017). Redox-based therapeutics in neurodegenerative disease. *Br J Pharmacol* **174**(12): 1750-1770.

McDougall SJ, Paull JR, Widdop RE, Lawrence AJ (2000). Restraint stress : differential cardiovascular responses in Wistar-Kyoto and spontaneously hypertensive rats. *Hypertension* **35**(1 Pt 1): 126-129.

McDougall SJ, Widdop RE, Lawrence AJ (2005). Central autonomic integration of psychological stressors: focus on cardiovascular modulation. *Auton Neurosci* **123**(1-2): 1-11.

McEwen BS, Bowles NP, Gray JD, Hill MN, Hunter RG, Karatsoreos IN*, et al* (2015). Mechanisms of stress in the brain. *Nature neuroscience* **18**(10): 1353-1363.

Medecine USNLo (2017). Depression: How effective are antidepressants?

Melo I, Drews E, Zimmer A, Bilkei-Gorzo A (2014). Enkephalin knockout male mice are resistant to chronic mild stress. *Genes, brain, and behavior* **13**(6): 550-558.

Menard C, Pfau ML, Hodes GE, Kana V, Wang VX, Bouchard S*, et al* (2017). Social stress induces neurovascular pathology promoting depression. *Nature neuroscience* **20**(12): 1752-1760.

Mendelson WB, Martin JV, Perlis M, Giesen H, Wagner R, Rapoport SI (1988). Periodic cessation of respiratory effort during sleep in adult rats. *Physiology & Behavior* **43**(2): 229-234.

Metcalf MD, Yekkirala AS, Powers MD, Kitto KF, Fairbanks CA, Wilcox GL*, et al* (2012). The delta opioid receptor agonist SNC80 selectively activates heteromeric mu-delta opioid receptors. *ACS Chem Neurosci* **3**(7): 505-509.

Miller GE, Chen E, Parker KJ (2011). Psychological stress in childhood and susceptibility to the chronic diseases of aging: moving toward a model of behavioral and biological mechanisms. *Psychol Bull* **137**(6): 959-997.

Miller MW, Sadeh N (2014). Traumatic stress, oxidative stress and post-traumatic stress disorder: neurodegeneration and the accelerated-aging hypothesis. *Molecular psychiatry* **19**(11): 1156-1162.

Miyaji Y, Yoshimura S, Sakai N, Yamagami H, Egashira Y, Shirakawa M*, et al* (2015). Effect of edaravone on favorable outcome in patients with acute cerebral large vessel occlusion: subanalysis of RESCUE-Japan Registry. *Neurol Med Chir (Tokyo)* **55**(3): 241-247.

Modrego PJ (2010). Depression in Alzheimer's disease. Pathophysiology, diagnosis, and treatment. *J Alzheimers Dis* **21**(4): 1077-1087.

Montandon G, Bairam A, Kinkead R (2006). Long-Term Consequences of Neonatal Caffeine on Ventilation, Occurrence of Apneas, and Hypercapnic Chemoreflex in Male and Female Rats. *Pediatr Res* **59**(4): 519-524.

Mora F, Segovia G, Del Arco A, de Blas M, Garrido P (2012). Stress, neurotransmitters, corticosterone and body-brain integration. *Brain research* **1476**: 71-85.

Mortola JP, Dotta A (1992). Effects of hypoxia and ambient temperature on gaseous metabolism of newborn rats. *Am J Physiol* **263**(2 Pt 2): R267-272.

Multhaup G, Ruppert T, Schlicksupp A, Hesse L, Beher D, Masters CL*, et al* (1997). Reactive oxygen species and Alzheimer's disease. *Biochem Pharmacol* **54**(5): 533-539.

Myers B, McKlveen JM, Herman JP (2012). Neural Regulation of the Stress Response: The Many Faces of Feedback. *Cell Mol Neurobiol*.

Narita M, Kuzumaki N, Miyatake M, Sato F, Wachi H, Seyama Y*, et al* (2006). Role of delta-opioid receptor function in neurogenesis and neuroprotection. *Journal of neurochemistry* **97**(5): 1494-1505.

Nattie E, Li A (2012). Chapter 4 - Respiration and autonomic regulation and orexin. In: Anantha S (ed). *Progress in Brain Research*. Elsevier. Vol Volume 198, pp 25-46.

Neumann ID, Wigger A, Kromer S, Frank E, Landgraf R, Bosch OJ (2005). Differential effects of periodic maternal separation on adult stress coping in a rat model of extremes in trait anxiety. *Neuroscience* **132**(3): 867.

Nishinaka Y, Mori H, Endo N, Miyoshi T, Yamashita K, Adachi S*, et al* (2010). Edaravone directly reacts with singlet oxygen and protects cells from attack. *Life Sci* **86**(21-22): 808-813.

Noble F, Banisadr G, Jardinaud F, Popovici T, Lai-Kuen R, Chen H*, et al* (2001). First discrete autoradiographic distribution of aminopeptidase N in various structures of rat brain and spinal cord using the selective iodinated inhibitor [125I]RB 129. *Neuroscience* **105**(2): 479-488.

Noble F, Roques BP (2007). Protection of endogenous enkephalin catabolism as natural approach to novel analgesic and antidepressant drugs. *Expert Opin Ther Targets* **11**(2): 145-159.

Noda M, Furutani Y, Takahashi H, Toyosato M, Hirose T, Inayama S*, et al* (1982). Cloning and sequence analysis of cDNA for bovine adrenal preproenkephalin. *Nature* **295**(5846): 202-206.

Noor JI, Ikeda T, Mishima K, Aoo N, Ohta S, Egashira N*, et al* (2005). Short-term administration of a new free radical scavenger, edaravone, is more effective than its long-term administration for the treatment of neonatal hypoxic-ischemic encephalopathy. *Stroke* **36**(11): 2468-2474.

Nozaki C, Le Bourdonnec B, Reiss D, Windh RT, Little PJ, Dolle RE*, et al* (2012). delta-Opioid mechanisms for ADL5747 and ADL5859 effects in mice: analgesia, locomotion, and receptor internalization. *J Pharmacol Exp Ther* **342**(3): 799-807.

Nozaki C, Nagase H, Nemoto T, Matifas A, Kieffer BL, Gaveriaux-Ruff C (2014). In vivo properties of KNT-127, a novel delta opioid receptor agonist: receptor internalization, antihyperalgesia and antidepressant effects in mice. *Br J Pharmacol* **171**(23): 5376-5386.

Nunez MJ, Novio S, Amigo G, Freire-Garabal M (2011). The antioxidant potential of alprazolam on the redox status of peripheral blood leukocytes in restraint-stressed mice. *Life Sci* **89**(17-18): 650-654.

Ogliari A, Tambs K, Harris JR, Scaini S, Maffei C, Reichborn-Kjennerud T*, et al* (2010). The relationships between adverse events, early antecedents, and carbon dioxide reactivity as an intermediate phenotype of panic disorder: a general population study. *Psychother Psychosom* **79**(1): 48-55.

Öhman A (2000). Fear and Anxiety, Overlaps and Dissociations In: Lewis M, Haviland-Jones JM, Feldman Barrett L (eds). *Handbook of emotions* Third Edition edn.

Okuyama T, Kitamura T, Roy DS, Itohara S, Tonegawa S (2016). Ventral CA1 neurons store social memory. *Science* **353**(6307): 1536-1541.

Ong EW, Cahill CM (2014). Molecular Perspectives for mu/delta Opioid Receptor Heteromers as Distinct, Functional Receptors. *Cells* **3**(1): 152-179.

Onogi T, Minami M, Katao Y, Nakagawa T, Aoki Y, Toya T*, et al* (1995). DAMGO, a mu-opioid receptor selective agonist, distinguishes between mu- and delta-opioid receptors around their first extracellular loops. *FEBS Lett* **357**(1): 93-97.

Oslowski CM, Urano F (2011). Measuring ER stress and the unfolded protein response using mammalian tissue culture system. *Methods Enzymol* **490**: 71-92.

Ossipov MH, Dussor GO, Porreca F (2010). Central modulation of pain. *J Clin Invest* **120**(11): 3779-3787.

Oster-Granite ML, McPhie DL, Greenan J, Neve RL (1996). Age-dependent neuronal and synaptic degeneration in mice transgenic for the C terminus of the amyloid precursor protein. *The Journal of neuroscience : the official journal of the Society for Neuroscience* **16**(21): 6732-6741.

Ozmen I, Naziroglu M, Alici HA, Sahin F, Cengiz M, Eren I (2007). Spinal morphine administration reduces the fatty acid contents in spinal cord and brain by increasing oxidative stress. *Neurochem Res* **32**(1): 19-25.

Pan YX (2005). Diversity and complexity of the mu opioid receptor gene: alternative pre-mRNA splicing and promoters. *DNA Cell Biol* **24**(11): 736-750.

Pandey KB, Rizvi SI (2013). Resveratrol up-regulates the erythrocyte plasma membrane redox system and mitigates oxidation-induced alterations in erythrocytes during aging in humans. *Rejuvenation Res* **16**(3): 232-240.

Panneerselvam M, Ali SS, Finley JC, Kellerhals SE, Migita MY, Head BP*, et al* (2013). Epicatechin regulation of mitochondrial structure and function is opioid receptor dependent. *Mol Nutr Food Res* **57**(6): 1007-1014.

Papp LA, Klein DF, Gorman JM (1993). Carbon dioxide hypersensitivity, hyperventilation, and panic disorder. *The American journal of psychiatry* **150**(8): 1149-1157.

Patki G, Solanki N, Atrooz F, Allam F, Salim S (2013). Depression, anxiety-like behavior and memory impairment are associated with increased oxidative stress and inflammation in a rat model of social stress. *Brain research* **1539**: 73-86.

Paxinos G, Watson C (1998). *The rat brain in stereotaxic coordinates*, 4th Edition edn. Academic Press: San Diego.

Pecina M, Love T, Stohler CS, Goldman D, Zubieta JK (2015). Effects of the Mu opioid receptor polymorphism (OPRM1 A118G) on pain regulation, placebo effects and associated personality trait measures. *Neuropsychopharmacology : official publication of the American College of Neuropsychopharmacology* **40**(4): 957-965.

Perrine SA, Hoshaw BA, Unterwald EM (2006). Delta opioid receptor ligands modulate anxiety-like behaviors in the rat. *Br J Pharmacol* **147**(8): 864-872.

Pert A, Simantov R, Snyder SH (1977). A morphine-like factor in mammalian brain: analgesic activity in rats. *Brain research* **136**(3): 523-533.

Peters A, Sethares C, Moss MB (1998). The effects of aging on layer 1 in area 46 of prefrontal cortex in the rhesus monkey. *Cereb Cortex* **8**(8): 671-684.

Petrovich GD, Canteras NS, Swanson LW (2001). Combinatorial amygdalar inputs to hippocampal domains and hypothalamic behavior systems. *Brain Res Brain Res Rev* **38**(1-2): 247-289.

Petrovich GD, Scicli AP, Thompson RF, Swanson LW (2000). Associative fear conditioning of enkephalin mRNA levels in central amygdalar neurons. *Behav Neurosci* **114**(4): 681-686.

Petrowski K, Wintermann G-B, Kirschbaum C, Bornstein SR (2012). Dissociation between ACTH and cortisol response in DEX-CRH test in patients with panic disorder. *Psychoneuroendocrinology* **37**(8): 1199-1208.

Pfau ML, Russo SJ (2015). Peripheral and Central Mechanisms of Stress Resilience. *Neurobiol Stress* **1**: 66-79.

Pfleiderer B, Zinkirciran S, Arolt V, Heindel W, Deckert J, Domschke K (2007). fMRI amygdala activation during a spontaneous panic attack in a patient with panic disorder. *The World Journal of Biological Psychiatry* **8**(4): 269-272.

Pigott TA (2003). Anxiety disorders in women. *The Psychiatric clinics of North America* **26**(3): 621-672, vi-vii.

Player MS, Peterson LE (2011). Anxiety Disorders, Hypertension, and Cardiovascular Risk: A Review. *The International Journal of Psychiatry in Medicine* **41**(4): 365-377.

Porges SW (1995). Cardiac vagal tone: a physiological index of stress. *Neuroscience and biobehavioral reviews* **19**(2): 225-233.

Poulin JF, Berube P, Laforest S, Drolet G (2013). Enkephalin knockdown in the central amygdala nucleus reduces unconditioned fear and anxiety. *The European journal of neuroscience* **37**(8): 1357-1367.

Poulin JF, Castonguay‐Lebel Z, Laforest S, Drolet G (2008). Enkephalin co‐expression with classic neurotransmitters in the amygdaloid complex of the rat. *Journal of Comparative Neurology* **506**(6): 943-959.

Poulin JF, Laforest S, Drolet G (2014). Enkephalin downregulation in the nucleus accumbens underlies chronic stress-induced anhedonia. *Stress* **17**(1): 88-96.

Pradhan AA, Becker JA, Scherrer G, Tryoen-Toth P, Filliol D, Matifas A*, et al* (2009). In vivo delta opioid receptor internalization controls behavioral effects of agonists. *PLoS One* **4**(5): e5425.

Pradhan AA, Walwyn W, Nozaki C, Filliol D, Erbs E, Matifas A*, et al* (2010). Ligand-directed trafficking of the delta-opioid receptor in vivo: two paths toward analgesic tolerance. *The Journal of neuroscience : the official journal of the Society for Neuroscience* **30**(49): 16459-16468.

Puigserver P, Spiegelman BM (2003). Peroxisome proliferator-activated receptor-gamma coactivator 1 alpha (PGC-1 alpha): transcriptional coactivator and metabolic regulator. *Endocr Rev* **24**(1): 78-90.

Quintino-dos-Santos JW, Müller CJT, Bernabé CS, Rosa CA, Tufik S, Schenberg LC (2014). Evidence That the Periaqueductal Gray Matter Mediates the Facilitation of Panic-Like Reactions in Neonatally-Isolated Adult Rats. *PLoS One* **9**(3): e90726.

Ragnauth A, Schuller A, Morgan M, Chan J, Ogawa S, Pintar J*, et al* (2001). Female preproenkephalin-knockout mice display altered emotional responses. *Proceedings of the National Academy of Sciences of the United States of America* **98**(4): 1958-1963.

Rajmohan V, Mohandas E (2007). The limbic system. *Indian J Psychiatry* **49**(2): 132-139.

Randall-Thompson JF, Pescatore KA, Unterwald EM (2010). A role for delta opioid receptors in the central nucleus of the amygdala in anxiety-like behaviors. *Psychopharmacology (Berl)* **212**(4): 585-595.

Reed V, Wittchen HU (1998). DSM-IV panic attacks and panic disorder in a community sample of adolescents and young adults: how specific are panic attacks? *J Psychiatr Res* **32**(6): 335-345.

Rei D, Mason X, Seo J, Graff J, Rudenko A, Wang J*, et al* (2015). Basolateral amygdala bidirectionally modulates stress-induced hippocampal learning and memory deficits through a p25/Cdk5-dependent pathway. *Proceedings of the National Academy of Sciences of the United States of America* **112**(23): 7291-7296.

Reisine T, Pasternak G in Goodman and Oilman's The Pharmacological Basis of Therapeutics. eds Hardman, J. G. & Limbird, L. E. edn, pp 521-555.

Reyes BA, Zitnik G, Foster C, Van Bockstaele EJ, Valentino RJ (2015). Social Stress Engages Neurochemically-Distinct Afferents to the Rat Locus Coeruleus Depending on Coping Strategy. *eNeuro* **2**(6).

Rezayof A, Hosseini SS, Zarrindast MR (2009). Effects of morphine on rat behaviour in the elevated plus maze: the role of central amygdala dopamine receptors. *Behav Brain Res* **202**(2): 171-178.

Rezin GT, Cardoso MR, Goncalves CL, Scaini G, Fraga DB, Riegel RE*, et al* (2008). Inhibition of mitochondrial respiratory chain in brain of rats subjected to an experimental model of depression. *Neurochem Int* **53**(6-8): 395-400.

Rhim H, Miller RJ (1994). Opioid receptors modulate diverse types of calcium channels in the nucleus tractus solitarius of the rat. *The Journal of neuroscience : the official journal of the Society for Neuroscience* **14**(12): 7608-7615.

Richards EM, Mathews DC, Luckenbaugh DA, Ionescu DF, Machado-Vieira R, Niciu MJ*, et al* (2016). A randomized, placebo-controlled pilot trial of the delta opioid receptor agonist AZD2327 in anxious depression. *Psychopharmacology (Berl)* **233**(6): 1119-1130.

Roberson-Nay R, Klein DF, Klein RG, Mannuzza S, Moulton JL, Guardino M*, et al* (2010). Carbon dioxide hypersensitivity in separation-anxious offspring of parents with panic disorder. *Biological psychiatry* **67**(12): 1171-1177.

Rodrigues SM, LeDoux JE, Sapolsky RM (2009). The Influence of Stress Hormones on Fear Circuitry. *Annual Review of Neuroscience* **32**(1): 289-313.

Ron D, Walter P (2007). Signal integration in the endoplasmic reticulum unfolded protein response. *Nat Rev Mol Cell Biol* **8**(7): 519-529.

Roos RA, Bots GT (1983). Nuclear membrane indentations in Huntington's chorea. *J Neurol Sci* **61**(1): 37-47.

Rosin DL, Chang DA, Guyenet PG (2006). Afferent and efferent connections of the rat retrotrapezoid nucleus. *The Journal of Comparative Neurology* **499**(1): 64-89.

Rossier J, Guillemin R, Bloom F (1978). Foot shock induced stress decreases leu5-enkephalin immunoreactivity in rat hypothalamus. *Eur J Pharmacol* **48**(4): 465-466.

Rothstein JD (2017). Edaravone: A new drug approved for ALS. *Cell* **171**(4): 725.

Rozov AV, Valiullina FF, Bolshakov AP (2017). Mechanisms of Long-Term Plasticity of Hippocampal GABAergic Synapses. *Biochemistry (Mosc)* **82**(3): 257-263.

Rusin KI, Giovannucci DR, Stuenkel EL, Moises HC (1997). Kappa-opioid receptor activation modulates Ca2+ currents and secretion in isolated neuroendocrine nerve terminals. *The Journal of neuroscience : the official journal of the Society for Neuroscience* **17**(17): 6565-6574.

Russell LK, Mansfield CM, Lehman JJ, Kovacs A, Courtois M, Saffitz JE*, et al* (2004). Cardiac-specific induction of the transcriptional coactivator peroxisome proliferator-activated receptor gamma coactivator-1alpha promotes mitochondrial biogenesis and reversible cardiomyopathy in a developmental stage-dependent manner. *Circ Res* **94**(4): 525-533.

Russo SJ, Murrough JW, Han MH, Charney DS, Nestler EJ (2012). Neurobiology of resilience. *Nature neuroscience* **15**(11): 1475-1484.

Rygula R, Abumaria N, Flugge G, Fuchs E, Ruther E, Havemann-Reinecke U (2005). Anhedonia and motivational deficits in rats: impact of chronic social stress. *Behav Brain Res* **162**(1): 127-134.

Ryter SW, Kim HP, Hoetzel A, Park JW, Nakahira K, Wang X*, et al* (2007). Mechanisms of cell death in oxidative stress. *Antioxid Redox Signal* **9**(1): 49-89.

Sah P, Lopez De Armentia M (2003). Excitatory synaptic transmission in the lateral and central amygdala. *Annals of the New York Academy of Sciences* **985**: 67-77.

Saitoh A, Kimura Y, Suzuki T, Kawai K, Nagase H, Kamei J (2004). Potential anxiolytic and antidepressant-like activities of SNC80, a selective delta-opioid agonist, in behavioral models in rodents. *J Pharmacol Sci* **95**(3): 374-380.

Saitoh A, Sugiyama A, Yamada M, Inagaki M, Oka J, Nagase H*, et al* (2013). The novel delta opioid receptor agonist KNT-127 produces distinct anxiolytic-like effects in rats without producing the adverse effects associated with benzodiazepines. *Neuropharmacology* **67**: 485-493.

Saitoh A, Yoshikawa Y, Onodera K, Kamei J (2005). Role of delta-opioid receptor subtypes in anxiety-related behaviors in the elevated plus-maze in rats. *Psychopharmacology (Berl)* **182**(3): 327-334.

Salim S (2014). Oxidative stress and psychological disorders. *Curr Neuropharmacol* **12**(2): 140-147.

Sardinha A, Freire RC, Zin WA, Nardi AE (2009). Respiratory manifestations of panic disorder: causes, consequences and therapeutic implications. *J Bras Pneumol* **35**(7): 698-708.

Scalia F, Winans SS (1975). The differential projections of the olfactory bulb and accessory olfactory bulb in mammals. *The Journal of Comparative Neurology* **161**(1): 31-55.

Schenberg L (2016). A neural systems approach to the study of respiratory-type panic disorder. In: Nardi A, RCR R (eds). *Panic Disorder*. Springer international Publishing: Switzerland, pp 9-77.

Scherrer G, Tryoen-Toth P, Filliol D, Matifas A, Laustriat D, Cao YQ*, et al* (2006). Knockin mice expressing fluorescent delta-opioid receptors uncover G protein-coupled receptor dynamics in vivo. *Proceedings of the National Academy of Sciences of the United States of America* **103**(25): 9691-9696.

Schimitel FG, de Almeida GM, Pitol DN, Armini RS, Tufik S, Schenberg LC (2012). Evidence of a suffocation alarm system within the periaqueductal gray matter of the rat. *Neuroscience* **200**: 59-73.

Schimitel FG, Torres Müller CJ, Tufik S, Schenberg LC (2014). Evidence of a suffocation alarm system sensitive to clinically-effective treatments with the panicolytics clonazepam and fluoxetine. *Journal of Psychopharmacology* **28**(12): 1184-1188.

Schonthal AH (2012). Endoplasmic reticulum stress: its role in disease and novel prospects for therapy. *Scientifica (Cairo)* **2012**: 857516.

Seidah NG, Chretien M (1997). Eukaryotic protein processing: endoproteolysis of precursor proteins. *Curr Opin Biotechnol* **8**(5): 602-607.

Selye H (1937). The Significance of the Adrenals for Adaptation. *Science* **85**(2201): 247-248.

Selye H (1950). Stress and the general adaptation syndrome. *Br Med J* **1**(4667): 1383-1392.

Selye H (1956). The stress of life. New York: McGraw-Hill.

Selye H, Fortier C (1950). Adaptive reaction to stress. *Psychosom Med* **12**(3): 149-157.

Shorter E (2009). The history of lithium therapy. *Bipolar Disord* **11 Suppl 2**: 4-9.

Sies H (1997). Oxidative stress: oxidants and antioxidants. *Exp Physiol* **82**(2): 291-295.
Sinha R (2008). Chronic stress, drug use, and vulnerability to addiction. *Annals of the New York Academy of Sciences* **1141**: 105-130.
Skrabalova J, Drastichova Z, Novotny J (2013). Morphine as a Potential Oxidative Stress-Causing Agent. *Mini Rev Org Chem* **10**(4): 367-372.
Smith HS (2009). Opioid metabolism. *Mayo Clin Proc* **84**(7): 613-624.
Sobczak M, Salaga M, Storr MA, Fichna J (2014). Physiology, signaling, and pharmacology of opioid receptors and their ligands in the gastrointestinal tract: current concepts and future perspectives. *J Gastroenterol* **49**(1): 24-45.
Sohal RS, Wolfe LS (1986). Lipofuscin: characteristics and significance. *Prog Brain Res* **70**: 171-183.
Soliz J, Tam R, Kinkead R (2016). Neonatal Maternal Separation Augments Carotid Body Response to Hypoxia in Adult Males but Not Female Rats. *Frontiers in Physiology* **7**(432).
Spatola CA, Scaini S, Pesenti-Gritti P, Medland SE, Moruzzi S, Ogliari A*, et al* (2011). Gene-environment interactions in panic disorder and CO(2) sensitivity: Effects of events occurring early in life. *Am J Med Genet B Neuropsychiatr Genet* **156B**(1): 79-88.
Spruill TM (2010). Chronic psychosocial stress and hypertension. *Curr Hypertens Rep* **12**(1): 10-16.
Stein MB, Millar TW, Larsen DK, Kryger MH (1995). Irregular breathing during sleep in patients with panic disorder. *The American journal of psychiatry* **152**(8): 1168-1173.
Steiner DF (1998). The proprotein convertases. *Curr Opin Chem Biol* **2**(1): 31-39.
Stumm RK, Zhou C, Schulz S, Hollt V (2004). Neuronal types expressing mu- and delta-opioid receptor mRNA in the rat hippocampal formation. *The Journal of comparative neurology* **469**(1): 107-118.
Sugiyama A, Nagase H, Oka J, Yamada M, Saitoh A (2014). DOR(2)-selective but not DOR(1)-selective antagonist abolishes anxiolytic-like effects of the delta opioid receptor agonist KNT-127. *Neuropharmacology* **79**: 314-320.
Suudhof TC (2008). Neurotransmitter release. *Handb Exp Pharmacol*(184): 1-21.
Svoboda KR, Adams CE, Lupica CR (1999). Opioid receptor subtype expression defines morphologically distinct classes of hippocampal interneurons. *The Journal of neuroscience : the official journal of the Society for Neuroscience* **19**(1): 85-95.
Sweis BM, Veverka KK, Dhillon ES, Urban JH, Lucas LR (2013). Individual differences in the effects of chronic stress on memory: behavioral and neurochemical correlates of resiliency. *Neuroscience* **246**: 142-159.
Szklarczyk K, Korostynski M, Cieslak PE, Wawrzczak-Bargiela A, Przewlocki R (2015). Opioid-dependent regulation of high and low fear responses in two inbred mouse strains. *Behav Brain Res* **292**: 95-101.
Tagliari B, Noschang CG, Ferreira AG, Ferrari OA, Feksa LR, Wannmacher CM*, et al* (2010). Chronic variable stress impairs energy metabolism in prefrontal cortex and hippocampus of rats: prevention by chronic antioxidant treatment. *Metab Brain Dis* **25**(2): 169-176.
Tagliari B, Scherer EB, Machado FR, Ferreira AG, Dalmaz C, Wyse AT (2011). Antioxidants prevent memory deficits provoked by chronic variable stress in rats. *Neurochem Res* **36**(12): 2373-2380.

Takahashi R (2009). Edaravone in ALS. *Exp Neurol* **217**(2): 235-236.
Taliaz D, Loya A, Gersner R, Haramati S, Chen A, Zangen A (2011). Resilience to chronic stress is mediated by hippocampal brain-derived neurotrophic factor. *The Journal of neuroscience : the official journal of the Society for Neuroscience* **31**(12): 4475-4483.
Taussig R, Iniguez-Lluhi JA, Gilman AG (1993). Inhibition of adenylyl cyclase by Gi alpha. *Science* **261**(5118): 218-221.
Tenorio-Lopes L, Gulemetova R, Drolet G, Bretzner F, Kinkead R (2016). Orexin 1 Receptors Are necessary for Phase-Specific Enhancement of The Hypercapnic Ventilatory Response in Female Rats Subjected to Neonatal Stress. *The FASEB Journal* **30**(1 Supplement): 772.778.
Tenorio-Lopes L, Gulemetova R, Kinkead R (2015). Testosterone Increase Hypercapnic Ventilatory Response of Adult Male Rats Subjected to Panic Attack Model. *The FASEB Journal* **29**(1 Supplement).
Thompson CI, Brannon AJ, Heck AL (2003). Emotional fever after habituation to the temperature-recording procedure. *Physiology & behavior* **80**(1): 103-108.
Tjoumakaris SI, Rudoy C, Peoples J, Valentino RJ, Van Bockstaele EJ (2003). Cellular interactions between axon terminals containing endogenous opioid peptides or corticotropin-releasing factor in the rat locus coeruleus and surrounding dorsal pontine tegmentum. *The Journal of comparative neurology* **466**(4): 445-456.
Torregrossa MM, Jutkiewicz EM, Mosberg HI, Balboni G, Watson SJ, Woods JH (2006). Peptidic delta opioid receptor agonists produce antidepressant-like effects in the forced swim test and regulate BDNF mRNA expression in rats. *Brain research* **1069**(1): 172-181.
Tremblay ME, Zettel ML, Ison JR, Allen PD, Majewska AK (2012). Effects of aging and sensory loss on glial cells in mouse visual and auditory cortices. *Glia* **60**(4): 541-558.
Troisi A, Frazzetto G, Carola V, Di Lorenzo G, Coviello M, D'Amato FR*, et al* (2011). Social hedonic capacity is associated with the A118G polymorphism of the mu-opioid receptor gene (OPRM1) in adult healthy volunteers and psychiatric patients. *Soc Neurosci* **6**(1): 88-97.
Troisi A, Frazzetto G, Carola V, Di Lorenzo G, Coviello M, Siracusano A*, et al* (2012). Variation in the mu-opioid receptor gene (OPRM1) moderates the influence of early maternal care on fearful attachment. *Soc Cogn Affect Neurosci* **7**(5): 542-547.
Tsankova NM, Berton O, Renthal W, Kumar A, Neve RL, Nestler EJ (2006). Sustained hippocampal chromatin regulation in a mouse model of depression and antidepressant action. *Nature neuroscience* **9**(4): 519-525.
Turmaine M, Raza A, Mahal A, Mangiarini L, Bates GP, Davies SW (2000). Nonapoptotic neurodegeneration in a transgenic mouse model of Huntington's disease. *Proceedings of the National Academy of Sciences of the United States of America* **97**(14): 8093-8097.
Twig G, Elorza A, Molina AJ, Mohamed H, Wikstrom JD, Walzer G*, et al* (2008). Fission and selective fusion govern mitochondrial segregation and elimination by autophagy. *EMBO J* **27**(2): 433-446.
Ulrich-Lai YM, Herman JP (2009). Neural regulation of endocrine and autonomic stress responses. *Nature reviews Neuroscience* **10**(6): 397-409.

van der Bliek AM, Shen Q, Kawajiri S (2013). Mechanisms of mitochondrial fission and fusion. *Cold Spring Harb Perspect Biol* **5**(6).

van Rijn RM, Harvey JH, Brissett DI, DeFriel JN, Whistler JL (2013). Novel screening assay for the selective detection of G-protein-coupled receptor heteromer signaling. *J Pharmacol Exp Ther* **344**(1): 179-188.

Veening JG, Swanson LW, Sawchenko PE (1984). The organization of projections from the central nucleus of the amygdala to brainstem sites involved in central autonomic regulation: A combined retrograde transport-immunohistochemical study. *Brain Research* **303**(2): 337-357.

Vergura R, Balboni G, Spagnolo B, Gavioli E, Lambert DG, McDonald J*, et al* (2008). Anxiolytic- and antidepressant-like activities of H-Dmt-Tic-NH-CH(CH2-COOH)-Bid (UFP-512), a novel selective delta opioid receptor agonist. *Peptides* **29**(1): 93-103.

Versaevel M, Braquenier JB, Riaz M, Grevesse T, Lantoine J, Gabriele S (2014). Super-resolution microscopy reveals LINC complex recruitment at nuclear indentation sites. *Sci Rep* **4**: 7362.

Vgontzas AN, Bixler EO, Lin HM, Prolo P, Mastorakos G, Vela-Bueno A*, et al* (2001). Chronic insomnia is associated with nyctohemeral activation of the hypothalamic-pituitary-adrenal axis: clinical implications. *J Clin Endocrinol Metab* **86**(8): 3787-3794.

Vialou V, Robison AJ, Laplant QC, Covington HE, 3rd, Dietz DM, Ohnishi YN*, et al* (2010). DeltaFosB in brain reward circuits mediates resilience to stress and antidepressant responses. *Nature neuroscience* **13**(6): 745-752.

Viau V (2002). Functional cross-talk between the hypothalamic-pituitary-gonadal and -adrenal axes. *J Neuroendocrinol* **14**(6): 506-513.

Vyas A, Mitra R, Shankaranarayana Rao BS, Chattarji S (2002). Chronic stress induces contrasting patterns of dendritic remodeling in hippocampal and amygdaloid neurons. *The Journal of neuroscience : the official journal of the Society for Neuroscience* **22**(15): 6810-6818.

Waksman G, Bouboutou R, Devin J, Bourgoin S, Cesselin F, Hamon M*, et al* (1985). In vitro and in vivo effects of kelatorphan on enkephalin metabolism in rodent brain. *Eur J Pharmacol* **117**(2): 233-243.

Waksman G, Hamel E, Fournie-Zaluski MC, Roques BP (1986). Autoradiographic comparison of the distribution of the neutral endopeptidase "enkephalinase" and of mu and delta opioid receptors in rat brain. *Proceedings of the National Academy of Sciences of the United States of America* **83**(5): 1523-1527.

Wallace DR, Dodson SL, Nath A, Booze RM (2006). Delta opioid agonists attenuate TAT(1-72)-induced oxidative stress in SK-N-SH cells. *Neurotoxicology* **27**(1): 101-107.

Wei LN, Law PY, Loh HH (2004). Post-transcriptional regulation of opioid receptors in the nervous system. *Front Biosci* **9**: 1665-1679.

Wei LN, Loh HH (2011). Transcriptional and epigenetic regulation of opioid receptor genes: present and future. *Annu Rev Pharmacol Toxicol* **51**: 75-97.

Welch WJ, Suhan JP (1985). Morphological study of the mammalian stress response: characterization of changes in cytoplasmic organelles, cytoskeleton, and nucleoli, and appearance of intranuclear actin filaments in rat fibroblasts after heat-shock treatment. *J Cell Biol* **101**(4): 1198-1211.

Westrate LM, Drocco JA, Martin KR, Hlavacek WS, MacKeigan JP (2014). Mitochondrial morphological features are associated with fission and fusion events. *PLoS One* **9**(4): e95265.

Whistler JL, Enquist J, Marley A, Fong J, Gladher F, Tsuruda P*, et al* (2002). Modulation of postendocytic sorting of G protein-coupled receptors. *Science* **297**(5581): 615-620.

Whitaker AM, Gilpin NW, Edwards S (2014). Animal models of post-traumatic stress disorder and recent neurobiological insights. *Behav Pharmacol* **25**(5-6): 398-409.

White DP, Schneider BK, Santen RJ, McDermott M, Pickett CK, Zwillich CW*, et al* (1985). Influence of testosterone on ventilation and chemosensitivity in male subjects. *Journal of Applied Physiology* **59**(5): 1452-1457.

Whitnall MH (1993). Regulation of the hypothalamic corticotropin-releasing hormone neurosecretory system. *Prog Neurobiol* **40**(5): 573-629.

Wiest G, Lehner-Baumgartner E, Baumgartner C (2006). Panic attacks in an individual with bilateral selective lesions of the amygdala. *Archives of Neurology* **63**(12): 1798-1801.

Wigglesworth VB (1964). The Union of Protein and Nucleic Acid in the Living Cell and its Demonstration by Osmium Staining. *Journal of Cell Science* **s3-105: 113-122**(Available from: http://jcs.biologists.org/content/s3-105/69/113.abstract).

Wigglesworth VB (1981). The distribution of lipid in the cell structure: an improved method for the electron microscope. *Tissue Cell* **13**(1): 19-34.

Williams RH, Jensen LT, Verkhratsky A, Fugger L, Burdakov D (2007). Control of hypothalamic orexin neurons by acid and CO2. *PNAS* **104**(25): 10685-10690.

Wilson MA, Junor L (2008). The role of amygdalar mu-opioid receptors in anxiety-related responses in two rat models. *Neuropsychopharmacology : official publication of the American College of Neuropsychopharmacology* **33**(12): 2957-2968.

Wolff S (1995). The concept of resilience. *Aust N Z J Psychiatry* **29**(4): 565-574.

Wolkowitz OM, Epel ES, Reus VI, Mellon SH (2010). Depression gets old fast: do stress and depression accelerate cell aging? *Depress Anxiety* **27**(4): 327-338.

Wong ML, Kling MA, Munson PJ, Listwak S, Licinio J, Prolo P*, et al* (2000). Pronounced and sustained central hypernoradrenergic function in major depression with melancholic features: relation to hypercortisolism and corticotropin-releasing hormone. *Proceedings of the National Academy of Sciences of the United States of America* **97**(1): 325-330.

Xing G, Barry ES, Benford B, Grunberg NE, Li H, Watson WD*, et al* (2013). Impact of repeated stress on traumatic brain injury-induced mitochondrial electron transport chain expression and behavioral responses in rats. *Front Neurol* **4**: 196.

Yang DS, Kumar A, Stavrides P, Peterson J, Peterhoff CM, Pawlik M*, et al* (2008). Neuronal apoptosis and autophagy cross talk in aging PS/APP mice, a model of Alzheimer's disease. *Am J Pathol* **173**(3): 665-681.

Yang Y, Xia X, Zhang Y, Wang Q, Li L, Luo G*, et al* (2009). delta-Opioid receptor activation attenuates oxidative injury in the ischemic rat brain. *BMC Biol* **7**: 55.

Yasuda K, Raynor K, Kong H, Breder CD, Takeda J, Reisine T*, et al* (1993). Cloning and functional comparison of kappa and delta opioid receptors from mouse brain. *Proceedings of the National Academy of Sciences of the United States of America* **90**(14): 6736-6740.

Yehuda R, Flory JD, Southwick S, Charney DS (2006). Developing an agenda for translational studies of resilience and vulnerability following trauma exposure. *Annals of the New York Academy of Sciences* **1071**: 379-396.

Yoshikawa K, Williams C, Sabol SL (1984). Rat brain preproenkephalin mRNA. cDNA cloning, primary structure, and distribution in the central nervous system. *J Biol Chem* **259**(22): 14301-14308.

Youle RJ, van der Bliek AM (2012). Mitochondrial fission, fusion, and stress. *Science* **337**(6098): 1062-1065.

Young IJ, Rowley WF (1970). Histochemical alterations of ventral horn cells resulting from chronic hemispherectomy or chronic dorsal root section. *Exp Neurol* **26**(3): 460-481.

Zhang H, Torregrossa MM, Jutkiewicz EM, Shi YG, Rice KC, Woods JH*, et al* (2006). Endogenous opioids upregulate brain-derived neurotrophic factor mRNA through delta- and micro-opioid receptors independent of antidepressant-like effects. *The European journal of neuroscience* **23**(4): 984-994.

Zhang J, Haddad GG, Xia Y (2000). delta-, but not mu- and kappa-, opioid receptor activation protects neocortical neurons from glutamate-induced excitotoxic injury. *Brain research* **885**(2): 143-153.

Zhang L, Hernández VS, Liu B, Medina MP, Nava-Kopp AT, Irles C*, et al* (2012). Hypothalamic vasopressin system regulation by maternal separation: Its impact on anxiety in rats. *Neuroscience* **215**(0): 135-148.

Zhang N, Komine-Kobayashi M, Tanaka R, Liu M, Mizuno Y, Urabe T (2005). Edaravone reduces early accumulation of oxidative products and sequential inflammatory responses after transient focal ischemia in mice brain. *Stroke* **36**(10): 2220-2225.

Zhang XY, Chen DC, Tan YL, Tan SP, Wang ZR, Yang FD*, et al* (2015). The interplay between BDNF and oxidative stress in chronic schizophrenia. *Psychoneuroendocrinology* **51**: 201-208.

Zhang YT, Zheng QS, Pan J, Zheng RL (2004). Oxidative damage of biomolecules in mouse liver induced by morphine and protected by antioxidants. *Basic Clin Pharmacol Toxicol* **95**(2): 53-58.

Zhang ZQ, Julien C, Barres C (1996). Baroreceptor modulation of regional haemodynamic responses to acute stress in rat. *J Auton Nerv Syst* **60**(1-2): 23-30.

Zhou C, Huang Y, Przedborski S (2008). Oxidative stress in Parkinson's disease: a mechanism of pathogenic and therapeutic significance. *Annals of the New York Academy of Sciences* **1147**: 93-104.

Zhu M, Li M, Yang F, Ou X, Ren Q, Gao H*, et al* (2011). Mitochondrial ERK plays a key role in delta-opioid receptor neuroprotection against acute mitochondrial dysfunction. *Neurochem Int* **59**(6): 739-748.

Zhu M, Li MW, Tian XS, Ou XM, Zhu CQ, Guo JC (2009). Neuroprotective role of delta-opioid receptors against mitochondrial respiratory chain injury. *Brain research* **1252**: 183-191.

Zhu W, Pan ZZ (2004). Synaptic properties and postsynaptic opioid effects in rat central amygdala neurons. *Neuroscience* **127**(4): 871-879.

Zhu W, Pan ZZ (2005). Mu-opioid-mediated inhibition of glutamate synaptic transmission in rat central amygdala neurons. *Neuroscience* **133**(1): 97-103.

Ziemann AE, Allen JE, Dahdaleh NS, Drebot II, Coryell MW, Wunsch AM, *et al* (2009). The Amygdala Is a Chemosensor that Detects Carbon Dioxide and Acidosis to Elicit Fear Behavior. *Cell* **139**(5): 1012-1021.

6 CONTRIBUTION SCIENTIFIQUE / COLLABORATION – ANNEXE

Neonatal maternal separation opposes the facilitatory effect of castration on the respiratory response to hypercapnia of the adult male rat: evidence for the involvement of the medial amygdala

AUTHORS:

Luana Tenorio-Lopes[1], Mathilde S. Henry[2], Danuzia Marques[3], Marie-Ève Tremblay[2], Guy Drolet[2], Frederic Bretzner[2], Richard Kinkead[1].

AFFILIATION:

[1]Department of Pediatrics, Université Laval; Centre de Recherche de l'Institut de Cardiologie et Pneumologie de Québec

[2] Department of Molecular Medicine, Université Laval; Centre de Recherche du CHU de Québec-Université Laval; Axe Neurosciences

[3]Departamento de Morfologia e Fisiologia Animal Fac. de Ciências Agrárias e Veterinárias;'Universidade Estadual Paulista. Jaboticabal, SP, Brazil

Ce chapitre renferme la version intégrale d'un article publié dans le *Journal of Neuroendocrinology. J Neuroendocrinol. 2017 Dec;29(12). doi: 10.1111/jne.12550.*

6.1 Résumé

Les manifestations respiratoires du trouble panique (PD) se caractérisent par une plus grande instabilité respiratoire et une meilleure réactivité au CO_2 par rapport aux individus normaux. Alors que la prévalence des PD est environ trois fois plus élevée chez les femmes que chez les hommes, les origines de ce dimorphisme sexuel restent incomprises. Tout comme les patients atteints du PD, les rates femelles adultes soumises à une séparation maternelle néonatale (NMS) montrent une augmentation de leur réponse ventilatoire au CO_2. Étant donné que cet effet induit par la NMS n'est pas observé chez les hommes, nous avons émis l'hypothèse que la testostérone empêchait l'hypersensibilité au CO_2 induite par la NMS. Les chiots soumis à la NMS ont été placés dans un incubateur 3 h / jour à partir des jours 3 à 12 après l'accouchement. À l'âge adulte (8 à 10 semaines d'âge), les rats ont ensuite été soumis à une intervention chirurgicale fictive ou à une castration. Quatorze jours plus tard, la respiration a été mesurée au repos (air ambiant) et pendant une exposition aiguë à l'hypercapnie (5 et 10% de CO_2 pendant 10 minutes) en utilisant la pléthysmographie. Pour mieux comprendre les mécanismes impliqués, l'expression de c-fos a été utilisée comme un indicateur de l'activation neuronale. Les cerveaux ont été recueillis après exposition à l'air ou au CO_2 pour la quantification par immunohistochimie des cellules positives c-fos dans des régions sélectionnées, comprenant le noyau paraventriculaire de l'hypothalamus (PVN), l'hypothalamus dorso-médial et le complexe amygdalien. La castration a conduit à une augmentation de 100% de la réponse hyperventilatoire à 10% de CO_2 chez les rats témoins. De façon inattendue, la castration n'a eu aucun effet sur la réponse hyperventilatoire des rats NMS. L'intensité de la réponse hypercapnique était inversement corrélée avec l'expression de c-fos dans la partie médiale de l'amygdale. Nous concluons que la testostérone prévient l'hyperréactivité au CO_2 tandis que la NMS atténue la sensibilité au sevrage hormonal. Nous proposons qu'une influence inhibitrice de l'amygdale médiale contribue à cet effet.

6.2 Abstract

Respiratory manifestations of panic disorder (PD) include a greater respiratory instability and enhanced responsiveness to CO_2 compared to normal individuals. While the prevalence of PD is ~3 times greater in women compared with men, the origins of this sexual dimorphism remain poorly understood. Much like PD patients, adult female rats previously subjected to neonatal maternal separation (NMS) show an increase in their ventilatory response to CO_2. Because this effect of NMS is not observed in males, we hypothesized that testosterone prevents NMS-induced hyper-responsiveness to CO_2.

Pups subjected to NMS were placed in an incubator for 3 h/day from postnatal days 3 to 12. Control pups remained undisturbed. At adulthood (8 to 10 weeks of age), rats were then subjected either to sham surgery or castration. Fourteen days later, breathing was measured at rest (room air) and during acute exposure to hypercapnia (5 and 10% CO_2 for 10 min each) using plethysmography. To gain insight into the mechanisms involved, *c-fos* expression was used as an indicator of neuronal activation. Brains were collected following air or CO_2 exposure for quantification of *c-fos* positive cells by immunohistochemistry in selected regions, including the paraventricular nucleus of the hypothalamus (PVN), the dorso-medial hypothalamus, and the amygdalar complex. Castration produced a 100% increase of hyperventilatory response to 10% CO_2 in control rats. Unexpectedly, castration had no effect on the hyperventilatory response of NMS rats. The intensity of the hypercapnic response was inversely correlated with *c-fos* expression in the medial amygdala. We conclude that testosterone prevents the hyper-responsiveness to CO_2 whereas NMS attenuates sensitivity to hormone withdrawal. We propose that an inhibitory influence from the medial amygdala contributes to this effect.

KEYWORDS: panic disorder; neonatal stress; hypercapnia; testosterone; *c-fos*; PVN, amygdala.

6.3 Introduction

Panic disorder (PD) is a psychiatric disorder characterized by frequent panic attacks that are acute and unexpected. A panic attack is defined as an episode of overwhelming distress during which the patient rapidly develops symptoms such as sweating, heart palpitations, and fear of death. For a sub-population of PD patients, respiratory manifestations are a hallmark of this disorder; symptoms include intense air hunger, shortness of breath, and hyperventilation (Hoppe *et al*, 2012; Schenberg, 2016). The pathophysiological mechanism triggering the occurrence of panic attacks involves complex, inter-related processes. On one hand, the increased prevalence of sleep disordered breathing (SDB) in PD patients along with excessive respiratory and behavioral responsiveness to CO_2 stimulation point to abnormalities in the respiratory network and mechanisms responsible for CO_2 sensing (Papp *et al*, 1993; Stein *et al*, 1995). On the other hand, the fact that panic attacks and PD diagnosis emerge at puberty (Reed and Wittchen, 1998) and show a higher prevalence in women strongly suggest that neuroendocrine disruption also contributes to the pathophysiology (Donner and Lowry, 2013; Pigott, 2003). Despite recent progress in our understanding of PD (Johnson *et al*, 2010; Schenberg, 2016), the lack of proper animal models reproducing these two aspects of the disease impedes progress.

Childhood adversities comprising parental loss or neglect are significant risk factors for PD (Battaglia *et al*, 2014; Roberson-Nay *et al*, 2010). Early life stress alters brain development and today, we know that insufficient interactions between the mother and her offspring augment responsiveness of the hypothalamic-pituitary-adrenocortical axis (HPA) to stressors throughout life (Francis and Meaney, 1999; Liu *et al*, 1997). Neonatal maternal separation (NMS) has mixed effects on behavioral indicators of anxiety in adult rodents (Neumann *et al*, 2005; Quintino-dos-Santos *et al*, 2014; Zhang *et al*, 2012). Over the past decade, however, our laboratory has demonstrated that NMS (3h/day from postnatal days 3 to 12 in rats) is sufficient to disrupt development of the neural circuits that regulate breathing in a persistent and sex-specific fashion (Behan and Kinkead, 2011; Kinkead *et al*, 2014). CO_2 inhalation is a potent anxiogenic stimulus and panic patients exposed to this condition are more responsive than "healthy" subjects (Gorman *et al*, 1994). At adulthood, the respiratory phenotype of rats subjected to NMS shows several features reported in PD patients including respiratory instability during sleep and a sex-specific augmentation of the hyperventilatory response to CO_2 (Genest *et al*, 2007b; Kinkead *et al*, 2009). Specifically, the ventilatory response to hypercapnia (HCVR) of NMS females was found to be 63% larger than in non-stressed controls, whereas this increased responsiveness was not observed in males (Genest *et al*, 2007a). Moreover, these effects of NMS on the CO_2 response may only emerge when the animals reach sexual maturity (Tenorio-Lopes *et al*, 2016).

There are substantial functional and anatomical interactions between the corticotrophic (hypothalamic-pituitary-adrenocortical; HPA) and gonadotrophic (hypothalamic-pituitary-gonadal; HPG) axes (Viau, 2002). Some stressors can increase testosterone secretion (Chichinadze and Chichinadze, 2008), while testosterone inhibits HPA function by acting on the paraventricular nucleus of the hypothalamus (PVN) (Viau, 2002). NMS results in a persistent and sex-specific (male bias) augmentation of basal HPA activity and data show that this form of neonatal stress also alters HPA-HPG interactions. As a result, acute exposure to stress augments testosterone levels in NMS males contrary to non-separated controls (Fournier *et al*, 2014). Based on these observations, it is plausible that in males, augmented levels of testosterone prevent NMS-related enhancement of the

hyperventilatory response to CO_2. Although rarely considered, such "protective" effects may therefore explain the sex-based differences in PD manifestation.

To test this hypothesis, we first compared respiratory activity of non-separated *versus* separated rats that were either subjected to sham surgery or castration. Measurements were made at rest and during acute exposure to two levels of hypercapnic stimulation. The symptoms experienced during a panic attack reflect the interactions between hypothalamic and amygdalar structures associated with the regulation of stress, fear, and ventilatory responses (including CO_2-sensing) (Sardinha *et al*, 2009). To gain mechanistic insight, we then performed *c-fos* immunohistochemistry to identify key structures within this network that are particularly responsive to each experimental stimulation. Parts of these results have been published in abstract form (Tenorio-Lopes *et al*, 2016; Tenorio-Lopes *et al*, 2015).

6.4 Methods

6.4.1 Animals and ethical approval

Experiments were performed on 104 adult male Sprague–Dawley rats (55 NMS and 49 non-stressed controls) between 59 to 68 days of age; Table 1 provides details of mean ages, body weights, and animal distribution amongst the experimental groups. All animals used in this study were born and raised in our animal care facilities. Rats were supplied with food and water *ad libitum* and maintained under standard laboratory conditions (21^{o}C, 12:12-h dark–light cycle: lights on at 06:00 and off at 18:00). The Animal Care Committee of Université Laval approved all the experimental procedures and protocols which were in accordance with the guidelines of the Canadian Council on Animal Care.

6.4.2 Mating and neonatal maternal separation (NMS) procedures

Virgin females were mated and delivered 12-15 pups. Two days after delivery, litters were culled to 12 pups, when necessary, with an equal number of males and females when possible. The NMS protocol was identical to the one used in our previous studies (Genest *et al*, 2004). Briefly, each litter was separated daily from the mother 3h/day (09:00–12:00) from post-natal days 3 to 12. Separated pups were placed in a temperature (35°C) and humidity (45%) controlled incubator and isolated one from another using a cardboard partition. Non-separated control animals (CTRL) were continuously maintained under standard animal care procedures throughout the neonatal period with minimal human intervention. Since short periods of handling has distinct effects on HPA development (Lehmann *et al*, 2002), these animals are the most desirable control group for investigations of the effects of NMS on central nervous system development (Fournier *et al*, 2015; Lehmann and Feldon, 2000). On postnatal day 21, rats were weaned and housed 2 per cage under standard animal care conditions until adulthood (8 - 10 weeks old), at which time the ventilatory measurements were performed. Note that, for each group, rats originated from at least eight different litters to ensure that treatment-related differences were not due to a litter-specific effect.

6.4.3 Series I – Gonadectomy and whole-body plethysmography

6.4.3.1 Surgical procedures

Within each group (NMS and CTRL), male rats were selected and randomly assigned to one of these experimental procedures: castration or sham surgery, as done previously (Fournier *et al*, 2014). Briefly, rats were anaesthetized by inhalation of isoflurane (3% in air). A vertical incision was made in the abdomen slightly above the bladder. In the castrated group, the gonads were retracted and removed; in sham-operated animals, a vertical incision was made and the gonads were identified but not removed. At the beginning of the surgery, rats received subcutaneous injections of a non-steroidal anti-inflammatory drug (carprofen; 2mg/ml, 20 mg/kg; Pfizer, Kirkland, QC, Canada), local analgesic (xylocaine 2% with bupivacaine 0.5%; Hospira, Montréal, QC, Canada) and fluids (2 ml of saline). Postoperative treatments continued for 24h. Animals were returned to the animal care facility and housed in pairs for a 2-week period of recovery until the experiments were performed.

6.4.3.2 Ventilatory measurements

Ventilation was measured in unrestrained and awake rats using a whole-body, flow-through plethysmograph (PLY3223 Buxco Electronics, Sharon, CT - USA) as previously shown (Fournier *et al*, 2015). Briefly, the system consists of a 2-liter Plexiglas experimental chamber. The system was calibrated by injecting a known volume (5 ml) into the chamber with a glass syringe at a rate corresponding to the air flow range typically generated by the rat. Fresh air (baseline) or a hypercapnic gas mixture was delivered into the experimental chamber at a constant rate with a bias flow regulator (PLY1020; Buxco Electronics, Sharon, CT). Room air or gas mixtures were delivered to the experimental chamber at a constant rate (1.3 to 1.6 l/min). Barometric pressure, chamber temperature (T_C), humidity and the rectal temperature of the animals (T_B) were also measured at the beginning of each experiment to express the tidal volume (V_T; and thus minute ventilation, $\dot{V}_E$) in ml normalised to BTPS (body temperature (37°C), ambient pressure, and water vapor saturation (47 mmHg)) (Drorbough and Fenn, 1955). Composition of the gas mixtures flowing in and out of the chamber was analyzed with an oxygen analyzer (model S-3A, Ametek, Pittsburgh, PA) for subsequent calculation of oxygen consumption ($\dot{V}O_2$) in an open system (Mortola and Dotta, 1992).

6.4.3.3 Protocol

Each rat was allowed to acclimatize to the chamber for ~45 min. Baseline (normocapnic) measurements were made when the animal was quiet and the ventilatory variables were stable. All measurements were performed between 13:00 to 15:00 to minimize changes in endocrine and respiratory activity associated with the circadian rhythm. The baseline values obtained were representative of the data recorded over the preceding 10 min. A gas mixture of 5% CO_2 in air was then delivered into the chamber for 10 min. In males, previous work using 5% CO_2 revealed modest effects of stress on the hypercapnic response (Genest *et al*, 2007b). The CO_2 level was therefore raised to 10% for an additional 10 min to determine whether NMS-induced changes are dose-dependent. At the end of hypercapnia, each rat was taken out of the chamber for a final body temperature measurement, followed by deep anesthesia with a mixture of ketamine (Pfeizer, Kirkland, QC, Canada; 80 mg/kg) and xylazine (Bimeda, Cambridge, ON, Canada; 10 mg/ kg).

6.4.3.4 Blood sampling and hormone analyses

Once the rat reached a deep level of anesthesia, a terminal blood sample was withdrawn from the left ventricle. The rat was then perfused to harvest brain tissue as described below. Blood samples were placed in a serum-gel clotting activator Microtube (Sarstedt AG & Co., Nümbrecht Germany). After centrifugation (12.000 rpm at 4°C for 12 min), blood serum was collected and stored in a −80°C freezer until assayed. Assays of total testosterone were conducted in duplicate using a testosterone ELISA kit (Cayman Chemical Company, Ann Arbor, MI, USA) and a microplate spectrophotometer (Quant; Bio-Tek Instruments Inc., Winooski, VT, USA). According to the manufacturer, the sensitivity of the kit is 0.1 nM/L and intra assay variation within the data range is 4.4%. Testosterone concentrations were calculated from the four-parameter logistic standard curve using Sigma-Plot 12.3 (Systat Software, San Jose, CA, USA).

6.4.4 Series II – Quantification of c-fos immunoreactive cells during baseline and hypercapnia

6.4.4.1 Brain tissue harvesting

Prior to deep ketamine/xylazine anesthesia, rats were either acclimatized to the plethysmography chamber while breathing room air for ~45 min (baseline) or maintained in the chamber for 30 min after the CO_2 inhalation (hypercapnia) protocol. Following blood sampling, transcardiac perfusion was performed with 0.9% saline followed by 4% paraformaldehyde (PFA) in 0.1M sodium tetraborate buffer (PFA/borax; pH 9.5 at 4°C). Brains were extracted from the skull, post fixed for 24h in 4% PFA/borax and then placed in a 20% sucrose - 4% paraformaldehyde solution for 48h at 4°C. Frozen brains were mounted on a microtome and the regions of interest were cut in 30µm-thick coronal sections. Sections were collected in a cold cryoprotectant solution (0.05M sodium phosphate buffer, 30% ethylene glycol and 20% glycerol) and stored at −20°C. Brains were harvested from castrated and sham rats subjected to NMS or CTRL protocols; the precise number of animals used in each group appears in the figures and Table 1. Because ventilatory activity was recorded in these animals, it was possible to correlate apnea frequency and hyperventilatory response intensity with *c-fos* expression in selected regions of interest.

6.4.4.2 Regions of interest

c-fos protein expression was used as a functional marker of neuronal activation during normocapnia and hypercapnia in the paraventricular nucleus of the hypothalamus (PVN; bregma: -1.80 to -1.88), the amygdalar complex (medial, central, and basolateral amygdala; bregma: -2.56 to -2.80 mm), and the dorso-medial hypothalamus (DMH; bregma -2.56 to -3.14 mm). These regions were chosen because: 1) the PVN is a key structure involved in the orchestration of the neuroendocrine response to stress (Ulrich-Lai *et al*, 2009), 2) the amygdalar complex plays an important role in regulating behavioral and physiological responses associated with fear and anxiety (Rodrigues *et al*, 2009); although clinical data raise doubts about the role of the amygdala in the initiation of panic attacks (Feinstein *et al*, 2013; Pfleiderer *et al*, 2007; Wiest *et al*, 2006), neurons of the basolateral amygdala have CO_2-chemosensing properties (Ziemann *et al*, 2009), 3) the DMH (also known as the "hypothalamic panic area") contains orexinergic neurons that are implicated in panic attacks given their stimulatory effects on the brainstem's cardio-respiratory network and their CO_2-chemonsensing properties (Johnson *et al*, 2012; Williams *et al*, 2007). The selection of anatomical levels was conducted with reference to illustrations from a rat brain stereotaxic atlas (Paxinos and Watson, 1998) and using major anatomical landmarks including the optic tract (white matter) and lateral ventricles. Specifically, dark field contrast microscopy was used to visualize neuronal perikarya in the target regions (see below).

6.4.4.3 Immunohistochemistry

Free-floating sections were washed in 0.05M PBS for 30 min, then incubated with $NaBH_4$ in PBS for another 30 min. Sections were then washed 15 min in PBS and 30 min in PBST (0.1M PBS with 0.4% Triton-X and 0.5% bovine serum albumin, BSA) and incubated

overnight at 4°C with primary antibody (rabbit anti-human *c-fos* polyclonal affinity-purified antibody; Cat. n° PC38, Ab-5, Calbiochem, La Jolla, CA, USA; diluted 1:1000). The primary antibody was omitted in negative controls. The next day, sections were washed with the buffer and incubated with the secondary antibody for 2h (biotinylated goat anti-rabbit IgG; Cat. n° BA-1000; Vector, Burlingame, CA, USA; diluted 1:200). Sections were washed again and then processed for 90 min using the avidin-biotin-immunoperoxidase method (Vectastain ABC Kit, Vector Laboratories, Burlingame, CA, USA). Sections were rinsed in PBS and then *c-fos* immunoreactivity was revealed by the addition of the chromogen 3,3-diaminobenzidine for 2 min (SigmaFast™ DAB with metal enhancer; Sigma Aldrich, St. Louis, MO, USA). All sections were washed in PBS and placed on clean glass slides, dried overnight, dehydrated and mounted with coverslips using SHUR/Mount™ (Triangle Biomedic Sciences, Durham, NC, USA). All washes and incubations (except with the primary antibody) were done at room temperature.

6.4.5 Data analysis

6.4.5.1 Ventilatory measurements

Baseline measurements of ventilatory variables were obtained by averaging the last 10 min of stable recording. The apnea frequency was determined by counting the number of apneas over 10 min of baseline recording as we have done previously (Montandon *et al*, 2006). Briefly, based on established criteria (Mendelson *et al*, 1988), an apnea was defined as an interruption of airflow lasting at least two breathing cycles. At the end of the hypercapnic exposure (5% followed by 10% CO_2; 10 min each) a 5 min average was measured for each variable.

6.4.5.2 Immunohistochemistry

Tissue sections were visualised with a Leica DM 4500B microscope - equipped with a Retiga 2000R digital camera. A series of high-resolution micrographs were taken by using Openlab 5.5.2 (Improvision, Waltham, MA). *c-fos* immunoreactive cells were counted at 5X magnification in sections with clear labeling, as revealed by a dark punctate in their nucleus (B panels in Figures 3, 4 and, 5). The analyses were performed blind to the experimental conditions using Image J software (U.S. National Institutes of Health System). The numbers of *c-fos*-positive perikarya observed within each structure were counted bilaterally (whenever possible). For each condition, images were captured on 3 sections per animal and averaged to produce a mean value for each section. Since statistical analysis provided no evidence of lateralisation, these values were then averaged to obtain a mean value for each animal. Numbers of animals in each group are reported in the figures.

6.4.6 Statistics

The effects of surgery and stress on the ventilatory responses were assessed both on absolute data and results expressed as a percentage change from baseline. Analyses were performed using Statview 5.0 (SAS Institute, Cary, NC, USA). Analysis of variance (ANOVA) assessed the effects of the following factors on ventilation and expression of c-*fos*-positive perikarya, as appropriate: castration (castration *versus* sham), CO_2 exposure (air *versus* CO_2), and neonatal maternal separation (NMS *versus* CTRL). All data are presented as mean ± SEM. When ANOVA results indicated that a factor (or interaction

between factors) was significant ($P \leq 0.05$), the analysis was followed by Bonferroni-corrected *post-hoc* pairwise comparisons to identify specific differences. For *c-fos* data, *post-hoc* comparisons involving a low number of replicates ($n < 5$) were verified using a Mann-Whitney U test (non-parametric). Potential relationships between *c-fos*-labeled structures and apnea frequency and CO_2 response were first identified using a correlation matrix; Fisher's r- to z transformation was used to determine whether a correlation coefficient was statistically different from zero.

6.5 Results

6.5.1 Effectiveness of the castration procedure, body weight, and impact on basal ventilatory activity.

While the animals were age-matched, the mean body weight of castrated rats was found to be lower than shams (Table 1). Rats subjected to neonatal NMS weighed more than controls (Table 1); this was most noticeable in castrated animals. Analysis of blood samples obtained in "resting" (normocapnic) rats showed that castration equally reduced circulating testosterone levels in both groups (Fig. 1A and Table 1). In sham-operated animals, testosterone levels did not differ between CTRL and NMS groups (Fig. 1A).

Although these changes had no effect on basal minute ventilation ($\dot{V}_E$), differences in breathing pattern were observed: the tidal volume (V_T) of castrated rats was greater than of sham-operated animals (Table 1), which was compensated by a slightly reduced breathing frequency (f_R; Table 1). The reduction in f_R was most noticeable in controls (Table 1); these variables were not affected by NMS alone. None of the metabolic indicators (O_2 consumption, body temperature) differed between groups (Table 1). During normocapnia, apnea frequency was not influenced by NMS or castration (data not shown). In castrated animals, however, the apnea frequency correlated positively with testosterone levels; this relationship was strongest in CTRL animals (Fig. 1B). Conversely, no correlation was observed in rats with intact gonads (Fig. 1C).

	SHAM		CASTRATED		ANOVA results		
Parameter (Baseline)	*Control*	*NMS*	*Control*	*NMS*	**NMS effect**	**Castration effect**	**Factorial interaction**
Age (days)	63.2 ± 0.6 (21)	63.8 ± 0.6 (21)	63.4 ± 0.6 (23)	63.4 ± 0.7 (20)	$P = 0.65$ $F_{(1,81)} = 0.211$	$P = 0.90$ $F_{(1,81)} = 0.016$	NS
Weight (g)	426 ± 6 (21)	437 ± 10 (21)	381 ± 7*** (23)	409 ± 10*† (20)	$P = 0.02$ $F_{(1,81)} = 5.207$	$P < 0.0001$ $F_{(1,81)} = 18.327$	NS
Minute ventilation (ml BTPS/100g)	55 ± 2.5 (21)	51 ± 1.5 (21)	53 ± 1.7 (23)	54 ± 2.8 (20)	$P = 0.53$ $F_{(1,81)} = 0.406$	$P = 0.90$ $F_{(1,81)} = 0.016$	NS
Breathing frequency (breaths/min^{-1})	103 ± 2.5 (21)	102 ± 3.3 (21)	90 ± 1.9*** (23)	101 ± 3.5† (20)	$P = 0.10$ $F_{(1,81)} = 2.715$	$P = 0.01$ $F_{(1,81)} = 6.830$	$P = 0.05$ $F_{(1,81)} = 3.979$
Tidal volume (ml BTPS/100g)	0.52 ± 0.02 (21)	0.50 ± 0.01 (21)	0.59 ± 0.02* (23)	0.54 ± 0.02 (20)	$P = 0.07$ $F_{(1,81)} = 3.370$	$P = 0.013$ $F_{(1,81)} = 6.395$	NS
Body temperature (°C)	37.4 ± 0.1 (21)	37.4 ± 0.1 (21)	37.5 ± 0.1 (23)	37.7 ± 0.1 (20)	$P = 0.53$ $F_{(1,81)} = 0.394$	$P = 0.21$ $F_{(1,81)} = 1.62$	NS
Oxygen consumption (ml STPD/min/100g)	1.9 ± 0.1 (21)	1.9 ± 0.1 (21)	1.9 ± 0.1 (23)	1.9 ± 0.06 (20)	$P = 0.59$ $F_{(1,81)} = 0.288$	$P = 0.94$ $F_{(1,81)} = 0.005$	NS
Convective requirement ratio ($\dot{V}E/\dot{V}O_2$)	32 ± 2.0 (21)	28 ± 1.1 (21)	29 ± 1.7 (23)	29 ± 2.3 (20)	$P = 0.29$ $F_{(1,81)} = 1.128$	$P = 0.61$ $F_{(1,81)} = 0.267$	NS
Testosterone (nMol/l)	11.6 ± 0.8 (7)	19 ± 6.1 (10)	0.41 ± 0.06*** (7)	0.6 ± 0.1* (5)	$P = 0.41$ $F_{(1,25)} = 0.699$	$P = 0.003$ $F_{(1,25)} = 10.957$	NS

Table 1: Comparison of age, weight, body temperature, ventilatory, metabolic, and testosterone values obtained during baseline. The values are compared between sham-operated and castrated rats exposed to control or neonatal maternal separation (NMS) protocol.

Data are reported as mean ± SEM. *****Significantly different from sham-operated animal ($P \leq 0.05$); *******Significantly different from sham-operated animal ($P \leq 0.0001$). † Significantly different from control ($P \leq 0.05$). Numbers in brackets indicate the number of replicates in each group.

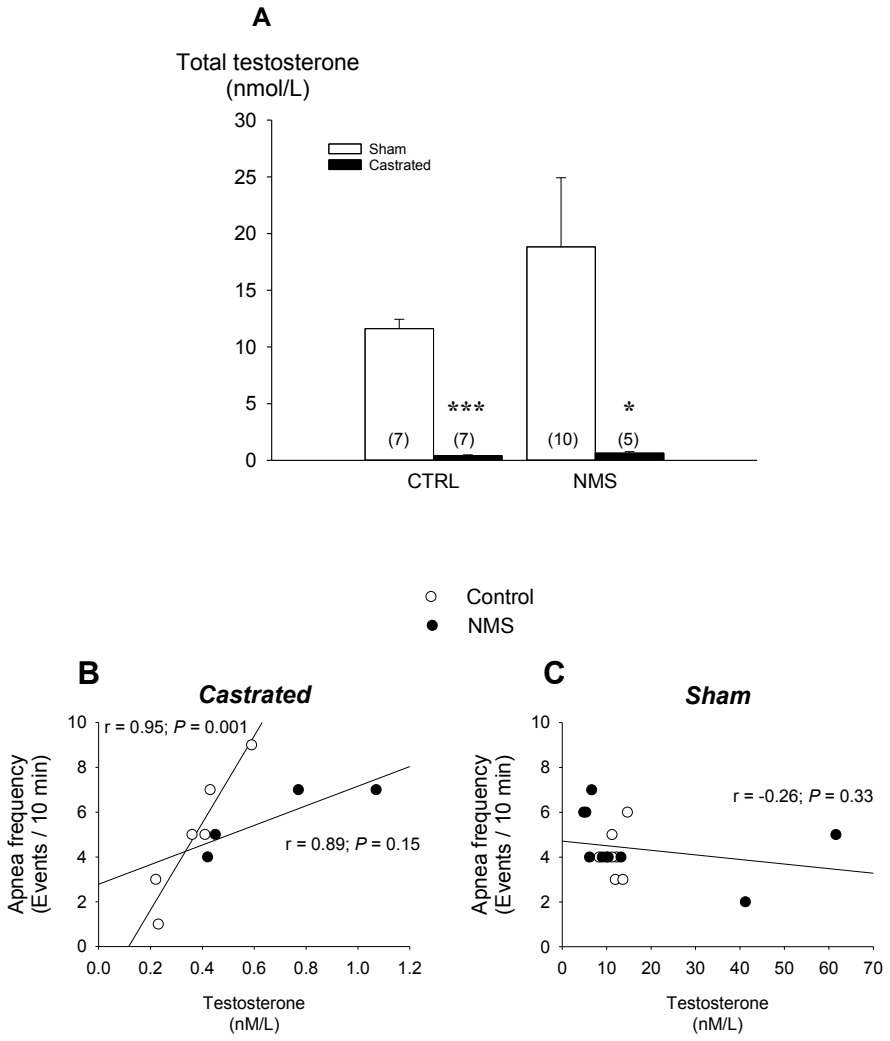

Figure 1: Consequences of castration on circulating testosterone levels and its relationship to apnea frequency under baseline conditions.
A) Blood samples were obtained from rats after 10 min of baseline recordings (normocapnia). The histograms compare results from animals exposed to neonatal maternal separation (NMS) or control (CTRL) protocols and also between castrated (black bars) and sham operated (white bars) animals. The relationship between basal testosterone levels and apnea frequency are compared between **B)** castrated and **C)** sham operated animals. Data are expressed as mean ± SEM. *****Significantly different from corresponding sham value ($P \leq 0.05$); *******Significantly different from corresponding sham value ($P \leq 0.0001$); supporting ANOVA results are reported in Table 1. Within histogram bars, the numbers between brackets indicate the number of replicates in each group.

6.5.2 Ventilatory response to hypercapnia (HCVR)

At 5% CO_2, the hyperventilatory response ($\dot{V}E$) was not influenced by castration or NMS (data not shown). At the end of the hypercapnic protocol (10% CO_2), however, there

was a significant interaction between castration and NMS ($F_{(1,45)}$ = 8.15; P = 0.007) such that the hypercapnic ventilatory response (HCVR) measured in CTRL rats was greater following castration than sham surgery; this effect of castration was not observed in NMS rats (Fig. 2). In these animals, surgery or stress had no significant effect on the V_T or f_R responses alone, nonetheless, the changes observed for each variable were sufficient to affect the outcome when combined since V_T and f_R are direct determinants of the hyperventilatory response ($\dot{V}E = V_T \times f_R$).

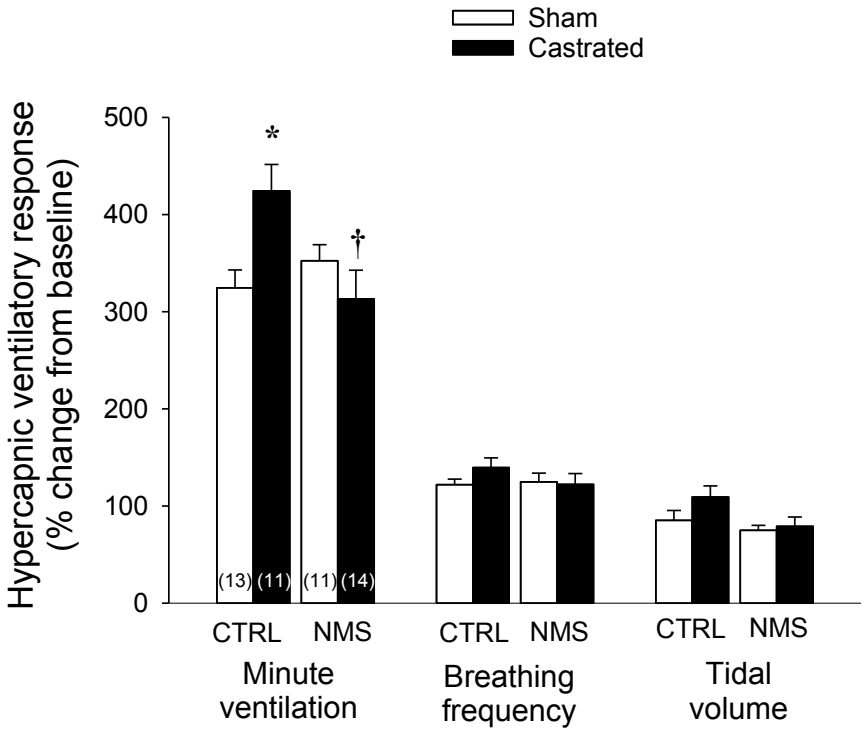

Figure 2: Castration increases the hypercapnic ventilatory response in control rats
Minute ventilation, tidal volume, and breathing frequency were measured during 10 min exposure to hypercapnia (10% CO_2; 10 min). The histograms represent responses expressed as percent change from baseline. Data are compared between rats exposed previously to neonatal maternal separation (NMS) or control (CTRL) protocols and also between castrated (black bars) and sham operated (white bars) animals. Data are expressed as mean ± SEM. *Post hoc* pair wise comparisons were performed only when ANOVA was significant. ***** Significantly different from corresponding sham value (P = 0.005). † Significantly different from corresponding control value (P = 0.01). Within the bars, numbers between brackets indicate the number of replicates in each group.

6.5.3 c-fos expression in the PVN at rest (room air) and following hypercapnic exposure (10% CO_2)

There was a significant effect of castration ($F_{(1,14)}$ = 9.742; P = 0.007), stress ($F_{(1,14)}$ = 11.360; P = 0.005) and hypercapnia ($F_{(1,28)}$ = 5.848; P = 0.02) on *c-fos* immunoreactivity in the PVN. Under basal conditions, the number of *c-fos* immunoreactive cells was

significantly greater in castrated NMS rats comparted with the sham NMS rats, however, this effect was not observed in the controls (Fig. 3). A significant interaction between CO_2 exposure and NMS was detected ($F_{(1,28)}$ = 6.270; P = 0.02), such that hypercapnia (10% CO_2) prevented the castration-induced increase in *c-fos* immunoreactivity in the PVN of NMS rats (Fig. 3C).

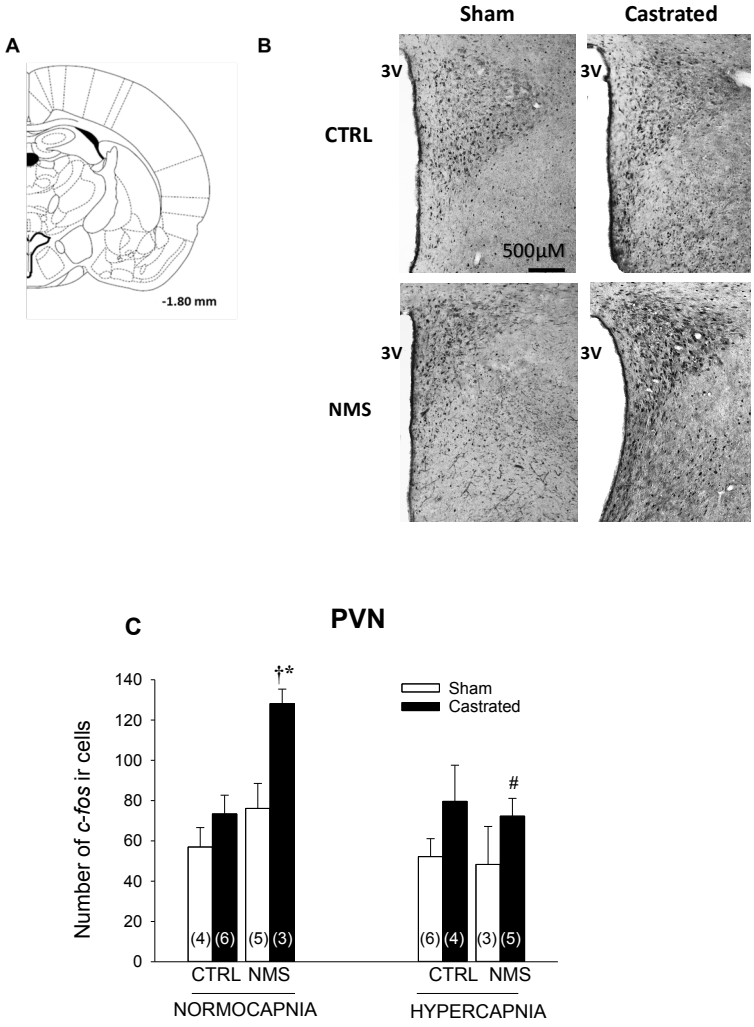

Figure 3: Castration increases the number of *c-fos* immunoreactive cells in the paraventricular nucleus of the hypothalamus (PVN) in rats subjected to neonatal maternal separation (NMS) under basal (normocapnic) conditions.
A) Schematic representation of the PVN at bregma -1.80 mm (Paxinos and Watson, 1994). **B)** Representative photomicrographs captured in rats exposed to normocapnia comparing *c-fos* immunoreactivity following castration or sham surgery in rats raised under standard conditions (CTRL; unstressed) or subjected to NMS. **C)** Mean number of *c*-fos immunoreactive cells expressed in the PVN during normocapnia and following hypercapnia (10% CO_2; 10 min). Data are compared between groups exposed to NMS or CTRL protocols and also between castrated (black bars) and sham (white bars) animals. Data are expressed as mean ± SEM. *Post hoc* pair wise comparisons were performed only when warranted by ANOVA. ***** Significantly different from corresponding sham value (*P* =

0.02). † Significantly different from corresponding control value (P = 0.007). # Significantly different from corresponding baseline (normocapnic) value (P = 0.005). Within histogram bars, the numbers between brackets indicate the number of replicates in each group.

6.5.4 c-fos expression in the amygdala at rest (room air) and following hypercapnic exposure (10% CO_2)

Within the amygdalar complex, mean data showed that at rest, the most important differences in *c-fos* expression were observed in the medial amygdala (MeA). In this structure, there was a significant effect of NMS ($F_{(1,14)}$ = 9.560; P = 0.008) and castration ($F_{(1,14)}$ = 13.697; P = 0.002) such that in NMS rats, the number of *c-fos* immunoreactive cells was higher in castrated- than sham-operated rats (Fig. 4B,C). Within the central region (CeA), basal *c-fos* expression was not affected by castration or NMS (Fig. 4D). In the basolateral amygdala (BLA), there was a significant effect of NMS ($F_{(1,14)}$ = 5.088; P = 0.04) and at rest, the number of *c-fos* immunoreactive cells was greater in NMS rats than in controls (Fig. 4E).

The effect of hypercapnia on *c-fos* immunoreactivity varied between amygdalar structures. In the MeA (Fig. 4C), there was a significant interaction between CO_2 and castration ($F_{(1,28)}$ = 13.111; P = 0.001). In this structure, CO_2 exposure consistently augmented the number of immunoreactive cells of rats with intact gonads; this response was not observed in castrated animals (Fig. 4C). A similar pattern was observed in the CeA. Again, there was a significant interaction between CO_2 and castration ($F_{(1,29)}$ = 3.993; P = 0.05) such that *c-fos* expression post-CO_2 was higher than at rest only in rats with intact gonads (Fig. 4D). Consequently, castrated rats had less immunoreactive cells than shams under hypercapnic conditions (Fig. 4D). In the BLA, NMS-related differences in *c-fos* expression were no longer observed upon hypercapnic exposure (Fig. 4E).

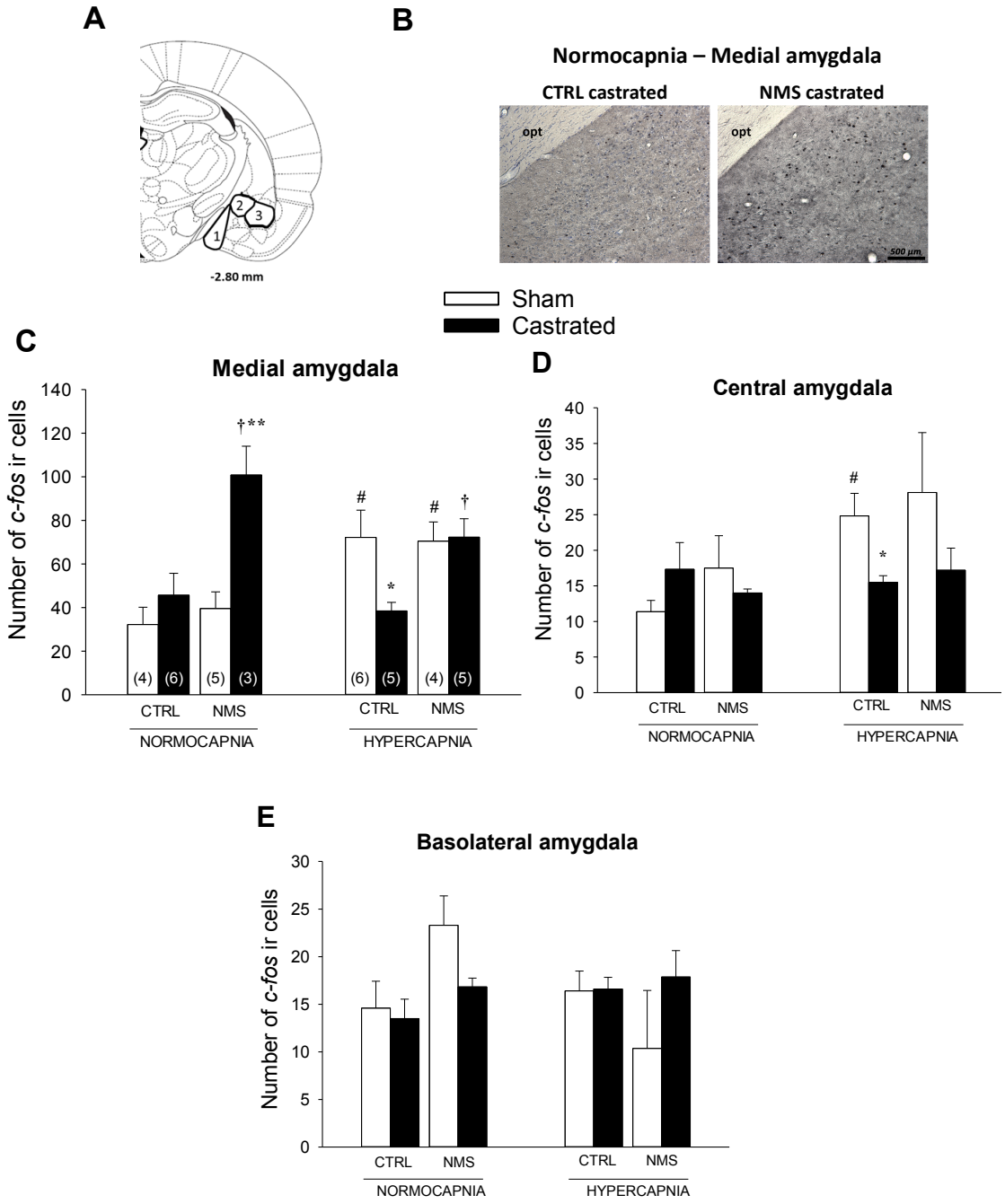

Figure 4: *c-fos* expression in different regions of the amygdala during normocapnia and hypercapnia

A) Schematic representation of the medial (1), central (2), and basolateral amygdala (3) at bregma -2.80 mm (Paxinos and Watson, 1994). **B)** Representative photomicrographs of the medial amygdala comparing basal (normocapnic) *c-fos* immunoreactivity following castration in rats exposed to neonatal maternal separation (NMS) *versus* control (CTRL) conditions. The mean number of *c-fos* immunoreactive cells expressed during normocapnia and following hypercapnia (10% CO_2; 10 min) are shown for the **C)** the medial, **D)** central, and **E)** basolateral amygdala. Data are compared between groups exposed previously to

NMS or CTRL protocols and also between castrated (black bars) and sham (white bars) animals. Data are expressed as mean ± SEM. *Post hoc* pair wise comparisons were performed only when warranted by ANOVA. † Significantly different from corresponding control value ($P \leq 0.01$). # Significantly different from corresponding baseline (normocapnic) value ($P \leq 0.05$). ** Significantly different from corresponding sham value ($P \leq 0.005$); * Significantly different from corresponding sham value ($P \leq 0.05$). Numbers between brackets indicate the number of replicates in each group.

6.5.5 c-fos expression in the dorsomedial hypothalamus (DMH) at rest (room air) and following hypercapnic exposure (10% CO_2)

There was no significant effect of castration, NMS or CO_2 on *c-fos* immunoreactivity in the DMH; however, there was a significant interaction between NMS and CO_2 ($F_{(1,24)} = 5.353$; $P = 0.03$); hence, following hypercapnia, the overall number of labeled cells in NMS rats was greater than in controls (Fig. 5B and C).

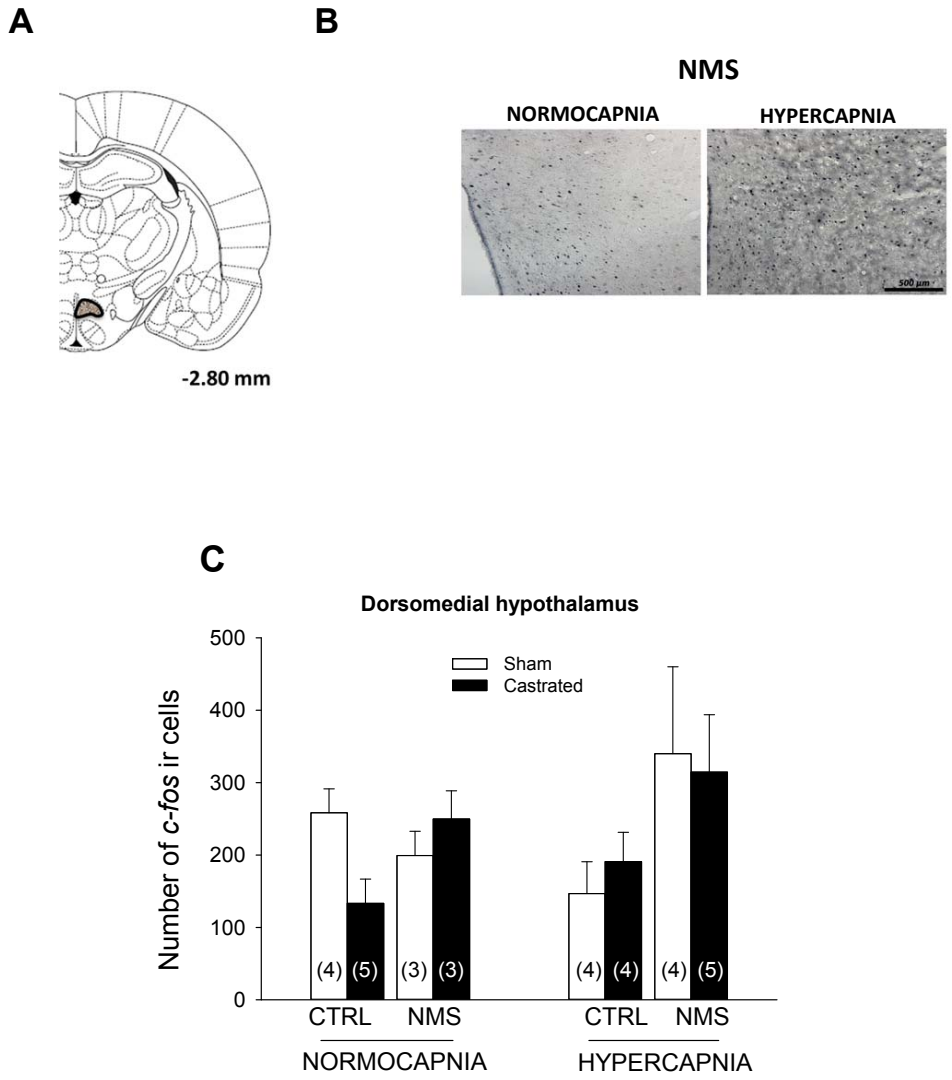

Figure 5: Neonatal maternal separation augments CO_2-induced increase in *c-fos* expression in the dorsomedial hypothalamus (DMH)
A) Schematic representation of the right DMH at bregma -2.80 mm (Paxinos and Watson, 1994). **B)** Representative photomicrographs of DMH comparing *c-fos* immunoreactivity in rats exposed to neonatal maternal separation (NMS) at rest (normocapnia) and following CO_2 exposure (10% CO_2; 10min). **C)** Average number of *c-fos* immunoreactive cells measured in the DMH during normocapnia and following hypercapnia. Data are compared between groups exposed previously to NMS or control (CTRL) protocols. Data are expressed as mean ± SEM. Numbers between brackets indicate the number of replicates in each group.

6.5.6 c-fos expression in the medial amygdala is inversely proportional to the intensity of the hyperventilatory response to CO_2.

As mentioned in the methods (section 2.6), a correlation matrix was initially used to identify potential relationships between *c-fos* expression following CO_2 exposure and the intensity of the hypercapnic ventilatory response. This exercise pointed to the MeA in which the number of *c-fos* positive cells was inversely proportional to the magnitude of the hyperventilatory response (Fig. 6). Of note, this relationship was especially strong in CTRL rats with intact gonads; however, neither NMS nor castration affected this relationship significantly.

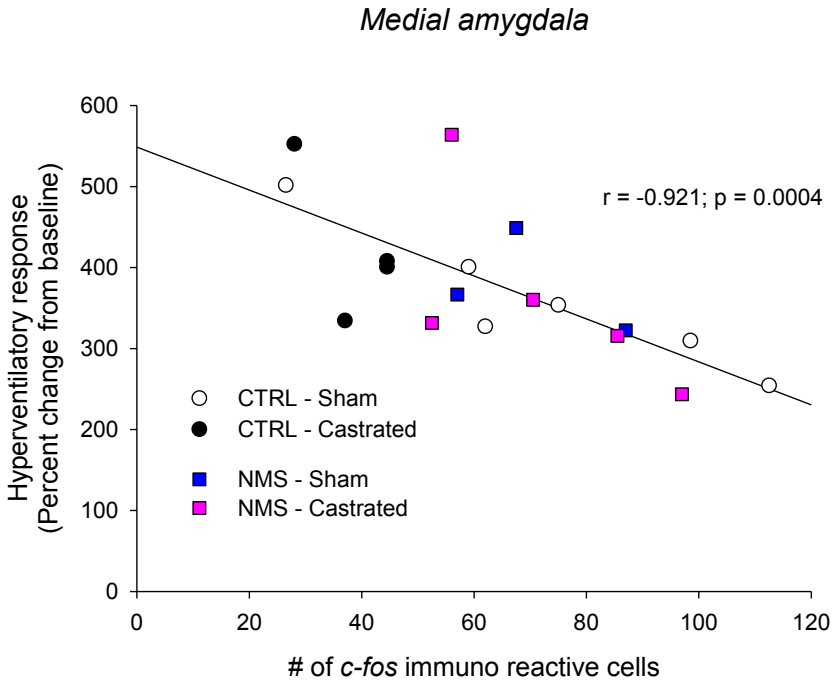

Figure 6: Intensity of the hyperventilatory response to CO_2 is inversely related to *c-fos* expression in the medial amygdala
Correlation between the hypercapnic ventilatory response to CO_2 (10% CO_2; 10 min) expressed as a percent change from resting values (normocapnia) and the number of *c-fos* positive cells following CO_2 exposure in the medial amygdala. Data are reported for all

animals; symbol shape (control *versus* neonatal maternal separation) and colors (sham *versus* castrated) identify data points from each experimental group.

6.6 Discussion

The propensity for panic disorder (PD) is higher in women than in men; disease onset coincides with puberty and its incidence declines markedly as women enter menopause (Lovick, 2014; Reed *et al*, 1998). These observations strongly suggest that sex hormones do not only explain sex-based differences in disorder manifestation, but also contribute to its pathophysiology. Panic disorder also occurs in men but the reduced occurrence in this population raises questions regarding the role of testosterone in the disease process. To better understand this issue, we aimed to determine whether testosterone protects males against PD in a rat model. Exposure to adverse experiences during early life is a significant risk factor for PD, notably increasing responsiveness to CO_2 in both humans and animal models (Battaglia *et al*, 2014; Genest *et al*, 2007b; Ogliari *et al*, 2010; Quintino-dos-Santos *et al*, 2014; Spatola *et al*, 2011). Because stress interferes with the gonadotropic axis (Viau, 2002), we predicted that castration would further enhance the hypercapnic ventilatory response (HCVR) in rats previously subjected to NMS. Our data show that castration does augment the HCVR but contrary to our initial prediction, this effect was significant only in controls, thereby indicating a more important inhibitory influence of testosterone in this group. *c-fos* analysis of hypothalamic and amygdalar regions associated with the regulation of stress, fear, and ventilatory responses (including CO_2-sensing) revealed region-specific sensitivity to NMS and castration and thus provide insight into the involvement of complex interactions between testosterone and these structures in the respiratory manifestations of PD.

6.6.1 Neonatal maternal separation, castration, and breathing at rest

Sleep-disordered breathing is a significant co-morbidity in PD patients (Levitan and Nardi, 2009). The etiology of this condition is multifactorial and complex; however, enhanced O_2-chemoreceptor function that predisposes to respiratory instability and/or obstruction of the airways during sleep are at the core of the problem (Dempsey *et al*, 2010). In addition, the higher prevalence of sleep-disordered breathing in men suggests that testosterone contributes to this respiratory impairment and current evidence indicates that testosterone levels are lower in men with sleep-disordered breathing (Luboshitzky *et al*, 2005). Protocols that aimed to supplement hypogonadal men augment the responsiveness to hypoxia in some subjects, thus promoting respiratory instability and apneas during sleep. No change in responsiveness to CO_2 was reported in these studies (Matsumoto *et al*, 1985; White *et al*, 1985). While these studies have inherent limitations (sample size, heterogeneity in administration protocols), they nonetheless suggest that a condition reducing testosterone augments sensitivity to subsequent increases in this hormone, and its consequences on apneas. Cleary, the testosterone levels observed following castration are very low thereby raising questions about the biological significance of our results. Despite this limitation and the limited number of animals, the fact that castration strengthened the relationship between apnea frequency and circulating testosterone levels, especially in control rats, is consistent with clinical observations linking hypogonadal conditions to an increased propensity for apneic events (Fig. 1). Based on previous results (Fournier *et al*, 2014), region-specific changes in androgen receptor expression within the brainstem resulting from NMS may explain the slope differences in these relationships, suggesting that testosterone supplementation could increase apnea frequency. With regards to mechanisms, the sum of the measurements obtained here indicates that respiratory disorders

related to neural control dysfunction become more apparent when the system is challenged (and/or testosterone levels augmented following castration). This finding is supported by results showing that under baseline conditions (Table 1), neither NMS nor castration augmented apnea frequency, and changes in breathing pattern were marginal with no alteration of the minute ventilation. Furthermore, indicators of metabolism did not differ between groups.

6.6.2 Impact of neonatal maternal separation and castration on basal c-fos expression in the hypothalamus and amygdala

Neonatal maternal separation (NMS) impacts the development of the hypothalamic-pituitary-adrenocortical (HPA) axis and its consequences persist throughout life. In adult males (but not females) previously subjected to NMS, quantification of *c-fos* m-RNA within the PVN, blood adrenocorticotropic hormone (ACTH), and blood corticosterone show that basal HPA activity is greater than in undisturbed controls (Genest *et al*, 2004). Following castration, male rats subjected to NMS showed the highest basal level of *c-fos* immunoreactive cells in the PVN (Fig. 3C); this effect was not observed in controls. This result is consistent with the inhibitory effect that testosterone exerts on HPA function by acting on the PVN (Viau, 2002). Interestingly, the MeA was the only structure found to be affected by both procedures (castration and NMS) during normocapnia (Fig. 4C). The MeA is sensitive to testosterone (Cooke, 2006) and GABAergic projections from the MeA are key to the regulation of PVN function and acute stress responses (Herman and Tasker, 2016b). However, this relationship appeared to be non-functional in NMS rats following castration. This may be due to abnormal GABAergic modulation owing to downregulation of KCC2 (a transmembrane anion transporter), as previously shown following chronic stress (Hewitt *et al*, 2009). That said, the relative stability in respiratory activity at rest is surprising considering the profound influence that the PVN exerts on baseline breathing (Genest *et al*, 2007a). This points to significant compensatory mechanisms within the respiratory network that ensure homeostasis. The source of this influence remains uncertain; however, the increased immunolabeling observed in the BLA of NMS rats suggest that this region could contribute to this effect. The lack of effect of castration in the BLA is consistent with its low level of androgen receptor expression relative to the MeA (Forbes-Lorman *et al*, 2014).

6.6.3 Impact of neonatal maternal separation and castration on the ventilatory, hypothalamic, and amygdalar responses to CO_2 inhalation

The rapid increase in arterial P_{CO_2} that follows CO_2 inhalation activates chemosensors among the periphery and brain, which then initiate robust hyperventilation. The CO_2 chemosensory circuit is an important aspect in PD pathophysiology; when chemosensitivity and/or responsiveness to CO_2 become excessive, physiological and emotional responses associated with fear and panic are observed (Schenberg, 2016). The carotid bodies are mainly known for their ability to sense O_2 in arterial blood; however, these peripheral chemoreceptors also contribute significantly to the HCVR and their activation by potassium cyanide injection (i.v.) is sufficient to trigger flight behaviors reminiscent of panic attack (Schimitel *et al*, 2012). While NMS augments the carotid body's response to hypoxia in males (but not females) it does not affect the responsiveness to CO_2 in either sex (Soliz *et al*, 2016). Consequently, the effects of NMS on the HCVR most likely originate from the central nervous system. CO_2-chemosensitive structures were first identified at the ventral surface of the medulla; however, more rostral structures are also equally capable of responding to CO_2/H^+ and initiating proper ventilatory and behavioral responses to maintain homeostasis (Nattie and Li, 2012). Amongst the structures investigated here, CO_2-sensing properties were already demonstrated for orexinergic neurons of the DMH in mice (Williams *et al*, 2007), while in stressed rats, this structure showed the strongest *c-fos* expression following hypercapnic exposure (Fig. 5C). The fact that this effect was not observed in control rats is consistent with the role that orexin plays in PD and the notion that early life stress is a significant risk factor for this disease (Battaglia *et al*, 2014; Johnson *et al*, 2010). However, the DMH response did not translate into an increased hyperventilation, thus pointing to a significant inhibition acting on the respiratory network during CO_2 exposure. While the CeA sends inhibitory projections to the DMH (Herman *et al*, 2016b), its involvement is unlikely because NMS did not affect *c-fos* expression in this structure. However, correlation matrix analysis indicates that, amongst the structures investigated, the MeA is the most likely source of this inhibitory influence owing to the inverse relationship observed between *c-fos* immunolabeling and hyperventilatory response (Fig. 6).

The MeA is commonly associated with olfactory pathways (Scalia and Winans, 1975); it is closely related to the modulation of responses to psychogenic stressors and can influence social, sexual, and defensive behaviors due to its reciprocal connections with the hypothalamus (Martinez *et al*, 2011). That CO_2 influences MeA *c-fos* expression is consistent with the notion that CO_2 is a "mixed" stressor that can recruit both systemic and psychogenic circuits (Kinkead *et al*, 2014), but to the best of our knowledge, there are no direct connections from the MeA onto respiratory brainstem neurons. However, the MeA can modulate respiration *via* the PVN. Considering that sex-based differences in the structural, neurochemical, and synaptic organization of the MeA are established during early life (Cooke and Woolley, 2005), it is therefore plausible that this structure contributes to the respiratory symptoms observed in PD.

The BLA receives inputs from multiple sensory systems and is involved in the consolidation of highly salient emotional stimuli (Sah and Lopez De Armentia, 2003). The BLA sends projections to the CeA (Poulin *et al*, 2008) that acts as the amygdala's output station to mediate behavioral and autonomic responses (Veening *et al*, 1984). In mice, BLA neurons show CO_2 sensing properties and activation of these cells by CO_2/H^+ triggers fear-related responses but not hyperventilation (Ziemann *et al*, 2009). Negligible differences in

c-fos expression of BLA neurons following CO_2 exposure do not support an increased activation (Fig. 4E) or a significant contribution of this structure to the abnormal respiratory phenotype that results from NMS.

GABAergic projections from the CeA regulate emotional homeostasis and responses to systemic stressors (Ulrich-Lai *et al*, 2009), and there is evidence indicating that the CeA and PVN could work independently (Carter *et al*, 2004). CeA activation in cats stimulates breathing (Harper *et al*, 1984); in rats, CeA efferents project near the nucleus of the solitary tract and CO_2-sensing neurons of the retrotrapezoid nucleus (Rosin *et al*, 2006). As for the PVN, the CeA's influence on these structures likely occurs *via* inhibition withdrawal (Ulrich-Lai *et al*, 2009). In female rats, data showing that CO_2-induced activation of the CeA is greater in NMS than in controls led us to propose that this structure plays an important role in the respiratory manifestation of PD (Kinkead *et al*, 2014). Here, we report that *c-fos* expression in the CeA was increased by CO_2, but NMS had no influence on the response (Fig. 4D). While it is tempting to conclude that the effects of NMS on the CeA's response to CO_2 are sex-specific, differences in the methods (measurement of mRNA *versus* proteins) and level of hypercapnic stimulation (5% *versus* 10%) between studies must be considered. Nevertheless, the significant reduction in *c-fos* expression in castrated rats indicates that testosterone is necessary for CeA activation during hypercapnia, but this effect is independent of NMS. This result points towards a novel role for this hormone in the regulation of the response to CO_2.

The PVN plays a key role in respiratory control and its action is influenced by limbic structures that respond to stressors in a region- and stimulus-specific manner (Ulrich-Lai *et al*, 2009). The anatomical relationships between the amygdalar regions investigated here and the PVN are indirect and homogeneous. Projections from the CeA and MeA are GABAergic whereas those from the BLA are glutamatergic (Ulrich-Lai *et al*, 2009). It is therefore conceivable that inputs from the MeA and BLA have opposite effects on PVN activity and responses. These relationships are influenced by NMS which augments PVN activation in males by biasing the balance between GABAergic and glutamatergic influences towards excitation (Genest *et al*, 2007a; Kinkead *et al*, 2008). The specific impact of each structure is yet to be addressed; however, the present work leads us to propose that in rats subjected to NMS, the influences that these amygdalar regions exert on the PVN and/or respiratory structures of the brainstem (*e.g.* nucleus of the solitary tract) are sufficient to maintain a normal HCVR, even when the inhibitory influence of testosterone is removed experimentally. In controls, a "standard" GABAeric modulation combined with the lack of MeA activation during CO_2 exposure leads to an enhanced hyperventilation when testosterone is reduced. Clinical data concerning the potential role of testosterone in PD is limited, but based on the present work, this investigation seems to be highly promising. However, the contribution of the amygdalar complex in the initiation of panic attacks in humans is uncertain. Patients with Urbach-Wiethe disease that show extensive bilateral calcifications of the amygdala can develop panic attacks spontaneously and in response to inhalation of 35% CO_2 (Feinstein *et al*, 2013). Conversely, an fMRI investigation of a PD patient showed amygdalar activation during a spontaneous panic attack. Clearly further clinical research is necessary to understand these discrepancies. However, keeping in mind the limitations inherent to species-related differences, the hypothesis that the amygdalar complex helps maintain a normal HCVR when facing a CO_2 challenge is in line with the clinical observations. Because the amygdala contributes to fear conditioning (Rodrigues *et al*, 2009), it is thus plausible that this structure either suppresses

or does not play a role in a novel or acute situation such as CO_2-induced panic response. However, the amygdala would most likely play a critical role in the formation of fear-induced situations as indicated by the fact that a significant proportion of PD patients have agoraphobia (Kessler *et al*, 2006) and patients with amygdalar atrophy do have disrupted emotional memory (Wiest *et al*, 2006).

6.6.4 Limitations, Conclusions, and Perspectives

Manifestations of panic attacks are diverse and can be triggered by different stimuli that may, or may not, involve memory. Consequently, the underlying neurological mechanisms are complex and comprehensive investigations of the origins of PD are challenging. Numerous structures have been associated with PD and here, we focused our study primarily on the paraventricular nucleus of the hypothalamus (PVN), the dorso-medial hypothalamus, and the amygdalar complex. That said, several additional structures could have been investigated. Amongst those, periaqueductal grey matter (PAG) is worth mentioning as it is considered the final common pathway of all defensive behaviors (including respiratory responses) and therefore plays an important role in the mediation of panic attacks (Quintino-dos-Santos *et al*, 2014; Schenberg, 2016; Schimitel *et al*, 2014). Thus, the PAG could be an alternative explanation for the results reported here. However, owing to its complex organisation a proper investigation of this structure could be an independent study.

Regardless of their nature, respiratory stimuli associated with suffocation can trigger panic attacks in both animal models and humans (Battaglia *et al*, 2014; Beck *et al*, 1999; Casanova *et al*, 2013; Schimitel *et al*, 2012). In normal (unstressed) rats however, chemical stimulation of the hypoxic chemoreflex by potassium cyanide infusion is more potent than CO_2 inhalation at evoking panic-related behaviors (Schimitel *et al*, 2012). While this may raise questions about CO_2's ability to elicit panic in rats, we must keep in mind that in the clinic, CO_2 inhalation elicits panic attacks in predisposed patients but not in healthy subjects (Klein, 1993). As pointed out by Quintino-dos-Santos *et al*. (Quintino-dos-Santos *et al*, 2014), CO_2 sensitivity in humans increases linearly with the number and severity of adverse life events (Ogliari *et al*, 2010; Spatola *et al*, 2011). Because NMS augments the ventilatory response to CO_2 in females (Genest *et al*, 2007b), we propose that this form adverse life event predisposes rats to panic attacks induced by CO_2 inhalation. Furthermore, we previously showed that in comparison to untreated controls, adult male (but not female) rats subjected to NMS are characterised by an augmented hypoxic ventilatory response to moderate hypoxia (12% O_2) and are hypertensive (Genest *et al*, 2004). This sex-specific phenotype shares features reported in both sleep disordered breathing and PD patients (Beck *et al*, 1999; Dempsey *et al*, 2010; Player and Peterson, 2011). Testosterone contributes to this persistent effect of NMS since castration brings the hypoxic ventilatory response back to control levels (Fournier *et al*, 2014). Here, castration augmented the ventilatory response to CO_2 in control but not NMS rats and the magnitude of this difference was comparable to the one between NMS and controls that was previously observed in females (Genest *et al*, 2007b). These differences in the effects of castration highlight the specificities in the chemosensory and neural pathways activated by O_2 and CO_2 and the region-specific effects that testosterone exerts on these networks regulating respiratory and behavioral responses.

Unlike these effects in males, NMS does not augment HPA axis function in females (Genest *et al*, 2004). Thus in line with clinical data, these results raise questions regarding the role of the HPA axis in PD. Empirical findings suggest that PD patients present a decreased reactivity of the HPA axis (Petrowski *et al*, 2012) and that panic attacks occur without any significant stress responses (de Souza Armini *et al*, 2015; Graeff, 2007); data showing that CO_2 did not augment *c-fos* immunolabeling in the PVN (Figure 3) are consistent with these observations. Paradoxically, experimental and clinical findings have established that early life exposure to adverse experiences, which disrupt HPA axis development, is a major risk factor for PD (Battaglia *et al*, 2014). Clearly, resolving this issue is well beyond the scope of our study but the present data, combined with previous work from our and other laboratories, nonetheless provide valuable clues regarding the impact of NMS on the neuroendocrine modulation of ventilatory responses to CO_2.

Our findings show that castration produced a robust increase of hyperventilatory response to hypercapnia in control rats, while castration had no effect on the hyperventilatory response of NMS rats. Furthermore, we also found that the intensity of the hypercapnic response was inversely proportional to *c-fos* expression in the MeA, thus suggesting an inhibitory influence from the MeA.

6.7 Acknowledgments

We are grateful to Dr. Roumiana Gulemetova and Stéphanie Fournier for the great technical assistance. We thank Dr Tara Janes for proofreading the manuscript. LTL was supported by National Council for Scientific and Technological Development CNPq - Brazil (206239/2014-9 – PDE) and the Canadian Institutes of Health Research (MOP 133686 to RK, GD, and FB).

1. Hoppe LJ, Ipser J, Gorman JM, Stein DJ. Panic disorder. In: Michael J. Aminoff FB, Dick FS, eds. *Handbook of Clinical Neurology*: Elsevier 2012: 363-74.
2. Schenberg L. A neural systems approach to the study of respiratory-type panic disorder. In: Nardi A, RCR R, eds. *Panic Disorder*. Switzerland: Springer international Publishing 2016: 9-77.
3. Stein MB, Millar TW, Larsen DK, Kryger MH. Irregular breathing during sleep in patients with panic disorder. *The American journal of psychiatry*. 1995; **152**(8): 1168-73.
4. Papp LA, Klein DF, Gorman JM. Carbon dioxide hypersensitivity, hyperventilation, and panic disorder. *The American journal of psychiatry*. 1993; **150**(8): 1149-57.
5. Reed V, Wittchen HU. DSM-IV panic attacks and panic disorder in a community sample of adolescents and young adults: how specific are panic attacks? *J Psychiatr Res*. 1998; **32**(6): 335-45.
6. Pigott TA. Anxiety disorders in women. *The Psychiatric clinics of North America*. 2003; **26**(3): 621-72, vi-vii.
7. Donner N, Lowry C. Sex differences in anxiety and emotional behavior. *Pflügers Archiv - European Journal of Physiology*. 2013; **465**(5): 601-26.
8. Johnson PL, Truitt W, Fitz SD, Minick PE, Dietrich A, Sanghani S, Traskman-Bendz L, Goddard AW, Brundin L, Shekhar A. A key role for orexin in panic anxiety. *Nat Med*. 2010; **16**(1): 111-5.
9. Roberson-Nay R, Klein DF, Klein RG, Mannuzza S, Moulton JL, Guardino M, Pine DS. Carbon dioxide hypersensitivity in separation-anxious offspring of parents with panic disorder. *Biological psychiatry*. 2010; **67**(12): 1171-7.
10. Battaglia M, Ogliari A, D'Amato F, Kinkead R. Early-life risk factors for panic and separation anxiety disorder: insights and outstanding questions arising from human and animal studies of CO_2 sensitivity *Neuroscience & Biobehavioral Reviews*. 2014; **46**(3): 455–64.
11. Liu D, Diorio J, Tannenbaum B, Caldji C, Francis D, Freedman A, Sharma S, Pearson D, Plotsky PM, Meaney MJ. Maternal care, hippocampal glucocorticoid receptors, and hypothalamic- pituitary-adrenal responses to stress. *Science*. 1997; **277**(5332): 1659-62.
12. Francis DD, Meaney MJ. Maternal care and the development of stress responses. *Curr Opin Neurobiol*. 1999; **9**(1): 128-34.
13. Zhang L, Hernández VS, Liu B, Medina MP, Nava-Kopp AT, Irles C, Morales M. Hypothalamic vasopressin system regulation by maternal separation: Its impact on anxiety in rats. *Neuroscience*. 2012; **215**(0): 135-48.
14. Neumann ID, Wigger A, Kromer S, Frank E, Landgraf R, Bosch OJ. Differential effects of periodic maternal separation on adult stress coping in a rat model of extremes in trait anxiety. *Neuroscience*. 2005; **132**(3): 867.
15. Quintino-dos-Santos JW, Müller CJT, Bernabé CS, Rosa CA, Tufik S, Schenberg LC. Evidence That the Periaqueductal Gray Matter Mediates the Facilitation of Panic-Like Reactions in Neonatally-Isolated Adult Rats. *PLoS One*. 2014; **9**(3): e90726.
16. Behan M, Kinkead R. Neuronal Control of Breathing: Sex and Stress Hormones. *Comprehensive Physiology*. 2011; **1**2101 - 39.
17. Kinkead R, Tenorio L, Drolet G, Bretzner F, Gargaglioni L. Respiratory manifestations of panic disorder in animals and humans: A unique opportunity to understand how supramedullary structures regulate breathing. *Respir Physiol Neurobiol*. 2014; **204**(0): 3-13.

18. Gorman JM, Papp LA, Coplan JD, Martinez JM, Lennon S, Goetz RR, Ross D, Klein DF. Anxiogenic effects of CO2 and hyperventilation in patients with panic disorder. *American Journal of Psychiatry*. 1994; **151**(4): 547-53.
19. Genest SE, Gulemetova R, Laforest S, Drolet G, Kinkead R. Neonatal maternal separation induces sex-specific augmentation of the hypercapnic ventilatory response in awake rat. *J Appl Physiol*. 2007; **102**1416-21.
20. Kinkead R, Montandon G, Bairam A, Lajeunesse Y, Horner RL. Neonatal maternal separation disrupts regulation of sleep and breathing in adult male rats. *Sleep*. 2009; **32**(12): 1611-20
21. Genest SE, Balon N, Gulemetova R, Laforest S, Drolet G, Kinkead R. Neonatal maternal separation and enhancement of the hypoxic ventilatory response: the role of GABAergic neurotransmission within the paraventricular nucleus of the hypothalamus. *J Physiol*. 2007; **583.1**299-314.
22. Tenorio-Lopes L, Gulemetova R, Drolet G, Bretzner F, Kinkead R. Orexin 1 receptors are necessary for phase-specific enhancement of the hypercapnic ventilatory response in female rats subjected to neonatal stress. *The FASEB Journal*. 2016; **30**(1 Supplement): 772.8.
23. Viau V. Functional cross-talk between the hypothalamic-pituitary-gonadal and -adrenal axes. *J Neuroendocrinol*. 2002; **14**(6): 506-13.
24. Chichinadze K, Chichinadze N. Stress-induced increase of testosterone: Contributions of social status and sympathetic reactivity. *Physiology & Behavior*. 2008; **94**(4): 595-603.
25. Fournier S, Gulemetova R, Joseph V, Kinkead R. Testosterone potentiates the hypoxic ventilatory response of adult male rats subjected to neonatal stress. *Exp Physiol*. 2014; **99**(5): 824-34.
26. Sardinha A, Freire RC, Zin WA, Nardi AE. Respiratory manifestations of panic disorder: causes, consequences and therapeutic implications. *J Bras Pneumol*. 2009; **35**(7): 698-708.
27. Tenorio-Lopes L, Gulemetova R, Kinkead R. Testosterone Increase Hypercapnic Ventilatory Response of Adult Male Rats Subjected to Panic Attack Model. *The FASEB Journal*. 2015; **29**(1 Supplement).
28. Genest SE, Gulemetova R, Laforest S, Drolet G, Kinkead R. Neonatal maternal separation and sex-specific plasticity of the hypoxic ventilatory response in awake rat. *J Physiol*. 2004; **554**(Pt 2): 543-57.
29. Lehmann J, Russig H, Feldon J, Pryce CR. Effect of a single maternal separation at different pup ages on the corticosterone stress response in adult and aged rats. *Pharmacol Biochem Behav*. 2002; **73**(1): 141-5.
30. Lehmann J, Feldon J. Long-term biobehavioral effects of maternal separation in the rat: consistent or confusing? *Rev Neurosci*. 2000; **11**(4): 383-408.
31. Fournier S, Gulemetova R, Baldy C, Joseph V, Kinkead R. Neonatal stress affects the aging trajectory of female rats on the endocrine, temperature, and ventilatory responses to hypoxia. *Am J Physiol Regul Integr Comp Physiol*. 2015; **308**(7): R659-R67.
32. Drorbough JE, Fenn WO. A Barometric method for measuring ventilation in newborn infants. *Pediatrics*. 1955; **16**81-6.
33. Mortola JP, Dotta A. Effects of hypoxia and ambient temperature on gaseous metabolism of newborn rats. *Am J Physiol*. 1992; **263**(2 Pt 2): R267-72.

34. Ulrich-Lai YM, Herman JP. Neural regulation of endocrine and autonomic stress responses. *Nat Rev Neurosci*. 2009; **10**(6): 397-409.
35. Rodrigues SM, LeDoux JE, Sapolsky RM. The Influence of Stress Hormones on Fear Circuitry. *Annual Review of Neuroscience*. 2009; **32**(1): 289-313.
36. Wiest G, Lehner-Baumgartner E, Baumgartner C. Panic attacks in an individual with bilateral selective lesions of the amygdala. *Archives of Neurology*. 2006; **63**(12): 1798-801.
37. Feinstein JS, Buzza C, Hurlemann R, Follmer RL, Dahdaleh NS, Coryell WH, Welsh MJ, Tranel D, Wemmie JA. Fear and panic in humans with bilateral amygdala damage. *Nat Neurosci*. 2013; **16**(3): 270-2.
38. Pfleiderer B, Zinkirciran S, Arolt V, Heindel W, Deckert J, Domschke K. fMRI amygdala activation during a spontaneous panic attack in a patient with panic disorder. *The World Journal of Biological Psychiatry*. 2007; **8**(4): 269-72.
39. Ziemann AE, Allen JE, Dahdaleh NS, Drebot II, Coryell MW, Wunsch AM, Lynch CM, Faraci FM, Howard Iii MA, Welsh MJ, Wemmie JA. The amygdala is a chemosensor that detects carbon dioxide and acidosis to elicit fear behavior. *Cell*. 2009; **139**(5): 1012-21.
40. Johnson PL, Samuels BC, Fitz SD, Lightman SL, Lowry CA, Shekhar A. Activation of the orexin 1 receptor is a critical component of CO_2-mediated anxiety and hypertension but not bradycardia. *Neuropsychopharmacology*. 2012; **37**(8): 1911-22.
41. Williams RH, Jensen LT, Verkhratsky A, Fugger L, Burdakov D. Control of hypothalamic orexin neurons by acid and CO_2. *PNAS*. 2007; **104**(25): 10685-90.
42. Paxinos G, Watson C. *The rat brain in stereotaxic coordinates* San Diego: Academic Press, 1998.
43. Montandon G, Bairam A, Kinkead R. Long-Term Consequences of Neonatal Caffeine on Ventilation, Occurrence of Apneas, and Hypercapnic Chemoreflex in Male and Female Rats. *Pediatr Res*. 2006; **59**(4): 519-24.
44. Mendelson WB, Martin JV, Perlis M, Giesen H, Wagner R, Rapoport SI. Periodic cessation of respiratory effort during sleep in adult rats. *Physiology & Behavior*. 1988; **43**(2): 229-34.
45. Lovick TA. Sex determinants of experimental panic attacks. *Neurosci Biobehav Rev*. 2014; **46P3**465-71.
46. Ogliari A, Tambs K, Harris JR, Scaini S, Maffei C, Reichborn-Kjennerud T, Battaglia M. The relationships between adverse events, early antecedents, and carbon dioxide reactivity as an intermediate phenotype of panic disorder: a general population study. *Psychother Psychosom*. 2010; **79**(1): 48-55.
47. Spatola CA, Scaini S, Pesenti-Gritti P, Medland SE, Moruzzi S, Ogliari A, Tambs K, Battaglia M. Gene-environment interactions in panic disorder and CO_2 sensitivity: Effects of events occurring early in life. *Am J Med Genet B Neuropsychiatr Genet*. 2011; **156B**(1): 79-88.
48. Levitan MN, Nardi AE. Nocturnal panic attacks: clinical features and respiratory connections. *Expert review of neurotherapeutics*. 2009; **9**(2): 245-54.
49. Dempsey JA, Veasey SC, Morgan BJ, O'Donnell CP. Pathophysiology of Sleep Apnea. *Physiol Rev*. 2010; **90**(1): 47-112.
50. Luboshitzky R, Lavie L, Shen-Orr Z, Herer P. Altered Luteinizing Hormone and Testosterone Secretion in Middle-Aged Obese Men with Obstructive Sleep Apnea. *Obesity Research*. 2005; **13**(4): 780-6.

51. Matsumoto AM, Sandblom RE, Schoene RB, Lee KA, Giblin EC, Pierson DJ, Bremner WJ. Testosterone replacement in hypogonadal men: effects on obstructive sleep apnoea, respiratory drives, and sleep. *Clin Endocrinol (Oxf)*. 1985; **22**(6): 713-21.
52. White DP, Schneider BK, Santen RJ, McDermott M, Pickett CK, Zwillich CW, Weil JV. Influence of testosterone on ventilation and chemosensitivity in male subjects. *Journal of Applied Physiology*. 1985; **59**(5): 1452-7.
53. Cooke BM. Steroid-dependent plasticity in the medial amygdala. *Neuroscience*. 2006; **138**(3): 997-1005.
54. Herman JP, Tasker JG. Paraventricular Hypothalamic Mechanisms of Chronic Stress Adaptation. *Frontiers in Endocrinology*. 2016; **7**(137).
55. Hewitt SA, Wamsteeker JI, Kurz EU, Bains JS. Altered chloride homeostasis removes synaptic inhibitory constraint of the stress axis. *Nat Neurosci*. 2009; **12**(4): 438-43.
56. Forbes-Lorman R, Auger AP, Auger CJ. Neonatal RU-486 (mifepristone) exposure increases androgen receptor immunoreactivity and sexual behavior in male rats. *Brain Research*. 2014; **1543**143-50.
57. Schimitel FG, de Almeida GM, Pitol DN, Armini RS, Tufik S, Schenberg LC. Evidence of a suffocation alarm system within the periaqueductal gray matter of the rat. *Neuroscience*. 2012; **200**: 59-73.
58. Soliz J, Tam R, Kinkead R. Neonatal Maternal Separation Augments Carotid Body Response to Hypoxia in Adult Males but Not Female Rats. *Frontiers in Physiology*. 2016; **7**(432).
59. Nattie E, Li A. Chapter 4 - Respiration and autonomic regulation and orexin. In: Anantha S, ed. *Progress in Brain Research*: Elsevier 2012: 25-46.
60. Scalia F, Winans SS. The differential projections of the olfactory bulb and accessory olfactory bulb in mammals. *The Journal of Comparative Neurology*. 1975; **161**(1): 31-55.
61. Martinez RC, Carvalho-Netto EF, Ribeiro-Barbosa ÉR, Baldo MVC, Canteras NS. Amygdalar roles during exposure to a live predator and to a predator-associated context. *Neuroscience*. 2011.
62. Cooke BM, Woolley CS. Sexually Dimorphic Synaptic Organization of the Medial Amygdala. *The Journal of Neuroscience*. 2005; **25**(46): 10759-67.
63. Sah P, Lopez De Armentia M. Excitatory synaptic transmission in the lateral and central amygdala. *Annals of the New York Academy of Sciences*. 2003; **985**: 67-77.
64. Poulin JF, Castonguay‐Lebel Z, Laforest S, Drolet G. Enkephalin co‐expression with classic neurotransmitters in the amygdaloid complex of the rat. *Journal of Comparative Neurology*. 2008; **506**(6): 943-59.
65. Veening JG, Swanson LW, Sawchenko PE. The organization of projections from the central nucleus of the amygdala to brainstem sites involved in central autonomic regulation: A combined retrograde transport-immunohistochemical study. *Brain Research*. 1984; **303**(2): 337-57.
66. Carter RN, Pinnock SB, Herbert J. Does the amygdala modulate adaptation to repeated stress? *Neuroscience*. 2004; **126**(1): 9-19.
67. Harper RM, Frysinger RC, Trelease RB, Marks JD. State-dependent alteration of respiratory cycle timing by stimulation of the central nucleus of the amygdala. *Brain Research*. 1984; **306**(1–2): 1-8.

68. Rosin DL, Chang DA, Guyenet PG. Afferent and efferent connections of the rat retrotrapezoid nucleus. *The Journal of Comparative Neurology*. 2006; **499**(1): 64-89.
69. Kinkead R, Balon N, Genest SE, Gulemetova R, Laforest S, Drolet G. Neonatal maternal separation and enhancement of the inspiratory (phrenic) response to hypoxia in adult rats: disruption of GABAergic neurotransmission in the nucleus tractus solitarius. *Eur J Neurosci*. 2008; **27**(5): 1174-88.
70. Kessler RC, Chiu W, Jin R, Ruscio A, Shear K, Walters EE. The epidemiology of panic attacks, panic disorder, and agoraphobia in the national comorbidity survey replication. *Archives of General Psychiatry*. 2006; **63**(4): 415-24.
71. Schimitel FG, Torres Müller CJ, Tufik S, Schenberg LC. Evidence of a suffocation alarm system sensitive to clinically-effective treatments with the panicolytics clonazepam and fluoxetine. *Journal of Psychopharmacology*. 2014; **28**(12): 1184-8.
72. Beck JG, Ohtake PJ, Shipherd JC. Exaggerated anxiety is not unique to CO_2 in panic disorder: A comparison of hypercapnic and hypoxic challenges. *Journal of Abnormal Psychology*. 1999; **108**(3): 473-82.
73. Casanova JP, Contreras M, Moya EA, Torrealba F, Iturriaga R. Effect of insular cortex inactivation on autonomic and behavioral responses to acute hypoxia in conscious rats. *Behav Brain Res*. 2013; **253**60-7.
74. Klein DF. False suffocation alarms, spontaneous panics, and related conditions. An integrative hypothesis. *Arch Gen Psychiatry*. 1993; **50**(4): 306-17.
75. Player MS, Peterson LE. Anxiety Disorders, Hypertension, and Cardiovascular Risk: A Review. *The International Journal of Psychiatry in Medicine*. 2011; **41**(4): 365-777
76. Petrowski K, Wintermann G-B, Kirschbaum C, Bornstein SR. Dissociation between ACTH and cortisol response in DEX-CRH test in patients with panic disorder. *Psychoneuroendocrinology*. 2012; **37**(8): 1199-208.
77. Graeff FG. Anxiety, panic and the hypothalamic-pituitary-adrenal axis. *Revista Brasileira de Psiquiatria*. 2007; **29**s3-s6.
78. de Souza Armini R, Bernabé CS, Rosa CA, Siller CA, Schimitel FG, Tufik S, Klein DF, Schenberg LC. In a rat model of panic, corticotropin responses to dorsal periaqueductal gray stimulation depend on physical exertion. *Psychoneuroendocrinology*. 2015; **53**136-47.